Communautés métazooplanctoniques de la zone épipélagique de deux environnements contrastés, le plateau des Kerguelen et la mer Méditerranée : caractérisation, distribution spatiale et rôle dans l'écosystème.

Antoine Nowaczyk

Thèse de doctorat
Aix Marseille Université
délivrée par l'Université de la Méditerranée

Ecole Doctorale en Sciences de l'environnement (ED-251)

Présentée par: **M. Nowaczyk Antoine**
Pour obtenir le grade de docteur en sciences de l'environnement.
Spécialité: **Océanographie**

Communautés métazooplanctoniques de la zone épipélagique de deux environnements contrastés, le plateau des Kerguelen et la mer Méditerranée : caractérisation, distribution spatiale et rôle dans l'écosystème.

Soutenue le 19 décembre 2011 à Marseille

Composition du Jury :

Pr. Bernard Quéguiner	Examinateur
Dr. Constantin Frangoulis	Rapporteur
Pr. Benoît Sautour	Rapporteur
Pr. Urania Christaki	Examinatrice
Dr. François Carlotti	Directeur de thèse
Dr. Delphine Thibault-Botha	Co-directrice de thèse

Remerciements :

Je tiens à remercier mes directeurs de thèse François Carlotti et Delphine Thibault Botha qui m'ont tout d'abord permis de découvrir le monde du zooplancton puis m'ont proposé ce sujet de thèse et ainsi continuer dans cette voie par la suite.

Je remercie les rapporteurs de cette thèse Benoît Sautour et Constantin Frangoulis pour la rapidité avec laquelle ils ont lu mon manuscrit et l'intérêt qu'ils ont porté à mon travail. Merci également aux autres membres du jury qui ont accepté de juger ce travail : Urania Christaki et Bernard Quéguiner.

Au cours de ce travail, j'ai participé à plusieurs programmes de recherches. Je remercie donc l'ensemble des personnes qui de près ou de loin ont élaboré et participé à ces programmes. Egalement merci à Bernard de Ligondes pour les sorties en mer bimensuelles lors du suivi SOMLIT ainsi qu'à Michel Lafont qui m'a dépanné plus d'une fois sur certains problèmes techniques.

Merci également à toutes les personnes du Centre d'Océanologie de Marseille (COM) grâce auxquelles j'ai pu effectuer ce travail. Merci également aux bonnes âmes qui ont réalisé certaines analyses pour moi comme Olivier Grosso pour les analyses en spectro de masse, Mireille Pujo-Pay pour une partie des analyses sels nuts et Dominique Lefèvre qui m'a beaucoup apporté sur les techniques de dosage des gaz.

Un remerciement tout particulier pour trois personnes qui m'ont soutenu tout au long de cette thèse et notamment pendant les périodes difficiles : Jean Blanchot pour ses « blanchotismes » qui mettent une bonne ambiance au 3ème étage et surtout pour sa grande générosité, Marc Pagano qui est sans doute l'une des personnes les plus dévouées que j'ai rencontrée, et enfin Floriane pour ses encouragements quotidiens.

Je ne peux pas terminer sans remercier mes deux compères thésards Lionel et Boris avec qui j'ai passé (et je continuerai) de bons moments derrière un ordinateur

(AOM) ou un bon barbecue dans la calanque après une journée de boulot. Et bon courage pour la suite à Nada et Marion et tous les autres thésards...

Enfin, merci à mes parents pour leurs soutiens moral et financier pendant ces longues années d'études.

Je n'ai sûrement pas nommé toutes les personnes sinon ce manuscrit ressemblerait plutôt à un annuaire mais il n'en reste pas moins que mes pensées y sont.

A Aurélie et à notre futur petit bout...

Table des matières

Liste des figures

Liste des tableaux

1 INTRODUCTION GÉNÉRALE

1.1 Caractéristiques du zooplancton et place dans les réseaux trophiques planctoniques marins

1.1.1 Diversité planctonique

Le zooplancton regroupe des organismes occupant un très large spectre de taille allant de quelques µm de large pour certains ciliés jusqu'à 2 m de diamètre pour certaines méduses (*Cyanea capillata*). D'après la classification en classe de taille proposée par Sieburth et al. (1978) le zooplancton se distribue en 5 classes de taille : nanoplancton (2-20 µm), microplancton (20-200 µm), mésoplancton (0,2-20 mm), macroplancton (2-20 cm) et jusqu'au mégaplancton (>20 cm) (Fig. 1-1). Le nanoplancton est essentiellement dominé par des protistes aussi bien autotrophe (Cryptophyte ou Chlorophyte) qu'hétérotrophes ou mixotrophes (ciliés ou flagellés). Ces derniers sont également une composante importante du microplancton qui comprend également de larges cellules phytoplanctoniques telles que les diatomées ou les dinoflagellés ainsi que les premiers stades de développement de métazoaires (nauplii de crustacés) mesurant ~90 µm de longueur pour les plus petites espèces (*Oithona* sp.) (Almeda et al., 2010). Le mésozooplancton est principalement dominé par des métazoaires crustacés filtreurs tels que les copépodes. Les copépodes marins représentent environ 2500 espèces (Razouls et al., 2005-2011) soit 60 % des métazoaires holoplanctoniques (Lenz, 2000) mais peuvent atteindre 99 % de l'abondance mésozooplanctonique (Razouls et al. 1997 ; Blain et al., 2001). Le mésozooplancton regroupe aussi des organismes « gélatineux » filtreurs de particules (salpes, dolioles et appendiculaires) et des prédateurs (hydroméduses, siphonophores, scyphozoaires et cténaires) dont certains sont en fait des composants du macrozooplancton et du mégazooplancton. Ainsi le zooplancton marin regroupe une grande diversité de phylum d'organismes unicellulaire (Protozoa, Actinopoda, Retaria, Cercozoa et Ciliophora) et pluricellulaire (Cnidaria, Ctenophora, Rotifera, Platyhelminthes, Nemertea, Annelida, Mollusca, Arthropoda, Chaetognatha et Chordata). Cette diversité de tailles et d'espèces occupant toutes les niches écologiques explique en partie la diversité fonctionnelle que l'on retrouve au sein du zooplancton.

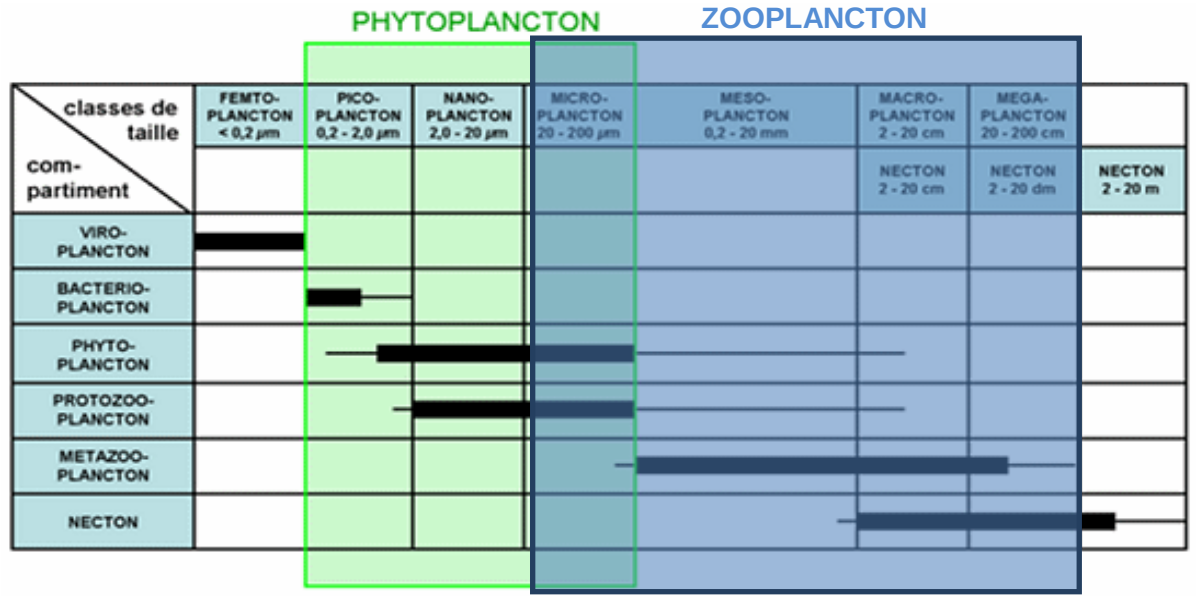

Figure 1-1. Distribution des différents groupes planctoniques en fonction de leur taille (d'après Sieburth et al., 1978).

1.1.2 Rôle du zooplancton dans le réseau trophique

Le mésozooplancton représente un vecteur important dans les transferts de matière et d'énergie dans l'écosystème pélagique marin, notamment par sa position intermédiaire entre les bas niveaux trophiques (organismes unicellulaires) et les niveaux trophiques supérieurs (Banse, 1995). La longueur du réseau trophique pélagique des producteurs primaires jusqu'aux poissons planctonophages peut être courte (3 niveaux : phytoplancton, crustacés zooplanctoniques et poissons) ou plus complexe (6 niveaux : phytoplancton, nanoflagellés hétérotrophes (HNF), ciliés, crustacés zooplanctoniques, zooplancton carnivore et poissons). Au sein du réseau trophique pélagique, le mésozooplancton exerce une pression trophique sur les producteurs primaires tels que les diatomées et les dinoflagellés (Vehmaa et al., 2011) mais aussi sur le protozooplancton hétérotrophe tels que les ciliés et les flagellés hétérotrophes (Calbet & Saiz, 2005) et même sur les petits métazoaires, dont, parfois, leur propre progéniture (Basedow & Tande, 2006; Galluci & Ólaffson, 2007). La production du zooplancton est fonction de la concentration en nourriture, ce qui implique un contrôle exercé par les bas niveaux trophiques vers les échelons supérieurs (control « bottom up ») (Fig. 1-2). De plus, la taille et le type de cellule dominant les producteurs primaires exercent un contrôle sur la diversité de la communauté mésozooplanctonique de part la sélectivité des tailles de proies (Sommer & Stibor, 2002) (Fig. 1-3).

L'écosystème pélagique est également contrôlé par les échelons trophiques supérieurs tels que les grands prédateurs de poissons planctonophages, réduisant ainsi la pression trophique sur le zooplancton par diminution du nombre de prédateurs. Ainsi, le développement de la communauté zooplanctonique ne dépend pas uniquement de la concentration en nourriture disponible mais aussi de la pression trophique qu'elle subit par les organismes zooplanctonophages (contrôle « top down »). Enfin, dans certains cas de perturbation de l'écosystème pélagique marin, le zooplancton gélatineux domine l'écosystème planctonique et exerce une pression trophique à la fois sur le même échelon trophique (copépodes) et sur l'échelon supérieur (larves et juvéniles de poissons planctonophages) (Richardson et al., 2009).

Le réseau trophique pélagique est particulièrement complexe (Reynolds, 2008) de par la diversité fonctionnelle de chaque échelon trophique. Par exemple, dans les eaux oligotrophes des océans, le transfert de matière par le métazooplancton vers les niveaux supérieurs ne passe pas uniquement par les producteurs primaires mais fait également intervenir les microorganismes de la boucle microbienne (Azam et al., 1983).

Au sein même du métazooplancton, la diversité fonctionnelle influe sur la sélection du type de proie. Par exemple, chez les copépodes, la sélectivité vis-à-vis de la taille des proies est essentiellement liée à la taille et à la structure des appendices qui servent à la capture ou à la filtration des proies (Karlson & Bamstedt, 1994). Certains organismes gélatineux (appendiculaires, salpes et dolioles) se nourrissent par filtration d'organismes bien inférieurs à leur taille (pico- et nano-plancton) (Wiebe et al., 1979; Gorsky et al., 1999) et même potentiellement sur du femtoplancton (0,02-0,2µm) (Sutherland et al., 2010) « court-circuitant » ainsi un (des) échelon(s)/maillon(s) du réseau trophique classique. Ces organismes diminuent parallèlement l'apport énergétique vers les poissons planctonophage du fait de leur faible valeur nutritive par rapport aux crustacés. D'autres organismes gélatineux comme les siphonophores et les cténaires sont eux des prédateurs du mésozooplancton et certains peuvent même capturer de plus grands organismes tels que les petits poissons pélagiques. Ainsi les déviations des flux énergétiques le long du réseau trophique et la longueur du réseau trophique ont un impact important sur le ratio poisson planctonophage – phytoplancton (Sommer et al., 2002).

1.1.3 Rôle du zooplancton dans les flux biogéochimiques marins

Le zooplancton joue un rôle essentiel dans la pompe biologique du carbone par l'intermédiaire des flux verticaux de particules biogènes (Sundquist, 1993) (Fig. 1-4). L'exportation de la matière depuis la couche euphotique vers les couches méso- et bathy-pélagiques est effectuée à la fois par transport passif (Agassiz, 1888) réalisé par simple sédimentation des pelotes fécales (Turner, 2002; Robinson et al., 2010) et des produits de dégradation et à la fois par transport actif (Vinogradov, 1962) via les migrations verticales nycthémérales (Zhang & Dam, 1997) ou ontogéniques (Kobari et al., 2008) effectuées par le zooplancton. Les flux de carbone liés à la migration verticale représentent environ 20 à 30 % des flux de carbone lié au mésozooplancton (Zhang & Dam, 1997).

Les particules mucilagineuses telles que les logettes d'appendiculaires ou du mucus (Gorsky et al., 1984; Davoll & Youngbluth, 1990) ayant la particularité de s'agréger avec d'autres particules augmentent ainsi l'exportation de matière vers le fond. Ces particules formant la neige marine (Alldredge et al., 1998) sont dégradées et reminéralisées par les bactéries hétérotrophes et les organismes de la boucle microbienne mais peuvent être également ingérées par des organismes omnivores et détritivores du plancton et du necton (Yam & Tang, 2006; Koski et al., 2007). Cette biodégradation est bien plus rapide lorsqu'elle est effectuée par le zooplancton et le necton que par les bactéries et les protistes. Par exemple, le taux de dégradation de ces particules par ces derniers est en effet assez long, de l'ordre de < 3 jours pour les œufs non fécondés, < 8 jours pour les mues, de 3 à 11 jours pour les carcasses et de 3 à 50 jours pour les pelotes fécales (revu par Frangoulis et al., 2005).

Le zooplancton intervient également dans le recyclage des éléments nutritifs servant de moteur à la production dite « régénérée » (Conway & Whitledge, 1979). Les déchets métaboliques issus de l'assimilation du zooplancton sont excrétés sous forme dissoute libérant ainsi du carbone, de l'azote et du phosphore minéral dissous (NH_4 et PO_4) et organique (urée, acides aminées) dans le milieu (revu par Le Borgne, 1996). L'excrétion et le « sloppy feeding » sont les principales sources de carbone et d'azote organique dissous et dans une moindre mesure, la lixiviation des pelotes fécales plus spécifique à l'azote (Saba et al., 2011). Ce carbone organique dissous est un substrat très rapidement assimilé par les bactéries hétérotrophes (Hygum, 1997).

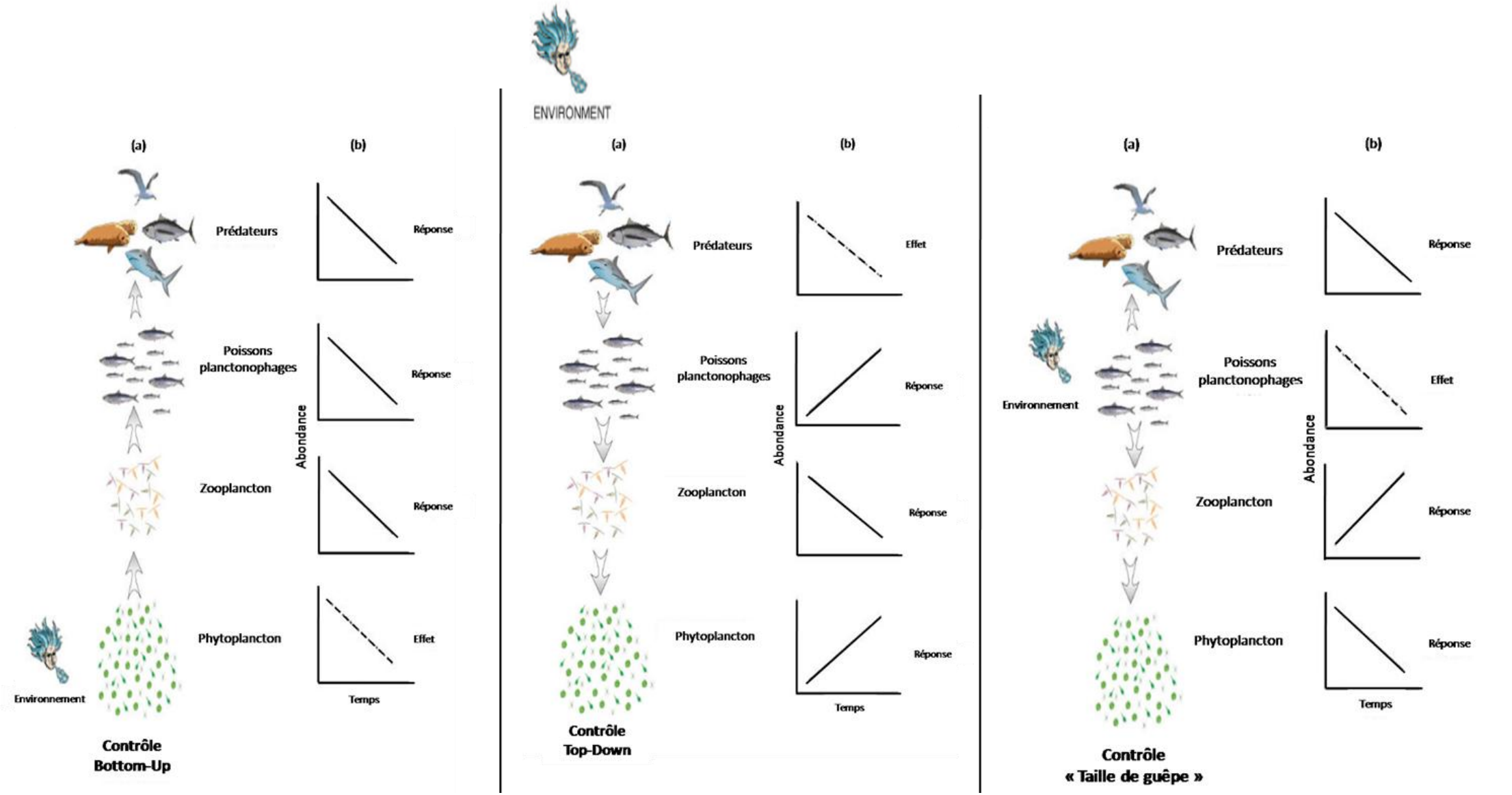

Figure 1-2. (a) Différents types de contrôles de l'écosystème pélagique marin simplifié par quatre échelons trophiques. (b) Contrôle et réponse des différents échelons trophiques en terme d'abondance en fonction du temps, (issue de Cury et al., 2001).

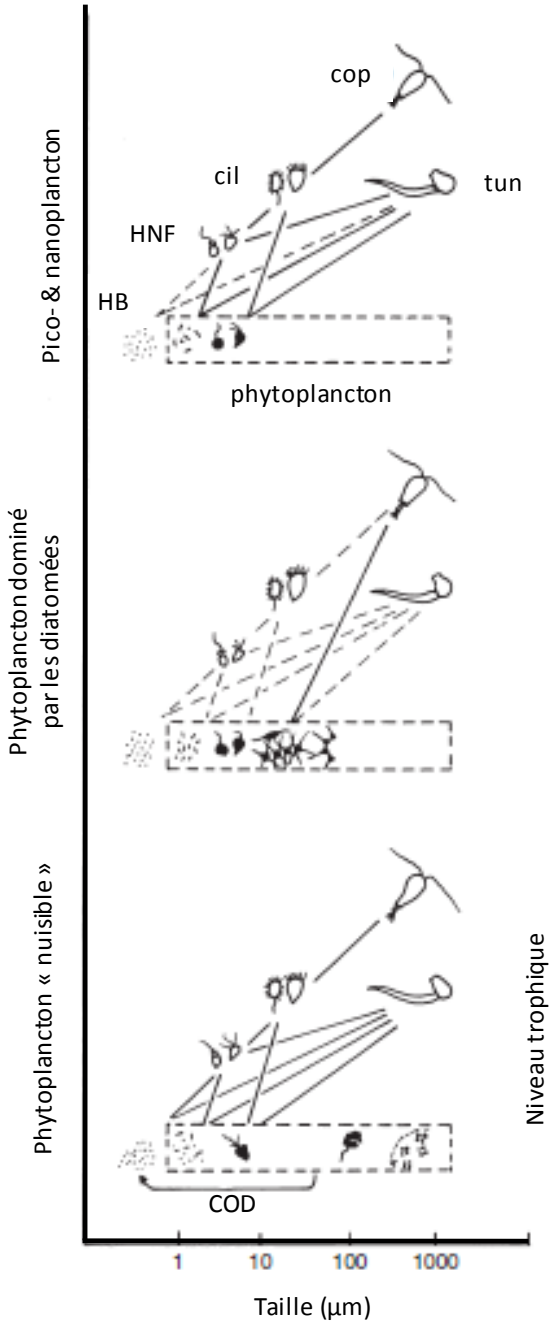

Figure 1-3. Représentation schématique du contrôle bottom up par la sélectivité des tailles de proies dans le milieu pélagique marin. Trait plein : prédation principale, tirets : prédation secondaire. HB : bactéries hétérotrophes, HNF : nanoflagellés hétérotrophes, cil : ciliés, cop, copépodes, tun : tuniciers, COD : carbone organique dissous (issue de Sommer & Stibor, 2002).

Les formes minérales sont rapidement utilisées par les producteurs primaires (bactéries et phytoplancton) notamment l'ammonium qui est la forme préférentiellement assimilable de l'azote, possédant ainsi un turn-over très rapide dans l'écosystème pélagique marin (Harrison et al., 1996; Conway, 1997). La contribution de l'excrétion du métazooplancton aux besoins

en sels nutritifs de la production primaire journalière est estimée entre 2 et 300 % pour l'azote et entre 17 et 200 % pour le phosphore (voir Frangoulis et al., 2005). Ceci indique que le métazooplancton peut, à lui seul, fournir la totalité des besoins en sels nutritifs des producteurs primaires notamment dans les zones peu productives où le rapport entre la biomasse de zooplancton et celle du phytoplancton est élevé (Alcaraz, 1988).

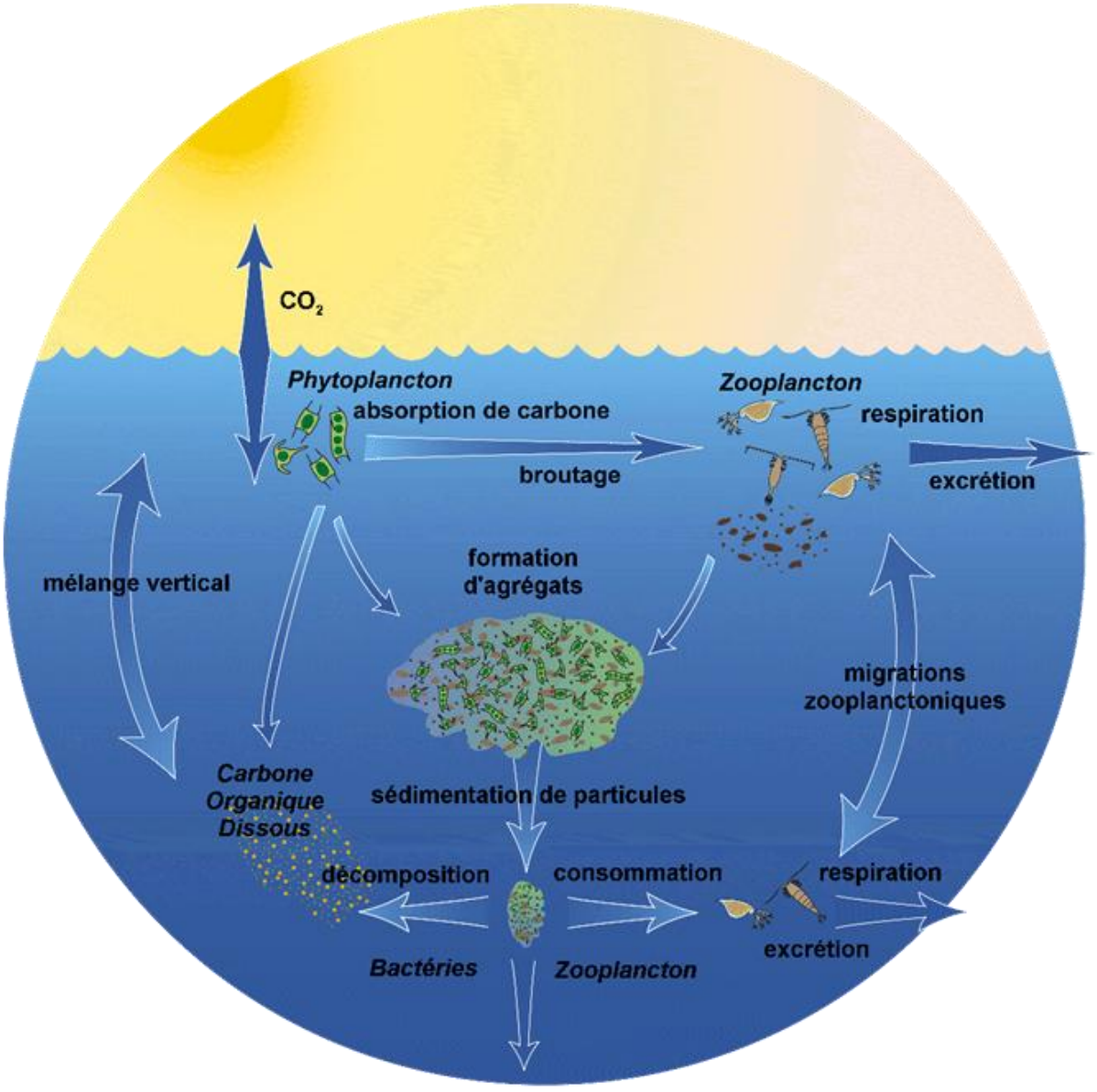

Figure 1-4. Représentation des flux de matière au sein de l'écosystème planctonique marin (issue de U.S. JGOFS).

Le zooplancton intervient également dans le cycle du carbone par l'intermédiaire de sa respiration qui restitue du carbone inorganique dissous (CO_2) dans le milieu. La contribution de la respiration du zooplancton est, par exemple, estimée entre 20 et 63 % des besoin en carbone de la production primaire en mer Catalane (Alcaraz et al., 2007).

Le transport actif de carbone, d'azote et de phosphore par la migration verticale nycthémérale du mésozooplancton est considéré comme un transfert significatif de la couche de surface vers la couche mésopélagique (Longhurst et al., 1990; Yebra et al., 2005). Cependant, en période de post floraison phytoplanctonique, lorsque la communauté mésozooplanctonique est peu abondante, cette contribution semble faible (< 5 % en termes de carbone) (Putzeys et al., 2011).

1.2 Description des écosystèmes étudiés

1.2.1 Bathymétrie et courantologie

1.2.1.1 Le plateau des Kerguelen

L'océan Austral a la particularité d'entourer entièrement le continent antarctique. Il est caractérisé par de forts courants cycloniques, formant des zones frontales, circulant dans le sens horaire dont les limites latitudinales varient en fonction des saisons (Fig. 1-5). Le Courant Circumpolaire Antarctique (ACC) forme la limite de l'océan Austral. Le plateau des Kerguelen est situé dans l'océan Austral du secteur indien entre 46°S et 64°S soit l'équivalent d'une distance maximale de 2 200 km. Il est entouré par le bassin d'Enderby à l'ouest et par le bassin Australo-Antarctique à l'est. Il résulte d'anciennes activités volcaniques datant d'environ 110 millions d'années. Une partie du plateau se situe au-dessus du niveau de la mer constituant les îles Kerguelen au nord et les îles Heard et MacDonald plus au sud. Il constitue une barrière importante de l'ACC circulant d'ouest en est. La majeure partie de ces masses d'eau (~100 Sv) est déviée au nord des îles Kerguelen (Fig. 1-6). Le plateau est séparé par le courant Fawn Trough dont le seuil atteint une profondeur de 2600 m permettant le passage d'une partie moins importante mais non négligeable (30-40 Sv) de l'ACC entre ces îles et le continent antarctique (Park et al., 1991; Park et al., 2008a,b; Rocquet et al., 2009).

La zone d'étude du projet KEOPS se situe sur la partie nord du plateau délimitée par le Front Polaire (PF) au nord et le Courant Fawn Trough (FTC) au sud. Le PF est actuellement défini comme la limite nord où les eaux de sub-surface ne dépassent pas l'isotherme 2°C, généralement localisé à ~ 100-300 m de profondeur (Park & Gambéroni, 1997). La complexité de la bathymétrie avec la présence de hauts fonds, de failles et de vallées permet d'expliquer en partie la courantologie locale (Park et al., 2008a).

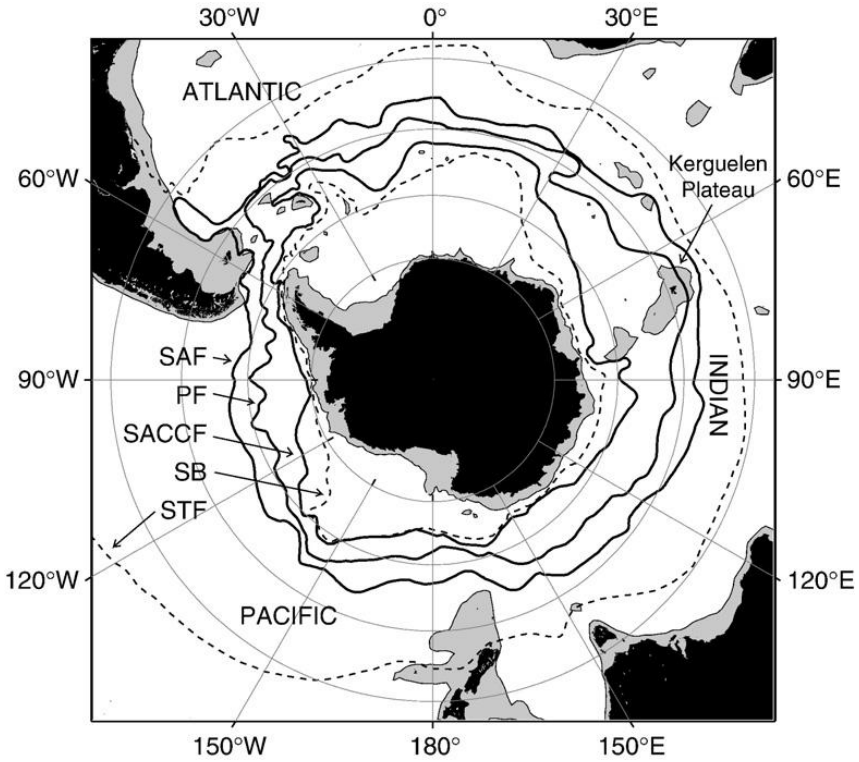

Figure 1-5. Distribution circumpolaire du front subtropical (STF), du front subantarctique (SAF), du front polaire (PF), du front sud ACC (SACCF), et de la limite sud du ACC (SB) (adapté de Orsi et al., 1995, repris de Rocquet et al., 2009).

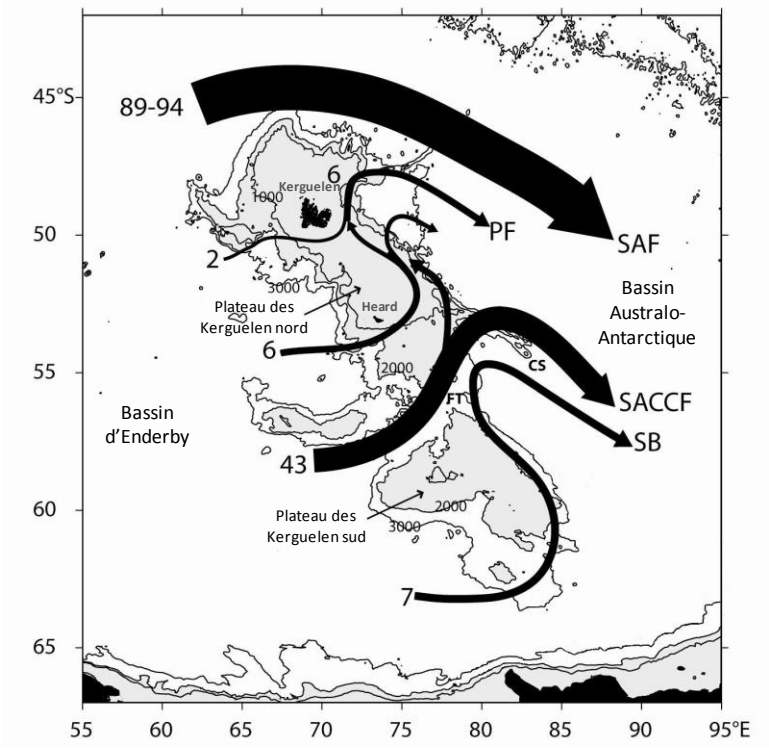

Figure 1-6. Circulation des branches principales du courant Circumpolaire antarctique (d'après Park et al., 2001 ; modifié) et bathymétrie de la région du plateau des Kerguelen. Sub-Antarctique Front (SAF), Front polaire (PF), Front du courant Circumpolaire Antarctique sud (SACCF), limite du courant Circumpolaire Antarctique sud (SB). Les chiffres précédents les courants indiquent leur débit en Sverdrup.

1.2.1.2 *La mer Méditerranée*

La Méditerranée est une mer intercontinentale, quasi fermée, possédant pour seule ouverture naturelle sur l'océan Atlantique, le détroit de Gibraltar, d'une largeur minimale de 14,4 km. Le canal de Suez se situe dans la partie est permettant une connexion artificielle avec la mer Rouge. Elle est subdivisée en deux bassins principaux : le bassin Ouest ou occidental et le bassin Est ou oriental tous deux séparés par le seuil de Sicile. Bien qu'elle ne constitue à elle seule que 0,82 % en surface et 0,32 % en volume de la totalité des océans mondiaux, elle est la mer quasi fermée la plus grande avec une surface équivalente au Golfe du Mexique soit 2 510 000 km² (Defant, 1961). Chaque bassin est lui-même divisé en sous bassins parfois eux même subdivisés en différentes zones géographiques de tailles inférieures portant le nom de mers, golfes ou baies (Fig. 1-7).

Figure 1-7 Localisation et topographie des principales sous régions de la mer Méditerranée.

La Méditerranée peut être considérée comme un océan en miniature avec des créations d'eau de fond, la présence de plusieurs bassins, de fosses océaniques, de seuils et de plateaux continentaux. La circulation générale des masses d'eau de surface est fortement influencée par les entrées d'eau Atlantique i.e. circulation thermohaline dans le sens ouest-est, le long des côtes nord-africaine jusqu'à la Sicile.

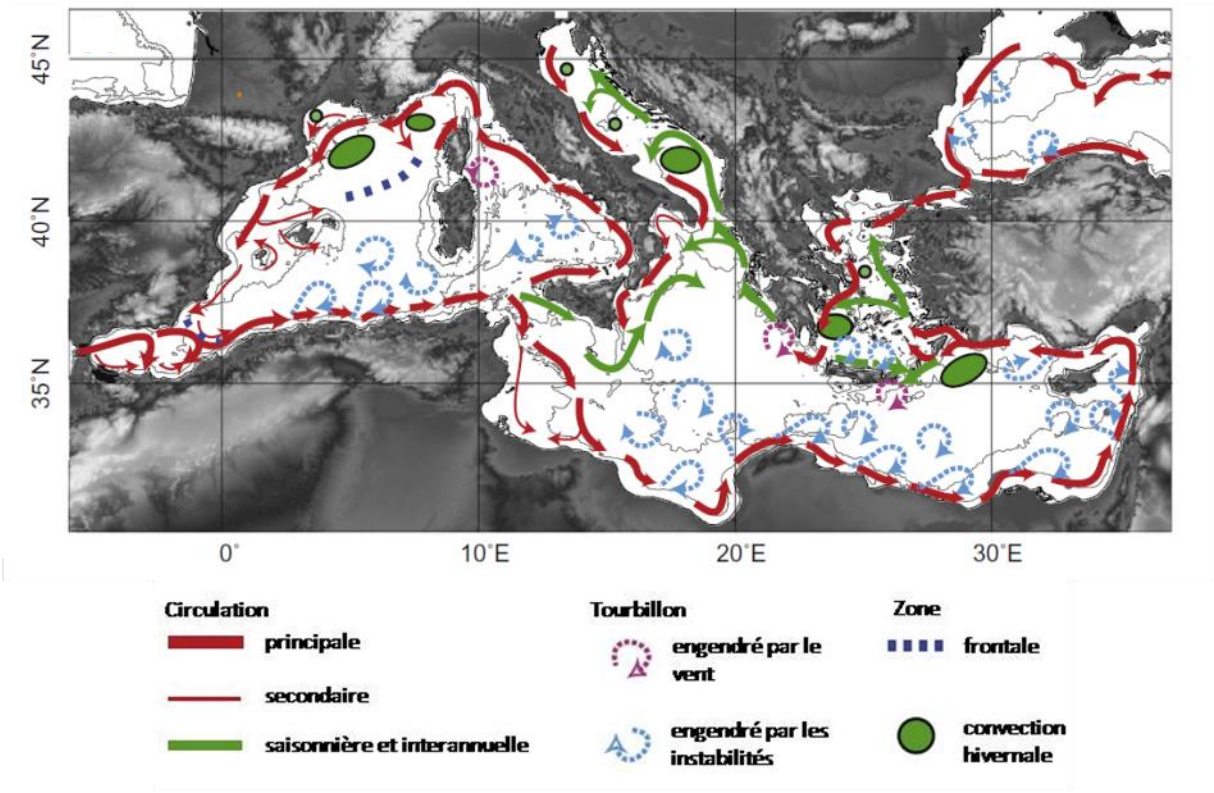

Figure 1-8. Circulation des masses d'eau de surface de la mer Méditerranée et de la mer Noire (issue de Durrieu de Madron et al., 2011, modifié de Millot & Taupier-Letage, 2005).

Ces masses d'eaux se subdivisent ensuite en deux, une partie s'orientant vers le nord le long des côtes italiennes formant par la suite le courant Nord (Millot, 1999), l'autre traversant le seuil de Sicile vers l'extrémité est du bassin Levantin (Fig. 1-8). Les masses d'eau de surface se densifient tout en se déplaçant vers l'est, on parle alors d'eau Atlantique modifiée (MAW : Middle Atlantic Water). Un approfondissement de la MAW est enfin observé à l'extrémité est du bassin Levantin créant les eaux Levantines Intermédiaires (LIW : Levantine Intermediate Water) reprenant alors une circulation vers l'ouest sous la couche euphotique.

Les eaux profondes sont créées au niveau de la marge continentale du Golfe du Lion dans le bassin Ouest (WMDW: West Mediterranean Deep Water) et en mer Adriatique dans le bassin Est (EMDW: Eastern Mediterranean Deep Water). Il existe en mer Egée, une autre zone de formation d'eaux profondes considérée pendant longtemps comme négligeable ; toutefois, selon des observations réalisées depuis 1946, cette zone semble devenir la seconde source d'eaux profondes du bassin Est allant jusqu'à des quantités trois fois supérieures à celles des eaux profondes créées en mer Adriatique (Robinson et al., 2001). La présence de seuils peu

profonds au niveau des connexions entre bassins (Gibraltar, Dardanelles et Sicile) empêche l'échange et la circulation d'eaux profondes avec l'océan Atlantique, la mer Noire et entre les deux principaux bassins méditerranéens. Ainsi les échanges d'eaux entre les bassins Est et Ouest se font à travers les eaux Levantines intermédiaires (Fig 1-9).

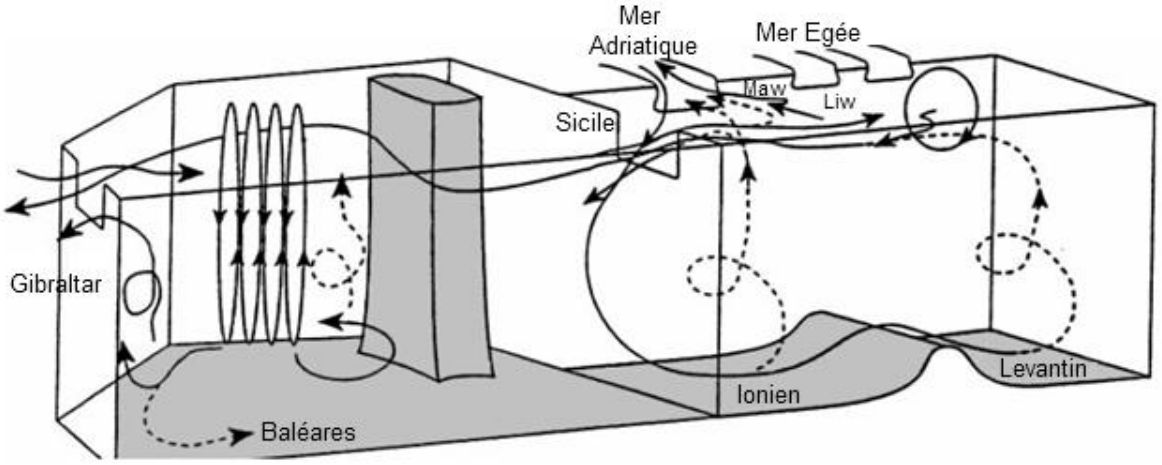

Figure 1-9. Représentation schématique des cellules thermohalines et de la circulation de l'Eau Levantine Intermédiaire (LIW) dans la mer Méditerranée (issue de Robinson et al., 2001).

1.2.2 Description des communautés zooplanctoniques des zones d'études

1.2.2.1 Communautés zooplanctoniques de l'océan Austral

Le mésozooplancton de l'océan Austral est principalement composé de copépodes dont l'abondance peut atteindre 99 % dans les 200 premiers mètres (Razouls et al., 1997; Blain et al., 2001). Les petits copépodes (<1,5 mm) dominent principalement en termes d'abondance (Atkinson & Sinclair, 2000) mais représentent en général moins de 5 % de la biomasse mésozooplanctonique totale. Au contraire, le grand zooplancton (>1,5mm) peut représenter jusqu'à 80 % de la biomasse totale (Ashjian et al., 2004). Cependant, ces proportions en termes d'abondance et de biomasse fluctuent à l'échelle de la saison.

La communauté des petits copépodes est dominée par les Oithonidae et les jeunes stades copépodites de nombreuses familles de copépodes. Le grand zooplancton est composé de copépodes dont certains adultes peuvent mesurer jusqu'à 10 mm (i.e. *Rhincalanus gigas*). Les euphausiacés représentent aussi un composant important du zooplancton Austral à l'interface

entre le mésozooplancton (larve) et le micronecton (adulte) (Nicol, 2003). Certaines espèces, dont *Euphausia superba* peuvent former des essaims importants représentant 2 10^6 tonnes de masse humide qui s'étend sur une surface de 100 km^{-2} et dans certains cas pouvant atteindre une densité de 480 000 ind m^{-3}, notamment le long de la péninsule antarctique (Hamner & Hamner, 2000; Atkinson et al., 2004; Nowacek et al., 2011). Ces euphausiacés ont un rôle clef dans l'écosystème antarctique puisqu'elles sont des proies pour les grands prédateurs tels que les baleines, les phoques, les pingouins, les oiseaux et les poissons (Costa & Crocker, 1996; Fraser & Trivelpice, 1996). Ils influent également sur la répartition verticale du zooplancton. Par exemple, le maximum d'abondance des copépodes se situe au-dessous de l'essaim d'euphausiacés afin d'échapper à leur prédation mais reste de ce fait sous le maximum de chlorophylle (Zhou et al, 2004; Ashjian et al., 2008).

Les copépodes de l'océan Austral possèdent des stratégies de cycles de vie différents selon les espèces (Atkinson, 1998). Certains grands copépodes comme *Calanoides acutus, Calanus propinquus* et *Rhincalanus gigas* possèdent un cycle de vie de 1 ou 2 ans et suivent des migrations verticales ontogéniques (Atkinson et al., 1997; Spiridonov & Kosobokova, 1997) (Fig. 1-10). Ces copépodes migrent dans la couche mésopélagique, vers 1000 m de profondeur et se mettent en état de vie ralentie (Hopkins et al., 1993 ; Atkinson, 1998 ; Pasternak et Schnack-Schiel, 2001) correspondant à la réduction du broutage et de l'activité métabolique principalement du début d'automne jusqu'au printemps (Schnack-Schiel et al., 1991). Pendant la période de floraison, le broutage et la croissance sont maximales afin de métaboliser et stocker les lipides sous forme de réserves qui seront ensuite utilisés pendant la période hivernale (Kattner et al., 1994 ; Kattner et Hagen, 1995 ; Mayzaud et al., 2011). Les espèces non migrantes comme les copépodes *Oithona similis*, *Microcalanus pigmaeus* et *Metridia* spp. ont généralement un régime alimentaire omnivore/détritivore, ce qui leur permet de ne pas être limités à la saison non productive pour se nourrir (Pasternak & Schnack-Schiel, 2001). Leurs périodes de nutrition et de croissance étant accrues, ces espèces se reproduisent tout au long de l'année et persistent ainsi dans la couche épipélagique (Fransz & Gonzales, 1995; Metz, 1996; Atkinson, 1998).

Pendant la période de pré- et post-floraison phytoplanctonique, les grands copépodes présentent une alimentation basée sur la carnivorie et les détritus, avec une sélectivité basée sur la taille des proies (Atkinson, 1994) ce qui leur permet de subvenir à leurs besoins lorsque la quantité en phytoplancton est insuffisante (Metz & Schnack-Schiel, 1995). Au contraire,

pendant la période où la concentration en phytoplancton est optimale, Huntley (1981) suggère qu'il n'y a pas de sélectivité des proies.

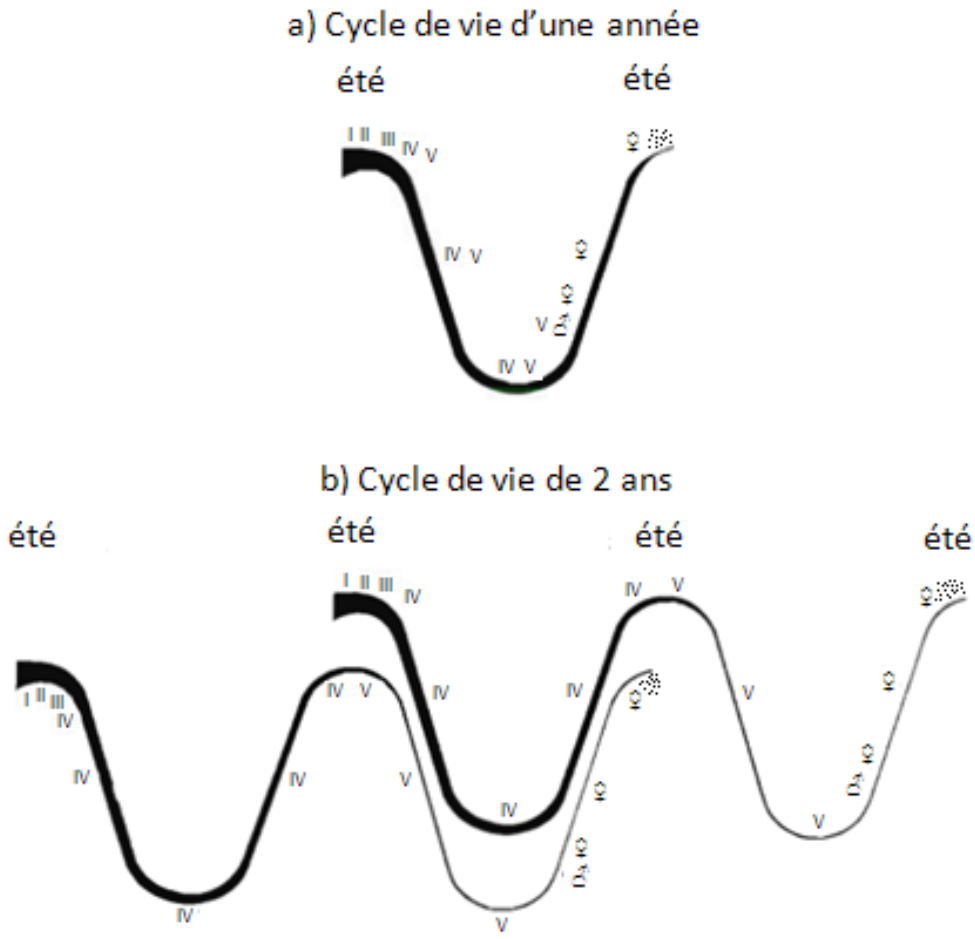

Figure 1-10. Représentation schématique des cycles de vie alternatifs de *Calanoides acutus*. Le cycle de 2 ans est représenté avec deux générations successives. Les chiffres correspondent aux stades copépodites. Les nuages de points symbolisent la période de ponte. L'amincissement des traits symbolise la mortalité. (issue de Atkinson et al., 1997).

Dans l'océan Austral, plusieurs espèces du mésozooplancton ont une distribution latitudinale claire. En effet, Deacon (1982) décrit le front polaire comme une barrière biogéographique du fait notamment de la différence en température de quelques degrés entre celui-ci et les zones adjacentes. Cependant pour le mésozooplancton, il ne semble pas que le front polaire agisse comme une barrière franche. Selon Atkinson & Sinclair (2000), l'abondance des espèces indique plutôt une distribution en fonction de zones géographiques de prédilection. Ces auteurs se sont basés sur un rapport d'abondance par zones géographiques afin de déterminer un indice différenciant les espèces « antarctiques » et « subantarctiques ». Les espèces endémiques de l'océan Austral représentent ~16.5 % de la communauté des copépodes et

sont essentiellement localisées dans les zones néritiques ou sous influence des glaces comme par exemple *Drepanopus pectinatus* qui ne se retrouve que sur le plateau continental du secteur indien (Crozet, Kerguelen et Heard) (Razouls et al., 2000). Dans ce secteur, le zooplancton se répartit selon un gradient nord-sud avec une diminution de la richesse spécifique des copépodes du nord vers le sud (Errhif et al., 1997) et des distributions spatiales différentes selon les espèces. Généralement, les petits copépodes comme *Oithona similis*, *O. frigida* et *Ctenocalanus citer* dominent la population aussi bien dans la zone antarctique que sub-antarctique. Pour les grands copépodes, *Pleuromamma borealis* semble plus présent dans la zone sub-tropicale, *Calanus simillimus* dans la zone délimitée par la convergence et la divergence antarctique et *Calanus propinquus* dans la zone antarctique

Ces distributions ont été étudiées à l'ouest du plateau des Kerguelen lors de plusieurs campagnes ANTARES à différentes périodes de l'année (Labat et al., 2002; Mayzaud et al., 2002a,b). Le schéma général montre que la biomasse est plus importante dans la zone du front polaire et du POOZ (Permanently Open Ocean Zone) en été et au printemps avec des valeurs comprises entre ~ 2 et 16 g PS m^{-2} dans les 200 premiers mètres. L'abondance des gros copépodes comme *Calanus simillimus*, *Calanoides acutus*, *Rhincalanus gigas* et *Metridia lucens* ainsi que celles des larves d'euphausiacés suivent ce même gradient nord-sud. Ces espèces qui dominent la biomasse se retrouvent également en forte densité sur le plateau des Kerguelen (Razouls et al., 1998). En été les salpes (*Salpa thomsoni*) et les ptéropodes (*Limacina* spp.) sont également présents mais seulement aux mêmes latitudes que le plateau. Leur impact sur la production primaire est non négligeable puisqu'ils en consomment environ 50 % et 3 % respectivement (Mayzaud et al., 2002b). Les amphipodes, les euphausiacés et certains copépodes sont les proies des poissons planctonophages mais également de juvéniles de grands poissons comme la légine (*Dissostichus eleginoides*) (Collins et al., 2007). Ce poisson est une espèce commerciale très exploitée sur le plateau des Kerguelen (Duhamel & Hautecoeur, 2009; Palomares & Pauly., 2011) et notamment au niveau de la marge océanique (Park et al., 2008b).

1.2.2.2 Communautés zooplanctoniques de Méditerranée

Comme dans la plupart des océans, les zones les plus productives en Méditerranée sont principalement localisées dans les zones côtières ou néritiques et notamment dans le Golfe du Lion, zone sous influence des apports fluviaux du Rhône. En effet, ces apports chargés en

sels nutritifs d'origine terrigène favorisent une forte production primaire correspondant en moyenne à 400 mg C m^{-2} j^{-1} au printemps et par conséquent permettent le développement du mésozooplancton dont la biomasse peut atteindre jusqu'à 28 mg PS m^{-3} pour une abondance de 8 000 ind m^{-3} dans les 200 premiers mètres (Gaudy et al., 2003 ; Youssara, 2003). Des biomasses élevées sont également observées dans le Golfe de Trieste en mer Adriatique, zone sous influence du Pô, avec 14 mg PS m^{-3} (Fonda Umani, 1996), ou également aux Baléares où la biomasse du mésozooplancton atteint 16 mg PS m^{-3} en janvier et en début d'été (Fernandez de Puelles et al, 2003 ; 2004) due aux conditions hydrologiques particulières comme des apports ponctuels d'eaux d'origine Atlantique plus riches.

Globalement les distributions spatiales de l'abondance et de la biomasse présentent une diminution de la côte vers le large qui s'accompagne d'une différentiation dans la composition des communautés (Champalbert, 1996 ; Gaudy et al., 2003 ; Siokou-Frangou et al., 2010). Les taxa les plus abondants en mer Méditerranée sont les copépodes qui représentent ~50 à 99 % de l'abondance du mésozooplancton ainsi que les appendiculaires (~1 à 22 %) et les cladocères (~1 à 11 %) aussi bien au niveau des zones néritiques (Solić et al., 1997 ; Calbet et al., 2001 ; Fernández de Puelles, 2003 ; Riandey, 2005 ; Ramfos et al., 2006) que dans les eaux du large (Saiz et al., 1999; Alcaraz, 2003; Mazzochi et al., 2003; Siokou-Frangou et al., 2009). Une différentiation côte-large de la composition spécifique de la communauté existe entre les zones côtières de Méditerranée (Est et Ouest), avec par exemple les copépodes calanoides tels que *Paracalanus parvus, Acartia clausi*, *Temora stylifera* et *Centropages typicus* plus abondant à la cote qu'au large (Mazzochi & Ribera d'Alcalà, 1995 ; Christou, 1998 ; Saiz et al., 1999 ; Calbet et al., 2001).

En zone hauturière, il existe cependant localement des régions productives, comme par exemple au niveau de structures hydrodynamiques à mésoéchelle, où les abondances et les biomasses zooplanctoniques atteignent parfois les valeurs observées en zones plus côtières. Par exemple, les zones frontales localisées en mer Catalane et en mer des Baléares (Alcaraz et al., 1994 ; 2007), en mer Ligure (Licandro & Icardi, 2009) en mer d'Alboran (Thibault et al., 1994 ; Youssara & Gaudy, 2001) et en mer Egée (Siokou-Frangou et al., 2009) ainsi que les tourbillons cycloniques comme au large de l'Algérie (Riandey, 2005 ; Riandey et al., 2005) qui possèdent une turbulence accrue permettant les remontées d'eau de fond plus riche en sels nutritifs de façon récurrente au cours du cycle annuel.

Ainsi la distribution globale de l'abondance du mésozooplancton en Méditerranée révèle de fortes valeurs locales aussi bien en zone côtière qu'en zone hauturière mais avec une plus forte variabilité spatiale dans le bassin Ouest et en mer Egée (Siokou-Frangou et al., 2010). Peu d'informations précises sur la distribution de la communauté zooplanctonique à l'échelle de la Méditerranée sont actuellement disponibles. Il existe cependant dans le bassin Est et au niveau du seuil de Sicile, une série de données sur la distribution spatiale et verticale du mésozooplancton (Mazzocchi et al., 1997 ; Siokou-Frangou et al., 1997, Fragopoulu et al., 2001). Il ressort de ces études que les abondances sont extrêmement faibles avec des valeurs comprises entre 200 ind m^{-3} au niveau du seuil de Sicile et ~50 ind m^{-3} dans la zone hauturière des bassins Ionien et Levantin. Aucune variabilité spatiale dans la composition de la communauté n'a été mise en évidence entre les différentes zone d'études du bassin Est. Dans le bassin Est et Ouest, deux études très succinctes sur l'abondance du zooplancton ont été réalisées entre Gibraltar et le bassin Ionien/Levantin (Dolan et al. 2002 ; Minutoli & Guglielmo 2009). Bien que les mailles utilisées dans ces études soient différentes (200 et 335 µm, respectivement) les valeurs présentent les maxima de densité localisés au même niveau, correspondant à des structures hydrodynamiques particulières (en mer Ligure et en mer d'Algérie) mais avec des valeurs ~3 fois supérieures obtenues avec le filet de 200 µm (600 ind m^{-3}). En revanche en zone hauturière non soumises à ces structures à mésoéchelle, les valeurs moyennes sont d'~200 ind m^{-3} (200 µm) et comparables à celles observées au seuil de Sicile mais environ 3 fois supérieures à celles du bassin Est pour la même période (automne) (Mazzocchi et al., 1997 ; Dolan et al. 2002). Enfin, une dernière étude très succincte (seulement 9 stations échantillonnées) sur le stock de mésozooplancton a été réalisée en juin 1999 dans les deux principaux bassins méditerranéens (Siokou-Frangou, 2004) et révèle la possibilité d'un gradient est-ouest de l'abondance du mésozooplancton, de 100 à 900 ind m^{-3}. Ainsi, il apparait en filigrane de toutes ces études une différence dans les stocks entre les deux principaux bassins avec des valeurs plus faibles dans le bassin Est (pouvant représenter moins de 50 ind m^{-3} pour une biomasse < 1 mg PS m^{-3} ; Mazzochi et al., 1997 ; Siokou-Frangou et al., 2004).

Concernant le cycle saisonnier, le mésozooplancton présente généralement deux pics d'abondance, à la fin du printemps et en automne. Ceux-ci sont consécutifs, avec un décalage d'environ 3 semaines, aux efflorescences phytoplanctoniques liées le plus souvent à la stabilisation du milieu après le brassage de la colonne d'eau par de forts vents notamment le long des côtes (Gaudy, 1985; Stergiou et al., 1997 ; Zervoudaki et al., 2007). Certaines

espèces présentent une saisonnalité importante alors que d'autres sont présentes toute l'année ou présentent une variation interannuelle marquée (Fig. 1-10). A cela s'ajoute des variations d'amplitude dans les pics d'abondances liées à des variations inter-annuelles et géographiques (Fig. 1-11). Ainsi les communautés se caractérisent par une diversité spécifique élevée qui varie au cours du cycle annuel (Lakkis, 1990a; Siokou-Frangou et al., 2009). Par exemple, dans une étude comparative pluriannuelle du cycle de *C. typicus* à différents sites côtiers de la Méditerranée, Mazzocchi et al. (2007) ont mis en évidence une certaine constante saisonnière dans la période des pics d'abondance (avril-juin) quelle que soit la zone d'étude considérée mais avec des variations importantes inter-sites. Certains facteurs influencent localement cette distribution comme en période d'anomalie positive de la NAO (North Atlantic Oscillation) où la distribution annuelle est bimodale en Méditerranée nord-ouest. L'influence de la NAO sur la production secondaire zooplanctonique en Méditerranée a d'ailleurs été mise en évidence dans plusieurs études (Fernández de Puelles et al., 2007; Molinero et al., 2005, 2008b; Garcia-Comas et al., 2011). Enfin d'autres facteurs peuvent expliquer les différences d'abondance à l'échelle de la Méditerranée comme la température ou la quantité en ressource nutritive (Di Capua & Mazzocchi, 2004; Molinero et al., 2009).

La mer Méditerranée possèdent une amplitude saisonnière de température importante généralement comprise entre 13°C en hiver jusqu'à plus de 27°C pour les eaux situées au-dessus de la thermocline. Or, la température du milieu marin est considérée comme un des facteurs majeurs gouvernant l'activité métabolique des organismes poïkilothermes du mésozooplancton (Ikeda, 1985). Cette gamme de température des eaux impose aux organismes planctoniques de la Méditerranée de posséder une certaine eurythermie avec une activité métabolique élevée notamment pendant la période estivale (Christou & Moraitou-Apostolopoulou, 1995). De ce fait la plupart des organismes présentent des taux de croissance relativement élevés et des temps de développement très courts (~ 2 à 3 semaines entre l'œuf et le stade adulte pour les copépodes) (Klein Breteler et al., 1994). Cette rapidité de croissance permet le développement de plusieurs générations au cours d'une année. Par exemple, pour *Centropages typicus*, on observe entre 5 à 7 générations au cours d'un cycle annuel (Mazzocchi et al., 2007).

Le second facteur majeur influençant le métabolisme est la taille des organismes (Peters, 1983). Le métazooplancton méditerranéen est dominé par des copépodes de petite taille,

essentiellement < 1 mm qui sont présents tout au long de l'année (Calbet et al., 2001). Dans les eaux du large du bassin Est méditerranéen, les petits copépodes (500-1000 µm) représentent entre 45 et 58 % de l'abondance de mésozooplancton (Koppelmann & Weikert, 2007), et peuvent représenter entre 69 et 77% de la biomasse et 45 et 50% de la production secondaire (Zervoudaki et al. 2006 ; 2007) dans une zone frontale en mer Egée. Ces études suggèrent un rôle éventuellement important de ces copépodes dans le contrôle « top down » des ciliés et des producteurs primaires notamment en période de forte production printanière.

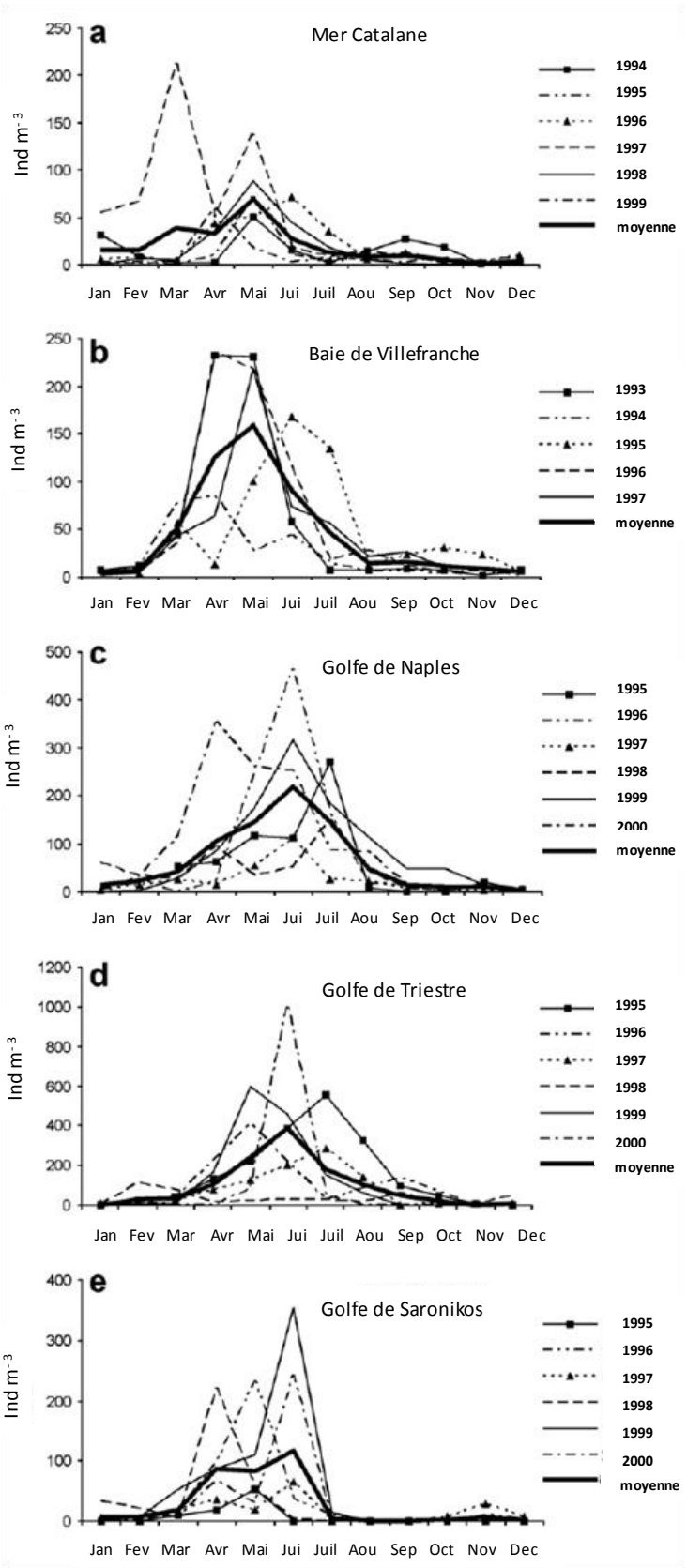

Figure 1-11. Cycles annuels de l'abondance de *Centropages typicus* situés à 5 stations côtières de Méditerranée de 1995 à 2000. Seuls les adultes sont représentés pour la mer Catalane (a) et la baie de Villefranche (b) ; adultes et copépodites pour les 3 autres sites (issue de Mazzocchi et al., 2007).

1.3 Objectifs de la thèse

1.3.1 Etat des connaissances

Le suivi à long terme développé sur de nombreux sites (i.e. station Papa, Aloha, Bats) où l'ensemble des compartiments biologiques pélagiques sont échantillonnés de façon récurrente a permis d'obtenir une idée relativement satisfaisante de la variabilité temporelle des communautés zooplanctoniques sous différentes latitudes. Par contre, les données disponibles ne permettent pas encore une étude approfondie de la variabilité spatiale à grande échelle, notamment en Méditerranée et dans la zone permanente de l'océan Austral (POOZ), zone non soumise au front polaire et à la formation de glace en hiver.

Selon la fréquence d'échantillonnage, les séries temporelles permettent de suivre la dynamique saisonnière ou annuelle mais également d'étudier les variations interannuelles. Ces données permettent également la paramétrisation et la validation de modèles de dynamique des populations qui permettent de mieux comprendre les mécanismes favorables ou non à la production de ces populations (Eisenhauer et al., 2009; Carlotti & Poggiale, 2010; Qiu et al., 2010).

En Méditerranée, le nombre de suivis à long terme reste très restreint et avec des périodes d'échantillonnage très variables. Il existe une hétérogénéité importante dans la représentation des deux principaux bassins avec de plus nombreux suivis temporels réalisés dans le bassin Ouest et en mer Adriatique (Fig. 1-12 et Tableau 1-1). La station la plus ancienne se situe dans la baie de Villefranche où les échantillonnages hebdomadaires ont débuté en 1966 et sont encore actuellement en cours.

En Méditerranée la plupart des suivis à long terme s'intéressent principalement à l'étude des communautés côtières, sauf pour les deux stations hauturières située au large de Naples, proche de l'île de Ponza, sur des fonds d'environ 3000 m qui a été étudiées seulement entre 1976 et 1979 et la station DYFAMED au centre de la mer Ligure (Buat-Ménard & Lambert, 1993) mais où le zooplancton n'y est étudié que de façon ponctuelle (Andersen et al., 2001a,b) ou très spécifique (Andersen et al., 1993; Berline et al., 2011).

Figure 1-12. Localisation des stations fixes à échantillonnage régulier dont le suivi du mésozooplancton est annuel (orange) et pluriannuel (rouge). Les détails concernant l'échantillonnage sont donnés dans le tableau 1-1.

Dans la zone permanente de l'océan Austral du secteur indien, la station KERFIX (Jeandel et al., 1998) située à 100 km au sud-ouest des îles Kerguelen (50°40'S - 68°25'E) et la station Bio (49°43'S - 70°56'E) située sur le plateau des Kerguelen, ont permis des échantillonnages mensuels de 1990 à 1995 et de 1993 à 1995 respectivement. Les objectifs de ces prélèvements étaient de quantifier les échanges d'oxygène et de gaz carbonique entre l'océan et l'atmosphère et de comprendre les variations saisonnières et interannuelles de l'activité biologique dans cette zone. Razouls et al. (1998) montrent en particulier que l'abondance des copépodes dans les 300 premiers mètres est 7 fois plus importante pendant la période productive qu'en hiver et que l'impact du broutage sur la communauté phytoplanctonique reste faible toute l'année (maximum de 2 % de la production primaire).

L'ensemble des données disponibles ne permet pas une approche intégrée de la variabilité spatiale à grande échelle (bassin, océan) bien que des campagnes océanographiques à grande échelle soient réalisées de façon ponctuelle. Par exemple, aucune étude spatiale du zooplancton sur le plateau des Kerguelen n'avait encore été réalisée. De même, peu de campagne ont étudié le zooplancton de façon synoptique à l'échelle de toute la Méditerranée. Pourtant les grandes campagnes océanographiques pluridisciplinaires permettent d'avancer sur les connaissances du fonctionnement de l'écosystème pélagique marin, et notamment sur

Table 1-1. Détails des stations fixes à long terme où une étude de la communauté mésozooplanctonique est réalisée en mer Méditerranée.

Site	Pays	Type de filet	Taille de maille (µm)	Type de trait	Profondeur d'échantillonnage (m)	période	fréquence	Référence
Bassin Ouest								
Golfe de Tigullio	Italie	double Bongo	335	oblique	60	1985-1989, 1991-1995	bimensuel	Licandro & Ibanez (2000)
Golfe de Naples	Italie	Nansen	200	vertical	50	1984-1990	bimensuel	Mazzochi et Ribera d'Alcalà (1995)
			200	vertical	50	1984-1991, 1995-2000	bimensuel, hebdomadaire	Ribera d'Alcalà et al. (2004)
			200	vertical	50	1984-1991, 1995-2006	bimensuel, hebdomadaire	Mazzochi et al. (2011)
			70, 200	vertical	200	2002-2003	bi/mensuel	Peralba et Mazzochi (2004)
Golfe de Tunisie	Tunisie	WP2	200	vertical	15	1993-1995	mensuel	Daly-Yahia (1998)
Majorque	Espagne	Bongo	100, 250	oblique	75	1993-1994	10 jours	Fernandez de Puelles et al. (2003)
			250	oblique	75	1994-2011	10 jours	Fernandez de Puelles et al. (2004)
			250, 333	oblique	75, 100	1994-1999	mensuel	Fernandez de Puelles et al. (2007)
			250	oblique	75, 100	1994-2003	mensuel	Fernandez de Puelles et al. (2009)
Castellon	Espagne	WP2	250	vertical	1, 20, 40, 60	1960-1961	mensuel	Vives (1966)
Baie de Blanes	Espagne	microplancton, JB	53, 200	vertical, oblique	25	1995-1996	hebdomadaire	Calbet et al. (2001)
Baie de Banyuls	France	JB	160, 200	vertical	55	1970-1972	hebdomadaire	Razouls (1972)
Baie de Marseille	France	Tregouboff	1000, 400, 250, 140	horizontal	0, 20, 40	1960-1961	10 jours	Gaudy (1962)
		WP2	200	vertical	55	2002-2003	bimensuel	Riandey (2005)
Baie de Toulon	France	-	90	vertical	15	1995-1996	mensuel	Jamet et al. (2001)
Baie de Villefranche	France	JB	330	vertical	75	1966-1993	hebdomadaire	Molinero et al. (2003; 2005; 2008)
						1974-2002	hebdomadaire	Garcia-Comas et al. (2011)
						1995-2005	hebdomadaire	Vandromme et al. (2010)
Baie de Calvi	France	WP2	180	horizontal	5	1978-1979	journalier	Dauby (1980)
Bassin Est								
Golfe de Trieste	Italie	WP2	200	vertical	18	1970-1986	mensuel	Cataletto et al. (1995)
Adriatic nord	Croatie	WP2	200	vertical	40	1984-1988	-	Lučić (1988)
Baie de Kaštela	Croatie	Nansen	300	vertical	23, 100	1962-1982	mensuel	Solic et al. (1997)
Dubrovnik	Croatie	Nansen	200	vertical	75	1996	1-3 semaines	Batistic et al. (2007)
Baie de Boka Kotorska	Serbie-Montenegro	Nansen	250	vertical	30, 100	1970-1972	mensuel	Vukanić (1971, 1975)
Golfe de Saronikos	Grèce	WP2	200	oblique	50	1984-1985	mensuel	Siokou-Frangou (1996)
			200	oblique	12	1989-1993	mensuel	Christou (1998)
Beyrouth	Liban	WP2	200	vertical	90	1997-1998	-	Lakkis (1990a)
Beyrouth-Tripoli			200, 300	horizontal, vertical	10-800	1970-1988	-	Lakkis (1990b)
Bassin Ouest-large								
Ile de Ponza	Italie	-	250	vertical	3000	1975-1979	mensuel	Scotto di Carlo et al. (1984)

la variabilité des communautés zooplanctoniques et leur impact sur les écosystèmes océaniques.

Cependant, quelques études à grandes échelles ont pu être réalisées. Par exemple, Longhurst (1998) a réalisé une étude mondiale du milieu marin afin de tenter de définir des biomes et à plus petite échelle des écorégions. Cette étude est basée essentiellement sur des images satellitaires de la couleur de l'eau (estimation de la biomasse phytoplanctonique) et de différents paramètres physiques et biologiques tels que 72 espèces de copépodes les plus abondants. De même, Mackas & Beaugrand (2010) ont réalisé une étude mondiale du zooplancton à partir de séries à long terme pouvant atteindre une durée de plus de 60 ans. Les variabilités en termes de biomasse, de structure de taille, de composition et de distributions spatiale et temporelle y sont discutées. A plus petite échelle spatiale, les séries temporelles effectuées par le Continuous Plankton Recorder ont permis une bonne définition de la distribution et de l'évolution du zooplancton de surface dans l'Atlantique Nord (Beaugrand et al., 2000, 2002, 2007). Cependant, ces données n'ont pas été réalisées dans le cadre de campagnes pluridisciplinaires et ne concernent pas les zones d'études de cette thèse.

1.3.2 Objectifs

Mon travail de thèse a été centré sur l'analyse des communautés zooplanctoniques de deux écosystèmes contrastés.

La campagne KEOPS (*KErguelen: compared study of the Ocean and the Plateau in Surface water*) s'est déroulée dans l'océan Austral, sur le plateau des Kerguelen au cours de la période de fin de floraison estivale. L'échantillonnage a été réalisé sur 3 radiales couvrant la partie sud du plateau soit environ 74 000 km².

La campagne BOUM (*Biogeochemistry from the Oligotrophic to the Ultra-oligotrophic Mediterranean*) a été réalisée en période de stratification estivale intense dans les deux principaux bassins de la Méditerranée sur une radiale couvrant une distance de plus de 3 000 km.

Dans ces deux campagnes, des mesures de stocks et de processus physiologiques ont été réalisées à bord et au laboratoire afin de mesurer l'impact des communautés zooplanctoniques sur l'écosystème pélagique.

Dans ce contexte les objectifs de la thèse sont :

- ✓ Caractériser la variabilité à grande échelle régionale des communautés zooplanctoniques dans deux sous régions contrastées de l'océan mondial.
- ✓ Analyser les facteurs environnementaux et trophiques potentiellement responsables de ces variations.
- ✓ Améliorer nos connaissances sur la physiologie du zooplancton afin de déterminer l'impact de ses communautés sur l'écosystème océanique.

Dans un premier temps, la méthodologie utilisée lors de cette thèse sera décrite. Ensuite pour chaque site d'étude, les communautés mésozooplanctoniques seront caractérisées, leurs variations spatiales analysées et les processus métaboliques notamment l'ingestion, la respiration et l'excrétion mesurés afin de quantifier leur impact sur l'écosystème pélagique. Tout d'abord, les résultats de la campagne KEOPS qui s'est déroulée en période de fin de floraison sur le plateau des Kerguelen et en zone HNLC (High Nutrient Low Chlorophyll) dans l'océan Austral seront présentés. Puis, les résultats issus de la campagne BOUM qui s'est déroulée de la Méditerranée Nord Occidentale jusqu'à l'extrémité est du bassin Levantin en période de stratification des eaux de surface en été seront développés. Enfin dans une conclusion générale les caractéristiques communes et les singularités structurelles et fonctionnelles des communautés zooplanctoniques de ces deux écosystèmes contrastés notamment au niveau des limitations nutritives (fer pour l'océan Austral ; phosphore pour la Méditerranée) seront résumés.

2 MATERIEL ET METHODES

2.1 Stratégies générales d'étude

Le travail de thèse s'appuie sur deux campagnes océanographiques pluridisciplinaires, l'une réalisée sur le plateau continental des Kerguelen dans l'océan Austral (KEOPS) et l'autre en Méditerranée (BOUM). L'échantillonnage et les expériences à bord ont été réalisés par François Carlotti (KEOPS) ou par moi-même (BOUM). L'ensemble des analyses au laboratoire ont été sous ma responsabilité.

2.1.1 KEOPS

La campagne KEOPS (*KErguelen compared study of the Ocean and the Plateau in Surface water*) s'est déroulée entre le 12 janvier et le 13 février 2005 à bord du N/O *Marion Dufresne* entre 49-54° S et 71-78° E. Trois radiales (A, B et C) couvrant chacune le plateau, le talus continental et l'océan profond ont été effectuées auxquelles s'est ajoutée une journée de mesure à la station KERFIX (50°40'S, 68°25'E). Les stations A3 (en plein centre du plateau) et C11 (position la plus océanique) ont fait l'objet de périodes d'échantillonnage intensives sur 24 heures à plusieurs reprises au cours de la mission. Pour chaque station des profils verticaux de température, de salinité, de PAR et de fluorescence ont été réalisés à l'aide d'une CTD-Rosette. Différents paramètres chimiques (oxygène et sels nutritifs) et biologique (chlorophylle *a*) ont aussi été mesurés à différentes profondeurs. Un échantillonnage plus complet était réalisé à une station sur deux (station à chiffre impaire) avec notamment des prélèvements et des mesures dédiés au zooplancton (filets Bongo et UVP : Underwater Video Profiler).

2.1.2 BOUM

La campagne BOUM (*Biogeochemistry from the Oligotrophic to the Ultra-oligotrophic Mediterranean Sea*) s'est déroulée du 18 juin au 20 juillet 2008 à bord du R.V. *l'Atalante*. Un transect de 3000 km composé de 2 legs réalisés dans les bassins Est et Ouest de la mer Méditerranée (43-33° N et 4-32° E). Le premier leg (18 au 29 juin) a débuté dans le bassin Ionien (station 1) jusqu'à l'extrémité est du bassin Levantin (station C). Ensuite, le deuxième leg (3 au 18 juillet) s'est déroulé à l'ouest de la première station (station B) puis à travers le seuil de Sicile et le bassin Algéro-Provencal pour se terminer dans le panache du Rhône (station 27). La stratégie d'échantillonnage consistait en une série de courtes stations (~ visitée pendant 2-3 h) distantes d'environ 100 km. Trois stations longues (A, B et C)

situées au centre des tourbillons anticycloniques ont été échantillonnées à de nombreuses reprises pendant 3 jours. A chaque station, des profils de température, salinité, PAR et de fluorescence étaient réalisés entre la surface et le fond à l'aide d'une CTD rosette. Les paramètres chimiques (oxygène et sels nutritifs) étaient mesurés à chaque station courte, alors que les paramètres biologiques i.e. les bactéries, le phytoplancton, le microzooplancton et le zooplancton, étaient mesurés à une station sur deux. Au niveau des 3 stations longues, en plus des paramètres de base décrits ci-dessus, des études de processus ont aussi été réalisées à bord (respiration et excrétion pour le zooplancton).

Les protocoles suivis pendant les deux études présentées ici sont semblables et sont décrits ci-dessous.

2.2 Prélèvement des organismes en mer

Le zooplancton a été récolté à l'aide d'un double filet Bongo avec une ouverture de 60 cm de diamètre (équivalent à 0,28 m^2) et un vide de maille de 330 µm (KEOPS) ou de 120 µm (BOUM). Un collecteur de même vide de maille était fixé au filet. Les traits de filets étaient effectués verticalement de 200 m à la surface à une vitesse de 1 m s^{-1}.

La distribution verticale des nauplii et des copépodes de petite taille a été étudiée à l'aide de bouteilles de prélèvements (Niskin) récoltées à différentes profondeurs.

2.3 Conservation et traitement des échantillons à bord

La totalité du contenu d'un collecteur a été rapidement transférée dans un splitter (boite de Motoda) à l'abri de la lumière et subdivisée en deux fractions homogènes.

La première moitié a été rapidement filtrée et les organismes ont été recueillis sur trois filtres de type GF/C. Les filtres ont été ensuite déposés dans des boites de Pétri identifiées et rapidement introduites dans une bombonne d'azote liquide afin de fixer instantanément les organismes pour les mesures ultérieure des contenus stomacaux en pigments. Ces boites ont ensuite été stockées dans un surgélateur à -80°C.

La seconde fraction était destinée à des mesures de biomasse totale (poids sec). Les organismes ont tout d'abord été tamisés sur une soie de même vide de maille que le filet afin d'éliminer les petites particules agrégées (eg : chaines de diatomées et de dinobiontes,

radiolaires) puis recueillis sur un filtre GF/C. Ce dernier a été préalablement calciné au laboratoire pendant 3h à 350°C afin d'éliminer les traces de carbone puis pré-pesé et enfin stocké dans une boite de Pétri identifiée. Les organismes ont ensuite été séchés à bord dans une étuve à 60°C pendant 3 jours. Lors de la mission KEOPS, la présence de très nombreuses chaines de diatomées n'a pas permis de réaliser cette mesure.

Les organismes contenus dans le second collecteur ont été conservés dans une solution à 4 % de formol/eau de mer tamponnée au borax pour l'analyse taxonomique.

Le contenu (12 L) de chaque bouteille Niskin a été filtré sur une soie de 50 µm et fixé dans une solution formol/eau de mer à 4 % (KEOPS) ou filtré sur une soie de 20 µm et fixé dans une solution lugol/eau de mer à 2 % (BOUM).

Afin de récolter des organismes pour les expériences métaboliques, des traits de filets supplémentaires ont été réalisés. Le contenu des collecteurs a été dilué avec précaution dans un seau de 10 L contenant de l'eau de mer filtrée à 0,2 µm et entreposé dans une pièce thermostatée. Les expériences ont été réalisées 1 à 2 heures après l'échantillonnage.

2.4 Traitement des échantillons

2.4.1 Mesure de la biomasse

Les filtres contenant les organismes déshydratés à bord ont été replacés dans une étuve à 60°C pendant 24h au laboratoire. Ensuite chaque filtre a été pesé et soustrait au poids du filtre sans organisme. Afin de calculer la biomasse, ce poids a ensuite été rapporté au volume échantillonné par le filet. La distance parcourue par le filet a été mesurée à l'aide d'un volucompteur placé au niveau de l'ouverture du filet (KEOPS) ou estimé à partir de la longueur de câble déroulé (BOUM).

2.4.2 Analyses taxonomiques

Afin de décrire la composition taxonomique du zooplancton, environ 500 individus d'un sous échantillon sont identifiés sous une loupe binoculaire (LEICA MZ6) en utilisant une cuve de Bogorov ou de Dollfus. La détermination a été faite le plus souvent jusqu'au niveau de l'espèce et de la différenciation des stades adultes et copépodites pour les copépodes. La description taxonomique s'est basée sur les travaux de Razouls (1994) et de Bradford-Grieve et al. (1999) pour la campagne KEOPS et sur les travaux de Rose (1933), Trégouboff & Rose (1957) et Razouls (2005-2011) pour la campagne BOUM.

2.4.3 Analyses au compteur optique à plancton (OPC 1L)

2.4.3.1 Description et principe de l'appareil

L'OPC 1L (Optical Plankton Counter: Focal Technologies Inc., Dartmouth, Nouvelle Ecosse, Canada) est un compteur optique à plancton de laboratoire permettant à la fois le comptage et la mesure de particules. L'appareil est inséré dans un circuit d'eau fermé et relié à un ordinateur permettant l'acquisition en direct des données. Il est constitué d'un faisceau lumineux à une longueur d'onde de 640 nm à travers lequel pénètre un tube en verre. Lorsqu'une particule est entraînée, elle induit une atténuation d'intensité lumineuse qui est détectée par un récepteur, convertie et enregistrée par l'unité de conversion comme une variation du signal électrique qui correspond à la taille digitale de la particule. Cette taille digitale est ensuite convertie en µm à l'aide d'une routine fournie par le constructeur. Cette surface est ensuite convertie en surface équivalent sphérique comme telle :

L'aire correspondant à une particule est assimilée à un disque de même surface. Le diamètre de ce disque est appelé ESD pour Equivalent Spherical Diameter et est donné en µm. Le terme sphérique vient du fait qu'un même organisme peut être détecté sous différents angles et donc pour un organisme donné, il existe une « gamme de taille» comprise entre le passage de face (taille minimale) et de profil (taille maximale).

La limite de détection de cet appareil est comprise entre 200 et 2000 µm d'ESD.

L'ESD est ensuite convertie en volume par la formule empirique d'une sphère. A partir de ce biovolume, une relation a été utilisée afin de le convertir en masse. La relation logarithmique obtenue par Riandey (2005) à partir du même appareil sur des communautés zooplanctoniques du Golfe de Guinée et de la mer d'Alboran a été utilisée :

$$Log\ (W) = 0{,}865\ log\ (BV) - 0{,}887$$

Où W = poids sec en mg et BV = Biovolume en mm^3

Afin d'estimer la biomasse en carbone, un facteur de conversion Carbone/Poids Sec de 50% a été utilisé (Postel et al., 2000).

2.4.3.2 Conditions d'utilisation et mode opératoire

Les conditions d'utilisation et les contraintes expérimentales ont été décrites par Herman (1988, 1992), Beaulieu et al. (1999) et Sourisseau (2002). Les échantillons sont introduits

dans une colonne d'eau à l'aide d'une seringue de 60 mL dont l'extrémité a été coupée afin de permettre le passage des gros organismes et de réguler facilement leur introduction. En effet, il est recommandé d'obtenir un passage d'organismes < 20 particules par seconde afin d'éviter une sous-estimation par superposition des particules (Sourisseau, 2002). Le nombre d'organismes compté par l'OPC étant visualisé en direct sur l'écran de l'ordinateur, il est donc facile de réguler cette introduction par simple pression sur la seringue. De même, le débit du circuit d'eau a été fixé à 18 L min^{-1} afin d'obtenir un comptage optimal selon Sourisseau (2002). Ce dernier a établi qu'il faut au minimum 1000 individus pour obtenir une bonne représentation du spectre de taille des particules. Dans cette étude le nombre minimum d'organismes passés à l'OPC a toujours été supérieur à 2000 afin d'obtenir un spectre le plus précis possible (fraction de 1/8 ou 1/16 de l'échantillon). Cette fraction est ensuite conservée dans un flacon différent afin de permettre toute vérification par la suite.

2.4.4 Analyses au ZooScan

2.4.4.1 Description et principe de l'appareil

Le ZooScan est un scanner couplé à un analyseur d'image permettant la numérisation des échantillons afin d'obtenir le comptage et la taille de chaque particule. Ce scanner diffère des scanners classiques sur plusieurs points. Il est constitué de LEDs sur et sous la vitre afin d'optimiser la luminosité. L'ensemble est imperméable de façon à accueillir des échantillons de zooplancton en milieu liquide. Il possède un système à bascule pour récupérer facilement l'intégralité de l'échantillon.

Le ZooScan est couplé à un logiciel gratuit d'analyse d'image : *Image J*. Un « «plug-in » a été développé pour *Image J* nommé ZooProcess qui permet de configurer les images de scanner par l'intermédiaire d'un autre logiciel nommé VueScan. Une fois le scan réalisé par celui ci, l'image est ensuite convertie pour être utilisée sous ZooProcess (changement de format). Les caractéristiques de l'échantillon (métadata) sont ensuite saisies dans ZooProcess (par exemple : la date, la profondeur, le type de filet, la fraction utilisée). L'analyse d'image est effectuée une fois la série des échantillons effectuée. Le logiciel individualise les particules sous forme de vignette (Fig. 2-1). Ensuite 46 paramètres sont calculés pour chaque particule. Afin de séparer les particules zooplanctoniques et non zooplanctoniques, on utilise le logiciel « Plankton Identifier » dont le principe est le suivant. Il sélectionne 1 000 vignettes au hasard dans la série de scans. Le tri est effectué visuellement pour chaque vignette que l'on insère dans le dossier correspondant (nommé : zooplancton ou détritus). Il est important d'avoir un

nombre de vignettes semblable dans chaque dossier afin de ne pas favoriser une classe dans la reconnaissance. Une analyse statistique (Random forest) permet de rechercher les correspondances entre les 46 paramètres de chaque vignette avec ceux obtenus dans chaque dossier (routine Tanagra de Plankton Identifier).

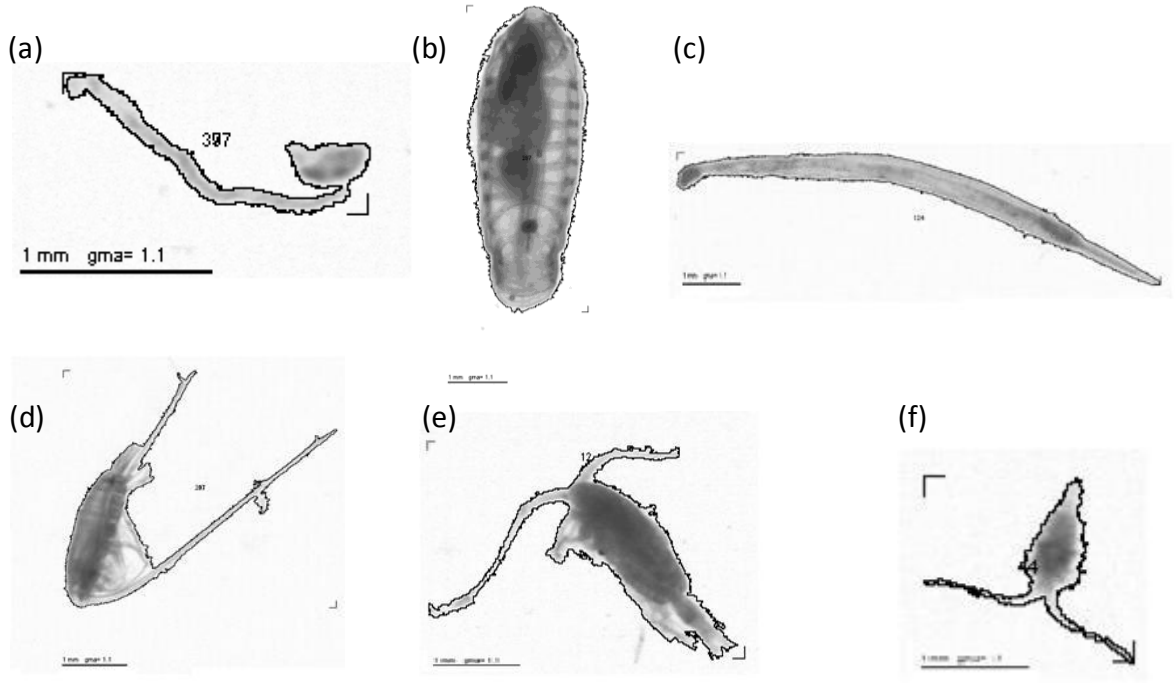

Figure 2-1. Sélection de vignettes d'organismes zooplanctoniques numérisés par le ZooScan. Les lignes noires correspondent aux contours détectés par le logiciel ZooProcess. (a) Appendiculaire, (b) Salpe, (c) Chaetognathe, (d) *Mesocalanus tenuicornis*, (e) *Pleuromamma* sp., (f) *Centropages typicus*.

Ces appareils permettent donc d'obtenir rapidement (~ 15 min OPC, 30-45 min ZooScan) une répartition en classe de taille de l'ensemble des organismes.

2.4.4.2 Préparation et traitement des échantillons

Tout d'abord, un cadre en plexiglas (type narrow) est disposé sur la vitre du scanner. Celui-ci correspond à la dimension du scan et permet de disposer les organismes dans le champ de numérisation (2400 dpi). Ensuite de l'eau à température ambiante (afin d'éviter le dégazage donc la formation de bulles d'air) est ajoutée jusqu'au niveau indiqué sur le cadre. Un scan à blanc (sans organisme) est réalisé une seule fois en début de série afin de détecter éventuellement les défauts présents sur la vitre et de les éliminer dans les scans des échantillons.

L'échantillon est fractionné afin d'obtenir un minimum de 1000 individus. Les organismes sont disposés sur le scanner dans un fond d'eau. Ils sont ensuite éloignés du bord du cadre et séparés les uns des autres manuellement à l'aide d'une épine en bois afin d'éviter de confondre plusieurs particules avec une seule de plus grande taille. Cela aurait pour conséquence de sous-estimer le nombre de particules et d'augmenter le nombre de particules de grande taille. La surface des individus est représentée par un nombre de pixel. Un pixel est équivalent à un carré de 10,56 µm de coté. La mesure de la taille des organismes est ensuite estimée comme pour l'OPC. Cette surface est convertie en un disque de même surface, dont le diamètre correspond à l'ESD qui est ici nommé ECD (Equivalent Circular Diameter) et donné en µm.

L'estimation de la biomasse est basée sur la relation où 1 mm^3 correspond à 1 mg de poids humide (densité = 1).

2.5 Etude *in vitro* du métabolisme

2.5.1 Mesure de la respiration

2.5.1.1 Incubation des organismes

L'eau de mer utilisée pour les expériences a été prélevée en surface à l'aide d'un seau puis filtrée sur 0,2 µm (filtre GF/F de 180 mm de diamètre) et enfin stockée dans deux bidons Nalgène de 10 L pendant 48 h dans une pièce thermo-régulée. La température de la pièce est ajustée en fonction de la température *in situ* à la profondeur du maximum de chlorophylle soit 15, 16 et 17°C pour les stations A, B et C respectivement. Les bidons sont laissés ouverts de façon à saturer et équilibrer l'eau en O_2 et en CO_2. Une heure avant les expériences, plusieurs flacons *DBO* à col rodé de 125 ou de 310 mL ont été remplis avec cette eau par siphonnage en prenant soin de ne pas introduire de bulle d'air à l'aide d'un tuyau en téflon préalablement nettoyé à l'acide chlorhydrique 10%. Les organismes zooplanctoniques sont transférés juste après la pêche dans un seau de 10 L rempli avec de l'eau de mer de surface préalablement filtrée sur 0,2 µm et stockée dans la pièce thermo-régulée. Les organismes sont ensuite passés avec précaution au travers d'un tamis de 1000 µm afin de d'obtenir deux classes de tailles. Les petits organismes (< 1000 µm) sont considérés globalement alors que les plus grands sont séparés par groupe taxonomique ou par espèce et par stade lorsque que cela a été possible à l'aide d'une loupe binoculaire. Chaque lot d'organisme a été vérifié afin d'éliminer les organismes carnivores (i.e chaetognathes) ou photosynthétiques (i.e *Ceratium*). Tous les

organismes sont conditionnés pendant environ 2h dans des coupelles en verre remplies de 100 mL d'eau de mer expérimentale. A la station C, le contenu du collecteur présentait une concentration importante de chaine de *Chaetoceros* et de *Ceratium* rendant la séparation par classe de taille impossible. De ce fait, les organismes ont été séparés individuellement et seules des expériences par taxons ont été réalisées.

Les lots homogènes d'individus sont ensuite introduits dans les flacons *DBO* de 125 ou de 310 mL selon la taille des organismes. Les individus sont déposés délicatement sur une soie puis transférés dans le flacon, avec un minimum de stress pour les organismes. Les gros organismes, comme les euphausiacés et les amphipodes, sont placés individuellement dans les flacons de 310 mL. Les organismes de taille moyenne (i.e. ostracodes et copépodes) sont placés individuellement ou par lots regroupant jusqu'à 15 individus alors que les plus petits sont placés par lots d'environ 150 individus dans les flacons de 125 mL. Le choix du nombre d'organismes est basé sur les travaux de Mayzaud et al. (2005). Chaque flacon est placé dans un bain marie, afin de limiter les possibles variations thermiques de la pièce thermo-régulée, pendant 15 à 24 h à l'obscurité. Une série de 6 à 7 flacons témoins (eau de mer expérimentale sans organisme) est placée dans les mêmes conditions. Les taux de respiration sont calculés par différence entre les flacons avec et sans organismes.

2.5.1.2 Consommation d'oxygène

La mesure de la consommation d'oxygène n'a été réalisée que durant la campagne BOUM. Une fois l'incubation terminée, chaque flacon est délicatement ouvert sans créer de surpression. L'eau est aspirée à l'aide d'un tuyau en téflon dont l'extrémité qui est introduite dans le flacon est entourée d'une soie de 10 µm afin de ne pas récolter les organismes et les possibles détritus. L'autre extrémité du tuyau est adaptée à une seringue qui permet d'amorcer le siphonage de l'eau. Un flacon de mesure de 30 ml contenant un barreau aimanté est rempli jusqu'à débordement.

Les mesures d'oxygène sont effectuées à l'aide d'un oxymètre (YSI 420) équipé d'une électrode de Clark adaptée au flacon de mesure qui est déposé sur un agitateur magnétique réglé à la même vitesse pour toutes les expériences. Les taux de consommation d'oxygène VO_2 (µl ind^{-1} j^{-1}) sont obtenus d'après l'équation :

$$VO_2 = [O_{2mes}] \frac{V}{32} \frac{22,4}{n} \frac{24}{t}$$

Où :

$[O_{2mes}]$: concentration d'oxygène dissous (mg O_2 L^{-1})
V: volume du flacon (mL)
32 : correspond à la masse atomique de l'O_2
22,4 : correspond au volume (L) occupé par 1 mole
n: nombre d'individus par flacon
t: temps expérience (h)

2.5.1.3 Mesure du rejet de $C0_2$

A la fin des expériences, du chlorure mercurique a été ajouté en excès (50 ou 100 µL) afin de stopper l'activité biologique. Les mesures ont été réalisées avec un coulomètre (UIC, inc) par titrage du CO_2 total (TCO_2) (Johnson et al., 1987 ; DOE, 1994). Le système de siphonnage de l'eau est couplé à un coulomètre dont le circuit est automatisé et fabriqué par le laboratoire. Le principe du dosage est le suivant :

Quelques gouttes d'HCl sont ajoutées à 25 mL d'échantillon, libérant ainsi le carbone organique dissous sous forme gazeuse (CO_2). Ce gaz est ensuite transporté par de l'azote gazeux dans une chambre contenant une solution d'éthanolamine et de thymolphthaléine ainsi que les électrodes du coulomètre. Le thymolphthaléine est un indicateur de pH qui est incolore en milieu acide et bleu en milieu basique. L'ajout du CO_2 dans cette solution a pour conséquence un changement de pH et de changer la coloration vers le bleu. Le dosage du point d'équivalence (équilibre acido-basique) est réalisé par l'ajout d'une base dont la formation est réalisée par réaction d'électrolyse entre les électrodes et l'éthanolamine. Le point d'équivalence est déterminé par photométrie en coulomb, le nombre de coulomb étant proportionnel à la quantité de CO_2. Les coulombs sont ensuite convertis en µmol CO_2 L^{-1} (cf. constructeur). Le taux de rejet de CO_2 est ensuite exprimé en µL en multipliant par 22.4 (1 mole de gaz parfait occupe 22.4 L). Au cours d'une série de mesures, un flacon expérimental témoin est mesuré après la mesure de 3 flacons afin de corriger la dérive potentielle du coulomètre.

2.5.2 Mesure de l'excrétion

Le protocole expérimental est identique à celui mis en place pour les expériences de respiration décrites ci-dessus. Le volume des flacons utilisés pour ces expériences est exclusivement de 310 mL. Trois aliquotes de 20 mL sont siphonnés, pour chaque sel nutritif, à l'aide d'une seringue équipée d'un filtre GF/F. Les mesures d'ammonium et de phosphore ont été réalisées immédiatement à bord du navire. La mesure d'ammonium a été réalisée par

fluorimétrie (Holmes et al., 1999) à l'aide d'un fluorimètre Jasco FP-2020. Le phosphore inorganique dissous a été mesuré par colorimétrie (Treguer & le Corre, 1975) à l'aide d'un Technicon autoanalyseur Bran Luebbe II.

2.5.3 Mesure de la fluorescence intestinale

Les échantillons récoltés en mer et placés à -80°C sont décongelés doucement (placé dans de la glace) et à l'obscurité, afin de limiter la dégradation des pigments chlorophylliens par la lumière. Une fraction de l'échantillon est placée dans une boite de Pétri avec de l'eau de mer froide (~ 0ºC) et filtrée à 0,2 µm. Les individus sont séparés individuellement à la loupe binoculaire et classés par groupe de taille/espèces dans des tubes à essai.

Les analyses ont été effectuées principalement sur 3 groupes. Le groupe I regroupe des copépodes de taille > 3 mm (*Calanus simillimus*, *Calanoides acutus* adultes et CV, *Rhincalanus gigas* adultes, CV-II et *Pleuromamma robusta* adultes et CV-IV). Le groupe II était composé de copépodes de petites taille < 3 mm (Paracalanidae, *Oithona* spp. et *Clausocalanus laticeps*). Les euphausiacés forment le troisième groupe. L'extraction des pigments est ensuite faite à l'obscurité et au froid (~0°C), dans 5 mL de méthanol 100 % pendant 1h (KEOPS) ou dans 5 mL d'acétone à 90 % pendant une nuit (BOUM).

La chlorophylle et les phéopigments sont estimés à partir de mesures de fluorescence avant et après acidification (quelques gouttes d'acide chlorhydrique 1 N) à l'aide d'un fluorimètre Turner III selon la méthode de Yentsch & Menzel (1963) modifiée par Holm-Hansen et al. (1965). Les phéopigments correspondent à la dégradation pigmentaire de la chlorophylle *a* dans le tractus digestif des copépodes. Le contenu stomacal en pigment (ng Chl *a* eq ind^{-1}) a été calculé d'après Wang & Conover (1986), où la chlorophylle *a* équivalente = Chl *a* + Pheopigments.

Le contenu pigmentaire est ensuite transformé en taux d'ingestion *in situ* (I en ng Chl *a* eq ind j^{-1}), en supposant un taux de broutage et de défécation à l'équilibre, d'après l'équation :

$$I = C_0 k \; x \; 24$$

où C_0 est le contenu pigmentaire du tube digestif (ng Chla eq ind^{-1}) et k le taux d'évacuation stomacal (en h^{-1}). Le taux d'évacuation stomacal, n'ayant pas été mesuré pendant les missions, une valeur de 0,67 h^{-1} basée sur des copépodes au sud des Kerguelen au printemps a été utilisée pour KEOPS (Mayzaud et al., 2002). La relation d'allométrie en fonction de la

température (0 - 17°C) obtenue par Dam et Peterson (1988) puis modifiée par Bamstedt et al. (2000) a été utilisée pour BOUM:

$$k = 0{,}0124\, x\, e^{(0{,}0767\, x\, T)}$$

où k est le taux d'évacuation stomacal (min^{-1}) et T la température (°C)

En supposant le taux d'ingestion constant sur 24h et en connaissant l'abondance des espèces (ind m^{-3}), le taux d'ingestion total de la communauté zooplanctonique (µg Chl *a* eq m^{-3} j^{-1}) a été calculé. L'impact du broutage sur le phytoplancton a été estimé en comparant ces valeurs aux valeurs de chlorophylle *a* et de production primaire *in situ* moyennées sur la couche 0-200 m.

Afin de pouvoir exprimer le taux d'ingestion en terme de carbone, un rapport C:Chl *a* de 106 (Razouls et al., 1998b) a été appliqué pour KEOPS et de 50 pour BOUM (Båmstedt et al., 2000). L'ingestion en carbone phytoplanctonique par les copépodes peut ensuite être calculée en termes de ration journalière (% du poids de carbone corporel ingéré par jour), ou de pression de broutage sur le phytoplancton (% du stock de carbone phytoplanctonique consommé par jour).

Caractérisation de la distribution spatiale, structure de la communauté du mésozooplancton dans deux écosystèmes contrastés et étude de la réponse fonctionnelle

3 CAS D'UNE ZONE NATURELLEMENT ENRICHIE EN FER EN FIN DE FLORAISON PHYTOPLANCTONIQUE DANS L'OCEAN AUSTRAL

3.1 Introduction

L'objectif principal de la mission KEOPS est d'améliorer nos connaissances sur la réponse de l'océan Austral au changement climatique globale et en particulier, d'étudier les effets de la fertilisation naturelle de l'océan par le plateau des Kerguelen sur la pompe biologique du CO_2 et sur les cycles de composés chimiques jouant un rôle dans la régulation du climat.

En effet, sur le plateau des Kerguelen, les apports naturels et réguliers en fer favorisent une forte production phytoplanctonique pendant une période d'environ 3 mois. Or, l'océan Australe se caractérise par un écosystème HNLC où la production primaire est limitée par la disponibilité en fer (Martin et al., 1990). La production primaire est dominée par de larges espèces phytoplanctoniques telles que les diatomées (Kopczynska et al., 1986 ; Quéguiner et al., 1997). Par exemple, la fraction > 10 µm représente jusqu'à 96 % de la silice biogénique. Cette prépondérance en diatomée est une caractéristique de tout l'océan Austral et notamment au niveau du plateau des Kerguelen (Cornet-Barthau et al., 2007; Armand et al., 2008). Des expériences d'enrichissement en fer sous forme de sulfate de fer ($FeSO_4$) ont été réalisées ces dernières décennies dans différentes parties du globe avec comme conséquence l'augmentation de la production primaire (Boyd et al., 2000; Gervais et al., 2002; Coale et al., 2004) mais la durée de la floraison phytoplanctonique est limitée à quelques jours ou jusqu'à 1 mois (voir Boyd et al., 2007, tableau 1). Dans certains cas, la réponse des producteurs primaires est même très limitée (Harvey et al., 2007).

Au cours de ces expériences d'enrichissement, le control top down du mésozooplancton sur les producteurs primaires est clairement mis en évidence dans différentes zones géographiques (Rollwagen Bollens & Landry, 2000; Tsuda et al., 2007), alors que dans l'océan Austral, il reste faible, voire négligeable (Zeldis, 2001; Buesseler et al., 2004). Pendant les campagnes SOIREE et SOFeX, les copépodes n'ont en effet consommé par jour que ~ 1 % du stock du phytoplancton équivalent à ~ 6 à 8 % de la production primaire.

Mais qu'en est-il au niveau de la zone d'enrichissement naturelle du plateau des Kerguelen? L'impact de la prédation du mésozooplancton sur les producteurs primaires est-il plus important ou aussi négligeable que dans les expériences de fertilisation anthropique?

L’étude réalisée ici avait pour objectif principal de caractériser à la fois les stocks (abondance et biomasse) et la structure des communautés métazooplanctoniques (taxonomie et classe de taille) sur le plateau des Kerguelen et dans la zone HNLC. Dans un second temps nous essayerons au travers des mesures de taux métaboliques de discuter du fonctionnement du mésozooplancton en période productive.

A la suite de cet article, la distribution spatiale spécifique sera mise en relation avec les paramètres environnementaux les plus représentatifs afin de déterminer s’il existe des différences spatiales aussi bien entre le plateau et la zone HNLC que sur le plateau lui-même.

3.2 "Zooplankton community structure, biomass and role in the carbon fluxes during the second half of a phytoplankton bloom in the eastern sector of the Kerguelen Shelf (January-February 2005)"

Available online at www.sciencedirect.com
ScienceDirect
Deep-Sea Research II 55 (2008) 720–733
DEEP-SEA RESEARCH PART II
www.elsevier.com/locate/dsr2

Zooplankton community structure, biomass and role in carbon fluxes during the second half of a phytoplankton bloom in the eastern sector of the Kerguelen Shelf (January–February 2005)

François Carlotti[a,b,*], Delphine Thibault-Botha[a,b], Antoine Nowaczyk[a,b], Dominique Lefèvre[c]

[a]*Laboratoire d'Océanographie et de Biogéochimie, Aix-Marseille Université, CNRS, LOB-UMR 6535, OSU/Centre d'Océanologie de Marseille, Campus de Luminy—Case 901, F-13288 Marseille Cedex 09, France*
[b]*CNRS (CNRS/INSU), UMR 6535, Campus de Luminy—Case 901, 163 Avenue de Luminy, F-13288 Marseille Cedex 09, France*
[c]*Laboratoire de Microbiologie, Géochimie et Ecologie Marines, Aix-Marseille Université, CNRS, LMGEM-UMR 6117, OSU/Centre d'Océanologie de Marseille, Campus de Luminy—Case 901, F-13288 Marseille Cedex 09, France*

Accepted 10 December 2007
Available online 14 March 2008

Abstract

During the KEOPS survey, zooplankton was sampled with vertical tows to estimate zooplankton stock and to study its composition and size structure both using traditional taxonomic identification and Optical Plankton Counter (OPC). Mesozooplankton OPC-biomass derived from OPC size spectra and integrated over 200 m was variable with average values about 10 g C m^{-2} along transects A and B and at the fixed station KERFIX, and only ~5 g C m^{-2} along transect C. Stations in the most oceanic area (A11, B11, and C11) presented biomass values 3 times lower than the mean value of their respective transects, highlighting a clear decrease of the biomass beyond the shelf. The mesozooplankton community was dominated by copepods, particularly by large- and medium-size calanoids and small Oithonidae. Large numbers of different copepodites stages and nauplii were found, as well as exuviae, indicating that individuals were in active growing phase over the whole area. Euphausiids, chaetognaths, appendicularians, amphipods, polychaetes, ostracods and salps were found as well.

Two reference stations, A3 located in the middle of the bloom on the shelf and C11 in the oceanic waters, were visited several times during the cruise. No particular temporal variations, neither in biomass nor in community structure, were observed, but differences in integrated biomass (average biomass at A3: 10.6 g C m^{-2}; at C11: 2.8 g C m^{-2}) between oceanic and shelf stations clearly show an enhanced secondary production on the shelf. Additional measurements at some stations were performed in order to quantify ingestion (gut contents) and respiration rates on key species and size groups. Gut pigment contents were higher during the first half of the survey at both stations, showing clear temporal changes probably linked to the prey field, with lower values always reported in the oceanic waters compared to the shelf.

Values of respiration and ingestion rates extrapolated from OPC size spectra using published allometric relationships are discussed.

Keywords: Zooplankton; Kerguelen Island; Heard Island; Biomass; Composition; Carbon budget

1. Introduction

The Southern Ocean is characterized by large areas of high surface-nutrient concentrations that are not linked to correspondingly high productivity as indicated by *in situ* and satellite-based chlorophyll measurements and primary productivity estimates, except in some shelf regions (Schlitzer, 2002). Such productive shelves can support

*Corresponding author at: Tel.: +33 491041644; fax: +33 491041643. Laboratoire d'Océanographie et de Biogéochimie, Aix-Marseille Université, CNRS, LOB-UMR 6535, OSU/Centre d'Océanologie de Marseille, Case 901, F-13288 Marseille Cedex 09, France.
E-mail address: francois.carlotti@univmed.fr (F. Carlotti).

0967-0645/$ - see front matter © 2008 Elsevier Ltd. All rights reserved.
doi:10.1016/j.dsr2.2007.12.010

3.2.1 Introduction

The Southern Ocean is characterized by large areas of high surface-nutrient concentrations that are not linked to correspondingly high productivity as indicated by *in situ* and satellite-based chlorophyll measurements and primary productivity estimates, except in some shelf regions (Schlitzer, 2002). Such productive shelves can support large stocks of mesozooplankton as shown around the South Georgia island (Ward et al., 1995; Atkinson et al., 1996), in the Prince Edward Archipelago (Froneman et al., 1999; Hunt & Pakhomov, 2003), in the Antarctic Peninsula (Hernández-León et al., 2000), in Terra Nova Bay (Fonda Umani et al., 2005), and around the Kerguelen Islands in the Indian sector of the Southern Ocean (Razouls et al., 1996, 1998; Mayzaud et al., 2002a, b). These regions are known to be breeding areas for many top predators (i.e. birds and seals), which reflect sufficient food availability at the levels of zooplankton and nekton (Pakhomov & McQuaid, 1996). Despite the potentially important role that these regions may play in the whole Southern Ocean ecosystem (Moore and Abbott, 2000), underlying mechanisms between physical features, such as fronts, eddies or internal waves and nutrients inputs, primary and secondary productions, are still poorly understood.

The interdisciplinary field experiment *KErguelen: compared study of the Ocean and the Plateau in Surface water* (KEOPS) program conducted during the late austral summer 2005 was designed to understand the mechanisms inducing the phytoplankton bloom and to quantify the carbon fixation and vertical fluxes over the area of the bloom on the Kerguelen Plateau, east of the Kerguelen Island—Heard Island line. The Kerguelen Islands are associated with eastwards-elevated chlorophyll concentrations linked to physical processes induced by the interplay between the eastward flow of the Antarctic Circumpolar Current (ACC) and the large topographic barrier of the shallow Kerguelen Plateau, which is oriented north-west/south-east along the 70°E meridian (Fig. 1). The recurrent south-east large bloom generally begins in November, peaks in January, and ends in late February (Blain et al., 2001, 2007; Schlitzer, 2002). In a previous study (Blain et al., 2001), a high chlorophyll plume observed north-east of the Kerguelen Island and north of the Polar Front has been correlated with both sufficient iron concentrations (dissolved Fe in the range 0.45–0.7 nM), and a more favorable light-mixing regime.

Several scientific programs have increased our understanding on the composition, structure and physiological activities of mesozooplankton and its impact on phytoplankton production particularly around the Kerguelen Island, at the field station KERFIX and on transect from

Kerguelen Island to the ice edge on the Antarctic continent (Mayzaud and Razouls, 1992; Semelkina, 1993; Razouls et al., 1996, 1997, 1998; Errhif et al., 1997; Tirelli and Mayzaud, 1999; Blain et al., 2001; Mayzaud et al., 2002a, b). Zooplankton biomass on the south-eastern part of the Kerguelen Island has been documented once by Semelkina (1993). However, it is still unknown how strongly the zooplankton stock responds to this long lasting phytoplankton bloom and whether it varies in space and time in relation to the phytoplankton and microzooplankton abundance and composition.

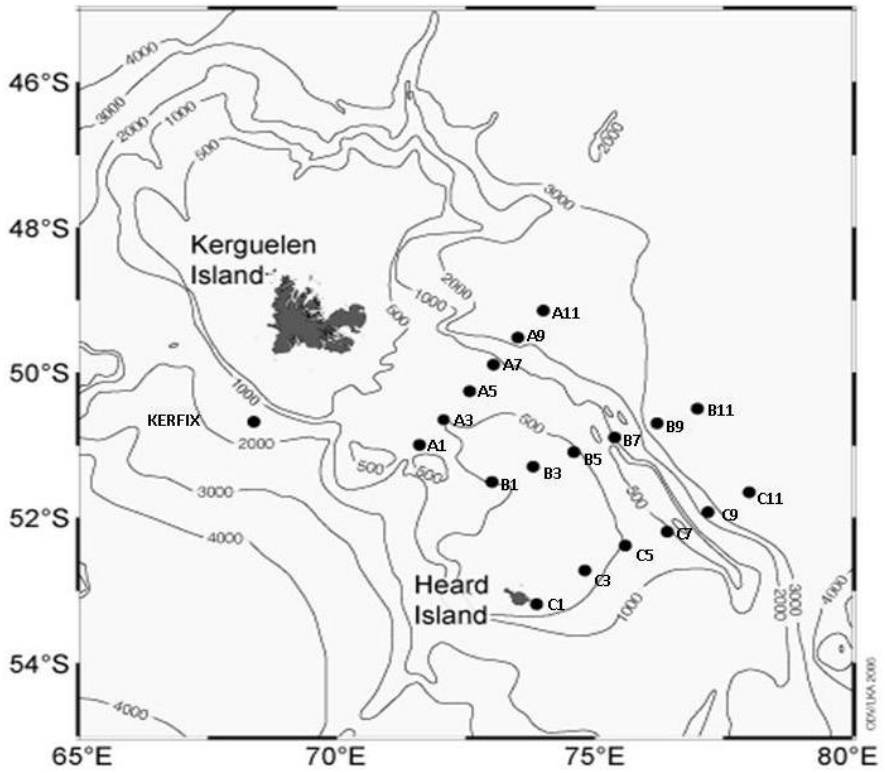

Figure 3-1. Map of the studied area and locations of sampling stations during the KEOPS cruise.

During the KEOPS survey, zooplankton were sampled in order (1) to identify whether differences in the standing stock and composition of mesozooplankton (using traditional taxonomic identification and Optical Plankton Counter) occurred between quite contrasted hydrological structures and (2) to characterize their dynamics at the end of a long-term natural iron-fertilized bloom. Additional physiological measurements were conducted at some stations to quantify respiration and ingestion rates on key species and size groups. Rates were then compared with size-dependent allometric relationships.

3.2.2 Material and Methods

3.2.2.1 Study site and sampling strategy

The KEOPS study was conducted between January 19 and February 13, 2005 on board the R.V. Marion Dufresne and covered an area of 50,000 km² on the east–south-east area of the Kerguelen Islands. Cruise tracks showing the three main transects located over the mid-shelf to the oceanic waters and sampling sites are presented in Fig. 3-1. Details on the location of the sampling positions are presented elsewhere (see Table 1 in Armand et al., 2008).

The physical and chemical oceanography pertinent to the KEOPS study are presented in Park et al. (2008a, b), van Beek et al. (2008), Mongin et al. (2008), Mosseri et al. (2008), and Blain et al. (2007). Information on phytoplankton stock and production, stock and grazing of microzooplankton, and copepod grazing is presented in companion papers (Armand et al., 2008; Christaki et al., 2008; Sarthou et al., 2008). Complementary information on satellite-image-derived primary production has been supplied by Uitz et al. 2009.

3.2.2.2 Mesozooplankton sampling

Zooplankton vertical net tows were conducted at stations with odd numbers. Three stations (A3 and B5 in the core of the bloom, and C11 in high-nutrients low-chlorophyll— HNLC— waters) were visited several times during the cruise, allowing us to study temporal variations. Mesozooplankton were sampled using double Bongo nets fitted with 330-µm mesh sizes mounted with filtering cod ends. Hauls were done from 200 m to the surface at $1ms^{-1}$. A flow-meter was used to obtain accurate sampled volumes. The content of one of the two nets was preserved in buffered seawater–formalin solution (4%) for further laboratory study of zooplankton community structure and biomass. The material of the second net was placed in small containers and immediately deep-frozen (-80 °C) for further gut content analysis. At stations A3 and C11, part of the material was immediately diluted with filtered seawater for respiration rate experiments (see the following text).

In addition, the abundance and vertical distribution of copepod nauplii were estimated at A3 (5 times) and C11 (once) using waters collected with the CTD/rosette at six depths (10, 20, 40, 60, 80 and 100 m). At each depth, 12 L of water was sieved through a 50 µm mesh. Samples were then preserved in 4% borax-buffered formalin seawater and counted once back in the laboratory in France.

3.2.2.3 Analysis of samples

Mesozooplankton community structure was described following two different approaches, the first was the traditional taxonomic determination using dissecting microscope, and the second was based on size spectrum analysis using a bench-top version of the Optical Plankton Counter Focals® OPC-1L (lab OPC).

Taxonomic determination was made at a limited number of key stations (A3, B5, C11 and KERFIX) using a LEICA MZ6 dissecting microscope and a Bogorov tray. Zooplankton were identified down to species level. For large calanoid copepod species, early (C1–C3) and late (C4 and C5) copepodite stages were counted separately.

Net tow samples from all stations were processed with a lab OPC. OPC has been recently used to study zooplankton community in various areas and has been validated by comparisons with traditional sampling methods (Huntley et al., 1995; Zhou and Huntley, 1997; Gallienne and Robins, 1998; Beaulieu et al., 1999; Grant et al., 2000; Woodd-Walker et al., 2000; Zhou and Tande, 2001; Edvardsen et al., 2002; Riandey et al., 2005; Sourisseau and Carlotti, 2006; Vanderploeg and Roman, 2006). Our lab OPC setup is similar to the one described by Beaulieu et al. (1999) and used in Riandey et al. (2005) and Sourisseau and Carlotti (2006). Organisms are gently introduced into the water circulation system. The crosssection of any particle is estimated (digital size) and is converted into equivalent spherical diameter (ESD) following a semi-empirical formula (Focal Technologies Inc., 1997). Any particle with an ESD larger than 250 µm is counted by the OPC. To avoid coincidence, we imposed a maximum count rate at 20 particles min^{-1} and a constant flow rate at 18 L min^{-1}. The shape of the size spectrum was obtained by counting at least 1000 particles (Sourisseau and Carlotti, 2006).

At most stations located on transects A and B, high densities of chains of diatoms (mainly *Thalassiossira antarctica*, see Armand et al., 2008) were also collected by the Bongo nets, which tended to clog the net. The presence of these diatoms led to a higher retention rate of small-size individuals. Therefore, before processing the samples through the OPC, samples had to be delicately cleared of large clump of diatom chains with fine forceps. Moreover, during the introduction of the sample into the glass tube of the water circulation system, we gently re-suspended the sample using a stainless steel grid (diameter 8 cm, mesh size 1 cm, open area ca. 70%, initially built for turbulent experiments, see Caparroy et al., 1998) that broke the agglomerates and detrital particles in smaller particles below the 250 µm ESD not

detected by the lab OPC. For data treatment, particles counted within the eight first digits (below 287 µm) were not taken into account.

The biovolume of a particle of a given ESD was calculated by assuming each particle as a sphere. In order to estimate the total biomass of the particles measured by the OPC, the total biovolume (BV, mm^3) was converted into biomass (*W*, mgDW) using the following relationship log (*W*) = 0.865 log (BV)-0.887 (Riandey et al., 2005). Carbon content has been assumed to be 50% of body dry weight.

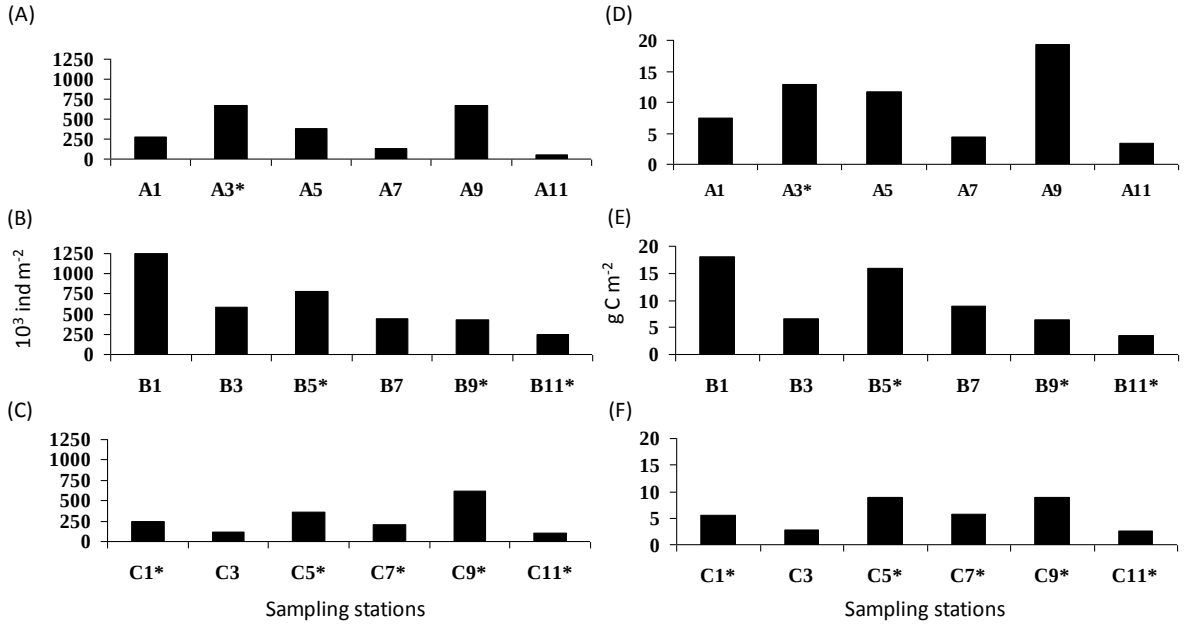

Figure 3-2. Integrated 0–200 m OPC abundance (A–C) and OPC biomass (D–F) for the different stations over the three transects. Transect A from 20 to 23 January; transect B from 29 January to 2 February; transect C from 5 to 9 February. Asterisk (*) indicates dark-night sampling. Positions of all stations and bathymetry are presented in Fig. 1.

The abundance and biomass of each specific ESD were then grouped into four ESD size fractions (287–500, 500–1000, 1000–2000, and >2000 mm), and summed to deliver the total abundance and biomass per sample over the upper 200 m. Abundance and biomass values are normalized to the volume of water filtered *in situ*. In this article, OPC abundance and OPC biomass will correspond to the values derived from the lab OPC treatment. ANOVA test (5% significance level) was used to test differences of abundances and biomass between stations or oceanic areas.

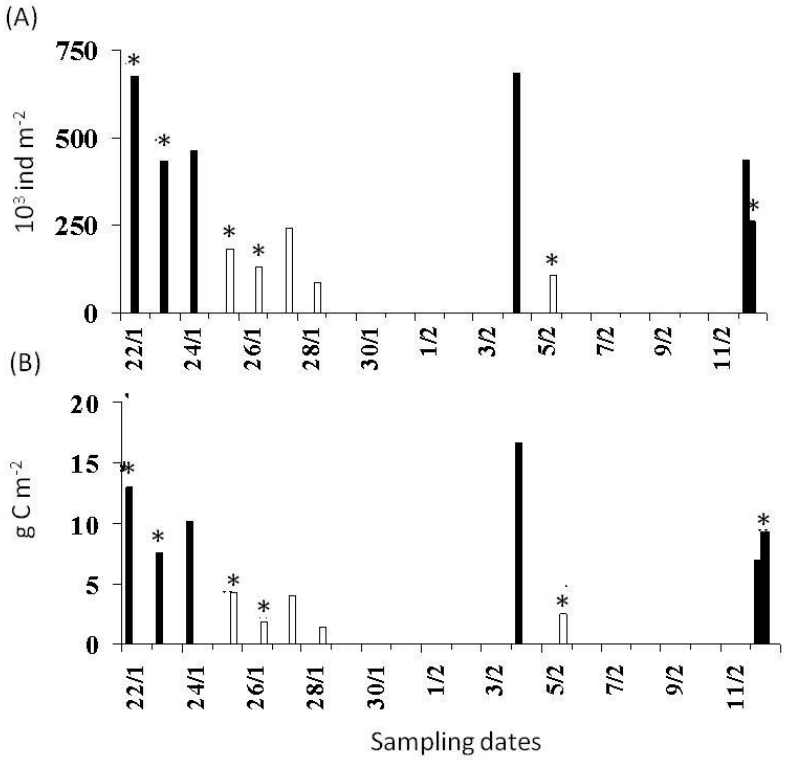

Figure 3-3. Temporal variation of integrated 0–200 m OPC abundance (A) and OPC biomass (B) at A3 (black) and C11 (white). Asterisk (*) indicates dark-night sampling.

3.2.2.4 Copepod gut fluorescence method

Samples were quickly thawed, then sorted into three groups (small, large copepods and euphausiids) using a dissecting microscope under dim light and with cold filtered seawater (at approximately 0–3 °C) and treated as described by Mackas and Bohrer (1976). Aliquots of 15 individuals of copepods larger than 3 mm, and aliquots of 50 individuals for smaller copepods, were picked and placed in glass tubes containing 10 mL of methanol in the cold and dark for extraction. Gut pigment analysis was done with a Turner Design fluorometer. Chlorophyll *a* and pheopigment concentration were measured according to the method of Yentsch and Menzel (1963) modified by Holm-Hansen et al. (1965). The gut pigment contents (ng Chl *a* eq ind^{-1}) were calculated according to Wang and Conover (1986), where ng chlorophyll *a* equivalents (ng Chl *a* eq) equal Chl *a* + pheopigment.

3.2.2.5 Individual respiration measured by coulometric total carbon dioxide technique

Respiration rates of key zooplanktonic species such as copepods, ctenophores, annelids, and euphausiids were measured during 24h stations (A3 and C11). We used a coulometric total

carbon dioxide technique to measure the CO_2 release (Mayzaud et al., 2005). Analysis of seawater TCO_2 throughout the cruises provided quality assessment of the precision and accuracy of the measurements.

The collected zooplankton was immediately placed in a large plastic cooler filled with surface seawater and kept at *in situ* temperature. Large individuals were rapidly sorted, and grouped on the basis of size and species or genera; each group was then placed in beakers filled with filtered seawater (0.45 µm) for less than 1 h. Individuals of a same species or genus were placed individually (for larger zooplankton organisms such as annelids, ctenophores and euphausiids) and by groups of 3–5 (for copepod species) in 125 mL flasks filled with filtered seawater saturated in oxygen. Animals were incubated in the dark at *in situ* temperature (2–3°C) for 15–20 h. Control bottles (0.45 µm-filtered seawater) without zooplankton were

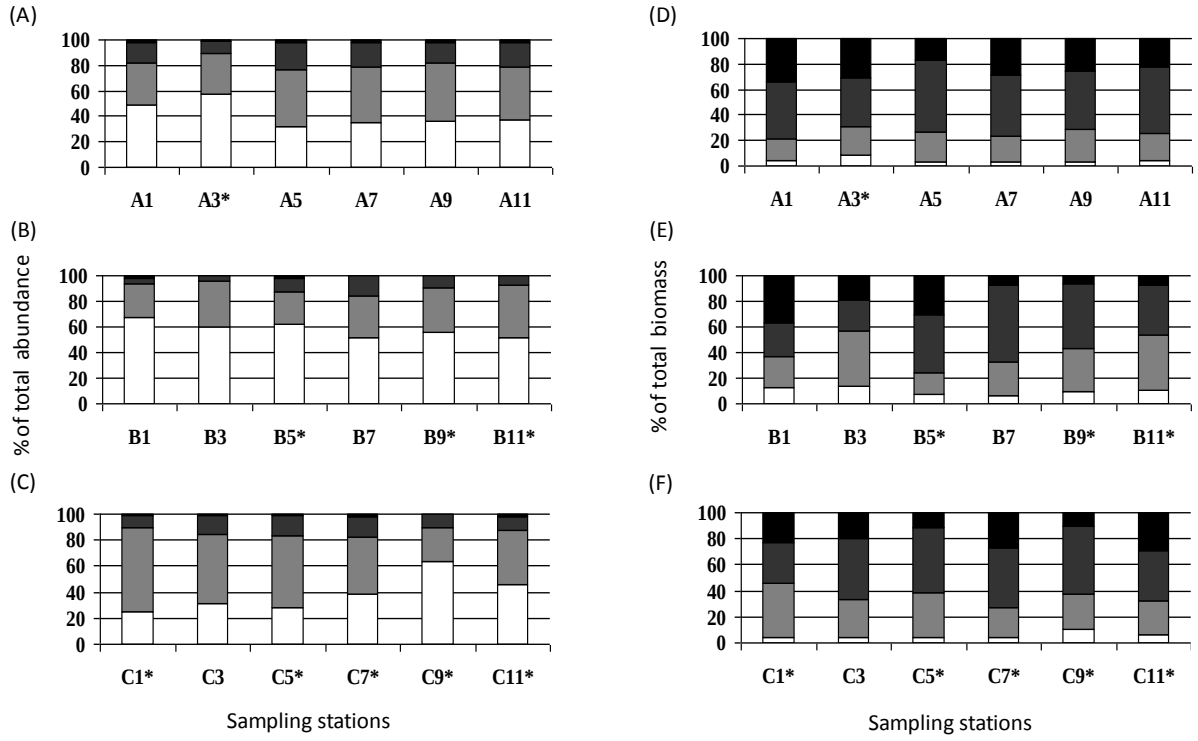

Figure 3-4. Size fraction distribution of OPC abundance (A–C) and OPC biomass (D–F) for the four size fractions: < 500 µm: white; 500–1000 µm: light gray; 1000–2000 µm: dark gray; >2000 µm: black. Asterisk (*) indicates dark-night sampling.

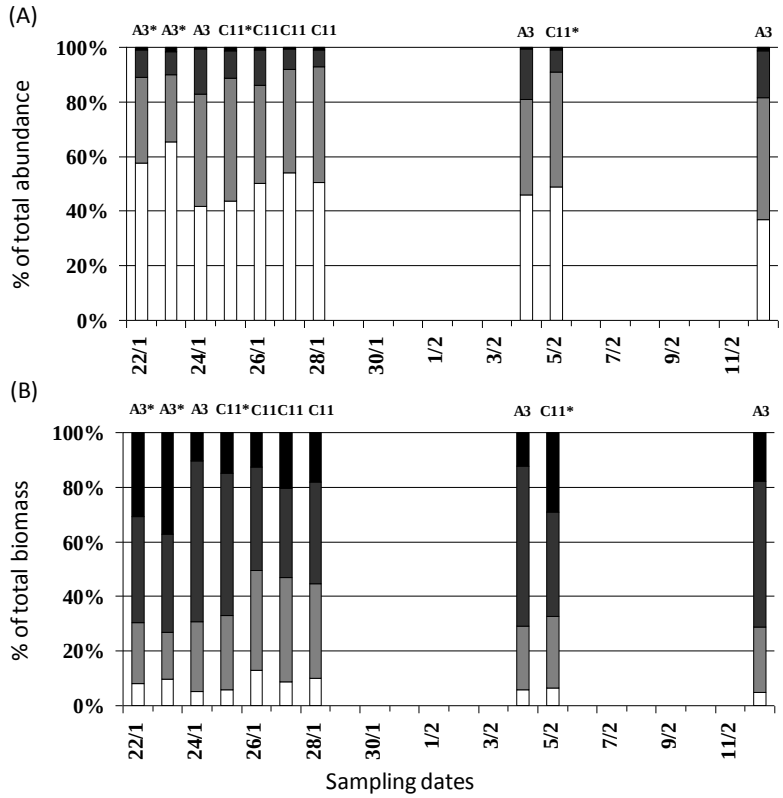

Figure 3-5. Size fraction distribution of OPC abundance (A) and OPC biomass (B) at A3 and C11 for the four size fractions: < 500 µm: white; 500–1000 µm: light gray; 1000–2000 µm: dark gray; > 2000 µm: black. Asterisk (*) indicates dark-night sampling.

incubated under the same conditions. CO_2 production was computed by difference between start and end of the incubations, corrected for possible changes in control bottles.

3.2.2.6 Ingestion and respiration derived from allometric relationships

In order to estimate the ingestion and respiration rates of the whole mesozooplankton, we applied two allometric relationships to the biomass size spectra delivered by the lab-OPC. First, Atkinson (1994) established a relationship between mass-specific ingestion (*I*, in mg C ind^{-1} day^{-1}) and individual body dry weight (DW, in mg) of grazers by pooling data from a large number of on board-incubation experiments: log I = 0.33(70.070) logDW-0.43, where ingestion was mainly based on natural phytoplankton. Rather than using the whole dataset of Atkinson (1994), which gives ingestion rates with a range of one order of magnitude for any body dry weight, we propose a new relationship log (*I*) = 0.523 log(DW)-0.43, which fits only the upper range of the mass-specific ingestion values of Atkinson (see his Fig. 4, 1994). This

new relationship delivers a daily ingestion rate equal to 3 % of the body carbon ingested per day by a copepod weighing 1 mg DW (i.e. copepod assemblages dominated by *Calanus propinquus*), comparable to the maximum value (3.3 %) measured during grazing experiments run by Sarthou et al. (see their Table 3-2, 2008). Similarly, a relationship established by Mayzaud et al. (2002a) between respiration rate (R, ml O_2 ind^{-1} day^{-1}) and body dry weight (DW, mg) of copepods from the Kerguelen area was used: $log\ R = 0.78\ (\pm 0.018)\ log\ DW + 1.28\ (\pm 0.016)$ (R^2 = 0.988). Respiration was converted to carbon assuming a RQ = 0.9 (Mayzaud et al., 2002a).

3.2.3 Results

3.2.3.1 Hydrology and trophic conditions

Different water masses were identified over the shelf, in the oceanic area, and at KERFIX (Park et al., 2008b). The upper 200 m of the water column consisted of Antarctic surface water with a wind-mixed layer (WML) ranging from 44 to 128 m in thickness, deepening from the shelf to oceanic waters. Over the whole area, the surface salinity varied very little, from 33.80 to 33.93 and decreased with depth by less than 0.5 within the upper 200 m. Surface temperature displayed, on the other hand, much stronger variation, with values between 1.74 and 1.98°C at C11 and between 3.57 and 3.97°C at A3, and decreased with depth, reaching a minimum value (-0.2°C at C11 and 1°C at A3) at 150–200 m depth, respectively (see Park et al., 2008b for more details).

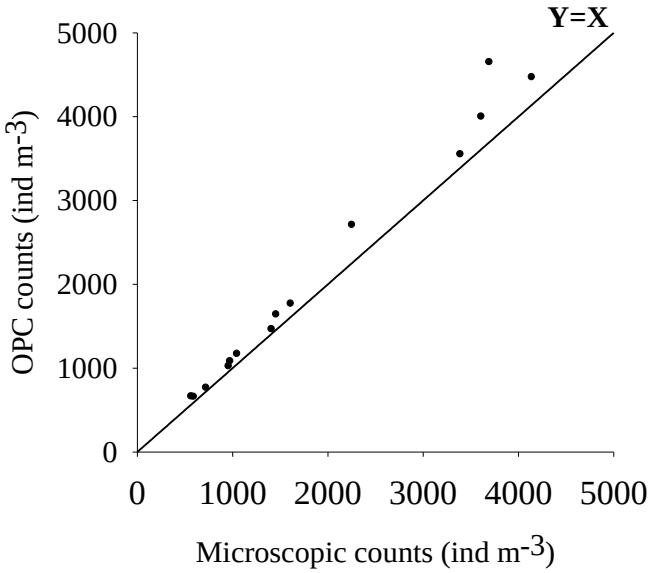

Figure 3-6. Comparison between OPC and microscope counts for stations A3 (six samples), C11 (five samples), B5 (one sample) and KERFIX (two samples).

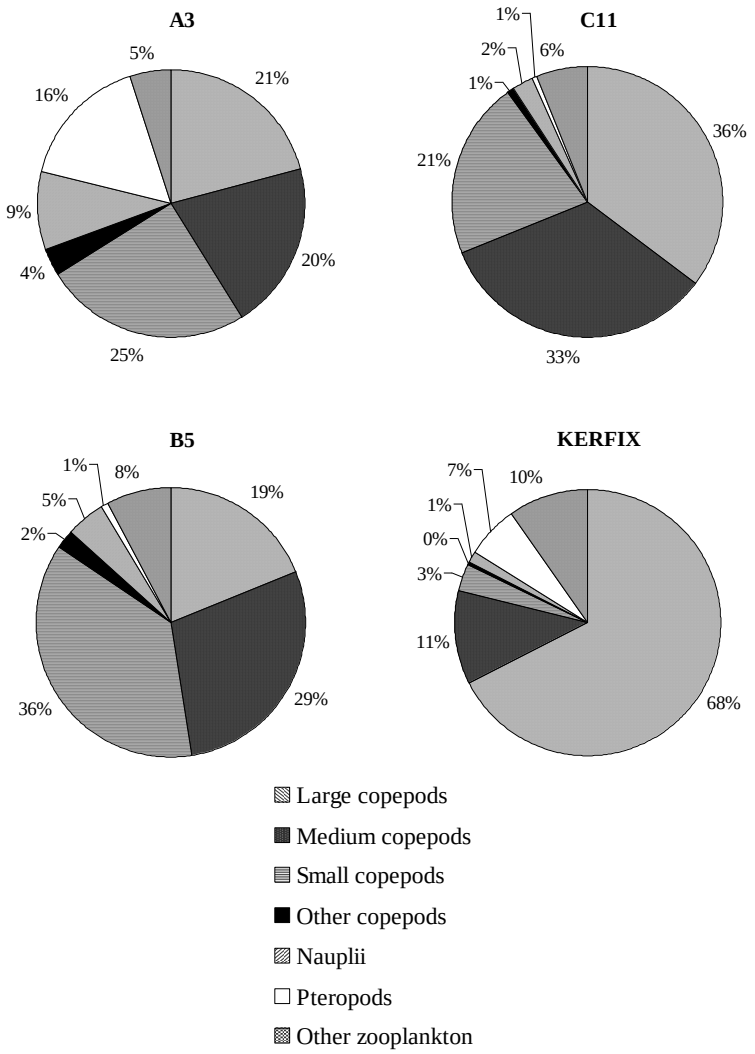

Figure 3-7. Composition of the zooplankton community within the top 200m at A3 (24 January), C11 (28 January), B5 (1 February), Kerfix (10 February). Large-size copepods are defined as all copepodites and adult stages of *Calanus simillimus*, *Calanus propinquus*, *Metridia lucens*, *Paraeuchaeta* sp., *Pleuromamma robusta* and *Rhincalanus gigas*. Medium size copepods are defined as late copepodite and adult stages of *Clausocalanus* spp. and *Microcalanus* spp. Small copepods are defined as adult stages of *Oithona similis*, *Oithona frigida* and *Oncaea* sp. ''Other copepods'' and ''Nauplii'' represent undefined copepodite and nauplii stages. Other zooplankton organisms are defined as appendicularians, chaetognaths, euphausiids, polychaetes, amphipods, ostracods and radiolarians.

Above the Kerguelen Shelf, A3 was located in the middle of the intense phytoplankton bloom (Blain et al., 2008). Satellite images indicated that the bloom started 2 months before the KEOPS-cruise and lasted to the end of February. The mean chlorophyll concentration in the upper 200 m was, on an average, 3 times higher on the shelf than off shore. Surface phytoplankton biomass ranged from 0.26 to 2.78 µg Chl *a* L^{-1} on the shelf, whereas in the HNLC region concentrations were overall very low (0.20–0.35 µg Chl *a* L^{-1}). The associated autotrophic (Armand et al., 2008), bacterial (Obernosterer et al., 2008) and microplanktonic (Christaki et al., 2008) communities revealed higher stocks and substantially higher biomass,

and higher rates of production and respiration over the shelf than in the surrounding HNLC waters. The diatom community structure above the shelf site changed over time depending on the diatom responses to nutrient availability (Armand et al., 2008), maintaining the highest biomass (50–100 µg C L^{-1}), whereas in the offshore waters, out of the bloom region, the diatom community showed little changes over the 25 day period, with biomass lower than 25 µg C L^{-1}.

3.2.3.2 OPC abundance and OPC biomass distributions

Over the three transects (A, B and C), zooplankton OPC abundance (mean ± S.D.) were, respectively, 364.7 ± 265.2 × 10^3, 624.0 ± 327.0 × 10^3 and 276.1 ± 195.1 × 10^3 ind m^{-2} (Fig. 3-2). For the whole dataset, total zooplankton OPC abundance integrated over the top 200 m (Fig. 2) ranged between 58 × 10^3 ind m^{-2} (minimum observed at A11) and 1249 × 10^3 ind m^{-2} (maximum observed at B1). The OPC biomass varied from 3.44 g C m^{-2} (station A11) to 19.36 g C m^{-2} (station A9). Average biomass along the transects was 9.91 ± 5.98, 9.93 ± 5.78

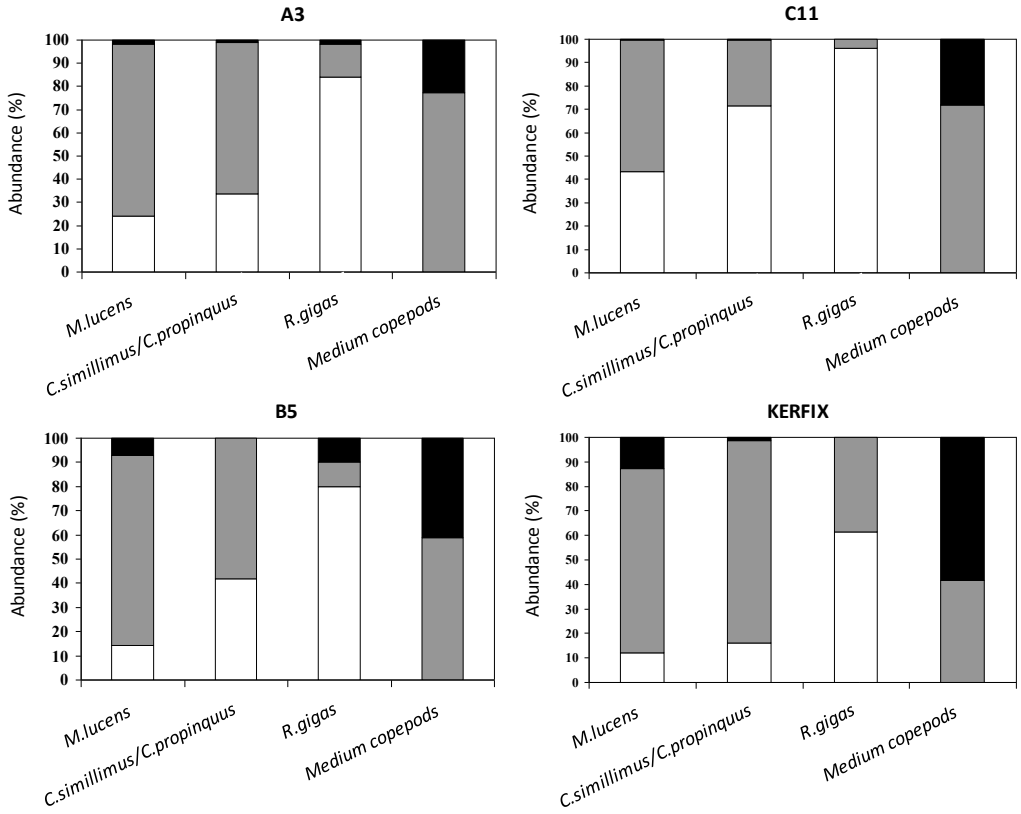

Figure 3-8. Mean stage frequencies of early copepodite stages (C1–C3) in white bars, copepodite stages (C4 and C5) in gray bars, and adults in black bars, in key copepod populations for different areas (see Fig. 3-1).

and 5.7 ± 2.79 g C m^{-2}, respectively, for transects A, B and C. Biomass over the transect C appears to have been the lowest among the three transects, although the differences between the three transects were not statistically different (ANOVA, $p > 0.05$). Any spatial pattern was difficult to extract due to the variability of the biomass between and among transects, partly linked to diurnal variations (see Mayzaud et al., 2002b). Within each transect, the lowest biomass was observed at the most oceanic stations (A11, B11, and C11), with values 3 times lower than the mean biomass value along the transect, but no cross-shelf gradient was detected by ANOVA tests.

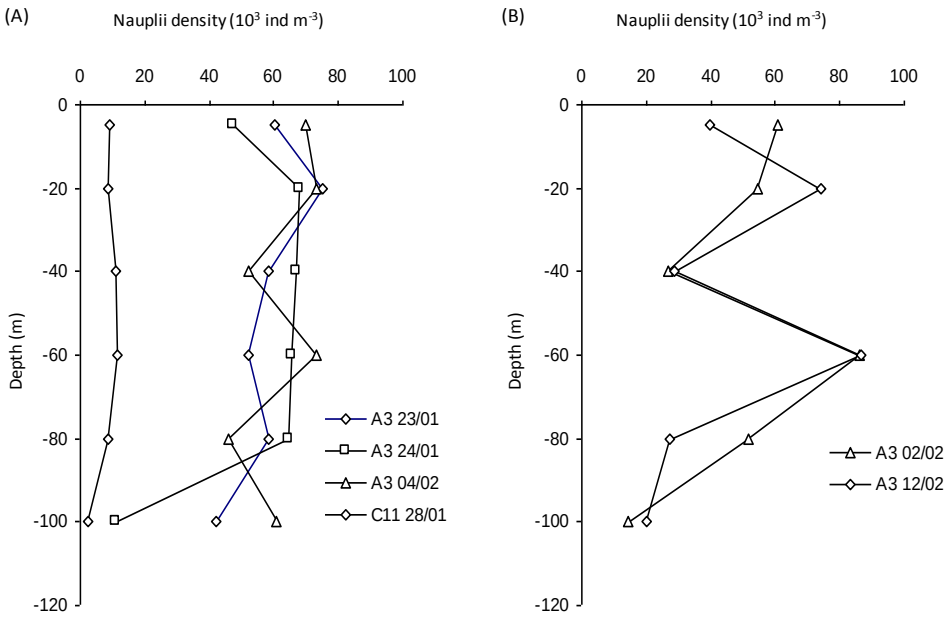

Figure 3-9. Vertical distribution of nauplii densities at six stations within the top 100 m: (A) day sampling; (B) night sampling.

Two stations, A3 and C11, were visited several times during the cruise, allowing us to study temporal variations in the zooplankton community (Fig. 3-3). At A3, OPC abundance varied from 261 × 10^3 to 681 × 10^3 ind m^{-2} (mean ± S.D.: 492.1 ± 161.1 ind m^{-2}), with a corresponding mean value of 10.6 ± 3.6 g C m^{-2}, whereas in C11 OPC abundance varied from 84.2 × 10^3 to 184 × 10^3 ind m^{-2} (mean ± S.D.: 150.0 ± 63.9 ind m^{-2}), with a corresponding mean value of 2.8 ± 1.2 g C m^{-2}. The OPC abundance and OPC biomass values at each A3 and C11 stations showed no significant decrease during the cruise, but inter-site variations were significant (ANOVA, $p < 0.05$) for OPC biomass.

Zooplankton OPC abundance over the three transects was mainly dominated by the two smallest size fractions (285–500 and 500–1000 µm), representing over 80% of the total OPC abundance (Fig. 3-4), whereas the bulk of the OPC biomass was made of large individuals. The size fraction distribution along the three different transects showed a relative homogeneity, except for the OPC biomass fraction > 2000 µm along transect B, and the OPC abundance and OPC biomass fractions 285–500 µm for transect C.

No temporal changes in size structure could be detected at A3 and C11 between the different sampling dates (Fig. 3-5). Individuals > 1mm were slightly more abundant at A3 than at C11.

3.2.3.3 Taxonomic distribution

Total abundance estimated from microscopic counts was compared to the OPC abundance (Fig. 3-6). OPC counts appear slightly higher than microscopic counts, which might be explained by pieces of exuviae as well as aggregates of diatoms that were not differentiated from zooplankton organisms by OPC. However, the use of the lab OPC to estimate zooplanktonic abundance appeared valid, despite the high concentration of diatom chains in the samples (see Section 2).

The mesozooplankton abundance (Fig. 3-7) was dominated by copepods (> 80%), especially by calanoid copepods of large size (*Calanus simillimus*, *C. propinquus*, *Metridia lucens*, *Paraeuchaeta sp.*, *Pleuromamma robusta* and *Rhincalanus gigas*) and medium size (late copepodite and adult stages of *Clausocalanus* spp. and *Microcalanus* spp.), and small copepods (Oithonidae and Oncaeidae). At A3, a large proportion of nauplii was found in the net samples linked to the presence of large quantities of chains of diatom. Undetermined copepodite forms were included under ‘‘other copepods’’. Other zooplankton taxa were represented by euphausiids, chaetognaths, appendicularians, amphipods, polychaetes, ostracods and salps. Non-copepod taxa represented around 4–8% of the overall total abundance. Pteropods quite abundant over the shelf (7–12 % of the total abundance) were counted separately. Moreover, a large proportion of exuviae (> 10 %) was counted at C11 and at KERFIX, but represented only 1–2 % at A3 and B5.

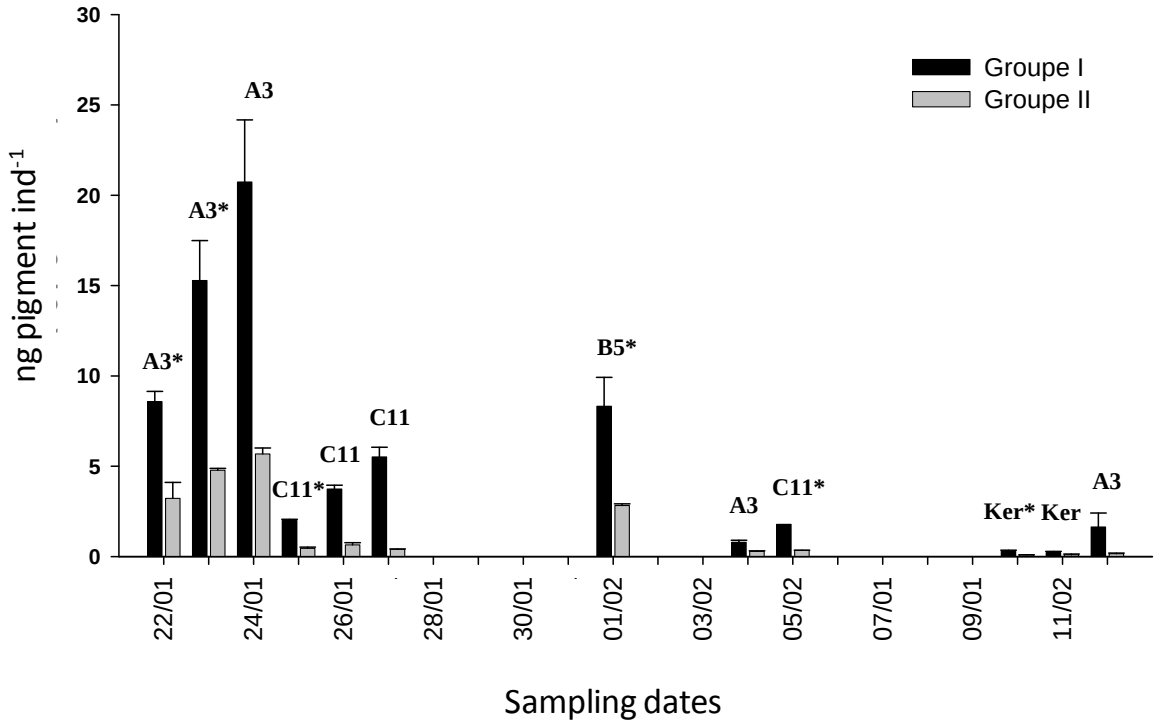

Figure 3-10. Copepod gut contents for two groups of copepods. Groups 1 (black bars) and 2 (gray bars): cephalothoracic length, respectively, upper and lower than 3 mm. Asterisk (*) indicates dark-night sampling.

Table 3-1 Individual respiration rates of key zooplanktonic taxa during KEOPS

Taxa, species and developmental stages	Respiration rates ($\mu g\ C\ ind^{-1}\ day^{-1}$)	No. of individuals	S.D.
R. gigas mainly C5	13.72	36	6.33
C4 and C5 of *C.propinquus* and *C.simillimus*	9.34	34	4.56
Ctenophores	53.89	4	20.01
Thomopteris sp.	819.00	4	154.60
Euphausiids	57.89-256.14	3	
Chaetognaths	79.65 and-103.50	2	

Large calanoid copepods (Fig. 3-8) were mainly represented by young developmental stages, very few adults being collected over the entire period. Young copepodite stages of *R. gigas* were clearly the most dominant form found for this species. For medium-sized copepods, copepodite stages C4 and C5 and adults were equally represented. *C. simillimus*, *C. propinquus*, *M. lucens*, and *Microcalanus* spp. had a higher proportion of adults at C11 than at A3.

The vertical distribution of nauplii density (Fig. 3-9) did not show any specific pattern within the top 80 m for the two stations A3 and C11, but density was 6 times lower at C11 (~10 nauplii L^{-1}) than at A3 (50–70 nauplii L^{-1}). The lowest densities were always reported below 100 m. Nauplii density did not display any temporal variations at A3 (Fig. 3-9A). Diel variation in the vertical distribution of the nauplii was studied twice at A3. A clear minimum was observed at 40 m for the two days studied (February 2 and February 12, 2005) during night samplings (Fig. 3-9B).

3.2.3.4 Metabolic rates

For both groups of copepods (small and large), gut pigment contents (Fig. 3-10) appeared to be highly variable. The highest values were found during the first half of the survey, with lower values reported in the HNLC waters than on the shelf. Then after 1st of February, phytoplankton appeared to represent only a minor component of the copepods diet at all stations. Our values indicate that the feeding on the phytoplankton component might be higher during the first half of the survey and lower later in the season. Individual respiration rates are presented in Table 1.

Rates of ingestion and respiration (Fig. 3-11) were derived from allometric relationships (see material and methods). Calculation from OPC size spectra gave respiration rates ranging from 40 mg C m^{-2} d^{-1} at C11 to 560 mg C m^{-2} d^{-1} at B1. In general, the trend observed in the spatial variations of the respiration was directly related to the spatial distribution of total OPC biomass rather than to the size structure of the community itself. Specific respiration rate did not show any strong variation (between 2.67 % and 3.48 %), with a very low value measured at A11 (1.44 %). Estimated ingestion rates from our allometric relationship ranged from 140 mg C m^{-2} d^{-1} at offshore stations to 1895 mg C m^{-2} d^{-1} (shelf station B1). Specific ingestion rates were estimated at about 4 % to 12 %.

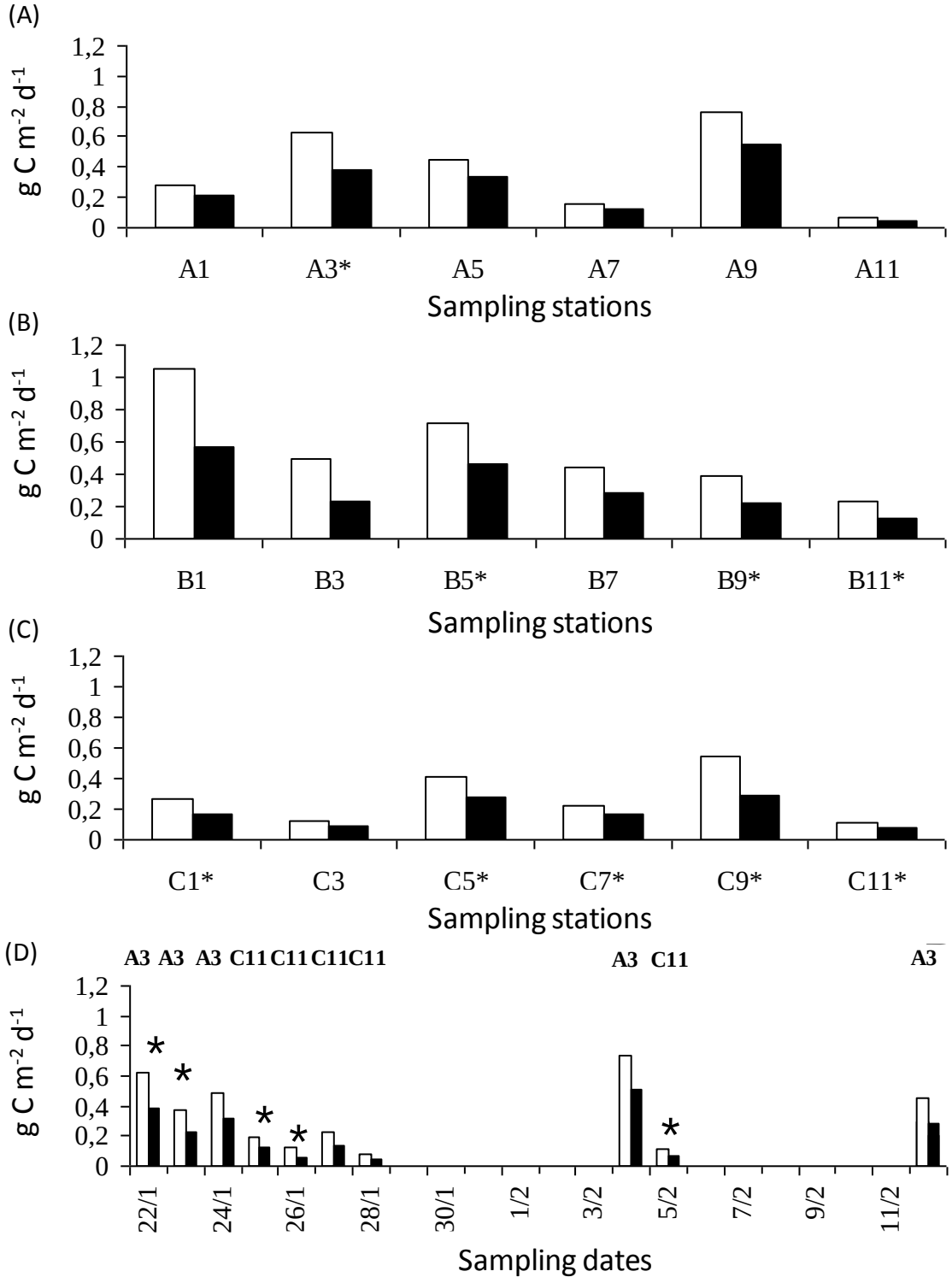

Figure 3-11. Estimated integrated ingestion (white) and respiration rates (black) for the whole mesozooplankton biomass for all sampled stations. (A) Transect A from 20 to 23 January; (B) transect B from 29 January to 2 February; (C) transect C from 5 to 9 February; (D) stations A3 and C11 for different visits (transect and time-series stations). Asterisk (*) indicates dark-night sampling.

3.2.4 Discussion

3.2.4.1 Zooplankton abundance, community structure and biomass

OPC systems, both laboratory and in situ versions, have been increasingly used since their development in the early 1990s (Vanderploeg and Roman, 2006), but only a few studies report their uses in Antarctic regions (Labat et al., 2002; Hernández-León and Montero, 2006). Nevertheless, our double approach confirmed the use of lab OPC to quickly examine Antarctic zooplankton samples. Mesozooplankton displayed high abundance and biomass during KEOPS, similar to those observed by Semelkina (1993) during the SKALP cruises conducted in the eastern region of the Kerguelen in February 1997 and 1998. The area (46–52°S, 64–73°E all around the Kerguelen Island from the shelf to oceanic waters with isobaths down to 4000 m) and time frame (February, April, July–August 1997 and February 1998) sampled during those cruises were much wider than during KEOPS. Nevertheless, according to Semelkina (1993), the sampling period and region of KEOPS corresponded to the space and time window of the highest densities of mesozooplankton in the upper 200 m. Such high densities also were found during spring blooms at similar latitudes in the Antarctic Ocean, particularly in the vicinity of islands, both in the Indian (Errhif et al., 1997) and the Atlantic sectors (Ward et al., 1995; Fransz and Gonzalez, 1997).

The mesozooplankton community was dominated by copepods, particularly copepodite stages of large calanoid copepods, small copepods and nauplii. Semelkina (1993) found in February 1997 and 1998 during SKALP almost the same dominance of copepods (81% of the mesozooplankton biomass) and the same dominant taxa and species of zooplankton. High densities of copepod nauplii also were found both in the net samples and the bottle samples, confirming the possible clogging of the net by the diatoms chains; these nauplii are not usually efficiently retained by a 330-µm mesh size. These high abundances of copepod nauplii appeared to represent an important component of the microbial food web (Christaki et al., 2008). Exuviae also were found in large numbers both at C11 and KERFIX, and to a lesser extent at A3 and B5. Distributions of exuviae are highly dependent on the physical properties of the water column such as advection and mixing, and are also probably consumed by micro- and meso-zooplankton.

Altogether, stage distribution of large copepods, densities of nauplii, and presence of exuviae show that growth and development rates of the organisms were particularly high on the shelf

over the whole period of KEOPS, a situation found in other shelves in summertime (Shreeve and Ward, 1998; Shreeve et al., 2002).

Differences in integrated OPC biomass between oceanic and shelf stations have been reported for several regions (Ward and Shreeve, 1999), mainly due to enhanced primary production over the shelf. Lower average OPC biomass observed along transect C, which took place at the end of the survey, can be related to different factors (i.e. bloom phase, hydrodynamics). Potential effects of the advanced phase of the bloom were not supported by the successive samplings done at A3 and C11 (see Fig. 3-3), which showed no strong temporal variation in biomass. Hydrodynamic features observed along transect C are a stronger candidate (Park et al., 2008b). At C11, lower nauplii and copepodite densities reflected lower local egg production by females, and presence of juvenile stages of copepods also might be related to advection from the shelf rather than to local production.

OPC biomass observed in the south-east region of the Kerguelen Islands during our survey were similar to those measured by Semelkina (1993) in February 1987 and April 1987. She mentioned biomass up to 200 mg DWm^{-3} in the upper 100 m, mainly due to swarms of *C. simillimus*. Other published biomass values around Kerguelen were always lower, but sampling sites differed from those of KEOPS. During ANTARES 2 and 3 cruises along the 62°E (Mayzaud et al., 2002a, b), three stations sampled in the north of the permanent open ocean zone (POOZ) presented biomass ranging from 0.6 to 16.0 g DWm^{-2} in February–March 1994 with a dominance of young copepodite stages (ANTARES 2), and from 2 to 8 g DWm^{-2} in October–November 1995 with dominance of late copepodite and adult stages (ANTARES 3). Observations made during our survey are consistent with those made during ANTARES 2. Thus, it can be assumed that the mesozooplanktonic biomass and population structures during KEOPS at the end of the bloom corresponded to the usual second seasonal peak of biomass in summer related to the recruitment of the new generation (Hopkins, 1971) and exceed estimates made in earlier dates in the season and in areas outside of the bloom distribution.

Diel vertical migration probably had an effect on the size spectrum of abundance of zooplankton, but lack of wire time did not allow us to investigating further this component. However, almost all zooplankton taxa do perform vertical migrations that influence their vertical distribution in space and time (Ward et al., 1995).

3.2.4.2 Mesozooplankton respiration and ingestion

Respiration rates measured during the survey are in the higher range of published values for Antarctic zooplankton. Regarding copepods, Mayzaud et al. (2002a, b) obtained slightly lower values for the same area, but later in the season (September–October). Our values were similar or higher than measurements made by Schnack et al. (1985) in the Peninsula region and Drits et al. (1994) in the Weddell Sea. For the other zooplanktonic organisms, our data are consistent with published respiration rates (Ikeda and Fay, 1981; Ikeda and Mitchell, 1982; Alcaraz et al., 1998).

Based on our measurements of respiration rates and the high dominance of copepods in the region, the use of the allometric relationship between respiration rates and body weight of copepods established by Mayzaud et al. (2002a) delivers a reasonable estimate of the total community respiration. The integrated respiration rates of the whole mesozooplankton community during KEOPS were high compared to Mayzaud et al. (2002a) due to the high biomass of zooplankton found during KEOPS. However, the specific respiration rate of the whole mesozooplankton community (~3.00 % ± 0.36) is a standard value for this area (Mayzaud et al., 2002a).

The integrated ingestion rates of the whole zooplankton community calculated with our allometric relationship (see Section 2) applied to the OPC size spectra is around 3 times the respiration rate (Fig. 3-11). In comparable bloom conditions, Schnack et al. (1985) and Mayzaud et al. (2002b) measured ingestion rates 2–4 times higher than the respiration rates to cover for carbon requirement for growth or reproduction.

In its early phase, the highest values of measured gut contents are comparable to gut fullness reported for Antarctic copepods in other areas (Atkinson et al., 1992a, b; Drits et al., 1994; Tirelli and Mayzaud, 1999; Mayzaud et al., 2002a). Low gut content observed afterwards may be subject to different hypotheses. Changes in gut levels and percentage of individuals with full guts depend on the relative distribution of phytoplankton and grazers (Atkinson et al., 1992b). These low gut content values cannot be related to a reduced energy uptake by the mesozooplankton, due to the high respiration rates and the active growth and development phase during the whole survey, but rather to a shift of prey consumed from fresh phytoplankton to phyto-detritus or animal sources.

In regions where phytoplankton is low, many factors contribute to the functional response of copepods, omnivory being the most efficient feeding strategy (Gentleman et al., 2003). The

various resources of mesozooplankton dominated by copepods are (1) phytoplankton both large cells, as diatoms, and small cells, (2) microzooplankton, mainly ciliates, (3) detritus, and (4) other zooplankton including cannibalism. Most of the dominant Antarctic copepods grow and reproduce whatever the phytoplankton concentration using other food resources such as microzooplankton (Atkinson, 1994, 1996; Mayzaud et al., 2002b) or small zooplankon, like nauplii and small copepodites (Metz and Schnack-Schiel, 1995; Atkinson, 1995) or on detritus (Michels and Schnack-Schiel, 2005).

In comparison with other estimates of grazing rates by copepods in Antarctica (Drits et al., 1994; Schnack et al., 1985; Mayzaud et al., 2002a; Schultes et al., 2006), the phytoplankton concentrations above the MLD (Uitz et al., submitted) at A3 (1–2 µg Chl *a* L^{-1}) and at C11 (0.15–0.2 µg Chl *a* L^{-1}) are, respectively, sub-optimal and limiting for copepods. Sarthou et al. (2008), based on a limited number of experiments, estimated the copepod grazing to be 1–10 % of the chlorophyll stocks. From our measurements of gut pigments contents, assuming a 30 % loss of pigment into non-fluorescence substance (Mayzaud and Razouls, 1992), we estimate the daily impact of grazing of the two sizes of copepods on the phytoplankton stocks > 10 µm. This impact at A3 decreased by a factor ~10 between the beginning and the end of the bloom, from 3.87 ± 2.86 % to 0.42 ± 0.12 % d^{-1} for large copepods and from 24.33 ± 14.31 % to 0.20 ± 0.08 % d^{-1} for the small copepods. Large and small copepods at C11 removed 1.98 ± 2.58 % and 4.86 ± 3.29 % d^{-1}, respectively. We calculated the daily ratio (% copepod body carbon per day) large and small copepods could cover from grazing on phytoplankton as > 10 µm. Only small copepods at A3 during the first part of our survey could have thrived on phytoplankton with values (51.83 ± 14.11 % body carbon d^{-1}) above the minimum of 20 % body carbon d^{-1}, implying that food was not limited (Herman, 1983). At C11 and at A3 during the later stage of the bloom daily ratios, based only on phytoplankton food sources, were never met (2.22 ± 1.19 % and 1.04 ± 0.46 % body carbon d^{-1} for large copepods, respectively, and 5.23 ± 1.51 % and 3.02 ± 1.08 % body carbon d^{-1} for small copepods, respectively). In both areas, stocks of ciliates and HNF are probably controlled by mesozooplankton, but they represent a low contributor to the mesozooplankton ingestion at A3 at the beginning of the bloom, whereas they could be a sufficient food complement at A3 during the later stage of the bloom and at C11, when feeding on phytoplankton was low. Other potential food resources as detritus (i.e. phytodetritus, fecal pellets, dead bodies) and cannibalism could occur but cannot be estimated.

3.2.5 Conclusions

Recent iron-fertilization experiments launched from research vessels triggered very large blooms, covering several square miles, but the long-term impact of such artificial bloom on higher trophic levels could not be detected due to the length of the experiments (from a few days to over a month) in comparison to the time-scale from weeks to months needed for zooplankton community to develop (Rollwagen-Bollens and Landry, 2000; Zeldis, 2001; Tsuda et al., 2005, 2006). Obviously during KEOPS, throughout the second half of the natural long-term bloom (>3 months), the mesozooplankton populations were already well established. The zooplankton biomass did not increase, and species composition, dominated by copepods, did not change significantly. Such apparent absence of numerical response to iron-enriched bloom at high latitudes has been observed during SOIREE, SEEDS and SERIES (Zeldis, 2001; Tsuda et al., 2005, 2006). In the Southern Ocean, many zooplankton species are able to maintain high stocks of overwintering forms during winter time (Atkinson, 1998), which use the bloom to initiate new generations or to complete their life cycle. The high numbers of juvenile forms of copepods during KEOPS and the high respiration rates indicate active growth and development. More investigations are needed to study the mesozooplankton response in term of physiological and demographical rates to show how much the variability in intensity and duration of the recurrent bloom in Kerguelen could influence the persistence of these populations. Gut content observations show that the direct mesozooplankton grazing on phytoplankton probably played a minor role in the control of the primary production as shown in many studies in Antarctic waters (Hopkins, 1987; Atkinson and Shreeve, 1995; Atkinson et al., 1996; Ward et al., 1995). However, its role as top predator of the planktonic system and particularly its control of the microzooplankton component should be investigated more thoroughly.

3.3 Complément d'étude sur les communautés zooplanctoniques.

Dans l'article précédent, la composition taxonomique du zooplancton n'avait été étudiée que dans un nombre limité de stations clés (A3, B5, C11 and KERFIX) ne permettant pas une analyse complète de la variabilité spatiale en relation avec les paramètres environnementaux. Pour pallier ce problème nous avons complété l'étude taxonomique en analysant l'ensemble des stations, nous permettant ainsi de réaliser une analyse multi-variée approfondie. L'analyse de co-inertie permet de croiser un tableau "environnement" (11 paramètres physiques, chimiques et biologiques intégrés sur les 200 premiers mètres) et un tableau "zooplancton" (taxons identifiés) en considérant l'ensemble des stations. Les abondances taxonomiques et leurs abréviations respectives sont présentées en Annexe 1. Les nauplii et les *Oncaea*/*Triconia* spp. ont été supprimés de l'analyse car leur échantillonnage au filet de 330 µm n'est pas satisfaisant. De même, la station KERFIX n'a pas été utilisée dans cette analyse en raison du manque de données environnementales.

Le premier plan factoriel explique 54 % de la variance dont 32 % par le premier axe. Dans le système « environnement », trois groupes de stations sont distincts. Le premier groupe concerne les stations B9, B11 et C11 qui sont les stations les plus océaniques, représentatives de la zone HNLC caractérisée par de plus fortes concentrations en ammonium et en petites cellules phytoplanctoniques. A l'opposé, les 3 premières stations des deux radiales les plus au Nord (A1, A3, A5 et B1, B3, B5) sont caractérisées par des valeurs en chlorophylle *a* et en production primaire plus importantes, représentatives de zones plus eutrophes. Ainsi le premier axe correspond à un axe « trophique » avec les stations moins productives à droite et les plus productives à gauche. Le dernier groupe de stations représenté par la radiale la plus au Sud (C) et l'extrémité Est des deux autres radiales sont donc des stations intermédiaires d'un point de vue trophique. Ainsi le centre du plateau des Kerguelen se différencie de la zone localisée plus au sud. Cette différenciation se retrouve également dans la distribution de la chlorophylle *a* (Uitz et al., 2009), ce qui peut aussi s'expliquer d'un point de vue physique, l'eau de surface de la radiale C étant en effet plus froide que celles situées plus au nord et présentant des structures turbulentes dus aux courants de marées plus importants (Park et al., 2008).

Dans le système « zooplancton », ces groupes de stations ne sont pas clairement identifiés bien que les stations A3, B1 et B5 soient, comme précédemment, distinctes des autres stations. Les stations caractéristiques de la zone HNLC ne possèdent donc pas une

communauté mésozooplanctonique distincte des stations localisées sur le plateau. Seuls *Pleuromamma robusta*, les appendiculaires, les polychètes et les ostracodes sont clairement distingués des autres taxons. Ces organismes sont souvent représentatifs des zones néritiques. A l'opposé, les copépodes carnivores *Paraeuchaeta* spp. sont quant à eux plutôt représentatifs d'un milieu profond et vivent le plus souvent sous la couche des 200 premiers mètres. La relation entre les coordonnées normalisées des stations sur le premier axe des deux systèmes (« environnement » et « zooplancton ») reflète le degré d'association entre les paramètres environnementaux et les taxons du mésozooplancton (Fig. 3-12). Cette relation n'est pas très forte (R^2 = 0,42; p <0,01) avec des valeurs très dispersées autour de la ligne d'égalité indiquant peu d'association entre les paramètres physiques, chimiques et biologiques et la distribution de la communauté mésozooplanctonique. Cependant, cette analyse ne tient pas compte des ressources trophiques autres que les producteurs primaires. Ainsi la prise en compte d'autres sources de nourriture potentielles comme le protozooplancton (HNF et ciliés) dans l'analyse aurait peut-être donné une structuration plus réaliste. Nous avons en effet démontré que les taux d'ingestion des copépodes sur les seuls producteurs primaires étaient insuffisants pour équilibrer leurs besoins métaboliques et donc qu'un autre type de nourriture que l'herbivorie était probable. Cela est également suggéré dans cette région par Razouls et al. (1998) et Mayzaud et al . (2002).

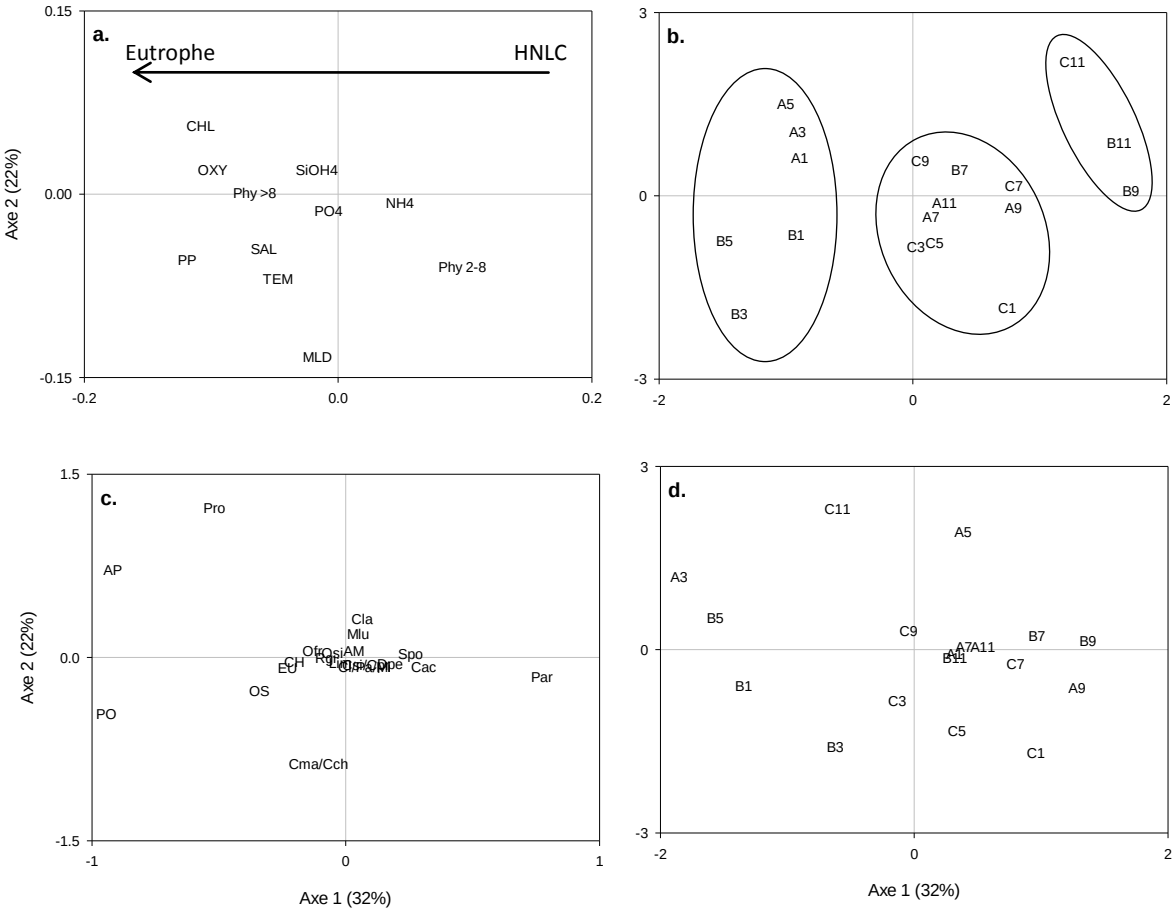

Figure 3-12. Analyse de co-inertie : plot des variables environnementales (a.) et des stations (b.) dans le système « Environnement » et plot des taxons du mésozooplancton (c.) et des stations (d.) dans le système « Zooplancton ». CHL : chlorophylle *a*, MLD : profondeur de la couche de mélange, OXY : oxygène, PP : production primaire, Phy 2-8 : phytoplancton entre 2 et 8 µm, Phy > 8 : phytoplancton > 8 µm, SAL : salinité, TEM : température.

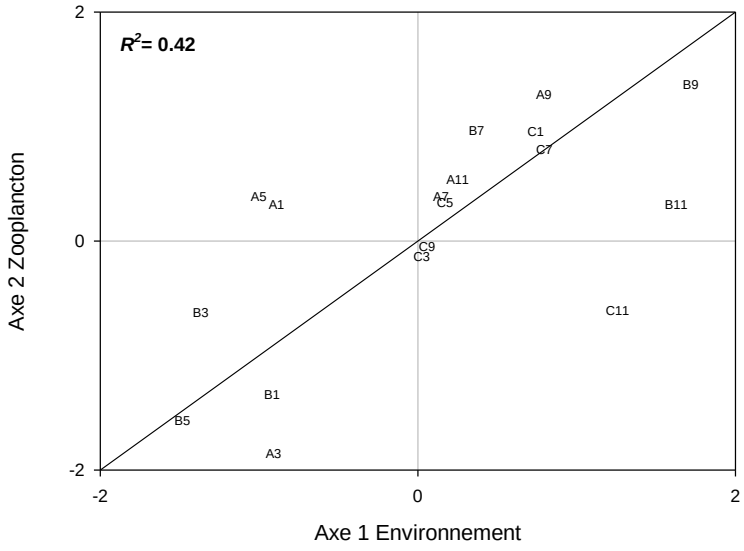

Figure 3-13. Analyse de co-inertie : relation entre les coordonnées normalisées des stations dans le premier axe des deux systèmes (« Environnement » et « Zooplancton »). La droite représente l'égalité entre les coordonnées dans les deux systèmes.

3.4 Conclusions générales sur KEOPS

Cette étude a mis en évidence que la zone productive du plateau des Kerguelen supporte une forte biomasse mésozooplanctonique comparée à la zone HNLC de l'océan Austral. Plusieurs éléments ont permis de démontrer que la communauté des copépodes était bien établie : dominance des stades copépodites, densité élevée de nauplii et quantité d'exuvies retrouvées dans les collecteurs suggérant des taux de croissance et de développement élevés. Cependant les mesures de fluorescence des contenus stomacaux ont révélé de faibles taux d'ingestion de phytoplancton ne permettant pas de couvrir les dépenses métaboliques basales, notamment vers la fin de la floraison, bien que les concentrations en chlorophylle soient élevées. De plus nous avons mesuré des taux de respiration importants pour l'océan Austral impliquant une activité métabolique élevée. Ceci implique donc que les copépodes se nourrissent sur un autre type de nourriture que les organismes photosynthétiques. Cette hypothèse est confortée par les résultats de Sarthou et al. (2008) qui, au cours de la même campagne, ont mesuré un faible impact du broutage des copépodes sur le phytoplancton, représentant 1 à 10 % seulement du stock de chlorophylle *a* par jour. De plus, Christaki et al. (2008) ont mesuré de faibles concentrations en ciliés alors que la concentration en producteurs primaires permettait le développement d'une population plus importante, suggérant une forte prédation des copépodes sur le protozooplancton. La prédation journalière par le zooplancton peut atteindre 57 % de la production des ciliés pour seulement 4 % de la production primaire en zone HNLC (Atkinson, 1996). Cependant dans le cas d'une expérience d'enrichissement en fer (EisenEX), les diatomées constituaient jusqu'à 88 % du carbone ingéré pour le copépode *C. simillimus* dont la population a une consommation journalière équivalent à 15 % du stock en diatomées (Schultes et al., 2006). Par contre, dans cette même étude les copépodes < 2 mm et *R. gigas* ne consommaient que 1.5 % par jour du stock phytoplanctonique. Ceci indique que chaque espèce de copépode possède sa propre sélectivité vis-à-vis des proies. De plus cette sélectivité peut changer au cours du temps comme cela a été montré pour *R. gigas* où en période de floraison estivale la source majeure de nourriture est le phytoplancton alors qu'au printemps et en automne, en période de pré- et post-floraison, les protozoaires, les nauplii et les détritus constituent une grande partie de son alimentation (Atkinson, 1998).

Ainsi, même en période productive, comme au cours de notre étude, les diatomées ne constituent qu'une partie du carbone ingéré par le zooplancton sur le plateau des Kerguelen. Comme la concentration des producteurs primaires est importante, l'impact du broutage est négligeable. De plus il est possible, comme cela a déjà été observé par Henjes et al., (2007) au

cours de l'expérience EisenEx, que le contrôle top down des copépodes sur le microzooplancton entretienne une production plus importante de diatomées en entrainant par effet cascade une diminution du nombre de ses consommateurs microzooplanctoniques. Cet effet de cascade permettrait ainsi potentiellement d'allonger la durée de floraison au-delà de 3 mois sur le plateau des Kerguelen.

4 CAS D'UN GRADIENT D'OLIGOTROPHIE EN MEDITERRANEE

4.1 Introduction

Un des principaux objectifs de la campagne BOUM est de donner une description des paramètres biogéochimiques et de la diversité biologique de la mer Méditerranée selon deux axes (de l'embouchure du Rhône au centre du bassin occidental, axe nord-sud et du centre de ce dernier aux côtes de la Syrie, axe ouest-est), durant la période où la stratification est maximale. Les variables environnementales classiques (température, salinité, alcalinité, concentration en oxygène dissous) ainsi que les pools organiques et minéraux du carbone et des éléments biogènes (C, N, P et Si), et les pigments ont été mesurés. D'autres variables plus spécifiques (fixation de l'azote, diversité des diazotrophes et temps de recyclage du phosphate minéral dissous) ont été également mesurées à quelques profondeurs choisies sur trois stations de longue durée. Un des intérêts est de pouvoir décrire les variations des caractéristiques biogéochimiques et biologiques le long d'un gradient d'oligotrophie (Moutin et al., 2011).

En effet, une des caractéristiques de la mer Méditerranée est sa faible concentration en phosphore inorganique dissous qui limite la production primaire (Berland et al., 1980; Thingstad & Rassoulzadegan, 1995; Thingstad et al., 2005). La circulation thermohaline anti estuarienne de la Méditerranée couplée aux apports en sels nutritifs des grands fleuves (Rhône, Pô) plus importants dans le bassin Ouest, favorisent un appauvrissement de l'ouest vers l'Est en sel nutritifs (Sournia, 1973; Krom et al., 1991 ; Moutin & Raimbault, 2002; Pujo-Pay et al., 2011). Globalement, les eaux de surfaces appauvries en sels nutritifs sont transportées en partie vers le bassin Est à travers le seuil de Sicile alors que les eaux intermédiaires plus denses du bassin Levantin (LIW) circulent vers le bassin Ouest sous la couche euphotique (200-500 m) (voir Pinardi & Masetti, 2000 pour plus de détails) exportant ainsi une partie des sels nutritifs (Krom et al., 2005).

Ainsi, la région la plus oligotrophe est située dans le bassin Levantin avec des rapports nitrate / phosphate des eaux profondes bien supérieurs (28:1) (Krom et al., 1991) à ceux de Redfield (16 :1) (Redfield et al., 1963) généralement observés dans les eaux profondes océaniques. De plus cette région est considérée comme ultra-oligotrophe avec des valeurs de production primaire faibles de l'ordre de 60-80 g C a^{-1} soit environ la moitié de celles observées dans la plupart des régions océaniques oligotrophes telles que la mer des Sargasses (Béthoux, 1989; Krom et al., 2003). La déficience en phosphore serait en partie liée à la pauvreté des apports en eaux douces terrestres se déversant dans la mer et des apports atmosphériques dont

notamment les poussières sahariennes (Guerzoni et al., 1999 ; Ludwig et al., 2009). L'intensité de ce gradient d'oligotrophie est quant à lui déterminé par la balance des processus biologiques telles que la production, l'exportation et la reminéralisation.

Il est admis que les sels nutritifs influencent la chaine trophique (contrôle « bottom up ») de par leur utilisation directe par les organismes autotrophes (bactéries, phytoplancton) et indirecte via les échelons trophique supérieurs (nanoflagellés, microzooplancton) qui se nourrissent principalement de ces organismes. Ainsi, ce gradient ouest-est en sels nutritifs a des répercussions sur la plupart des échelons trophiques. Par exemple, la production et l'abondance virale et bactérienne (Christaki et al., 2001, 2011; Van Wambeke et al., 2002, 2011), la concentration en phytoplancton et la production primaire (Dolan et al., 1999 ; Moutin et Raimbault, 2002; Barale et al., 2008; D'Ortienzo & Ribera d'Alcalà, 2009; Ignatiades et al., 2009) et l'abondance et la biomasse des organismes hétérotrophes de petite taille (Dolan et al., 1999, 2002; Turley et al., 2000; Christaki et al., 2001, 2011; Ignatiades et al., 2009) diminuent d'ouest en est. Nous pouvons donc parler de gradient trophique ouest-est en Méditerranée.

Cependant, aucune étude ciblée et synoptique sur la distribution du mésozooplancton n'a été réalisée de façon intégrée sur l'ensemble de la Méditerranée. Une seule étude, succincte, effectuée en juin 1999 à 9 stations semble indiquer une différence entre les bassins Ouest et Est en termes d'abondance et de biomasse mais pas en termes de composition taxonomique (Siokou-Frangou, 2004).

Dans une étude globale des océans, Longurst (1998) a tenté de mettre en évidence des zones biogéographiques du plancton en tenant compte des processus biogéochimiques. La Méditerranée y est décrite comme appartenant au biome des vents d'ouest atlantique caractérisé par un important mélange des eaux de surface jusqu'en profondeur en hiver et une stratification des eaux de surface à partir du début du printemps avec une production primaire rapidement limitée par les faibles concentrations en sels nutritifs. La mer Méditerranée y est considérée comme une bio-province dans sa globalité, regroupant également la mer Noire.

Nous pouvons donc nous demander comment se comporte la distribution du zooplancton aussi bien en termes de biomasse qu'en termes d'abondance taxonomique en Méditerranée. Est-ce qu'elle peut être considérée comme globalement homogène sur les deux bassins méditerranéens (Longurst, 1998), ou est-ce que cette distribution serait similaire aux gradients ouest-est des paramètres chimiques (Moutin et Raimbault, 2002; Pujo-Pay et al., 2011) et

biologiques (Turley et al., 2000; Moutin & Raimbault, 2002; Christaki et al., 2001) ou peut-on distinguer des écorégions ou bio-provinces pour le mésozooplancton (Bianchi & Morri, 2000)?

Le premier article présenté ci-après a pour objectif principal de caractériser à la fois les stocks (abondance et biomasse) représenté par le métazooplancton et la structure des communautés (taxonomie et taille) le long du gradient trophique. Dans un second temps nous essayerons (1) de mettre en relation cette distribution spatiale avec les paramètres environnementaux les plus représentatifs et (2) de voir s'il existe des zones géographiques distinctes pour le métazooplancton.

Par ailleurs nous pouvons nous demander si l'activité métabolique de la communauté mésozooplanctonique et son impact sur l'écosystème diffèrent le long de ce gradient d'oligotrophie.

Ainsi, le second article s'intéressera à l'activité métabolique des organismes clés de la communauté du mésozooplancton par des mesures de taux d'ingestion, de respiration et d'excrétion. Ensuite à partir de ces taux individuels et des abondances *in situ* présentées dans le premier article, l'impact de la communauté sur les organismes autotrophes sera estimé : contrôle « top down » par le broutage et control bottom up par le recyclage de composés inorganiques dissous.

4.2 "Distribution of epipelagic metazooplankton across the Mediterranean Sea during the summer BOUM cruise"

Biogeosciences, 8, 2159–2177, 2011
www.biogeosciences.net/8/2159/2011/
doi:10.5194/bg-8-2159-2011

Biogeosciences

Distribution of epipelagic metazooplankton across the Mediterranean Sea during the summer BOUM cruise

A. Nowaczyk, F. Carlotti, D. Thibault-Botha, and M. Pagano

Aix-Marseille Université, UMR6535, INSU-CNRS – Laboratoire d'Océanographie Physique et Biogéochimique, Centre d'Océanologie de Marseille, Campus de Luminy, Case 901, 13288 Marseille, France

Received: 14 March 2011 – Published in Biogeosciences Discuss.: 22 March 2011
Revised: 29 July 2011 – Accepted: 1 August 2011 – Published: 9 August 2011

Abstract. The diversity and distribution of epipelagic metazooplankton across the Mediterranean Sea was studied along a 3000 km long transect from the eastern to the western basins during the BOUM cruise in summer 2008. Metazooplankton were sampled using both a 120 µm mesh size bongo net and Niskin bottles in the upper 200 m layer at 17 stations. Here we report on the stock, the composition and the structure of the metazooplankton community. The abundance was 4 to 8 times higher than in several previously published studies, whereas the biomass remained within the same order of magnitude. An eastward decrease in abundance was evident, although biomass was variable. Spatial (horizontal and vertical) distribution of metazooplankton abundance and biomass was strongly correlated to chlorophyll-*a* concentration. In addition, a clear association was observed between the vertical distribution of nauplii and small copepods and the depth of the deep chlorophyll maximum. The distinction between the communities of the eastern and western basins was clearly explained by the environmental factors. The specific distribution pattern of remarkable species was also described.

1 Introduction

Although the Mediterranean Sea represents only ~0.82 % of the total surface of the global ocean, it is the largest quasi-enclosed sea composed of two large basins, the eastern and the western basins, separated by the Strait of Sicily, which are subsequently divided in several sub-basins. It could be assimilated to a mini-size ocean with continental shelves, deep basins and trenches. The surface circulation is driven mainly by the inflow of Atlantic water through the Strait of Gibraltar, its signature being modified as it travels eastward. The Mediterranean is displaying deep water mass formation sites which have shown large modifications through time (Pinardi and Masetti, 2000; Millot and Taupier-Letage, 2005; and review by Bergamasco and Malanotte-Rizzoli, 2010). It is a hot spot for marine biodiversity (Margalef, 1985; Bianchi and Morri, 2000; Coll et al., 2010) with a marine biota composed of endemic and allochtonous species of Atlantic and Red Sea origins (Furnestin, 1968; Bianchi and Morri, 2000). This ecosystem is overall oligotrophic, but paradoxically, significant production do occur which sustain large fisheries and marine mammals communities (Coll et al., 2010; Würtz, 2010). This "maxi-size laboratory" can be then considered as one of the most complex marine environment (Meybeck et al., 2007).

As a whole, the Mediterranean Sea is characterized by a strong eastward gradient in nutrients, phytoplankton biomass and primary production (reviewed in Siokou-Frangou et al., 2010) with ultra-oligotrophic conditions being found in the Levantine basin (Krom et al., 1991; Ignatiades, 2005; Moutin and Raimbault, 2002). From a handful of studies, a similar pattern has also been reported at the basin scale for mesozooplankton abundance (Dolan et al., 2002; Siokou-Frangou, 2004; Mazzocchi et al., 1997; Minutoli and Guglielmo, 2009) but no synoptic view through the western and eastern basins was run to confirm this trend. Moreover, no clear pattern was highlighted for the biomass which presents several hot spots located in the north-western Mediterranean, the Catalan Sea, the Algerian Sea and the Aegean Sea (reviewed in Siokou-Frangou et al., 2010). Currently, the existing datasets are not yet sufficient to get a comprehensive understanding of the metazooplankton distribution in the Mediterranean Sea.

Indeed, many field studies have been realised at regional scales and have highlighted the impact of mesoscale features on the distribution and diversity of metazooplankton in both Mediterranean basins (Ibanez and Bouchez, 1987; Pinca and

Correspondence to: A. Nowaczyk
(antoine.nowaczyk@univmed.fr)

Published by Copernicus Publications on behalf of the European Geosciences Union.

4.2.1 Introduction

Although the Mediterranean Sea represents only ~0.82 % of the total surface of the global ocean, it is the largest quasi-enclosed sea composed of two large basins, the eastern and the western basins, separated by the Strait of Sicily, which are subsequently divided in several sub-basins. It could be assimilated to a mini-size ocean with continental shelves, deep basins and trenches. The surface circulation is driven mainly by the inflow of Atlantic water through the Strait of Gibraltar, its signature being modified as it travels eastward. The Mediterranean is displaying deep water mass formation sites which have shown large modifications through time (Pinardi & Masetti, 2000; Millot & Taupier-Letage, 2005; and review by Bergamasco & Malanotte-Rizzoli, 2010). It is a hot spot for marine biodiversity (Margalef, 1985; Bianchi & Morri, 2000; Coll et al., 2010) with a marine biota composed of endemic and allochtonous species of Atlantic and Red Sea origins (Furnestin, 1968; Bianchi & Morri, 2000). This ecosystem is overall oligotrophic, but paradoxically, significant production do occur which sustain large fisheries and marine mammals communities (Coll et al., 2010; Würtz, 2010). This "maxi-size laboratory" can be then considered as one of the most complex marine environment (Meybeck et al., 2007).

As a whole, the Mediterranean Sea is characterized by a strong eastward gradient in nutrients, phytoplankton biomass and primary production (reviewed in Siokou-Frangou et al., 2010) with ultra-oligotrophic conditions being found in the Levantine basin (Krom et al., 1991; Ignatiades, 2005; Moutin & Raimbault, 2002). From a handful of studies, a similar pattern has also been reported at the basin scale for mesozooplankton abundance (Dolan et al., 2002; Siokou-Frangou, 2004; Minutoli and Guglielmo, 2009) but no synoptic view through the western and eastern basins was run to confirm this trend. Moreover, no clear pattern was highlighted for the biomass which presents several hot spots located in the north-western Mediterranean, the Catalan Sea, the Algerian Sea and the Aegean Sea (reviewed in Siokou-Frangou et al., 2010). Currently, the existing datasets are not yet sufficient to get a comprehensive understanding of the metazooplankton distribution in the Mediterranean Sea.

Indeed, many field studies have been realised at regional scales and have highlighted the impact of mesoscale features on the distribution and diversity of metazooplankton in both Mediterranean basins (Ibanez & Bouchez, 1987; Pinca & Dallot, 1995; Youssara & Gaudy, 2001; Riandey et al., 2005; Molinero et al., 2008; Licandro & Icardi, 2009; Mazzocchi et al., 2003; Siokou-Frangou, 2004; Pasternak et al., 2005; Zervoudaki et al., 2006; Siokou-Frangou et al., 2009). Mesoscale hydrodynamic structures are known also to enhance nutrient

concentrations, and therefore, plankton patchiness stimulating trophic transfers towards large predators.

The BOUM experiment (Biogeochemistry from the Oligotrophic to the Ultra-oligotrophic Mediterranean) was conducted in order to obtain a better representation of the interactions between planktonic organisms and the cycle of biogenic elements in the Mediterranean Sea across the western and eastern basins through a 3000 km survey. Our main goal here was to improve our knowledge on the role of planktonic metazoan (metazooplankton hereafter; Sieburth et al., 1978) in the biogeochemical cycle in such an open oligotrophic ecosystem by coupling standing stock estimations (abundance, biomass, and size classes) and metabolic measurements. The presentation of this work is carried out in two steps. The structural investigation is presented here and the functional part will be presented in another manuscript (Nowaczyk et al., in prep). Therefore, the present study investigates the metazooplankton community spatial distribution (vertical and horizontal) including small-size copepods (nauplii and different copepodite stages) often neglected in previous studies. Finally, we attempt to define the links between the spatial distribution of metazooplankton and the environmental characteristics.

4.2.2 Material and Methods

4.2.2.1 Cruise track and environmental parameters

Cruise transect

A 3000 km transect across the Mediterranean Sea was conducted during the BOUM cruise from 18 June to 20 July, 2008 on board the French N.O. *L'Atalante* (Fig. 4-1). The cruise eastward from the Ionian basin (IB) to the Levantine basin (LB) from June 18 to 29 June; then switched to a westward direction. After a transit period of three days, sampling continued from the Ionian basin through the Sicily Channel (SC), the Algero-Provencal basin (APB) to the Rhône River Plume (RRP). Sampling strategy consisted in 27 short-stay stations (~2-3h) distributed ~100 km apart and long-stay stations (4 days: stations A, B and C) located in the centre of important hydrological features (anticyclonic gyres) (see Moutin et al., 2011 for more details). Location of the sampling stations is presented in Fig. 4-1 and Table 4-1. Physico-chemical parameters and phytoplankton were sampled at all stations whereas the

metazooplankton, ciliates and heterotrophic nanoflagellates (HNF) were samples every other stations.

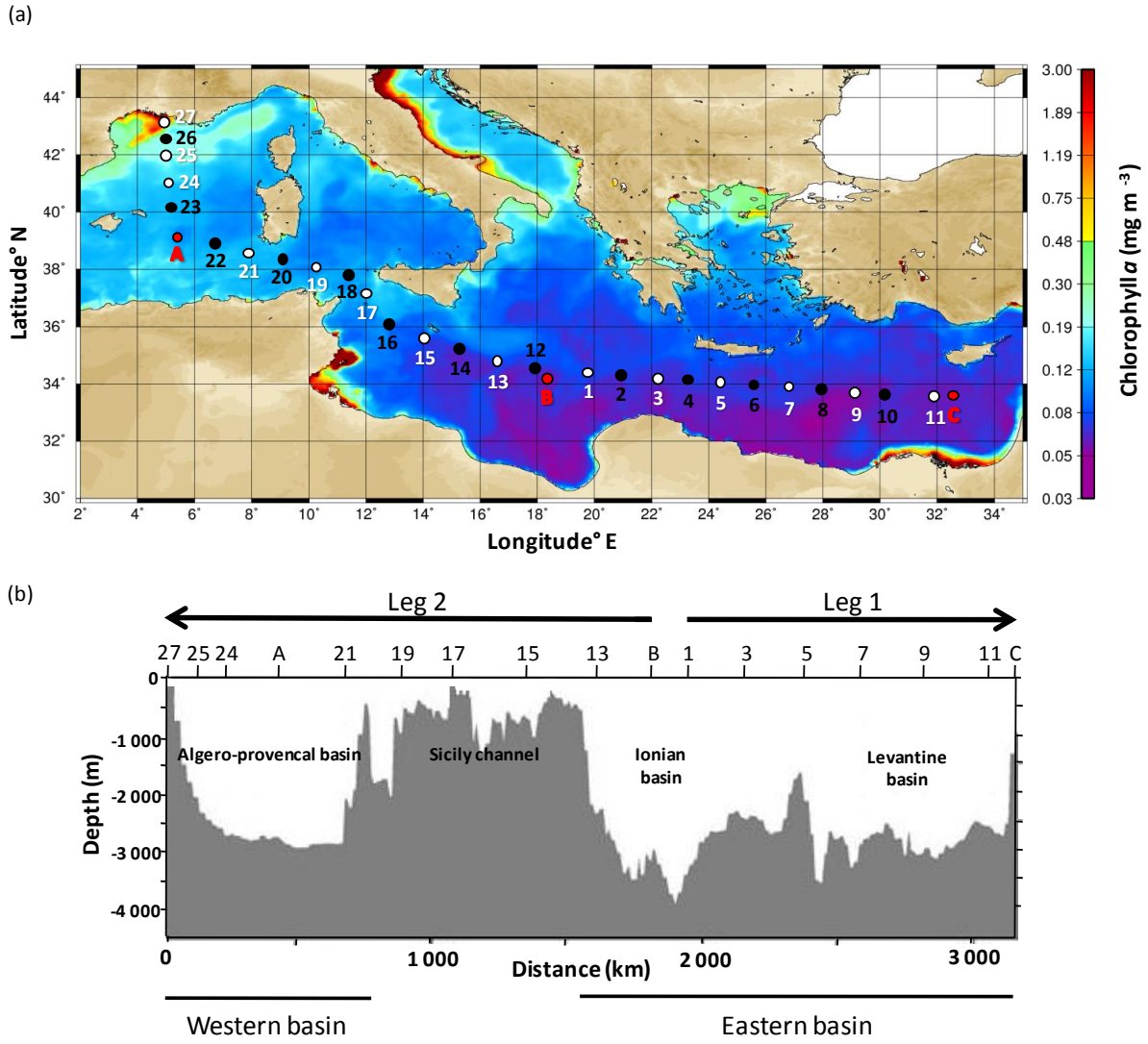

Figure 4-1. (a) Location of sampling stations superimposed on a SeaWIFS composite image of the sea surface integrated chlorophyll *a* concentration (permission to E. Bosc) during the BOUM transect (June 16th – July 20th 2008). Short-stay stations where zooplankton was sampled (white) and not sampled (black) and long-stay stations (red). (b) Bottom depth and geographic areas along the transect.

4.2.2.2 Sampling and analysis of environmental parameters

Vertical profiles of temperature, conductivity and oxygen were obtained using a Sea-Bird Electronic 911 PLUS CTD. Nutrients, chlorophyll, ciliates and HNF were sampled using Niskin bottles. Ammonium and phosphate concentration were immediately measured on board with an auto-analyzer (Bran+Luebbe auto-analyseur II) according to the colorimetric method as fully described in Pujo-Pay et al. (2011). Total chlorophyll-*a* was measured by the fluorimetric methods following a methanol extraction (Herbland et al., 1985). HNF samples

were filtered onto black nucleopore filters and stained with DAPI (Porter & Feig, 1980) and stored at -20°C on board until analysis, then enumerated using LEITZ DMRB epifluorescence microscope. Ciliates samples were fixed in 2 % Lugol's iodine-seawater solution, stored at 4°C and counted using an inverted microscope. These two methods were fully described in Christaki et al. (2011). The same method was used for nanophytoplankton and diatoms identification. The particular organic matter was determined according to the wet oxydation procedure described by Raimbault et al. (1999).

4.2.2.3 Zooplankton

Sampling strategy

Zooplankton was collected within the upper 200 m layer (100 m at st. 17 and 27) using double Bongo nets (60 cm mouth diameter) fitted with 120 µm mesh size and equipped with filtering cod ends. Vertical hauls were done at a speed of 1 m s^{-1}. No flowmeters were available but special care was taken while sampling to keep the cable vertical.

Volume sampled by the net was then reported to the depth of the tow and the opening surface of the net (0.28 m^2). Due to wire time constraints sampling was performed at different times of day and night. The length of time spent at stations A, B and C allowed us to collect zooplankton 3 times at noon and 4 times at midnight, on consecutive days.

Immediately after collection, the cod-end content of the first net was kept fresh and split into two parts with a Motoda box. The first part was processed immediately for biomass measurements. The second half of the sample was collected onto a GF/F filter, placed in a Petri dish, and then deep frozen in liquid nitrogen for further ingestion rates measurements (Nowaczyk et al., in prep). The cod-end content of the second net was directly preserved in 4 % buffered formalin-seawater solution for later taxonomic identification and abundance measurements. Discrete sampling was also performed to study vertical distribution of copepod nauplii and small copepods from water samples collected with the CTD/rosette. At each selected depth, the content of a 12 L Niskin bottle was gently collected onto a 20 µm mesh net and fixed in a 2 % Lugol's iodine-seawater solution. Seven depths were sampled between the surface and 200 m depth at stations A, B and C and only to a depth of 150 m at short-stay stations. The sampling depths were distributed according to the deep chlorophyll maximum depth.

Table 4-1. Position and characteristics (latitude, longitude, bottom depth, geographical region, date, sampling time and shortest distance to the coast) of the zooplankton sampling stations during the BOUM cruise.

Station ID	Latitude (°N)	Longitude (°E)	Bottom depth (m)	Region	Date	Sampling time (h:min)	Distance to the coast (km)
27	43°12	4°55	106	Rhône River Plume	7/18/08	23:10	14
25	41°59	5°00	2267	Algero-Provencal Basin	7/18/08	11:40	140
24	41°05	5°03	2659	"	7/18/08	01:05	130
A day	39°05	5°21	2798	"	7/15/08	11:30	120
A night	39°05	5°21	2786	"	7/15/08	23:30	120
21	38°37	7°54	2055	"	7/11/08	06:30	58
19	38°05	10°13	556	Sicily Channel	7/10/08	11:30	91
17	37°10	12°00	117	"	7/09/08	13:50	82
15	35°40	14°06	588	"	7/08/08	19:00	33
13	34°53	16°42	2097	Ionian Basin	7/08/08	01:30	240
B night	34°08	18°26	3007	"	7/04/08	01:45	260
B day	34°08	18°26	3197	"	7/05/08	11:55	260
1	34°19	19°49	3210	"	6/21/08	05:00	210
3	34°10	22°09	2382	"	6/22/08	01:15	140
5	34°02	24°29	2616	Levantin Basin	6/22/08	19:00	110
7	33°54	26°50	2780	"	6/23/08	13:25	135
9	33°45	29°10	3033	"	6/24/08	07:30	270
11	33°34	31°56	2514	"	6/25/08	04:30	135
C day	33°37	32°39	798	"	6/27/08	14:55	110
C night	33°37	32°39	817	"	6/27/08	23:35	110

Biomass measurement

The subsample for bulk biomass measurement was filtered onto pre-weighted and pre-combusted GF/F filter (47 mm) which was quickly rinsed with distilled water and dried in an oven at 60°C for 3 days onboard. Dry-weight (mg) of samples was calculated from the difference between the final weight and the weight of the filter and biomass (mg DW m^{-3}) was extrapolated from the total volume sampled by the net. Once back on land, carbon and nitrogen contents were measured. Dried samples were grinded, homogenized then split into 3 equal fractions (~0.8-1 mg DW), placed in tin caps and analyzed with a mass spectrometer (INTEGRA CN, SerCon).

Microscope counts

Taxonomic identification and counts of zooplankton were done back in the land laboratory using a LEICA MZ6 dissecting microscope. Very common taxa were counted in sub-samples (1/32 or 1/64), and the whole sample was examined for either rare species and/or large

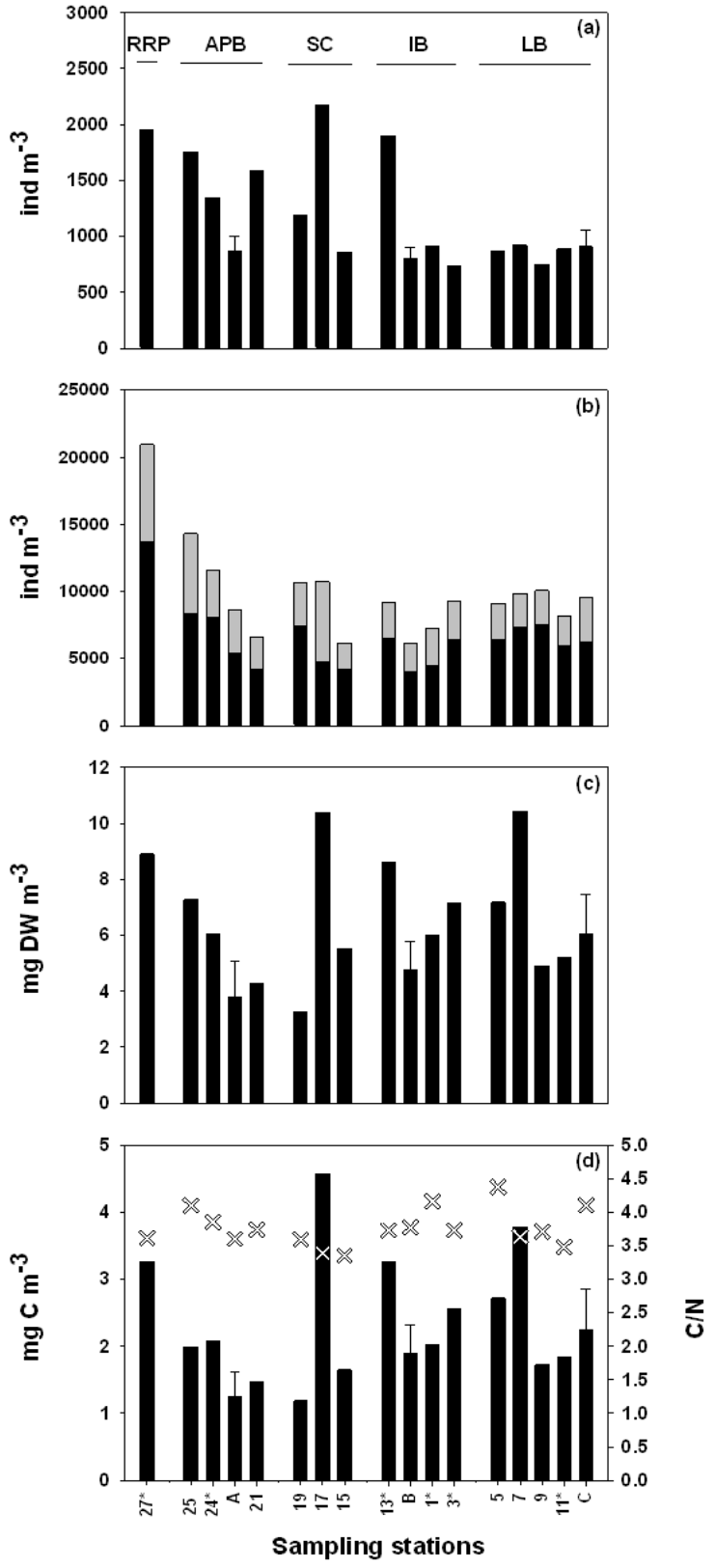

Figure 4-2. Spatial distribution of zooplankton integrated abundance obtained by net sampling (a) and by Niskin bottle (b) including nauplii (black) and small copepods (grey), biomass as dry weight (c) and as carbon (d) with C/N ratio (cross). Mean and standard deviation for stations A, B and C. (*) night sampling. See text for details on the five Mediterranean areas.

organisms (i.e. euphausiids, amphipods). Identification of the copepods community was made down to species level and developmental stage when possible. Sex determination was also done on the most abundant species. Species/genus identification was made according to (Rose, 1933; Trégouboff & Rose, 1957; Razouls et al., 2005-2011). Holoplankton organisms other than copepods as well as meroplankton were identified down to taxa levels.

Digital imaging approach using the Zooscan

After homogenization, another fraction of each preserved sample containing a minimum of 1000 particles was placed on the glass plate of the ZooScan. Organisms were carefully separated one by one manually with a wooden spine, in order to avoid overlapping. Each image was then run through ZooProcess plug-in using the image analysis software Image J (Grosjean et al., 2004; Gorsky et al., 2010). Several measurements of each organism were then computerized. Organism size is given by its equivalent circular diameter (ECD) and can then be converted into biovolume, assuming each organism is an ellipsoid (more details in Grosjean et al., 2004). The lowest ECD detectable by this scanning device is 300 µm. To discriminate between aggregates and organisms, we used a training set of about 1000 objects which were selected automatically from 35 different scans. Each image was classified manually into zooplankton or aggregates and each scan was then corrected using the automatic analysis of images.

The size spectrum of each sample was then measured using the NB-SS (Normalized Biomass Size Spectrum) calculation (Yurista et al., 2005; Herman and Harvey, 2006) where biovolume is converted into wet weight (1 mm^3 = 1 mg). The slope of NB-SS linear regression for each sample gives information on the community size-structure. Low negative slopes, close to zero, reveal high percentages of large organisms while high negative slopes are linked to higher percentages of small organisms (Sourisseau and Carlotti, 2006).

Data analysis

Nauplii abundance presented here only concern the discrete bottle sampling and not the integrated dataset as they have been under-sampled even with a fine mesh bongo.

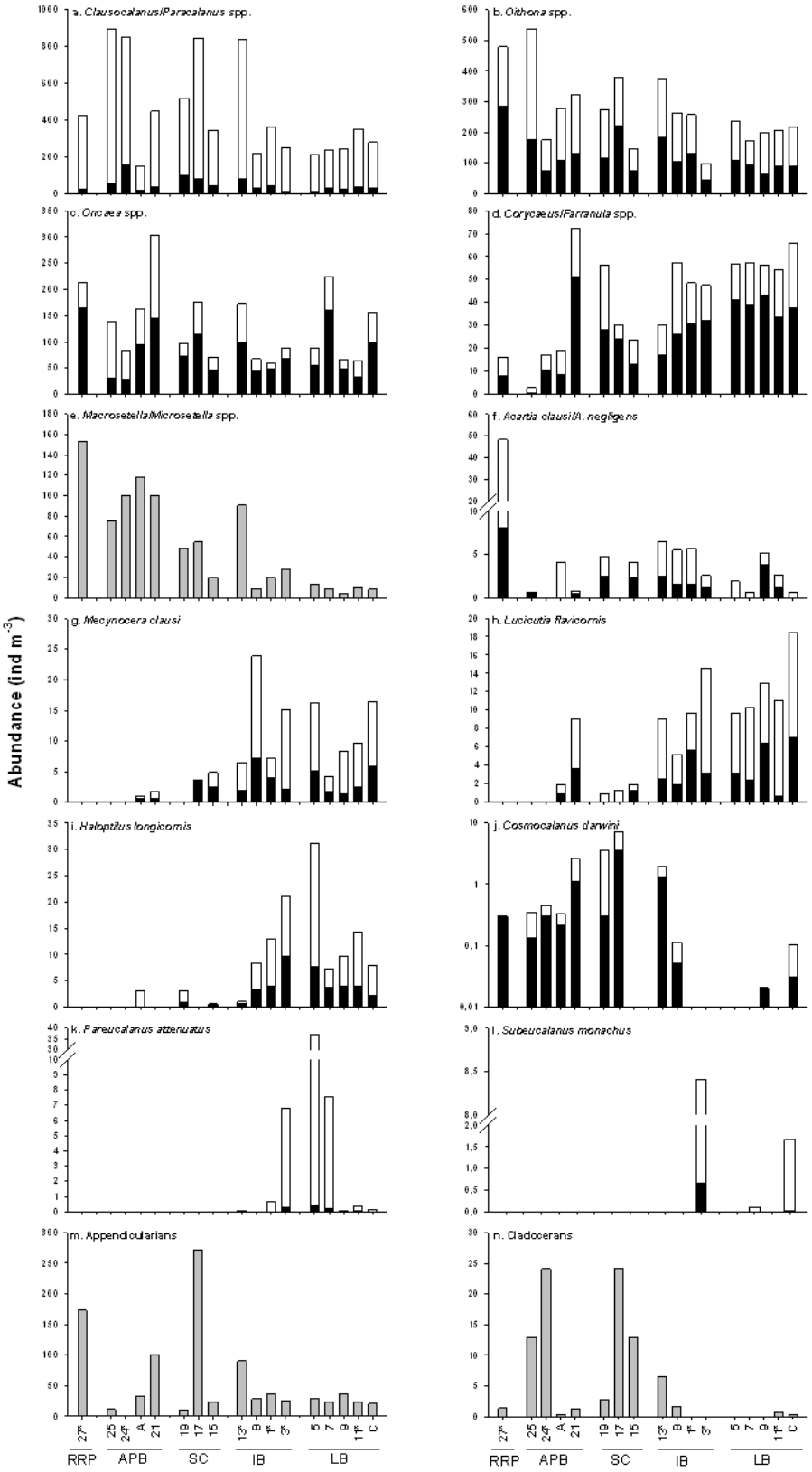

Figure 4-3. Spatial distribution of the important zooplankton species across the Mediterranean transect: (a) *Clausocalanus* spp. and *Paracalanus* spp., (b) *Oithona* spp., (c) *Oncaea* spp., (d) *Corycaeus* spp. and *Farranula* spp., (e) *Macrosetella* spp. and *Microsetella* spp., (f) *Acartia clausi* and *Acartia negligens*, (g) *Mecynocera clausi*, (h) *Lucicutia flavicornis*, (i) *Haloptilus longicornis*, (j) *Cosmocalanus darwini*, (k) *Pareucalanus attenuatus*, (l) *Subeucalanus monachus*, (m) Appendicularians and (n) Cladocerans. Nauplii (white), copepodit (black) and undifferentiated (grey) stages. (*) night sampling. Mean and standard deviations for stations A, B and C. Note: logarithmic scale in Fig. j.

Based on both microscope and ZooScan abundance and biomass datasets, one way Anovas were used to examine differences among geographic areas and paired t-tests were run to study the diel variations at the long-stay stations. Only one day and one night samples were counted and taxonomic composition described at each of these 3 stations. Thus, day-night comparison was assessed using paired t-test on the 6 data points. In order to reduce variability among stations, normalization was done by dividing each data by the maximum value of the pair. Pearson correlation and stepwise multiple regression analysis were conducted in order to explain the variability in zooplankton distribution. Relationships were tested between zooplankton parameters (abundance, biomass) and physical (temperature, salinity), biogeochemical (oxygen, PON, POP and particular N/P ratio), and biological (Chlorophyll-*a*, heterotrophic nanoflagellates, nanophytoplankton, diatoms, and ciliates) parameters. Regarding the Niskin bottle sampling, small copepods and nauplii variability was study at discrete depth scale but also integrated over the upper 200 m. Metazooplankton abundance and biomass variability assessment was on the other hand performed from the net sample data. Variables were log(x + 1) transformed when normalized tests failed.

The spatial variability of the environmental parameters and the metazooplankton community characteristics was assessed using multivariate analysis performed with ADE4 software (Thioulouse et al., 1997). The same environmental variables as in the correlation analysis (see above) was used but we added the mixed layer depth, and DIN, DIP, DON and DOP concentrations; we limited the metazooplankton community to the 74 more representative taxa (> 10 % occurrence). A principal component analysis (PCA) was performed on the environmental parameters, and a factorial correspondence analysis (COA) on the metazooplankton characteristics. The results of these two analyses were then associated through a co-inertia analysis (Dolédec & Chessel, 1994). A cluster classification (percentage similarity, Bray-Curtis Index) was run on the observation (stations) scores from the first factorial plane using complete linkage and multidimensional scaling analysis (MDS) with PRIMER 6.0 software (Clarke & Warwick, 1995). The significance among groups was then tested using a non-parametric MANOVA (PERMANOVA plug-in for PRIMER).

Table 4-2. Mean integrated abundance (± standard deviation) in the upper 200 m depth of total zooplankton, copepods, other holoplankton and meroplankton and percentage abundance of the major species and taxa within each category, for the different regions. Unidentified copepods and copepods < 0.1 % were grouped as other copepods. Amphipods, isopods and gelatinous larvae were grouped as others. * Nauplii abundance is given only for information and is not included in the total abundance.

Taxa	Symbole	Rhône river plume	Algero Provencal basin	Sicily channel	Ionian basin	Levantin basin	Algero Provencal eddy	Ionian eddy	Levantin eddy
Total (ind m^{-3})		1948	1561 ± 205	1407 ± 687	1181 ± 630	855 ± 75	872 ± 129	806 ± 92	906 ± 151
Copepods (ind m^{-3})		1636	1457 ± 229	1230 ± 519	1073 ± 570	771 ± 83	773 ± 110	742 ± 74	828 ± 134
Other holoplankton (ind m^{-3})		228	102 ± 107	173 ± 184	107 ± 59	81 ± 19	90 ± 28	60 ± 20	69 ± 13
Meroplankton (ind m^{-3})		83.6	2.4 ± 3.7	3.6 ± 1.9	1.3 ± 1.1	2.7 ± 1.8	9.4 ± 9.2	4.0 ± 1.7	9.4 ± 4.4
Nauplii* (ind m^{-3})		105	67 ± 54	92 ± 35	128 ± 128	74 ± 18	64 ± 18	100 ± 15	67 ± 7
Copepods (%)		84.0	93.3	87.4	90.8	90.2	88.6	92.1	91.4
Clausocalanus /*Paracalanus* spp.	ClPa	21.7	46.8	40.4	41.0	30.6	17.1	26.9	30.5
Oithona spp.	Oi	24.6	22.1	19.0	20.6	23.8	31.7	32.6	24.1
Oncaea spp.	On	10.9	11.2	8.1	9.0	12.9	18.6	8.4	17.3
Macrosetella /*Microsetella* spp.	MiMa	7.9	5.9	2.9	3.9	1.0	13.5	1.1	0.9
Corycaeus/Farranula spp.	CoFa	0.8	2.0	2.6	3.6	6.6	2.2	7.1	7.3
Acartia clausi	Acl	2.5	< 0.1	0.1	0.0	0.0	0.0	0.0	0.0
Acartia negligens	Ane	0.0	< 0.1	0.1	0.4	0.3	0.5	0.7	0.1
Calanus helgolandicus	Che	< 0.1	0.1	0.0	0.0	0.0	< 0.1	0.0	0.0
Calocalanus pavo	Cpa	0.0	0.0	0.4	1.3	0.9	0.0	0.4	0.5
Calocalanus spp.	Ca	0.4	0.4	1.0	2.6	2.5	1.5	4.1	2.3
Candacia spp.	Cd	0.1	< 0.1	0.1	0.1	0.1	< 0.1	< 0.1	< 0.1
Centropages typicus	Cty	0.2	0.3	1.4	< 0.1	0.0	0.0	0.0	0.0
Cosmocalanus darwini	Cda	< 0.1	0.1	0.3	0.1	< 0.1	< 0.1	< 0.1	< 0.1
Ctenocalanus vanus	Cva	2.1	0.0	0.6	0.8	0.8	0.0	0.0	0.0
Eucalanus hyalinus	Ehy	0.0	0.1	< 0.1	< 0.1	< 0.1	< 0.1	0.0	0.0
Euchaeta spp.		0.2	0.1	0.1	0.2	< 0.1	< 0.1	< 0.1	< 0.1
Euterpina acutifrons	Eac	4.1	0.0	0.1	0.4	0.0	0.0	0.0	0.0
Haloptilus spp.		0.0	< 0.1	0.1	1.0	1.8	0.4	1.0	0.9
Lucicutia spp.		0.0	0.2	0.1	0.9	1.3	0.2	0.7	2.1
Mecynocera clausi	Mcl	0.0	< 0.1	0.2	0.8	1.1	0.1	3.0	1.8
Mesocalanus tenuicornis	Mte	< 0.1	< 0.1	0.0	< 0.1	0.0	< 0.1	< 0.1	0.0
Nannocalanus minor	Nmi	3.3	0.7	5.5	0.0	0.3	0.4	1.3	0.0
Neocalanus gracilis	Ngr	0.0	< 0.1	< 0.1	0.2	0.1	0.1	0.1	< 0.1
Pareucalanus attenuatus	Pat	0.0	0.0	0.0	0.2	1.3	0.0	< 0.1	< 0.1
Pleuromamma abdominalis	Pab	0.0	0.2	0.0	0.1	< 0.1	0.2	< 0.1	< 0.1
Pleuromamma gracilis	Pgr	0.6	0.1	0.2	0.4	0.1	0.4	0.1	< 0.1
Scolecithricella spp.	Sa	0.4	0.0	0.2	0.2	< 0.1	0.0	0.6	0.3
Scolecithrix spp.	Sx	0.0	0.0	< 0.1	0.2	0.8	0.0	0.1	0.4
Spinocalanus spp.	Sp	0.6	< 0.1	0.8	< 0.1	0.3	< 0.1	0.2	0.1
Subeucalanus monachus	Smo	0.0	0.0	0.0	0.2	< 0.1	0.0	0.0	0.0
Temora stylifera	Tst	< 0.1	< 0.1	< 0.1	0.3	0.3	0.0	0.0	0.1
Other copepods		3.5	3.0	3.0	2.3	3.1	1.7	3.7	2.7
Other holoplankton (%)		11.7	6.6	12.3	9.1	9.5	10.3	7.4	7.6
Appendicularians	AP	8.9	2.4	7.2	4.3	3.3	3.7	3.6	2.3
Chaetognaths	CH	0.2	0.5	0.6	1.9	1.3	1.0	0.6	0.4
Cladocerans	CL	0.1	0.8	0.9	0.2	< 0.1	< 0.1	0.2	< 0.1
Doliolids	DO	0.0	< 0.1	0.0	< 0.1	0.3	0.0	0.0	0.0
Euphausiids/Mysids	EU MY	0.6	< 0.1	0.1	0.1	< 0.1	0.1	0.1	< 0.1
Ostracods	OS	< 0.1	2.3	0.8	1.2	3.0	3.7	1.4	2.7
Polychaetes	PO	0.5	0.3	0.1	0.4	0.3	0.8	0.1	0.2
Pteropods	PT	1.0	0.2	2.0	0.5	1.1	0.6	1.3	0.6
Salps	SA	< 0.1	0.0	0.4	0.1	0.0	< 0.1	< 0.1	< 0.1
Siphonophores	SI	0.4	< 0.1	0.2	0.3	0.1	< 0.1	0.1	0.9
Others		< 0.1	< 0.1	< 0.1	0.1	0.1	0.4	< 0.1	0.4
Meroplankton (%)		4.3	0.2	0.2	0.1	0.3	1.1	0.5	1.0
Decapod larvae	DE	0.1	0.1	< 0.1	0.0	< 0.1	0.0	< 0.1	< 0.1
Echinoderm larvae	EC	0.8	< 0.1	< 0.1	0.0	0.1	0.0	0.3	1.0
Fish eggs		0.1	< 0.1	< 0.1	< 0.1	< 0.1	< 0.1	< 0.1	< 0.1
Fish larvae	FI	< 0.1	< 0.1	< 0.1	< 0.1	0.1	0.1	< 0.1	< 0.1
Jellyfishes	JE	0.2	< 0.1	0.1	0.1	< 0.1	0.9	0.1	< 0.1
Lamellibranch larvae	LA	3.1	0.1	0.1	0.0	0.1	0.1	< 0.1	0.0

4.2.3 Results

4.2.3.1 Characterization of the study area

The cruise took place during the stratified period. The eastern basin, sampled during the first leg, showed a surface layer (0-20 m) with temperature above 22°C and up to 27°C at station C. Intermediate waters (60-200 m) displayed temperatures between 15 and 18°C, with warmer waters eastwards. Along the westward transect (second leg), temperature within the surface layer remained very high (> 25°C) as far as the Sicily channel. Salinity was much higher in the eastern basin and in particular from station 5 eastwards, where it remained above 39 down to 200 m. Associated with the increasing trend in oligotrophy from west to east, chlorophyll-*a* vertical distribution showed the deepening of the deep chlorophyll maximum (DCM) from 50 m at station 25, down to 80 m at station 19, to 100 m at station 3 and to 120 m at station C (Fig. 4-4a). The chlorophyll-*a* values at the DCM ranged from 0.237 at 100 m (st. 4) to 0.897 µg L^{-1} at 75 m (st. 20). Ciliate standing stock decreased also from west to east and maximum values were located as well as at the depth of the DCM; nevertheless ciliate abundance displayed high variability between stations. Mixotrophic ciliates represented an appreciable amount of the ciliate biomass (Christaki et al. 2011). More details on the chemical, biological and physical environmental conditions are presented in (Pujo-Pay et al., 2010; Crombet et al., 2011; Moutin et al., 2011).

4.2.3.2 Zooplankton abundance and biomass distribution

Zooplankton abundance in the upper 200 m layer estimated from the microscope counts (Fig. 4-2a) varied over the five geographic areas (RRP, APB, SC, IB and LB), with values (mean ± sd) of 1948, 1286 ± 409, 1407 ± 687, 1031 ± 492 and 872 ± 93 ind m^{-3}, respectively. No significant spatial differences were found between these five areas (Anova, $p > 0.05$). However, the general trend showed higher abundances in the western basin than in the eastern basin. Open water stations located in the western basin presented significantly ($p < 0.05$) higher abundance than those of the LB, but not to those in the entire eastern basin, due to the high abundance at station 13 (1901 ind m^{-3}). Abundance was higher at the stations located in coastal regions (st. 27) and in the centre of the SC (st. 17) than in open water, with the lowest abundance located at station 3 (732 ind m^{-3}). As for the total abundance pattern, nauplii and small copepods abundance did not show any significant differences between the five

geographic areas ($p > 0.05$) (Fig. 4-2b). Nevertheless, at the basin scale, only small copepods abundance presented a significant higher abundance ($p < 0.05$) in the western basin (4450 ± 2035 ind m^{-3}) than in the eastern basin (2627 ± 340). In addition, in the western basin, a clear northward increase in both the nauplii and small copepods abundance with values ranging from 20929 (st. 27) to 6620 ind m^{-3} (st. 21) was observed while it was not clear for the total abundance.

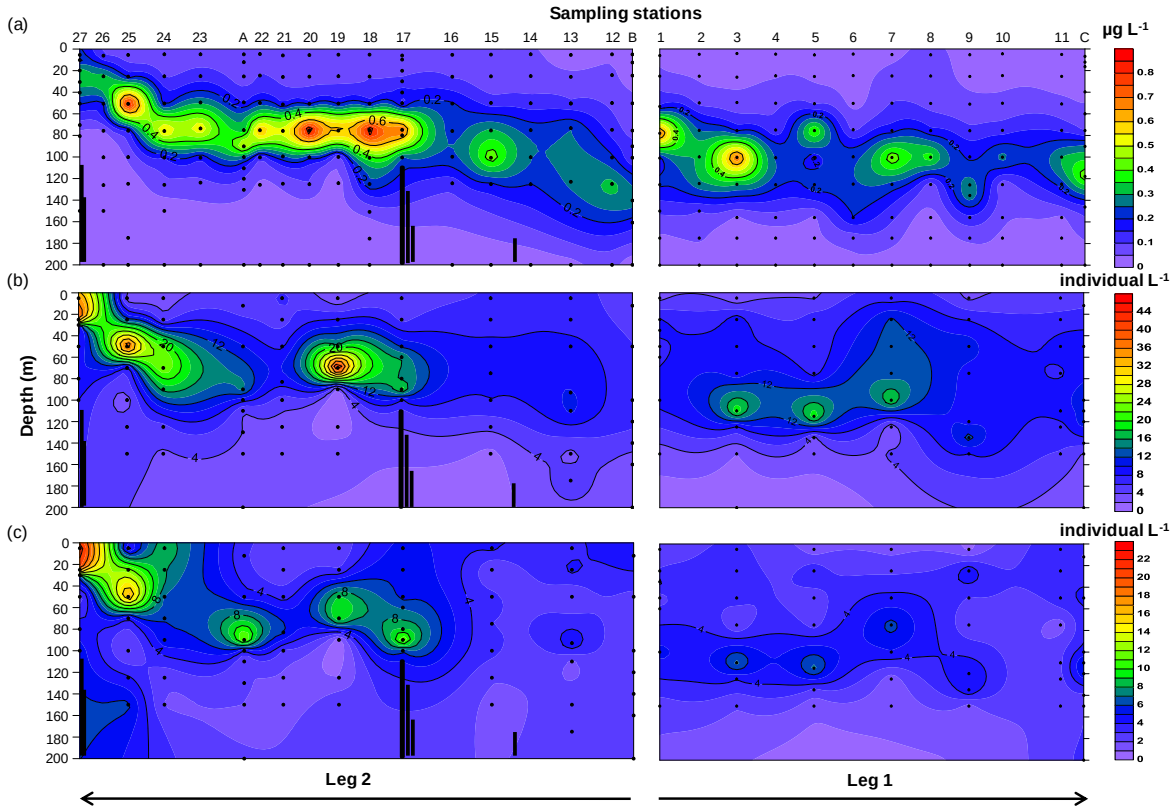

Figure 4-4. Spatial distribution of chlorophyll-a concentration (a), copepods nauplii (b) and small copepods (c) within the upper 200 m layer across the Mediterranean Sea. Bottom depth in black.

Zooplankton biomass (mg DW m^{-3}) was weakly but significantly correlated with abundance (ind m^{-3}) ($R^2 = 0.298$, $n = 20$, $p < 0.01$). Biomass displayed large spatial variability, with the values ranging from 3.2 mg DW m^{-3} (st. 19) to 10.4 mg DW m^{-3} (st. 17), equivalent to 1.2 to 4.6 mg C m^{-3} and 0.33 to 1.35 mg N m^{-3}, respectively (Fig. 4-2c, d). Station 7 displayed a low abundance but a rather large biomass, which can be explained by the presence of large amphipods. A clear increase of DW biomass occurred northward in the APB (st. 21 to st. 27), but no clear pattern was observed in the other regions. In addition, no significant spatial

differences were found between the five geographic areas (Anova, $p > 0.05$). Mean zooplankton carbon and nitrogen contents represented 36.3 ± 3.7 % and 9.6 ± 1.2 % of the DW respectively. Zooplankton C/N ratio was fairly constant (mean: 3.78 ± 0.29) with values ranged from 3.35 to 4.37 at station 15 and 5 respectively.

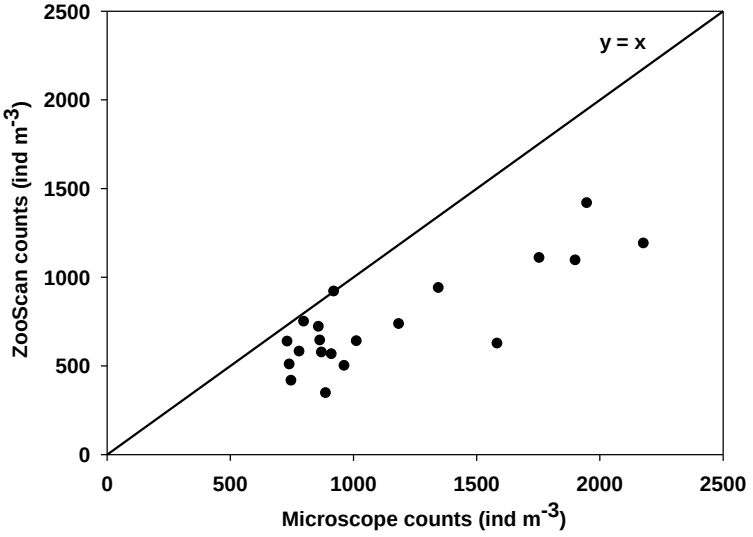

Figure 4-5. Comparison between microscope and ZooScan counts for all stations sampled with the Bongo net.

4.2.3.3 Metazooplankton community composition and distribution

Over 74 taxa were identified from net tows during this study (Table 4-2) with 56 genera/species of copepods, 6 taxa of meroplankton and 12 taxa of holoplankton. Nauplii were present in the net samples but this technique, even when using a 120µm mesh net, did underestimate their real abundance, which was confirmed by the comparison with the integrated abundance obtained with the Niskin bottle sampling (see 3.4) and were given in table 4-2 for information purpose only. Copepods represented 90.4 ± 3.0 % of total metazooplankton abundance and were dominated by 4 taxa: *Clausocalanus*/*Paracalanus* spp., *Oithona* spp., *Oncaea* spp. and *Macrosetella*/*Microsetella* spp. which represented ~80 % of the copepod community. The three first taxa were evenly distributed along the transect but presented a local higher abundance (Fig. 4-3a, b, c), whereas *Macrosetella/Microsetella* spp. were 7 times more abundant in the western than in the eastern Mediterranean Sea (Fig. 4-3e). *Euterpina acutifrons* and meroplanktonic larvae were very common in neritic and coastal

waters (e.g. st. 17 and 27 in table 4-3). With the exception of one or two stations, *Corycaeus/Farranula* spp. and *Oncaea* spp. populations were the only taxa dominated by adult stages (50 to 80 %).

Less abundant copepod species also displayed interesting geographical distribution. The genera *Corycaeus*/*Farranula* and *Calocalanus* spp. were less abundant in a large part of the western basin (Fig. 3d and Table 2). *Mecynocera clausi*, *Lucicutia flavicornis*, *Haloptilus longicornis*, *Pareucalanus attenuatus* and *Subeucalanus monachus* (Fig. 4-3g, h, i, k, l respectively) were clearly characteristic species of the eastern basin being absent or with a very low occurrence in the western basin. *Acartia* species were located throughout the Mediterranean Sea (Fig. 4-3f). However, *A. clausi* replaced *A. negligens* in the north part of the western Mediterranean (st. 27 and 25) and at station 19 (Table 4-2). The subtropical copepod species *Cosmocalanus darwini* (Fig. 4-3j) was found in the two basins and is reported here for the first time in the Mediterranean Sea. Both adult and copepodite stages were collected.

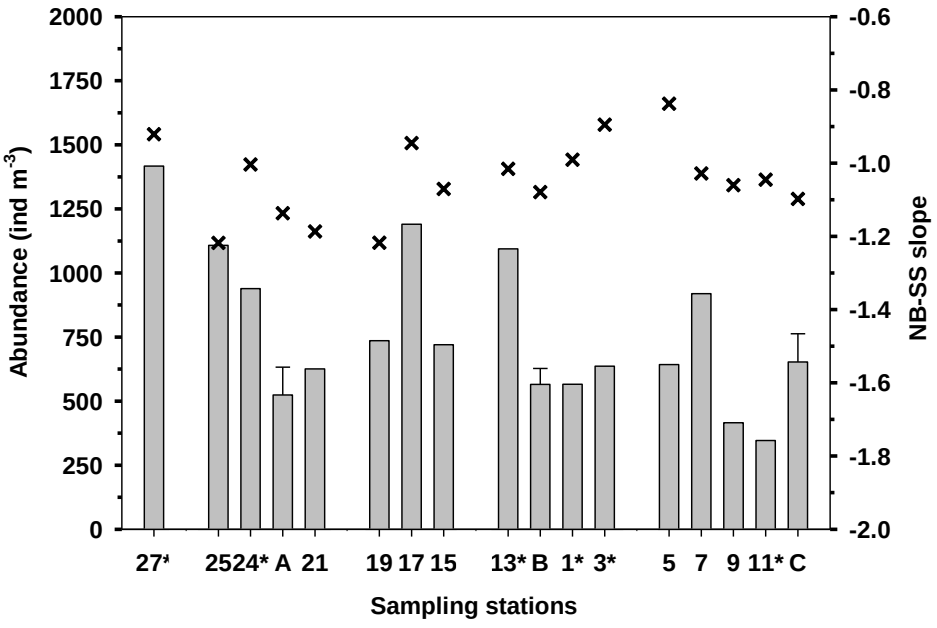

Figure 4-6. Spatial distribution of mesozooplankton abundance (vertical bar) from the ZooScan counts and values of NB-SS slope (dark cross) along the BOUM transect. Mean values for stations A, B and C between day and night sampling. (*) night sampling. See text for details on the 5 regions.

Non-copepod holoplanktonic species, mainly appendicularians, ostracods, pteropods and chaetognaths, made up 9.3 ± 2.0 % of the metazooplankton abundance while meroplanktonic species were scarce (1.0 ± 1.4 %) except at the RRP (4.3 %). Cladocerans (Fig. 4-3n) were absent in the central sector of the eastern basin. Appendicularians (Fig. 4-3m) were 3 to 10

times more abundant at stations 27 and 17 than in the rest of the transect. It is also interesting to note that station C presented a high abundance (up to 11.6 ind m^{-3}) of echinoderm larvae (Asteroidae).

Spatial impact of the mesoscale features, the anticyclonic gyres, when compared to the neighbouring stations was more or less obvious (see table 4-2 and figure 4-3). *Clausocalanus/Paracalanus* spp. were 2 to 4 time less abundant at stations A and B than at the adjacent stations, and only 1.5 less abundant at station C than at station 11. *Mecynocera clausi* and *Corycaeus/Farranula* spp. were on the other hand more abundant in the gyres than in the neighbouring stations especially obvious for the gyre B and C.

4.2.3.4 Discrete sampling

The discrete depth sampling within the top 200 m collected small-sized copepods (< 1 mm) and nauplii. The community of small copepods was composed of adult and copepodite stages of *Oithona* spp., *Oncaea* spp., *Corycaeus/Farranula* spp., *Macrosetella*/*Microsetella* spp., and copepodite stages of *Clausocalanus*/*Paracalanus* spp.. Distinct spatial patchiness was observed in the distribution of both nauplii and small copepods throughout the Mediterranean Sea (Fig. 4-4). The depth of the maximum nauplii density matched that of small copepods for most stations with the exception of stations 7 and 24. An eastward deepening of the depth of the highest abundance was observed from 25 m to 90 m in the western basin and from 100 m to 135 m in the eastern basin. Nauplii abundance was integrated over the upper 200 m except at stations 17 and 27 were depth range was limited to 100 m. Integrated abundance ranged from 4177 ind m^{-3} (st. 15) to 13729 ind m^{-3} (st. 27). It was 1.4 (st. 24) to 3.1 (st. 7) times higher than that of small copepods. The eastern basin showed an overall lower integrated abundance than the western basin and the SC for both nauplii and small copepods. Integrated values of nauplii and small copepods obtained using bottles sampling were 104 times and 4 times higher, respectively, than for samples collected with nets.

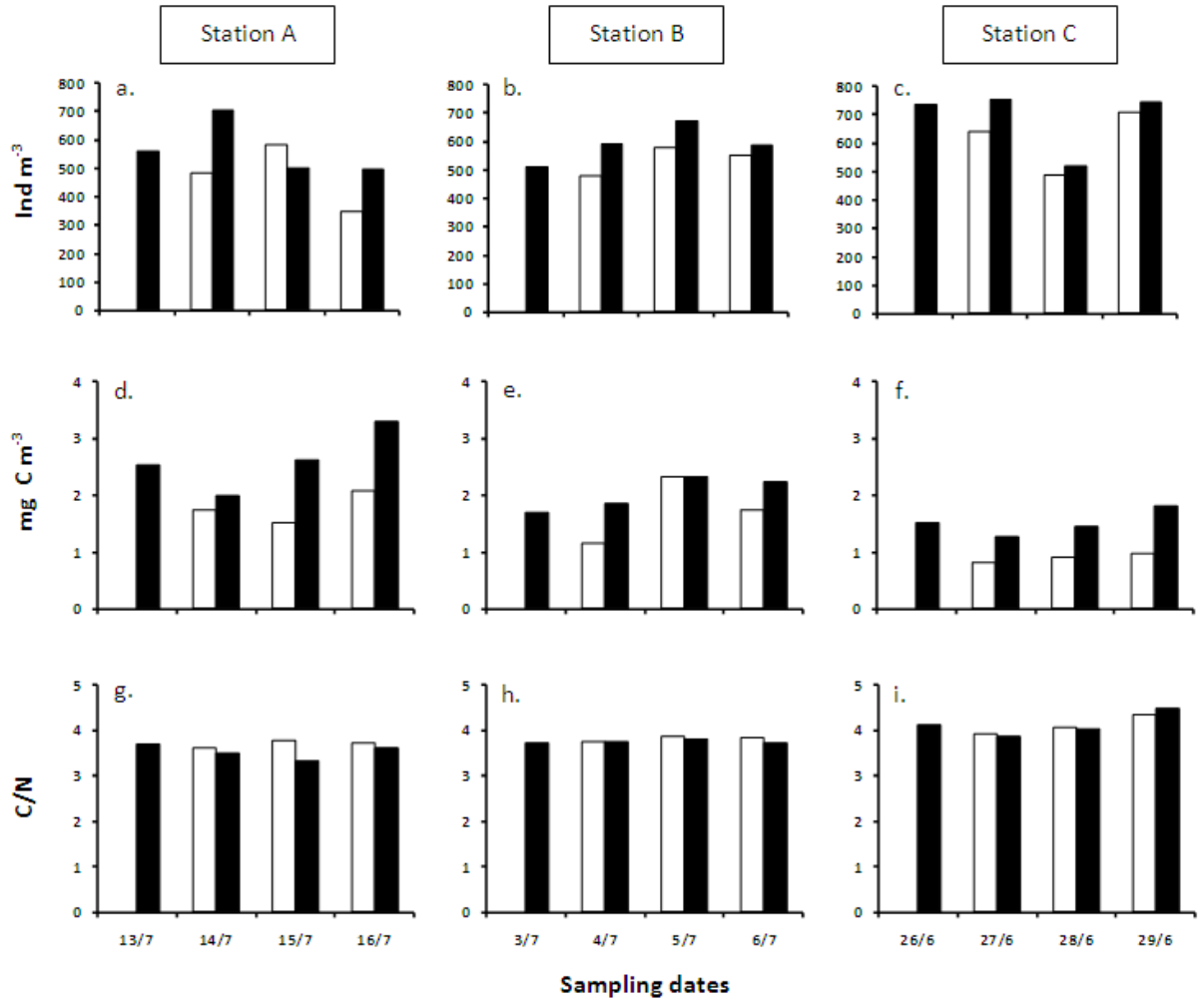

Figure 4-7. Impact of sampling time (day: white; night: black) on zooplankton abundance integrated in the upper 200 m (ZooScan counts) (a, b, c), carbon biomass (d, e, f) and C/N ratio (g, h, i) at stations A, B and C.

4.2.3.5 Zooplankton size structure

The automatic recognition system ZooScan (ZC) and the dissecting microscope (MC) (Fig. 4-5) showed a significant linear regression with ZC = 0.50 MC + 169.93 (R^2 = 0.69, p < 0.001, n = 20). The lower detection limit for the ZooScan is 300 µm ECD, which led to an underestimation of the total number of organisms counted by ~33 ± 15.9 % (corresponding to 35.4 ± 14.9 % when nauplii were computed) when compared to the microscope technique. This underestimation corresponded to the fraction < 300 µm ECD equivalent to a copepod with a total length of 500 µm. No clear pattern between the five geographic areas or between the western and eastern basins were found for this single size fraction (p > 0.05). Nevertheless, the overall spatial distribution of the metazooplankton abundance was similar between the two methods (Figs. 4-2a and 4-6). Biovolume (ZooScan determinations, data not

shown) and biomass (Fig. 4-2c) also shown similar spatial variations. Abundance and NB-SS slopes (Fig. 4-6) did not show any clear relationship between the five geographic areas (p > 0.05). Nevertheless, the NB-SS slopes showed clear basin scale differences, with significantly lower slope in the eastern basin (IB + LB) than in the western basin (APB) (p = 0.032), indicating a higher relative abundance of large organisms (> 2mm; such as *Haloptilus longicornis, Pareucalanus attenuatus* and *Subeucalanus monachus*) (Fig. 4-3i, k, l).

4.2.3.6 Day-night variation

At the three long-stay stations, significant higher abundance (~17 %; p < 0.001) and biomass (~40 %; p < 0.001) of organisms > 300 µm ECD observed at night highlighted the impact of the diel vertical migration on the structure of the community (Fig. 4-7). This increase was mainly explained by medium (500-1000 µm) and large-sized (> 1000 µm) organisms. Several specific taxa displayed higher night abundance within the upper 200 m. This included the copepods *Euchirella messinensis* and *Neocalanus gracilis* (p < 0.05), *Pleuromamma abdominalis* and *P. gracilis* (p < 0.01), as well as other taxa such as euphausiids, fish larvae (p < 0.001), pteropods and doliolids (p < 0.05).

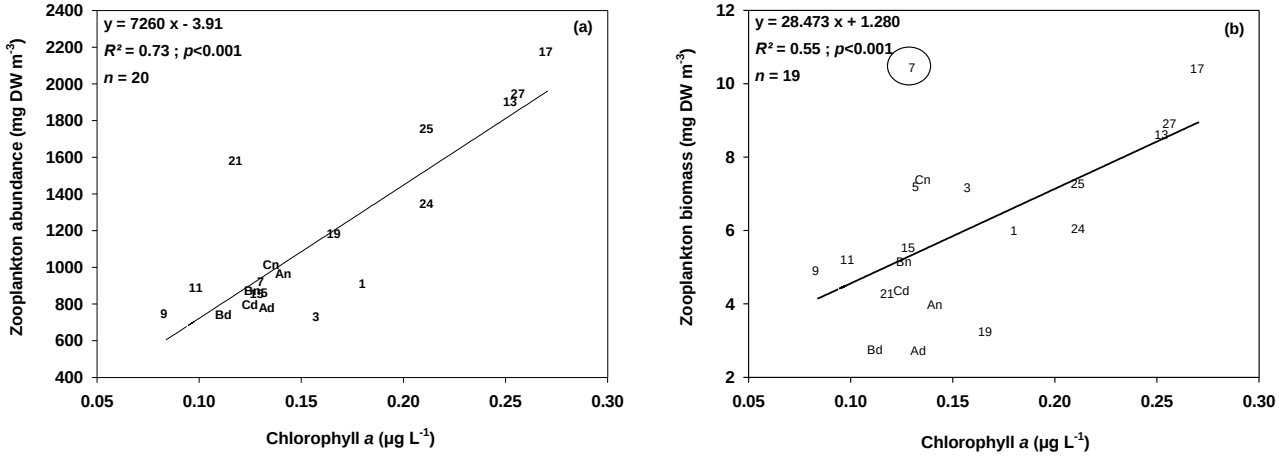

Figure 4-8. Relationship between chlorophyll *a* concentration (µg L^{-1}) and zooplankton abundance (a) (microscope counts) and net zooplankton biomass (b) across the whole Mediterranean Sea. For A, B and C stations, day sampling (d) and night sampling (n). See table 1 and figure 1 for localization of stations. Note: st 7 biomass value was removed from the analysis.

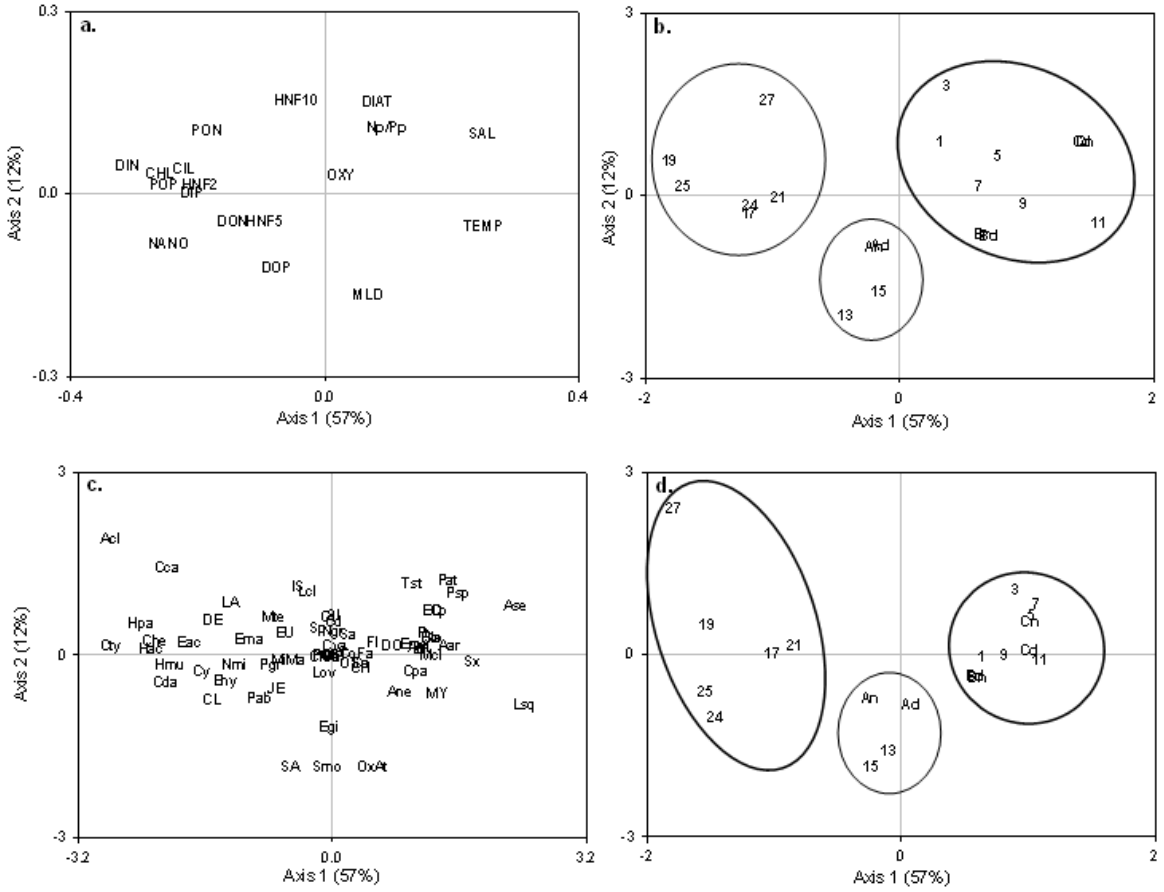

Figure 4-9. Co-inertia analysis: plots of the environmental variables (a) and the stations (b) in the "Environment" system and plot of the taxa (c) and the stations (d) in the "Zooplankton" system. Circles corresponded to cluster group tested with non parametric MANOVA. Mixed Layer Depth (MLD), *Aetideus armatus* (Aar), *Arietellus setosus* (Ase), *Calanoides carinatus* (Cca), *Clytemnestra* spp. (Cy), *Copilia* spp. (Cp), *Euaetideus giesbrechti* (Egi), *Euchaeta marina* (Ema), *Euchirella messinensis* (Eme), *Haloptilus acutifrons* (Hac), *H. longicornis* (Hlo), *H. mucronatus* (Hmu), *Heterorabdus papilliger* (Hpa), *Lubbockia squillimana* (Lsq), *Lucicutia clausi* (Lcl), *L. flavicornis* (Lfl), *L. ovalis* (Lov), *Phaenna spinifera* (Psp), *Sapphirina* spp. (Sa), Amphipods (AM), Cirriped larvae (CI), Isopods (IS), *Oxygyrus*/*Atlanta* spp. (OxAt) and *Pterotrachea* spp. (Pt). Other abbreviations as in Tables 2 and 3.

The C/N ratio was overall stable (3.82 ± 0.26, n = 21) but decreased slightly during the night in spite of there being no significant difference between day and night samples.

4.2.3.7 Relationships between metazooplankton and environmental parameters

No significant correlations between the different physico-chemical variables (temperature, salinity and oxygen) and the net metazooplankton abundance or biomass were found, while abundance of nauplii and small copepods from discrete samples were significantly correlated with oxygen level (Table 4-3). All metazooplankton parameters - both integrated and discrete data - were strongly correlated with chlorophyll-*a* concentrations (Fig. 4-8). Discrete abundance of nauplii and small copepods was strongly correlated with nanophytoplankton,

diatoms and POP concentrations. PON concentration was the only variable showing a significant relationship with both the net and discrete metazooplankton data.

Chlorophyll-*a* was included in all multiple regression models for biomass and integrated or discrete abundance (Table 4-4). Nanoplankton were selected as an explanatory variable in the model for integrated metazooplankton abundance as well as heteroflagellates in the models for integrated abundance of nauplii (HNF > 10 µm) and small copepods (total HNF).

The first factorial plane of the co-inertia analysis explained 69 % of the variance, with 52 % by the first axis. In both systems ("Environment" and "Zooplankton"), the three same groups of stations were observed (Fig. 4-9). Besides, the segregation obtained with the MDS analysis, based on the observation scores of the 2 first axes of both systems, showed the same grouping (not shown). The first group was composed of all stations located in the western basin, except for station A, and the western stations in the Sicily Channel (st. 19 and 17). The second group comprised all the stations located in the eastern basin except for station 13. The third group was composed of the eastern station in the SC (st. 15), the eastern station in the IB (st. 13) and the anticyclonic gyre A. The first group was characterized by high values of nutrients, chlorophyll-*a*, nanophytoplankton and ciliates (Fig. 4-9a) and the second group by elevated temperature and salinity and high diatoms concentration. In the "Zooplankton" system, the first group was mainly identified by the copepods *A. clausi*, *C. typicus* and *Calanoides carinatus* while the second group by the copepods *A. setosus*, *L. squilimana* and *H. longicornis* (Fig. 4-9c, d). In both systems the third group of stations occupied an intermediate position on the factorial plane. Other taxa (appendicularians, pteropods, polychetes, the calanoid copepods *Clausocalanus/Paracalanus* and the cyclopoid and poecilostomatoid copepods *Oithona* and *Oncaea*) were located near the barycentre. The relationship between the normalized coordinates of the stations on the first axis of both systems ("Environment" and "Zooplankton") which reflects the degree of association between zooplankton and environment was highly significant ($R^2 = 0.89$).

Table 4-3. Simple correlation analysis between zooplankton parameters and environmental factors: significance degree of *p* values (*: $p < 0.05$; **: $p < 0.01$; ***: $p < 0.001$, underlined stars mean negative correlation; ns: not significant). Integrated water column zooplankton abundance (ind m^{-3}) and biomass (mg DW m^{-3}) were obtained from net sampling ($n = 20$); discrete abundance of nauplii and small copepod (ind m^{-3}) was issued from Niskin bottles ($n = 111$ to 140).

Variable	Symbole	Net Biomass	Abundance				
			Net Total	Integrated		Discrete depths	
				Small copepods	Nauplii	Small copepods	Nauplii
Temperature	TEMP	ns	ns	ns	ns	ns	ns
Salinity	SAL	ns	ns	ns	ns	ns	ns
Oxygen	OXY	ns	ns	ns	ns	***	***
HNF 2-5 µm	HNF2	ns	ns	ns	ns	ns	ns
HNF 5-10 µm	HNF5	ns	ns	ns	ns	*	**
HNF >10 µm	HNF10	ns	ns	ns	**	ns	ns
HNF total	HNFT	ns	ns	*	ns	ns	**
Nanophyto.	NANO	ns	***	ns	ns	**	***
Diatoms	DIAT	ns	ns	ns	ns	***	***
Chlorophyll *a*	CHL	**	***	***	**	***	***
Ciliates	CIL	ns	ns	ns	ns	*	*
Part. Org. Phos.	POP	ns	*	ns	ns	***	***
Part. Org. Nitr.	PON	*	ns	*	*	***	***
N/P particular	Np/Pp	ns	ns	ns	ns	ns	ns

4.2.4 Discussion

4.2.4.1 Pattern of metazooplankton abundance and biomass along the BOUM transect

Zooplankton abundance values recorded, when using 120 µm bongo nets, during the BOUM transect, were 4 to 8 times higher than in previously published studies (Mazzocchi et al., 1997; Siokou-Frangou et al., 1997; Pasternak et al., 2005; Riandey et al., 2005), whereas biomass were of the same magnitude. Strong discrepancies with previously recorded abundance may arise from (1) the use of different sampling mesh-size (120 µm during BOUM and > 120 µm in all previous studies) and (2) differences in sampling periods. Mesh size is a very important factor in the evaluation of metazooplankton abundance (Calbet et al., 2001; Turner, 2004). Zervoudaki et al. (2006) reported in a frontal area of the Aegean Sea, an increase of 2 to 20 times in abundance when smaller organisms (45-200 µm) were considered. The most pronounced differences were observed for copepod nauplii, copepodites and adults of small organisms such as *Clausocalanus/Paracalanus* spp., *Oithona* spp., *Oncaea* spp. and *Macrosetella*/*Microsetella* spp. Therefore it is clear that abundance is significantly higher when sampling is performed with a 80 µm mesh size, but concomitant increase in biomass is not obvious (Thibault et al., 1994; Gaudy et al., 2003) probably due to the fact that small

organisms have a low specific weight. According to the seasonal pattern of zooplankton production in temperate oceanic areas (Harvey, 1955), our abundance should be intermediate between maximum late spring values and vernal minimum values. Nevertheless, for the seasonal period (June-July), our values (700-2500 ind m^{-3}) recorded in the 0-200 m layer with a 120 µm net were higher than that of Siokou-Frangou (2004; 50-900 ind m^{-3}) recorded in the upper 100 m with a 200 µm mesh net. This discrepancy highlights the difficulty when comparing different zooplankton datasets and the lack of common protocols.

The present work contributed to widening the characterization of the zooplankton distribution in the Mediterranean Sea. Our synoptic survey through the western and eastern basins confirms the eastward decrease of zooplankton abundance that has already been reported during other trans-Mediterranean surveys (Dolan et al., 2002; Siokou-Frangou, 2004; Minutoli and Guglielmo, 2009). In contrast, the biomass distribution did not show any large scale trend with average (~6.3 mg DW m^{-3}) and maximal (~10.4 mg DW m^{-3}) values similar between regions, in agreement with biomass data compilations for various Mediterranean regions (Champalbert, 1996; Koroleff, 1969; Alcaraz et al., 2007; Siokou-Frangou et al., 2010). The apparent paradox between the trend in abundance and no trend in biomass might be explained by difference in size-spectra between the eastern and western basins. The presence of a few dominant large species, such as *Haloptilus longicornis, Pareucalanus attenuatus* and *Subeucalanus monachus* in the eastern basin, or the large amphipod *Phronima sedentaria* at station 7 could explain high local biomass. For example, the contribution of the three large copepod species to the total biomass was estimated, using length-weight relationship (Webber and Roff, 1995; Hopcroft et al., 2002) to be 1.7 % (st. 13), 24.3 % (st. 3) and 30.5 % (st. 5). Therefore, large organisms contributed to the low NB-SS slopes observed in the eastern basin (see fig. 6). In contrast in the western basin, high abundance was linked with the predominance of small organisms such as *Oncaea* spp. and *Macrosetella/Microsetella* spp. This higher abundance of small organisms was confirmed by the Niskin bottle sampling.

Table 4-4. Equation parameters of the multiple linear regression models using forward stepwise method explaining the zooplankton parameters distribution. Integrated zooplankton abundance (ind m^{-3}) and biomass (mg DW m^{-3}) were obtained from net sampling (n = 20); discrete abundance of nauplii and small copepod (ind m^{-3}) was issued from Niskin bottles (n = 111 to 140). Symbols of variables are described in table 3.

	Beta	Beta standard error	P-level
Integrated nauplii abundance			
R^2 = 0.53; adjusted R^2 = 0.47; F = 8.61; P = 0.003			
Constant	3.63	0.08	
HNF10	0.27	0.09	0.008
CHL	3.15	1.22	0.021
Integrated small copepods abundance			
R^2 = 0.57; adjusted R^2 = 0.51; F = 9.82; P = 0.002			
Constant	3.10	0.12	
CHL	4.17	1.14	0.002
HNFT	0.32	0.14	0.039
Integrated metazooplankton abundance			
R^2 = 0.75; adjusted R^2 = 0.71; F = 21.89; P < 0.001			
Constant	1.87	0.3	
NANO	0.37	0.14	0.016
CHL	3.4	1.48	0.036
Integrated metazooplankton biomass			
R^2 = 0.55; adjusted R^2 = 0.49; F = 9.18; P = 0.002			
Constant	-19.84	6.77	
CHL	6.24	1.52	< 0.001
SAL	12.70	4.21	0.009

	Beta	Beta standard error	P-level
Discrete nauplii abundance			
R^2 = 0.56; adjusted R^2 = 0.54; F = 31.51; P < 0.001			
Constant	-12.79	2.22	
O2	5.58	0.86	<0.001
CHL	2.29	0.36	<0.001
TEMP	1.01	0.37	0.007
Discrete small copepods abundance			
R^2 = 0.32; adjusted R^2 = 0.31; F = 17.97; P < 0.001			
Constant	1.20	0.08	
CHL	1.33	0.35	<0.001
PON	1.97	0.59	0.001

In the western basin metazooplankton and small copepods abundances as well as the total biomass displayed a North-South decreasing gradient. D'Ortienzo and Ribera d'Alcalà (2009) reported also this clear north-south gradient in the lower trophic level (chlorophyll-*a* levels)

with a “northern blooming area”, an “intermittently-blooming central area” and a “non blooming area” in the south.

The high biomass and abundance variability between stations potentially arises from day-night variations, because sampling was conducted at different times of the day. When comparing day-night samplings at the three long stay stations, diel variation led to an increase of 17 % in term of abundance and over 40 % in term of biomass due to increasing numbers of medium and large organisms (> 500 µm ECD) at night as already observed in studies dedicated to the diel migration (Andersen et al., 1998; Andersen et al., 2004; Andersen et al., 2001a; Riandey et al., 2005). Variability in zooplankton abundance and biomass could also be explained by the 3 identified anticyclonic gyres characterized by a clear downwelling (Moutin et al., 2011) with, as consequence, a deepening in nutrients (Pujo-Pay et al., 2011) and low phytoplankton and microzooplankton biomass (Christaki et al., 2011; Crombet et al., 2011). On the other hand, freshwater and terrestrial mineral input from the Rhône River (Cruzado & Velásquez, 1990) could explain high nutrient levels and high phytoplankton and metazooplankton biomass in the river plume area (st. 27), as already evidenced by Gaudy et al. (2003). Variability resulted also probably from local hydrodynamic conditions linked to the bottom topography. The station 17 was very shallow with bottom depth ~100 m and presented typical characteristic of a coastal stations with high values of chlorophyll, high abundance of metazooplankton and a neritic community. This was also reported in other neritic areas of the western basin such as the Balearic Sea (Fernandez de Puelles et al., 2004; 2009). Station 13 located over the margin area (slope between SC and IB) was also a site where local enhancement can be observed.

Globally, the horizontal distribution of the metazooplankton in terms of abundance and biomass was mainly driven by the chlorophyll-*a* concentration (table 4-3, 4-4 and Fig 4-9). Our study established empirical relationships (linear regression) between metazooplankton abundance or biomass and chlorophyll-*a* concentration throughout the Mediterranean Sea. Chlorophyll-*a* (and subsequently zooplankton) distribution was mainly driven by the eastward gradient in oligotrophy which is a consequence of the thermohaline circulation and the nutrient inputs from rivers (Krom et al., 1991; Ignatiades, 2005; Moutin & Raimbault, 2002; D’Ortenzio & Ribera d’Alcalà, 2009).

In the Mediterranean Sea, the bulk of epipelagic mesozooplankton is generally concentrated within the upper 100 m (Scotto di Carlo et al., 1984; Weikert & Trinkaus, 1990; Brugnano et

al., 2010) and mainly within the upper 50 m in both the eastern basin (Mazzocchi et al., 1997) and the Ligurian Sea (Licandro & Icardi, 2009). Here, the bulk of both nauplii and small copepods presented a patchy vertical distribution (down to 120 m) throughout the Mediterranean Sea, mainly driven by the deep chlorophyll maximum (DCM) depth. Clear association between vertical distribution of epipelagic mesozooplankton and DCM has previously been shown during the summer stratified period (Alcaraz, 1985, 1988; Alcaraz et al., 2007). Higher grazing activity by copepods is also often associated with DCM as demonstrated by increased phaeophorbide concentration (Latasa et al., 1992). Here, the nauplii abundance vertical distribution showed a maximum matching the DCM except at a few stations where temperature at the maximum nauplii concentration was ~15°C. The multiple regression analysis confirmed the combined effort in the search for the optimal food availability (DCM) and the best thermal conditions for development (Chinnery & Williams, 2004; Koski et al., 2011). Nauplii and small copepod vertical distributions were also correlated with oxygen, PON and POP, but these variables are indirectly linked to phytoplankton abundance through photosynthesis, respiration and organic composition. Their distribution was also associated with heterotrophic nanoflagellates and ciliates, suggesting a link with the microbial loop, which is known as a potential food source for small planktonic organisms (Calbet & Saiz, 2005; Henriksen et al., 2007). Horizontal distribution of the abundance of nauplii, small copepods and metazooplankton was correlated with the distribution of HNF > 10 µm, total HNF and nanophytoplankton respectively. The affinity of nauplii for small motile prey such as HNF was evidenced experimentally by Henrikzen et al. (2007), that of small copepods for phytoplankton and microheterothrophs (Nakamura & Turner, 1997; Zervoudaki et al., 2007) and of metazooplankton for nanophytoplankton performed at different season of the year (Pinca & Dallot, 1995; Gaudy & Youssara, 2003; Alcaraz et al., 2007; Zervoudaki et al., 2007) is also well known. Finally physical forcing can also affect vertical distribution as shown by Andersen et al. (2001), with nauplii of copepods and euphausiid being influenced by a deepening of the mixed layer and a dilution of the phytoplankton biomass in the water column following a wind event.

4.2.4.2 Pattern of zooplankton assemblages in relation with environmental parameters

The zooplankton composition recorded during the BOUM transect was in general agreement with the published data on the Mediterranean Sea community (Siokou-Frangou et al., 1997; Gaudy et al., 2003; Pasternak et al., 2005; Riandey et al., 2005). The overall metazooplankton community was dominated by copepods and especially by small size species (< 1mm). *Clausocalanus/Paracalanus* spp. and *Oithona* spp. were the dominant genera, as is generally observed (Gallienne & Robins, 2001; Gaudy et al., 2003; Peralba & Mazzocchi, 2004; Zervoudaki et al., 2007).

We found a clear distinction in taxonomic composition between the western and the eastern basins mainly driven by ecological characteristics. Several copepods species showed a clear eastward pattern. For example, *Macrosetella/Microsetella* spp., *Acartia clausi* and *Centropages typicus* were more abundant in the western basin; while, *Calocalanus pavo, Corycaeus/Farranula* spp., *Haloptilus longicornis, Lucicutia flavicornis, Mecynocera clausi* and *Pareucalanus attenuatus* were present mainly in the eastern basin. The spatial distribution of most species reported here has been confirmed by Siokou-Frangou et al. (2010). Other taxonomic groups presented also a clear spatial pattern. Cladocerans were nearly absent from the eastern basin, which may be also explained by the difference in the sampling dates between the two basins (> 2 weeks). Indeed, these organisms are known to display explosive growth over very short time-periods linked to their parthenogenetic reproduction (Christou & Stergiou, 1998; Atienza et al., 2007; 2008). The distance to the coast could also explain local high abundance, such as in the Sicily Channel, of these organisms, known to have a neritic affinity (Fernandez de Puelles et al, 2007). These differences in the percentage contribution of some important species to the whole copepod assemblage might reflect differences in species biogeography, but might also be indicative of different associations between structural and functional features. In the co-inertia analysis (Fig 4-9), the eastern basin was characterized by high diatoms concentration associated with higher abundance, compared to other stations, of large-size herbivorous copepods i.e. *Pareucalanus attenuatus* (st. 5 and 7) and *Subeucalanus monachus* (st. 13) both restricted to the eastern basin. High abundance of these copepods also corresponded to hot spots of biogenic silicon dominated by the microphytoplankton *Chaetoceros* spp. in the eastern basin (Crombet et al., 2011). *Subeucalanus monachus* has already been reported in high abundance in the Rhodes cyclonic gyre where nutrients rich

waters have been upwelled leading to high phytoplankton biomass dominated by large diatoms (Siokou-Frangou et al., 1999). One novelty observed during the BOUM cruise is the presence of *Cosmocalanus darwini* reported for the first time in the Mediterranean Sea, both in the western and eastern basins. We found copepodites stages as well as females indicating the reproductive success of this species. However, it is difficult to conclude about its origin in the Mediterranean Sea. This species is common in the Red sea (Razouls et al., 2005-2011; web site) and is expected to undergo lesseptian dispersion but this species was found in lower abundance in the eastern basin than in the western basin.

On the other hand, the western basin was characterized by high nutrient concentrations, high abundance of nanophytoplankton and small and medium (< 1.5mm prosome length) herbivorous/omnivorous copepods (i.e. *Acartia clausi*, *Centropages typicus*, *Euterpina acutifrons*). The association of these small copepods species with nanophytoplankton-rich conditions has already been demonstrated in the Mediterranean (Pinca & Dallot, 1995; Gaudy & Youssara, 2003; Alcaraz et al., 2007; Zervoudaki et al., 2007).

Mesoscale hydrodynamic structures could also play an important role in the variability of zooplankton abundance and community structure. Anticyclonic gyres displayed lower abundance of metazooplankton and less marked vertical distribution than neighbouring stations where higher chlorophyll concentration at the DCM was observed. These gyres showed a metazooplankton community characterized by lower *Clausocalanus/Paracalanus* (herbivorous) and more *Corycaeus/Farranula* spp. (omnivorous) that could reflect changes in food availability (increase in oligotrophy, lower chlorophyll concentration) (Legendre & Rassoulzadegan, 1995).

The position of station A in the co-inertia analysis is peculiar, highlighting the response of the zooplankton community structure to the environmental forcing. Geographically belonging to the western basin, the physical conditions prevailing at station A led to a different zooplankton composition (i.e. less *Clauso/Paracalanus* spp., and more *Corycaeus/Farranula* spp. and *P. gracilis*) than other stations in the APB; therefore station A emerged on the co-inertia analysis half way between its geographical group and the group where station B and C were located. Nevertheless, the gyre located at station C did not display a lower abundance and biomass than surrounding LB stations. Its functioning could be slightly different from the two other gyres resulting in stronger (0.441 µg L^{-1}) and deeper (120 m depth) DCM. Moreover, its location close to the Cyprus coast could explain the high abundance of

echinoderm larvae through the aggregation effect of the gyre (Pedrotti and Fenaux, 1996). Indeed, these structures are known to affect mesozooplankton community structure and functioning (Youssara & Gaudy, 2001; Zervoudaki et al., 2006; Alcaraz et al., 2007; Molinero et al., 2008; Siokou-Frangou et al., 2009; Hafferssas & Seridji, 2010).

In conclusion, we found a clear eastward pattern in term of metazooplankton abundance but not for the biomass which showed a high variability between stations. The causes of this variability were numerous and of different aspect. The horizontal and vertical distribution of the metazooplankton was strongly linked to the chlorophyll-*a* concentration but also to other parameters such as microzooplankton or physical forcing (i.e. stratification, temperature). These environmental parameters influenced also the species distribution and size structure of the community. It is obvious that the type and the size of the available food (nanophytoplankton and/or diatoms) should also influence the presence of smaller or larger species.

4.3 "Role of the metazooplankton community in the functioning of the oligotrophic and ultra-oligotrophic Mediterranean Sea (BOUM Cruise)"

4.3.1 Introduction

The whole Mediterranean Sea (MS) is globally characterized by low nutrient concentrations i.e. oligotrophic. Moreover a strong eastward gradient in nutrient deficiency exists, reaching ultra-oligotrophic conditions in the Levantine basin with a strong limitation in phosphorus availability (Durrieu de Madron et al., 2011, Pujo-Pay et al., 2011). This gradient results from the general thermohaline circulation and the nutrient inputs from large rivers. Weak phytoplankton biomass and primary production ensue from this general deficiency in nutrients (reviewed in Siokou-Frangou et al., 2010). The degree of oligotrophy at any station along this gradient depends of its distance from the nutrient sources and the adequacy between biological processes such as production, remineralization, and export (Crise et al., 1999). As in most oligotrophic marine areas, the MS functioning is at large dominated by the microbial food web (Thingstad and Rassoulzadegan 1995; Christaki, Van Wambeke et al. 1996; Turley, Bianchi et al. 2000; Siokou-Frangou).

Mesoscale hydrological structures, in addition to the surface general circulation, affect, locally, the productivity patterns and biogeochemical fluxes by enhancing nutrient concentration and therefore the biological activities. In the MS, the most important structures are large river plumes (Rhône, Po and Nile) (Cruzado & Velasquez, 1990; Revelante & Gilmartin, 1992), frontal systems found in the Almeria-Oran region, the North Balearic-Catalan region and the North-East Aegean Sea (Estrada & Salat, 1989; L'Helguen et al., 2002; Zervoudaki et al., 2006), and deep convection areas in the Gulf of Lion, the South Adriatic gyre, the Rhodes gyre, and the Algerian gyre (Lévy et al., 1998; Gacic et al., 2002; Azzaro et al., 2007).

Increased zooplankton biomass and abundance have often been observed in relation with these structures (Pagano et al., 1993; Thibault et al., 1994; Isla et al., 2004; Riandey et al., 2005; Zervoudaki et al., 2007) and could be linked to either passive accumulation or increase of zooplankton production (Alcaraz et al 2007). However, the biological and ecological processes associated with these increases in biomass in Mediterranean mesoscales structures are poorly documented. Zooplankton metabolism has been studied so far mainly in neritic and shallow coastal areas (Gaudy et al., 2003) but rarely in open waters (Pérez et al., 1997; Gaudy

et al., 2003). Moreover they all have been very limited to local or regional scales, only Minutoli and Guglielmo (2009) measured respiration rates at the scale of the whole MS. A complete data set including trophic and metabolic rates is still clearly needed.

One objective of the BOUM project (Biogeochemistry from the Oligotrophic to the Ultra-oligotrophic Mediterranean) was to obtain a better representation of the interactions between planktonic organisms and the cycle of biogenic elements, in different regions of the MS. Here we present results on the metabolic rates of metazooplankton measured in three anticyclonic gyres located throughout the entire basin. Together with detailed information on the metazooplankton distribution (Nowaczyk et al, 2011), we aimed then at answering the following questions:

- Does the metazooplankton respond identically to the three anticyclonic gyres?

- What is the grazing pressure of metazooplankton on the Primary Production in this oligotrophic environment?

- How much metazooplankton contributes to the *in situ* pools of Carbon, Nitrogen and Phosphorus?

4.3.2 Materials and methods

4.3.2.1 Cruise track and sampling

Samples were collected in the centre of anticyclonic gyres located in the Algero-Provencal (station A), the Ionian (station B) and the Levantine (station C) Basins (Fig. 4-10) on 13/07/08, 04/07/08 and 26/06/08 respectively.

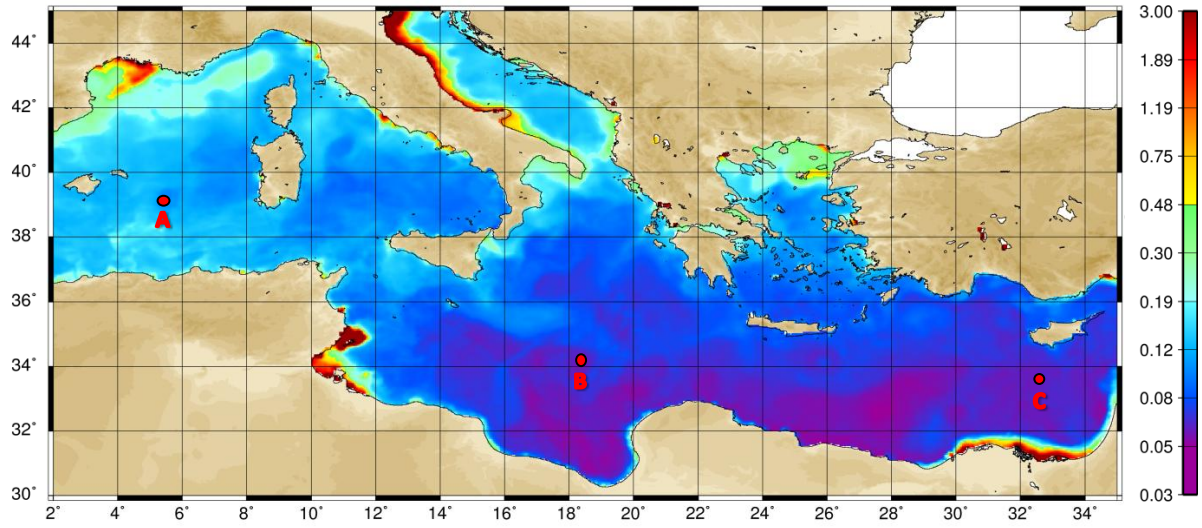

Figure 4-10 Location of sampling stations superimposed on a SeaWIFS composite image of the sea surface chlorophyll *a* concentrations (permission to E. Bosc) integrated during the BOUM transect (16 June-20 July 2008).

Zooplankton was collected around midnight using a double bongo nets (60 cm mouth diameter) fitted with 120 µm mesh size and equipped with filtering cod ends. Low speed (1 m s^{-1}) vertical hauls were carried out from 200 m to the surface.

Two hauls were done. From the first haul, one cod end was dedicated to abundance measurements and half of the second one for biomass estimation (Nowaczyk et al., 2011). The remaining of the second cod-end was immediately filtered on a GF/F filter, stored in a Petri dish and frozen in liquid nitrogen (-80°C) until further gut pigment content analysis. The second haul was dedicated to the metabolic experiments and lived animals were immediately sorted and prepared for the experiments within 1 to 2 h.

4.3.2.2 Gut fluorescence – grazing impact on phytoplankton

Grazing of copepod and ostracod on phytoplankton was assessed using the gut fluorescence technique (Macckas & Bohrer, 1976). Once back in the lab, animals were rapidly thawed, and sorted with a dissecting microscope under dim light using cold sea water (at approximately 0°C).Copepods were grouped into two size classes (< 1000 µm and > 1000 µm). Several sets of 100-150 and 5-30 individuals for the small and large fractions respectively were sorted out at each station. Ostracods (15-30 individuals) were also analyzed. Pigment contents were extracted in 5 ml of 90% acetone over-night at 4°C in the dark and then measured with a Turner Designs III fluorometer before and after acidification using 1 N HCl. Chlorophyll *a* and phaeopigment concentrations were measured according to Yentsch & Menzel (1963), modified by Holm-Hansen et al. (1965). Gut pigment contents (*GPC* in ng Chl*a* eq ind^{-1}) were calculated according to Wang & Conover (1986), where chlorophyll *a* equivalents = Chl *a* + phaeopigment. Gut clearance rate constant for copepods, *k* (min^{-1}), was calculated using the equation of Dam & Peterson (1988) modified by Dam (see Bamstedt et al., 2000). For ostracods, *k* was estimated at 80% of that of copepods at any given temperature (Perissinotto, 1992). GPC were transformed into *in situ* daily ingestion rates (I in ng Chl*a* eq ind^{-1} d^{-1}) assuming the animals were feeding at equilibrium (i.e. defecation rate = ingestion rate) and at constant rate over 24 h, following this equation:

$$I = GPC \times k \times 60 \times 24$$

Ingestion was converted into carbon using a carbon/chlorophyll ratio of 50 (Bamstedt et al., 2000).

The grazing impact of each taxon can be then estimated by multiplying its daily ingestion rate by its *in situ* abundance. Grazing pressure was assessed on >2 µm fraction of the phytoplankton biomass and primary production.

4.3.2.3 Metabolism measurements

Respiration and excretion experiments were performed using the same set up. Water for experiments was collected at the surface using a bucket, filtered through 0.2 µm and kept in 10 L jars for 48 h in a temperature-controlled room. The jars were kept untapped in order to saturate the water in oxygen and CO_2. The temperature of the room was adjusted to the *in situ*

temperature measured at the depth of the Deep Chlorophyll Maximum (DCM), i.e. 15°C, 16°C and 17°C, for stations A, B and C, respectively. Before the experiment, 125 mL or 310 mL *DBO* flasks were filled up by draining water from the 10 L jars. Zooplankton organisms, just after collection, were placed in 10 L buckets filled with surface seawater previously stored in the temperature-controlled room then gently sieved through a 1000 µm mesh size separating large and small organisms. The small zooplankton fraction (< 1000 µm) mainly composed of *Oithona* spp. and *Oncaea* spp. and copepodite of *Clausocalanus* spp. and *Paracalanus* spp., was considered globally. Large (> 1000 µm) organisms were considered either globally or separated according to species/taxa and stage (when possible). At station C, as the net was clogged by long chains of *Chaetoceros* and *Ceratium*, organisms had to be picked out individually by hand; thus, only taxon-specific experiments were run.

Animals were conditioned for ca. 2h in 100 mL glass beakers filled with filtered seawater. They were then introduced into the experimental flasks. Small organisms were placed by sets of up to 150 individuals per flasks, while large organisms were placed either individually *(Euchaeta spinosa*) or by sets of up to 15 (*Lucicutia* sp.). Very large organisms such as euphausiids and amphipods were placed individually into 310 mL flasks. Generally 2-3 replicates were run for small organisms and 1-4 replicates for large taxa (see Tables 4-5 and 4-7) according to availability in the samples.

Incubations were conducted in a water bath in the dark during 15 to 24 hours. Control bottles without zooplankton (3-6) were kept under the same conditions.

At the end of experiment, animals were preserved in 4% buffered formaldehyde seawater solution for confirmation of species identification and length measurements. The size were considered as: prosome length for copepods, from the eye base to the junction of abdomen and telson for euphausiids, from the base of the head to the base of junction of abdomen and telson for amphipods, the anterior nectophore length measurement for siphonophores and total length for other taxa. Length was converted into carbon content using published length-weight relationships (Uye 1982; Ikeda 1990; Mauchline 1998).

Respiration measurements

Respiration rates of zooplankton organisms were measured using two different methods, the oxygen consumption and the carbon dioxide release.

At the end of the incubation period, 20 mL of seawater was gently siphoned from each bottle to measure oxygen concentration using an YSI 420 oxymeter equipped with a Clark-type electrode. Mercuric chloride was then added in excess in each bottle to stop all respiration activities. Total inorganic carbon was measured using a colorimetric titration (Johnson et al., 1987) with a coulometer, as described in Mayzaud et al. (2005). Oxygen consumption and CO_2 production rates were computed by difference between the flasks containing animals and the controls at the end of the incubations.

The respiratory quotient (RQ) was then calculated from the ratio between the carbon dioxide produced and the oxygen consumed. For each taxon, daily individual respiration rate was multiplied by its depth-integrated abundance. For those taxa where respiration rates were not measured, values were taken from the literature (Mauchline et al., 1998). Integrated daily CO_2 production by the mesozooplankton was calculated by summing the production of the different taxa.

In order to characterize the respiratory activities, we will follow the classification made by Prosser (1961), with standard or "basal" activity corresponding to the amount of oxygen needed to support maintenance level, while "routine" described activity level with limited moving capacities such as found in the bottle incubation conditions, and then "active" level when activity reach maximal level. We will consider routine level as 1.9 times that of basal level, while active level is 6 times higher (Buskey, 1998). The contribution of the CO_2 production by zooplankton to the carbon requirement for primary production was estimated by comparing primary production (Moutin et al 2011) and CO_2 produced by the metazooplankton.

Excretion measurements

At the end of each experiment, oxygen measurements were carried out as described above. Dissolved ammonia and phosphorus were measured on three 20 mL sub-samples withdrawn with a syringe fitted with a GF/F filter and immediately analyzed on board. Ammonium (NH_4^+) was measured by fluorimetry according to Holmes et al (1999) on a Jasco FP-2020 fluorimeter with a precision of ± 2 nM and a detection level of 3 nM. Inorganic phosphorus (PO_4) was measured using the automated colorimetric technique (Treguer & le Corre, 1975) on a segmented flow Bran Luebbe autoanalyser II with a precision of ± 0.005 µM and a detection limit of 0.01 µM. Excretion rates were computed from the difference in concentrations between the experimental flasks and the controls at the end of the incubations.

Excretion rates for the whole zooplankton community were calculated by multiplying PO4 and NH4 excretion rates by the *in situ* abundances of the organisms, and were then compared to the phytoplankton demand for N and P. Phytoplankton nutrient uptake was estimated by converting the primary production using the following ratios: C:N:P = 200:20:1 at station A and 230:21:1 at stations B and C (Pujoy-Pay et al., 2011).

4.3.3 Results

4.3.3.1 Characterization of the study area

Stations A, B and C are located in the centre of 3 distinct anticyclonic gyres characterized by clear downwelling of surface waters (see Moutin et al submitted for more details). At station A, the downwelling signal is detectable down to 800 m but the core of the eddy is limited to 100-250 m. At station B, the eddy extends down to 1500 m and the core depth is 200-600 m.

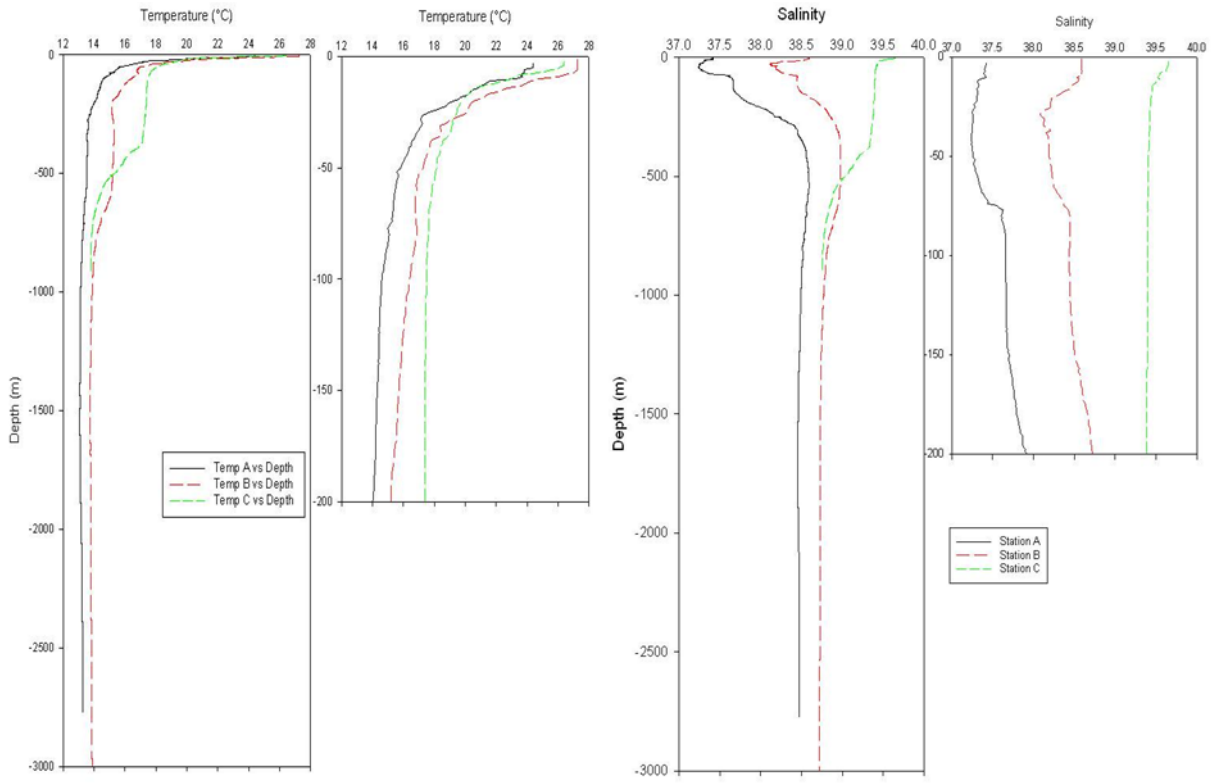

Figure 4-11. Vertical profile of temperature (left) and salinity (right) within the total water column and upper 200m at station A, B and C.

At station C the eddy is detectable down to the floor (900 m) and the core depth is 150-400 m. Surface salinity increases eastward from 37.4 to 39.6 while warmer surface water is observed at stations B and C (27-28°C) than at station A (25°C). The three sites are characterized by a

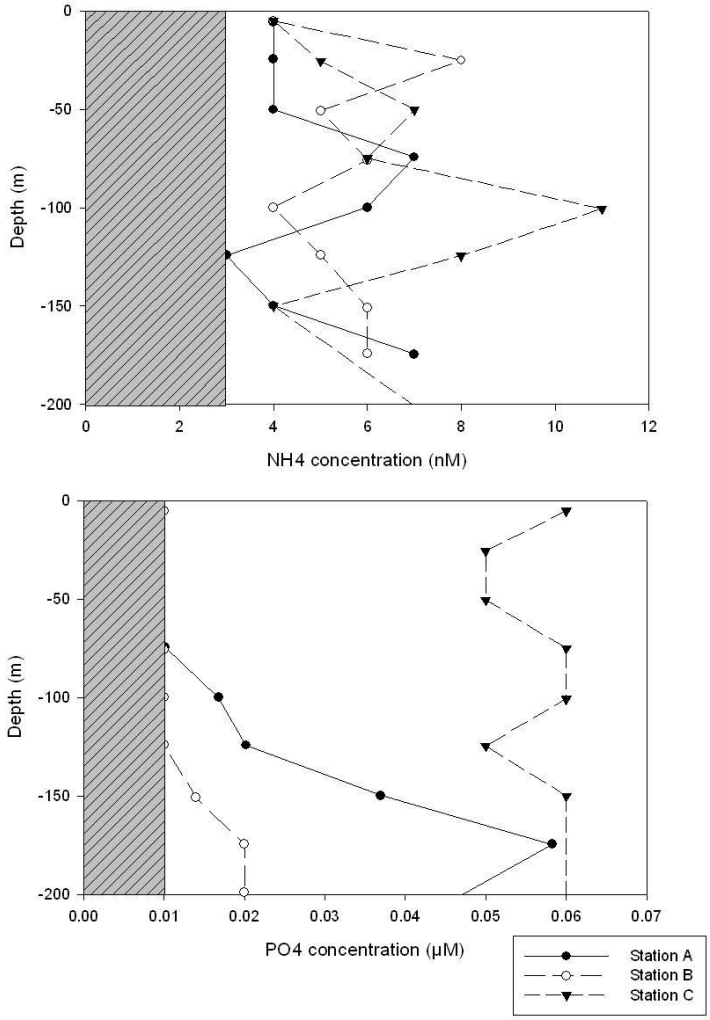

Figure 4-12. Vertical distribution of NH_4 (top) and PO_4 (bottom) within the upper 200m at station A, B and C. Detection limit in grey.

strong surface stratification. A clear deep halocline is observed at station A (~400 m) and station B (~300 m). At station C, salinity remains ~ 39.5 down to 400 m then freshens to typical deep water salinity (~38.6) (Fig. 4-11). Deep Chlorophyll Maxima (DCM) was localized at ~80 m ~150 m and ~110m at stations A, B and C (Fig 3a) with a corresponding temperature of 15°C, 16°C and 17°C respectively. The fluorescence signal is stronger at stations A (0.8 µg $Chla.L^{-1}$) and C (0.75 µg $Chla.L^{-1}$) than at station B (0.3 µg $Chla.L^{-1}$). Ammonium concentrations did not present any specific pattern for the three gyres, with values ranging from 3 to 11 nM (Fig. 4-12). On the other hand a clear spatial differences is observed in the PO4 distribution, with stations A and B characterized by very low PO4 concentrations (< detection limit) down to 75 m and 125 m respectively, increasing then slightly with depth, reaching 0.055 µM at station A but only 0.02 µM at station B.

Concentrations observed at station C were constant throughout the upper 200 m ~ 0.05-0.06 µM.

4.3.3.2 Respiration rates

Mean respiration rates (µl O_2 h^{-1} and µl CO_2 h^{-1}) and Respiratory Quotient (RQ) values are presented in Table 4-5. Measurements were made on seven different zooplankton taxa (amphipods, copepods, euphausiids, ostracods, jellyfishes, annelids and siphonophores), some regrouping species with different trophic and physiological characteristics. Individual respiration rates were therefore highly variable. Oxygen consumption rates ranged from 0.07 µL O_2 ind^{-1} h^{-1} for small copepods to 20.32 µL O_2 ind^{-1} h^{-1} for the annelid *Alciopa* sp. , and CO_2 production rates from 0.08 to 14.78 µg C ind^{-1} h^{-1}. Respiration rates were lower for small copepods such as *Lucicutia flavicornis* (0.26 µL CO_2 ind^{-1}) than for larger ones such as *Euchaeta spinosa* (3.15 µL CO_2 ind^{-1}). Large organisms showed high individual respiration rate ranging from 2.41 to 18.07 µl CO_2 ind^{-1} for the 4 species of amphipods and from 6.68 to 11.06 µl CO_2 ind^{-1} for the 3 species of euphausiids.

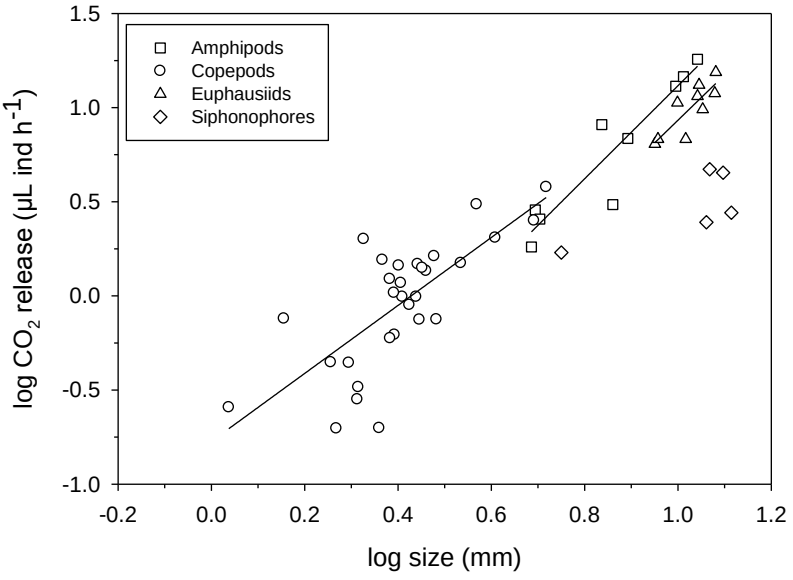

Figure 4-13. Log-log relationship between the individual hourly CO_2 release rates and the mean size of the zooplankton species. Equations were given in tab 4-6.

We considered here that the temperature at which the experiments were conducted (15, 16 and 17°C) did not impact significantly the metabolic activities. Respiration was strongly

correlated to the size of the organisms, but appeared less depend on the weight. The slope of the regression for the euphausiids and amphipods were not statistically different, while copepods at a lower slope (fig 4-13, Table 4-6).

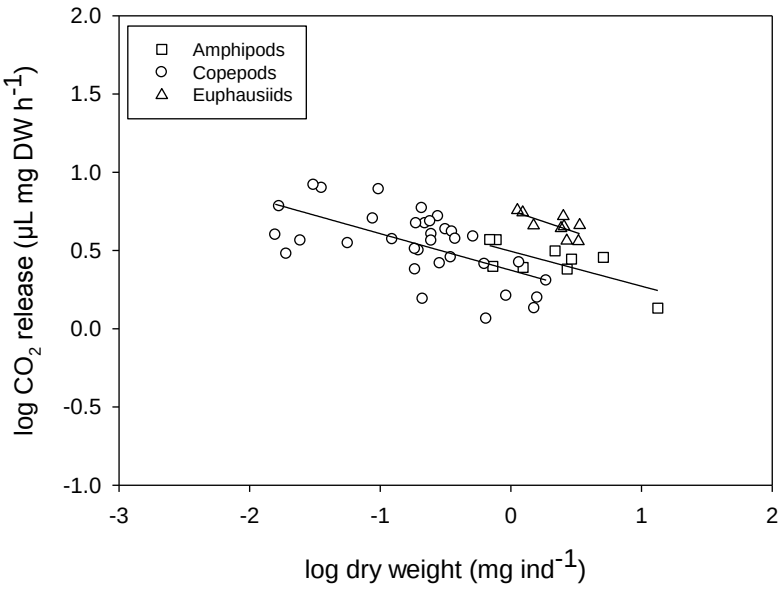

Figure 4-14. Log-log relationship between the weight-corrected hourly CO2 release and the mean dry weight of the three main taxa of crustacean zooplankton. Equations were given in tab 4-6.

Weight-corrected respiration rates for the three groups of crustaceans displayed rather identical inverse relationships (Fig.4-14) (-0.223 to -0.281). The release in CO_2 is higher than the consumption of oxygen in most cases, except for large amphipods and euphausiids (Fig 4-14). The slope of the regression between these two metabolic activities for copepods and euphausiids were similar (0.86 ± 0.35 and 0.83 ± 0.16, respectively). Amphipods had overall the highest RQ. (1.03 ± 0.3).

Table 4-5. Respiration rates (µl O_2 ind^{-1} h^{-1} and µl CO_2 ind^{-1} h^{-1}) and respiratory quotient (atomic ratio) for key taxa and zooplankton<1000 µm at stations A, B and C.

	Taxa + Stages	nb exp	Size (mm)	Dry weight (mg ind^{-1})	Respiration		RQ CO_2/O_2
					(µl O_2 ind^{-1} h^{-1})	(µl CO_2 ind^{-1} h^{-1})	
Station A							
Copepods							
	Copepods <1000 µm	2	nd	0.016 ± 0.001	0.074 ± 0.004	0.083 ± 0.028	1.13 ± 0.44
	Cosmocalanus darwini ♀	1	1.80	0.09	0.57	0.44	0.79
	Euchirella messinensis ♀	1	4.06	1.51	2.17	2.04	0.94
	Euchirella messinensis C3-5	2	3.37 ± 0.47	0.90 ± 0.36	2.24 ± 1.41	1.91 ± 1.64	0.78 ± 0.24
	Euchirella messinensis C1-2	2	2.02 ± 0.07	0.20 ± 0.02	0.82 ± 0.20	0.38 ± 0.08	0.47 ± 0.02
	Neocalanus gracilis C5+♀	2	2.68 ± 0.30	0.27 ± 0.08	1.24 ± 0.47	0.99 ± 0.52	0.78 ± 0.13
	Pleuromamma abdominalis ♂+♀	2	2.52 ± 0.07	0.23 ± 0.02	1.17 ± 0.12	1.01 ± 0.04	0.87 ± 0.06
Amphipods							
	Lycaea sp.	3	4.95 ± 0.22	0.73 ± 0.04	2.72 ± 0.43	2.41 ± 0.54	0.89 ± 0.18
	Anchylomera blossevillei ♂+♀	3	8.32 ± 1.76	3.40 ± 1.52	9.30 ± 2.72	9.86 ± 4.15	1.07 ± 0.28
	Platyscelus serratulus	1	11.02	13.34	12.42	18.07	1.45
	Scina crassicornis	2	8.57 ± 1.86	1.97 ± 1.03	6.01 ± 1.43	4.77 ± 2.43	0.77 ± 0.22
Euphausiids							
	Euphausia krohni	3	9.46 ± 0.81	1.28 ± 0.19	9.43 ± 2.61	6.68 ± 0.23	0.74 ±0.19
	Nematoscelis megalops	1	12.05	3.36	13.85	15.43	1.11
	Stylocheiron abbreviatum	2	10.50 ± 0.73	2.49 ± 0.09	15.33 ± 1.04	11.06 ± 0.61	0.72 ± 0.01
Ostracods							
	Conchoecia sp.	1	0.84	0.012	0.25	0.25	0.99
Siphonophores							
	Chelophyes appendiculata	4	12.37 ± 1.99	nd	4.04 ± 0.91	3.61 ± 1.16	0.94 ± 0.36
Station B							
Copepods							
	Copepods <1000 µm	2	nd	0.022 ± 0.004	0.071 ± 0.001	0.074 ± 0.023	1.04 ± 0.34
	Euchaeta marina ♀	4	2.72 ± 0.13	0.34 ± 0.04	1.66 ± 0.20	1.37 ± 0.10	0.82 ± 0.21
	Euchaeta spinosa ♀	2	5.07 ± 0.22	1.73 ± 0.19	4.23 ± 1.07	3.15 ± 0.90	0.74 ± 0.03
	Euchirella messinensis C4+C5+♀	2	3.21 ± 0.30	0.77 ± 0.21	1.95 ± 0.25	1.56 ± 0.09	0.81 ± 0.15
	Euchirella messinensis C2+C4	1	2.12	0.52	2.04	2.01	0.98
	Haloptilus longicornis ♀	2	2.17 ± 0.17	0.05 ± 0.01	0.27 ± 0.01	0.24 ± 0.06	0.89 ± 0.17
	Mesocalanus tenuicornis C5+♀	1	2.42	0.18	0.85	0.60	0.70
	Neocalanus gracilis C5+♀	2	2.72 ± 0.10	0.27 ± 0.03	0.89 ± 0.07	0.82 ± 0.11	0.92 ± 0.05
	Pleuromamma abdominalis ♂+♀	2	2.48 ± 0.09	0.22 ± 0.02	1.58 ± 0.72	1.20 ± 0.04	0.86 ± 0.42
Euphausiids							
	Euphausia krohni	4	11.63 ± 0.50	2.97 ± 0.44	13.55 ± 1.45	11.63 ± 1.72	0.88 ± 0.03
Polychetes							
	Alciopa sp.	3	23.03 ± 6.28	nd	20.32 ± 5.67	14.78 ± 2.56	0.86 ± 0.47
Station C							
Copepods							
	Euchaeta marina ♂+♀	1	2.52	0.29	nd	0.46	nd
	Lucicutia flavicornis C5+♀	1	1.09	0.03	nd	0.26	nd
	Scolecithricella minor	1	1.43	0.10	nd	0.76	nd
Jellyfishes							
	Oceania armata	4	6.14 ± 0.70	nd	nd	2.81 ± 0.28	nd
Polychetes							
	Lopadorhynchus appendiculatus	1	13.70	nd	nd	1.93	nd
Siphonophores							
	Chelophyes contorta /Eudoxoides spiralis	1	5.62	nd	nd	1.7	nd

Table 4-6. Linear relationships (log Y = a log X +y0) between CO_2 exhausted (Y; µl CO2 mm^{-1} h^{-1} and µl CO_2 mg DW^{-1} h^{-1}) and length (X, mm) or dry weight (X, µg) for all dataset. Results of the regression analysis are shown.

taxa	a	y_0	X	r^2	*p*	n
Amphipods	2.471	-1.355	Length	0.87	0.0002	9
	-0.223	0.495	Dry weight	0.54	0.0234	9
Copepods	1.805	-0.773	Length	0.55	< 0.0001	34
	-0.234	0.374	Dry weight	0.37	0.0001	34
Euphausiids	2.406	-1.473	Length	0.70	0.0051	9
	-0.281	0.755	Dry weight	0.51	0.0305	9

4.3.3.3 Excretion rates

Excretion rates (Table 4-7) ranged from 0.003 to 1.48 µg N ind^{-1} h^{-1} and from 0.07 to 25.5 ng P ind^{-1} h^{-1} for small copepods and euphausiids respectively. Atomic metabolic ratios (O/N, O/P and N/P) showed a great variability ranging for O/N from 9.9 (*Euchirella messinensis*) to 28.5 (small copepods), while O/P values varied from 51.4 (*Chelophyes contorta*/*Eudoxoides spiralis*) to 278.5 (*Euchirella messinensis*), corresponding for these siphonophores and the copepod to an N/P ratio of 2.0 and 18.3 respectively.

4.3.3.4 Gut pigment contents, in situ ingestion rates and metabolic budgets

Gut pigment content and ingestion rates showed clear differences between the taxonomic groups considered (Table 4-8) and the three sites considered. Large copepods (>1000µm) displayed the highest gut pigments contents and small copepods the lowest, while ostracod had intermediate values. As small organisms were more abundant than larger ones, community ingestion rates were between 4 and 10 times higher for small copepods than for large copepods. Community ingestion rates by the ostracods was very limited (<0.5 mg Chl*a* eq m^{-2} d^{-1}). Community ingestion was the highest at station B for the small copepods, then decreased at station C with minimum values observed at station A. The daily ration based on phytoplankton (46.4 to 87.7 %) was in excess of the 20% body carbon minimum requirement for the small copepods in order to cover their basal metabolism rate but barely reached that

minimal value for the large copepods (5.2 to 22.6 %). Ostracods ingested from 37.6 to 68.4 % of their body carbon per day as phytoplankton.

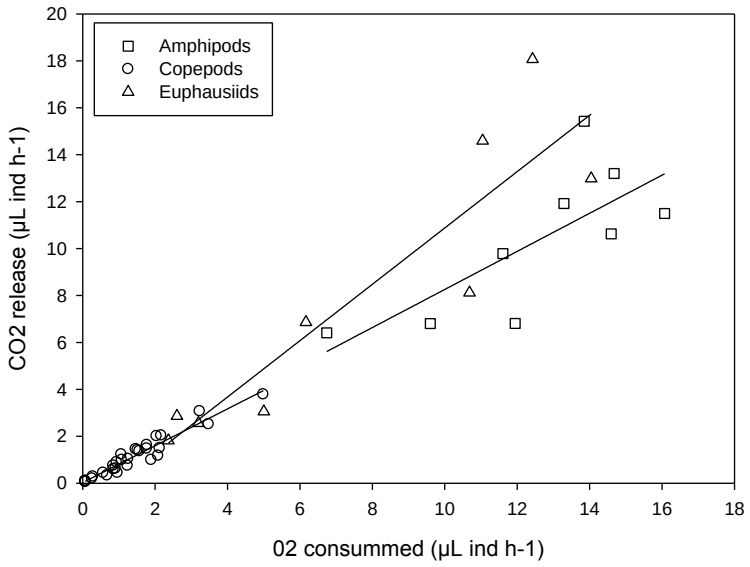

Figure 4-15. Relationship between the O_2 consumed and the CO_2 exhausted by the three main taxa of crustacean zooplankton.

Table 4-7. Respiration rates (µl O_2 ind^{-1} h^{-1}), excretion rates (µg N ind^{-1} h^{-1} and µg P ind^{-1} h^{-1}) and O:N, O:P, N:P atomic ratios for zooplankton < and > 1000 µm and key taxa at stations A, B and C.

Taxa	nb exp	Size (mm)	Dry weight (mg ind^{-1})	Respiration (µl O_2 ind^{-1} h^{-1})	Excretion		Atomic ratios		
					(µg N ind^{-1} h^{-1})	(µg P ind^{-1} h^{-1})	O:N	O:P	N:P
Station A									
copepods < 1000 µm	3	nd	0.009 ± 0.002	0.06 ± 0.01	0.003 ± 0.001	0.0007 ± 0.0002	28.46 ± 10.83	232.64 ± 99.37	8.43 ± 2.85
copepods > 1000 µm	3	2.84 ± 0.42	0.314 ± 0.130	0.44 ± 0.21	0.044 ± 0.22	0.008 ± 0.004	14.63 ± 0.92	158.89 ± 21.41	10.92 ± 1.92
Euchirella messinensis ♀	1	4.57	2.128	2.06	0.26	0.032	9.90	181.39	18.31
Euphausia sp.	1	14.85	5.38	13.64	1.48	0.255	11.52	148.1	12.86
Station B									
copepods < 1000 µm	3	nd	0.007 ± 0.002	0.05 ± 0.01	0.006 ± 0.001	0.0008 ± 0.0001	10.61 ± 0.29	173.78 ± 28.90	16.29 ± 5.26
copepods > 1000 µm	3	nd	0.332 ± 0.040	0.79 ± 0.10	0.043 ± 0.13	0.010 ± 0.007	25.80 ± 13.13	275.45 ± 145.15	13.37 ± 12.93
Euphausia krohni	3	10.71 ± 0.66	1.970 ± 0.062	6.01 ± 1.93	0.576 ± 0.385	0.096 ± 0.082	16.98 ± 6.92	226.01 ± 95.52	11.17 ± 1.82
Station C									
Euchaeta marina ♂+♀	2	2.76 ± 0.22	0.143 ± 0.032	0.87 ± 0.64	0.044 ± 0.020	0.014 ± 0.009	22.89 ± 7.79	257.37 ± 286.38	9.68 ± 9.22
Euchirella messinensis C4+C5	1	3.31	0.833	0.79	0.04	0.008	24.59	278.49	11.32
Lucicutia flavicornis C5+♀	3	1.14 ± 0.05	0.035 ± 0.004	0.13 ± 0.03	0.003 ± 0.002	0.0015 ± 0.0003	28.90 ± 2.48	149.37 ± 30.61	5.23 ± 1.51
Pleuromamma abdominalis ♀	1	2.41	0.207	0.61	0.050	0.010	15.30	156.25	10.21
Pleuromamma abdominalis C4+C5	1	2.02	0.128	0.30	0.017	0.004	22.32	183.52	8.22
Euphausia krohni	1	10.34	1.75	5.24	0.466	0.090	14.06	161.48	11.49
Sergestidae larvae	1	17.60	nd	2.83	0.241	0.036	14.69	215.92	14.70
Anchylomera blossevillei	1	6.99	2.33	7.11	0.569	0.113	15.64	174.95	11.19
Thomopteris sp.	1	2.09	nd	0.35	0.038	0.006	11.56	164.79	14.26
Chelophyes contorta /*Eudoxoides spiralis*	1	4.11	nd	0.53	0.026	0.029	25.75	51.42	2.00
Oceania armata	1	5.94 ± 0.64	nd	1.28	0.124	0.018	12.83	193.58	15.09

Table 4-8. Gut pigment contents, daily individual and community ingestion rates and grazing impact on > 2 µm phytoplankton biomass and primary production at stations A, B and C for copepods < and > 1000 µm and ostracods.

Station ID	Groups	n	Gut pigment content (ng Chl *a* eq ind^{-1})	Individual ingestion rate (ng Chl *a* eq ind^{-1} d^{-1})	Daily ration (%)	Community ingestion rate (mg Chl *a* eq m^{-2} d^{-1})	Daily grazing impact (%)	
							Chl *a* > 2µm	PP > 2 µm
A	Copepods <1000 µm	4	0.41 ± 0.16	24.96 ± 9.64	46.4 ± 17.5	3.78	27.98	> 100
"	Copepods >1000 µm	3	2.19 ± 2.32	133.19 ± 141.24	10.7 ± 3.8	0.76	5.65	52.75
"	Ostracods	1	1.27	62.00	68.4	0.50	3.67	34.23
B	Copepods <1000 µm	3	0.91 ± 0.15	53.14 ± 8.96	87.7 ± 17.0	6.74	90.34	> 100
"	Copepods >1000 µm	2	1.97 ± 1.55	115.01 ± 90.52	5.2 ± 5.1	0.62	8.26	32.93
"	Ostracods	1	1.14	53.32	58.9	0.11	1.48	5.9
C	Copepods <1000 µm	3	0.59 ± 0.03	32.89 ± 1.88	71.1 ± 4.1	5.58	36.63	> 100
"	Copepods >1000 µm	3	3.94 ± 3.12	219.44 ± 174.07	22.6 ± 8.4	1.79	11.73	79.51
"	Ostracods	1	1.06	47.28	37.6	0.24	1.60	10.87

We considered the C breathed out by the small and large copepods community measured during our study, 0.214 µg C µg C^{-1} d^{-1} and 0.278 µg C µg C^{-1} d^{-1} respectively, as the routine respiratory level, threshold above which energy can be invested into growth and reproduction. We then calculated the basal level activity and the active level for the two sizes of copepods (Fig 4-16). The three respiratory activities were compared to the amount of energy gained through feeding. When only phytoplankton >2µm is considered as food source, as estimated by the gut fluorescence technique, small ones met their basal and routine needs at all three stations, but covered their active level requirements only at station A. Large copepods gained at all three stations enough energy through phytoplankton to meet routine level. Most copepod species can actively feed on other particles such as microzooplankton and detritus. We assumed that all particles are ingested at the same rate, therefore multiplied the clearance rate obtained from our gut measurements (F = I / [Chl*a*>2µm]) by the biomass of each other food category. For small copepods, as they were already gaining enough energy to cover largely their routine and at station A their active metabolic needs, additional food source in the form of nano/micro heterotrophs and detritus should allow them to invest energy into growth and reproduction. Metabolic balance was not fulfilled for large copepods with phytoplankton and phytoplankton + nano/microheterotrophs except at station B. These organisms were only able to invest energy towards growth and reproduction when detritus was added to their potential diet and only at station B and C.

4.3.3.5 Impact of zooplankton on primary production

Given their high abundance, small copepods (<1000 µm) had the highest community ingestion rate on phytoplankton (3.78 to 6.74 mg Chl*a* eq m^{-2} d^{-1}). Daily grazing impact upon both phytoplankton stock and primary production were therefore higher for small copepods (>100 % of the primary production) than for large copepods (33 to 72 %) and for ostracods (6 to 33 %) (Table 4-8).

Daily release of CO_2 by the zooplankton community always largely exceeded the daily carbon requirement for the phytoplankton production (Table 4-9).

Table 4-9 Summary of carbon released and ammonium and phosphate excreted daily by the metazooplankton and their contribution to primary production requirements at station A, B and C. *: Ostracods only.

Variables	Station A				Station B				Station C			
	Copepods < 1000 µm	Copepods > 1000 µm	Other zooplankter	Total	Copepods < 1000 µm	Copepods > 1000 µm	Other zooplankter	Total	Copepods < 1000 µm	Copepods > 1000 µm	Other zooplankter	Total
Inorganic C released (mg C m^{-2} d^{-1})	171	90	123*	384	169	142	98	409	160	168	95	423
% phytoplankton C requirement	124	65	89*	278	82	98	71	251	114	109	65	288
NH_4 excreted (µmol m^{-2} d^{-1})	724	711	1135	2570	1285	815	581	2681	1041	973	480	2494
% phytoplankton N requirement	73	72	115	260	114	72	52	238	108	101	51	260
PO_4 excreted (µmol m^{-2} d^{-1})	89	56	83	228	82	58	44	184	82	76	50	208
% phytoplankton P requirement	398	252	376	1026	337	240	183	760	399	371	251	1021

The daily integrated nutrient recycling by metazooplankton through excretion was equivalent to 182 to 245 % and to 2 to 22 % of the *in situ* ammonium and phosphate concentrations respectively. The copepods were responsible of ~70 % in average of the total metazooplankton excretion (Table 4-9). Although small copepods had a lower excretion rates, theirs contributions were higher than largest copepods at each station. Phytoplankton requirements in term of nitrogen were largely fulfilled (238 to 260 %) by the metazooplankton community ammonium release. Phosphorus was also released in excess to phytoplankton production (760 to 1026 %) by the metazooplankton.

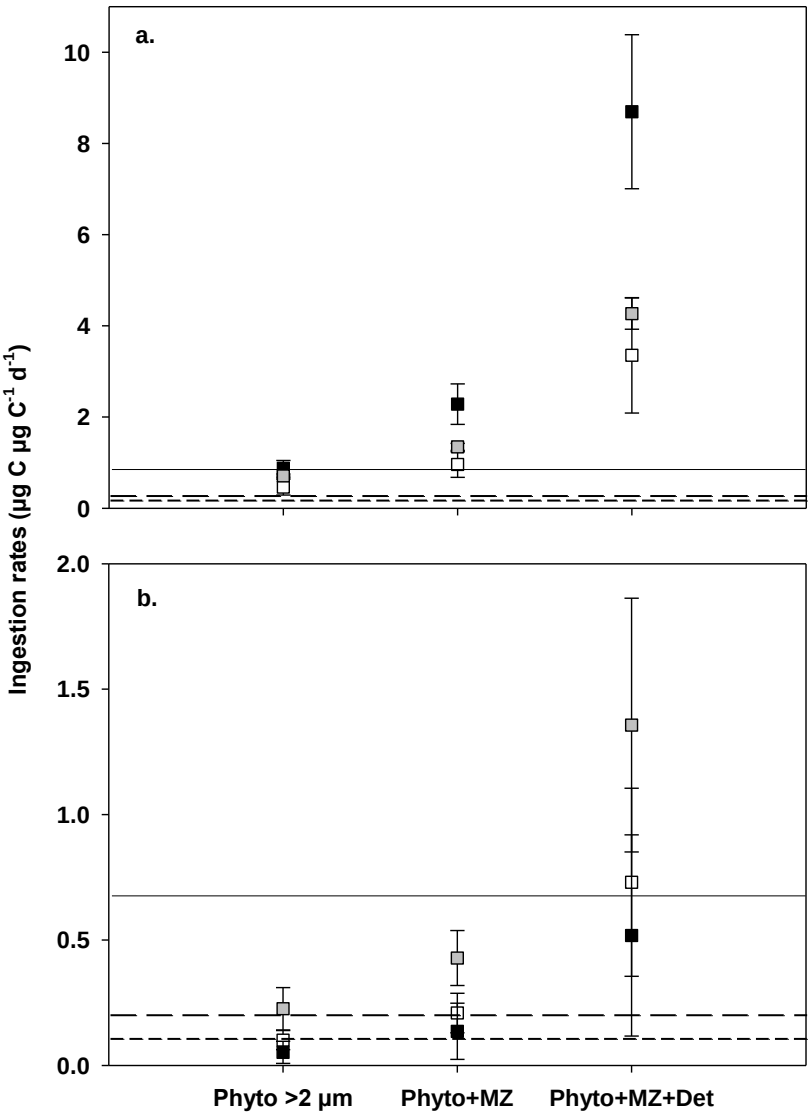

Figure 4-16. Weight specific ingestion rates including standard deviation for copepods (a.) < 1000 µm and (b.) >1000 µm calculated for rations based on phytoplankton > 2µm, phytoplankton + microbial components and phytoplankton + microbial components + organic detritus at the stations A (white), B (black) and C (grey). Values with standard deviation. Basal (short dash line), routine (long dash line) and active (plain) respiratory levels are represented for comparison.

4.3.4 Discussion

4.3.4.1 Respiration rates and RQ estimation

Few studies attempted so far to quantify the respiration by measuring directly CO_2 production in marine zooplankton (Raymont & Krishnaswamy, 1968; Rakusa-Suszczewski et al., 1976; Kremer, 1977). More recently, Mayzaud et al. (2005) presented a relationship between the

CO_2 production and the individual size (or weight) for various zooplankton taxa in the North Atlantic Ocean. Respiration rates measured here based on oxygen consumption were in the same range than those performed at the same temperature (Mauchline, 1998). CO_2 production rates here for copepods (0.08 to 3.15 µg C ind^{-1} h^{-1}) are in the same range than those measured by Mayzaud et al. (2005) in the Gulf of Biscaye (0.015 to 1.22 g C ind^{-1} h^{-1}).

In our study, the plots of CO_2 released versus size or weight showed important dispersion especially for copepods (low R^2). The experimental conditions that are known to affect the metabolic activities may partly explain this variability. The container size or high densities of organisms have been shown to influence metabolic rates (Ikeda et al, 2000). Here, we used two container sizes (125 and 310 mL), but Marshall & Orr (1958) found no appreciable effect even for container of equivalent or smaller size (30 to 160 ml) on *Calanus* oxygen consumption. We also kept animal concentrations low, never exceeding 0.3 and 1.2 ind mL^{-1} for the excretion and respiration measurement, respectively. These maximum concentrations were higher than the *in-situ* concentrations but largely lower than the 200 or 400 ind mL^{-1}, considered as critical for excretion measurements by Hargrave & Geen (1968) and Nival et al. (1974).

The variability within the type of zooplankton (copepods, euphausiids and amphipods) could arise from heterogeneity in species composition, especially for copepods which were composed of organisms with different feeding diets (herbivorous, omnivorous and carnivorous) and foraging strategies (filter feeders and active predators) which could impact their metabolic activity (Abou Debs, 1984). For example, *Paracalanus* spp. which is known to be a typical filter-feeder (Paffenhöfer and Mazzocchi, 2003) or *Macrosetella/Microsetella* spp., feeding on sinking detritus aggregates (Maar et al, 2006). *In situ* trophic condition preceding the capture of experimental animals could also influenced their metabolic activities, as shown in Kouassi et al. (2006). For example, diatoms represented a larger part of the available phytoplankton (higher chlorophyll biomass) at station C than at stations A and B explaining part of the inter-stations variability.

Despite high variability, we observed no significant difference between the slopes of the weight corrected CO_2 release rates *vs.* body weight for amphipods, copepods and euphausiids, whereas the intercept for euphausiids were significantly higher. The same trends were observed by Mayzaud et al. (2005). Furthermore the slope of our model for copepods is close to that obtained by Mayzaud et al. (2005) while our intercept is higher which could be due to

higher temperature in our study. This reflects that the global respiration functioning is uniform for crustacean even if the species are different.

In theory, the RQ ratio could range from 0.71 to 1, depending on the nutritive substrate used by the organisms (Ikeda et al., 2000). Our RQ ratios present nevertheless a larger variability with values ranging from 0.43 to 1.13. Nevertheless, the RQ average for a given taxa, correspond at the weighed values. An RQ of 0.97 is usually used to convert the oxygen consumption to carbon unit, nevertheless, the RQ ratio varied between the taxa considered. Moreover, the significant differences between the intercepts of the weight specific CO_2 respiration rates *vs.* individual weight relationships for three crustaceans' taxa are consistent with the difference in RQ ratios, higher intercepts for large crustaceans compared to copepods corresponding to lower RQ. Mayzaud et al. (2005) observed the same differences between large and small crustaceans and proposed that they are related to differences in the development of the muscular mass rather than a simple shift in respiratory metabolic substrate.

The metabolic quotients (O/N, O/P and N/P) were more variable between species than the RQ ratio, as already observed by Mousseau et al (2009). In our study, there was no significant relationship between metabolic quotients and RQ, probably due to low data number (n=7 data not showed). These ratio vary according to the metabolic substrate (Mayzaud & Conover, 1988) and indicates if the metabolism of the organism is rather based on carbohydrates, lipids or proteins, the pivot value is set at 24 (Ikeda et al., 2000). Metabolic O/N ratios lower than 24 indicate a protein-derived metabolism. In this study low and high O/N for small and large copepods respectively, at stations B and no significant difference at station C (no available data for station C) suggest difference in trophic conditions for the copepods between the two sites.

4.3.4.2 Trophic condition for zooplankton and trophic pathways

Small copepods and ostracods could balance their metabolic needs for respiration by a food ration containing only available phytoplankton (>2µm). This suggested a low predation of small organisms on micro-heterotophs (ciliates and HNF). For large copepods (>1000 µm), they did not balance there metabolic budget only with phytoplankton. Even including the micro-heterotrophe and organic detritus grazed at the same clearance rate (no selectivity), the budget was not entirely balanced in some case. To balance easily there budget, they need

another source of food. The diet of large copepods seems to be essentially omnivorous including carnivorous feeding

4.3.4.3 Zooplankton impact on phytoplankton

The high grazing impact on phytoplankton by small copepods at station B is due to a higher ingestion rate and a lower phytoplankton biomass (7.46 mg Chl*a* m^{-2}) than at stations A and C (13.52 and 15.25 mg Chl*a* m^{-2} respectively). Our results show the importance of copepods grazing pressure in the oligothrophic water with a high impact on primary production (>100 %) implying that the primary production could be controlled by copepod and especially by small copepods. Grazing impact both on phytoplankton biomass and primary production were high when we compared with the studies of Alcaraz (1988) performed nevertheless at the same season and at the same temperature in the Catalan Sea. Nutrients release by the metazooplankton covered between ~13-16 %; ~67-76 % and 20-23 % of the requirements for the primary production in term of N, P and C respectively. These lower metazooplankton contributions could be explain by the higher phytoplankton concentration, in fact at the DCM. Alcaraz (1988) reported a maximum value largely above 2 µg L^{-1} while in our study the maximum value was ~0.5 µg L^{-1}. In a more productive area as the Gulf of Lion, Gaudy et al. (2003) showed that the zooplankton contribution varied largely between coastal and the offshore areas and between seasons. They reported a mesozooplankton contribution higher in winter than during spring and a P requirement for the primary production >100 % as observed during our study. Our results were, nevertheless, in agreement with the supported observation that the ratio of primary production supported by the nutrients excreted by zooplankton is very low or negligible in coastal and estuarine areas (Smith, 1978) and can be one of the most important sources of nutrients in the oceanic zones (Verity, 1985).

4.4 Conclusion générale sur BOUM

Une étude spatiale basée sur une série temporelle de 10 ans d'images satellitaires de la chlorophylle *a* de surface a couvert l'intégralité de la Méditerranée (D'Ortienzo & Ribera d'Alcalà, 2009). Elle permet de distinguer 7 clusters (régions) différents sur la base de la quantité annuelle en chlorophylle, de la concentration maximale lors des floraisons de phytoplancton et également de la période à laquelle apparaissent ces floraisons. Ces clusters peuvent être regroupés en 4 groupes géographiques distincts des plus oligotrophes aux plus eutrophes : « non blooming area, intermittently blooming area, blooming area and coastal area » (Fig 4-17). On y distingue une différentiation nord-sud dans le bassin Algéro-Provencal avec une zone plus productive au nord et plus faible au sud et une zone intermédiaire au centre. Les bassins Ionien et Levantin sont par contre plus homogènes et considérés comme « non blooming area ». Notre étude, bien que ponctuelle, permet de retrouver plus ou moins cette distribution spatiale, en termes d'abondance et de biomasse du zooplancton. Par contre la composition taxonomique montre un aspect différent avec, pour certaines espèces, une distinction claire entre le bassin Est et le bassin Ouest. Cependant nos prélèvements de zooplancton ayant été réalisés sur un nombre limité de stations et sur une seule radiale, ne nous permettent pas de réellement caractériser des bio-provinces.

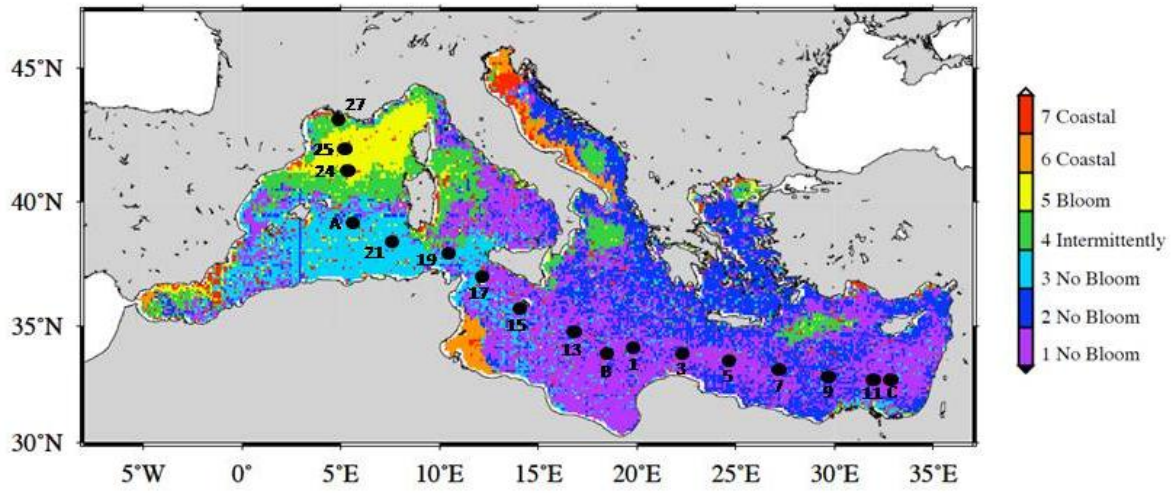

Figure 4-17. Distribution spatiale des 7 clusters dérivés de l'analyse d'images satellitaires SeaWIFS de la chlorophylle *a* de surface (issue de D'Ortienzo et Ribera d'Alcalà, 2009) et localisation des stations d'échantillonnage du zooplancton lors de la mission BOUM.

Très peu d'études sur la bio-régionalisation des espèces marines ont été réalisées en mer Méditerranée notamment sur le zooplancton. Basée essentiellement sur la biodiversité marine benthique, Bianchi et Morri (2000) distinguent 10 secteurs biogéographiques majeurs en mer Méditerranée. Par la suite Bianchi (2004) spécifie deux secteurs supplémentaires : le sud de la mer Tyrrhénienne et le sud de la mer Egée. Enfin, un treizième secteur biogéographique a été défini : le détroit de Messine qui est caractérisé par certaines espèces de macrophytes benthiques endémiques (Bianchi, 2007) (Fig. 4-18).

En superposant la distribution spatiale de la chlorophylle *a* obtenue par D'Ortienzo et Ribéra d'Alcalà (2009) avec les écorégions obtenue par Bianchi (2007) nous observons certaines similitudes entre ces deux études et entre celles-ci et nos propres résultats:

- une homogénéisation dans le bassin Est (également pour le métazooplancton en termes de stock dans notre étude),
- une différenciation entre le nord, le centre et le sud de la mer Adriatique,
- une différenciation entre le nord, le centre et le sud dans le bassin Ouest (également retrouvée dans notre étude en termes de stock de zooplancton)
- une distinction entre mer d'Alboran et mer Tyrrhénienne.

Notre étude n'a pas concerné la mer d'Alboran, mais il est connu que cette région est une des régions les plus productives notamment pour le mésozooplancton grâce à la présence de structures physiques à méso-échelle tels que des tourbillons cycloniques et des zones frontales quasi-permanentes (Seguin et al., 1994; Youssara & Gaudy, 2001 ; Gaudy & Youssara, 2003; Riandey et al., 2005) et de l'influence des eaux de l'Atlantique (Gómez et al., 2001).

Une étude réalisée par Fonda Umani (1996) sur la production et la biomasse planctonique dans son ensemble distingue clairement 3 zones géographiques en mer Adriatique: (1) eaux du large du centre et du sud caractérisées par une communauté « océanique » à forte diversité taxonomique et stable au cours de l'année ; (2) eaux du large du nord caractérisées par un mélange de communautés incluant des espèces néritique et des espèces plutôt méditerranéennes et du sud de l'Adriatique présentes toute l'année ; et (3) zone côtière caractérisée par une population néritique à faible diversité. Bianchi (2007) décrit également 3 bio-provinces en mer Adriatique mais distingue les régions nord, centre et sud. On peut remarquer que la distinction entre le Centre et le Sud aurait peut être pu également apparaitre

dans l'étude de Fonda Umani (1996) si celle-ci s'était étendue jusqu'à la pointe sud-est de l'Italie.

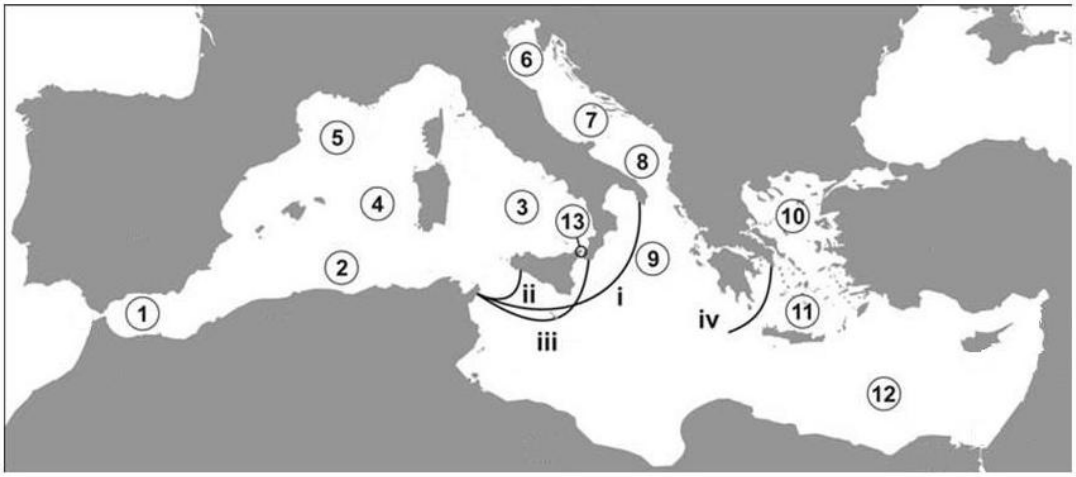

Figure 4-18. Majeurs régions biogéographiques : (1) Mer d'Alboran, (2) Côtes Algérienne et nord Tunisienne, (3) Mer Tyrrhénienne sud, (4) Mer des Baléares et mer de Sardaigne, (5) Golfe du Lion et mer Ligure, (6) Mer Adriatique nord, (7) Mer Adriatique centre, (8) Mer Adriatique sud, (9) Mer Ionienne, (10) Mer Egée nord, (11) Mer Egée sud, (12) Mer Levantine, (13) Détroit de Messine. i,ii,iii,iv : positions des limites entre le bassin Ouest et le bassin Est selon différents auteurs (issue de Bianchi, 2007, modifié).

Concernant la mer Egée, l'étude de Bianchi (2007) distingue clairement le nord et le sud. On retrouve cette distinction régionale dans une étude sur les ciliés par Pitta et Giannakourou (2000) qui montre une différence significative entre ces deux secteurs avec, dans la partie nord, des valeurs de biomasse et d'abondance supérieures et une diversité taxonomique plus importante en raison notamment de l'influence de la mer Noire. Ces différences se retrouvent également au niveau de la structure de taille avec une dominance de cellules plus larges au nord (18-50 µm) par rapport au Sud (< 18 µm). De même, une étude de Siokou-Frangou et al. (2004) sur le mésozooplancton indique des différences entre 3 régions (nord et sud de la mer Egée et la mer Noire) aussi bien au niveau des stocks qu'au niveau de la composition taxonomique rejoignant ainsi l'étude précédente.

Ainsi l'abondance et dans une moindre mesure, la biomasse du zooplancton présentent des distributions régionales fortement liées à la quantité de phytoplancton. Cette concentration du phytoplancton est la plupart du temps liée à des phénomènes physiques à méso-échelle qui favorisent la production primaire. Cependant, ces zones d'intense production sont souvent caractérisées par des communautés phytoplanctoniques différentes de celles des zones adjacentes. De plus, Ignatides et al. (2009) ont mis en évidence que le gradient est-ouest en

sels nutritifs à l'échelle de la Méditerranée et les structures physiques seraient déterminants dans la production et la diversité des communautés phytoplanctoniques. Or, la diversité des niveaux trophiques inférieurs est généralement supposée induire la diversité des niveaux trophiques supérieurs (Dolan, 2005; Dolan et al., 2005). Ainsi, la diversité de la ressource serait à la base de la diversité des consommateurs. Si Irigoien et al. (2004) considèrent qu'une telle relation n'existe pas pour le plancton, Dolan (2002) l'a récemment démontré pour la relation phytoplancton-microzooplancton. Cependant, cette relation entre composition taxonomique des communautés de producteurs et de consommateurs reste hypothétique puisqu'elle a rarement été observée.

Il a été montré également des différences significatives de composition entre les communautés zooplanctoniques à l'intérieur des structures physiques à mésoéchelle et celles des zones adjacentes, notamment en mer Egée (Zervoudaki et al., 2006, 2007; Siokou-Frangou et al., 2009) et en mer Catalane (Alcaraz et al., 2007).

Ainsi, bien qu'il s'agisse d'organismes tributaires des courants, le mésozooplancton observe une distribution spatiale liée aux conditions trophiques aussi bien au niveau de l'abondance et de la biomasse que de la composition taxonomique et de la structure de taille entre le bassin Ouest et le bassin Est méditerranéen.

Dans un second temps, l'impact du zooplancton sur les producteurs primaires a été étudié dans les trois gyres anticycloniques localisées dans les bassins Levantin, Ionien et Algéro-Provençal. Cette étude a tout d'abord permis de vérifier les résultats et les hypothèses émis par Mayzaud et al. (2005) concernant les différences entre les valeurs mesurées et théoriques du quotient respiratoire (RQ) et également des différences entre taxons liées au développement de la masse musculaire plutôt qu'à un simple shift dans le substrat métabolique respiratoire. Des relations allométriques entre la respiration exprimée en carbone et les paramètres individuels (taille, poids) par taxon ont également été réalisées.

L'impact du mésozooplancton sur les producteurs primaires est important puisqu'il est capable de brouter plus de 100 % de la production primaire journalière mais profitant plus aux petits copépodes qui peuvent satisfaire ainsi leurs besoins métaboliques de base et de routine avec seulement du phytoplancton comme source de nourriture. Les grands copépodes sont par contre dépendant d'autres sources de nourriture pour leur métabolisme de routine mais qui ne couvrent pas leur métabolisme actif. La station localisée dans le bassin Levantin semble la

plus favorable au développement du métazooplancton qui semble être principalement lié à des concentrations en diatomées élevées. De même, la répartition spatiale des tailles de copépodes est influencée par ces diatomées comme par exemple pour *Subeucalanus monachus* qui est présent aux stations où les concentrations en diatomées de grandes tailles sont plus importantes. Cette difficulté à satisfaire leurs besoins métaboliques est certainement accrue par la présence d'un grand nombre d'endoparasites (Alvez-de-Souza et al., 2011, Annexe 2). En effet, au cours de cette campagne, une très large proportion de copépodes a été retrouvée parasitée à la station C atteignant potentiellement 16 % de la communauté. Ces dinobiontes endoparasites peuvent potentiellement modifier l'activité métabolique de l'hôte et surtout diminuer son alimentation. Dans la baie de Marseille, au cours de ce travail de thèse, une autre espèce de dinobiontes parasitant les crustacés a pu être étudiée et a permis de mettre en évidence son cycle de vie (Gómez et al., 2009, Annexe 3).

Enfin, les copépodes peuvent libérer, par l'intermédiaire de déchets métaboliques, l'équivalent de plus de 100 % des besoins en éléments nutritifs (C, N et P) de la production primaire journalière pour toutes les stations. Les valeurs obtenues sont élevées par rapport aux autres données disponibles dans d'autres régions de la Méditerranée mais d'un même ordre de grandeur que dans des eaux aussi oligotrophes. Les valeurs sont d'autant plus élevées que le nombre de petits copépodes est plus important puisque nous avons utilisé une maille plus fine que dans les études précédentes.

5 CONCLUSION GENERALE ET PERSPECTIVES

Ce travail a permis des caractériser les communautés métazooplanctoniques et certains traits métaboliques et physiologiques à large échelle spatiale en s'appuyant sur deux écosystèmes contrastés. Cette approche a permis de mettre en évidence les similitudes et les différences dans la structure et le fonctionnement de ces écosystèmes planctoniques (Tableau 5-1).

5.1 Relation entre communautés zooplanctoniques et environnement

Au niveau du plateau des Kerguelen, nous avons mis en évidence une structuration claire des paramètres environnementaux. Cependant, cela ne se retrouvait pas au niveau des taxons du mésozooplancton et la relation entre les communautés zooplanctoniques et les facteurs environnementaux était faible. Au contraire, en Méditerranée, une relation forte entre les paramètres environnementaux, notamment les concentrations en chlorophylle *a*, et la distribution des communautés métazooplanctoniques a été observée.

En première analyse, il semble donc que la relation entre les communautés zooplanctoniques et les conditions environnementales soit très différente dans les deux régions considérées. Cependant les deux analyses n'ont pas été conduites avec le même panel de variables environnementales, d'avantage de variables trophiques ayant été prises en compte lors de l'étude en Méditerranée que lors de celle sur le plateau des Kerguelen. Il était donc important de pouvoir refaire les analyses de manière à ce qu'elles soient comparables. Nous avons donc réalisé une nouvelle analyse multivariée pour chaque campagne en considérant les 8 variables environnementales communes (température, salinité, profondeur de la couche de mélange, concentrations en oxygène, PO_4, NH_4, $SIOH_4$ et chlorophylle *a* et les taxons zooplanctoniques propres à chaque site) (Fig. 5-1).

Dans le cas de la Méditerranée, la relation entre le zooplancton et les paramètres environnementaux est forte (R^2 = 0,83 ; p <0,001) et met en évidence un effet possible du gradient trophique est-ouest sur la distribution de la communauté du mésozooplancton. Par contre cette relation est beaucoup plus faible sur le plateau des Kerguelen (R^2 = 0,60 ; p <0,01) et ne permet pas d'identifier d'association nette entre les variables environnementales et les groupes de taxons zooplanctoniques.

Cette différence entre les deux sites d'étude est sans doute liée à des délais différents de réponse des organismes zooplanctoniques aux variations environnementales en relation avec

	Plateau des Kerguelen Campagne KEOPS (12 janvier - 13 février 2005)	Mer Méditerranée Campagne BOUM (18 juin - 20 juillet 2008)
Caractéristiques du milieu		
Description succincte des écorégions	Sud Est des Kerguelen et zone hauturière	Bassin Est et Ouest, zone hauturière exepté Gibraltar
Période (saison)	Estivale	Estivale
Période (état de la floraison phytoplanctonique)	Milieu et fin de floraison phytoplanctonique de 3 mois	Post floraison phytoplanctonique
Température	Basse et faible amplitude (- 0,4 à 2,5°C)	Elevée et forte amplitude (13 à 28°C)
Nutriments	Apports constants en fer	Oligotrophie, limité en phosphore
Chlorophylle *a* intégrée	Modérée (~ 0,15 à 1,5 µg L^{-1})	Faible (0,08 à 0,3 µg L^{-1})
Caractéristiques du métazooplancton		
Biodiversité	Faible (28 taxons identifiés)	Modérée (80 taxons identifiés)
Biomasse	Elevée (~ 15 à 36 mg PS m^{-3})	Modérée (~ 3 à 10 mg PS m^{-3})
Taille maximale des copépodes	10 mm (*Rhincalanus gigas*)	6 mm (*Pareucalanus attenuatus*)
Distribution spatiale spécifique	Homogène	3 types de population distincts
	Faiblement liée aux paramètres environnementaux	Fortement liée aux paramètres environnementaux
Métabolisme		
Part des producteurs primaires pour subvenir aux besoins métaboliques	Insuffisant quelque soit la taille	Suffisant pour les copépodes < 1000 µm, pas pour > 1000 µm
Type de régime alimentaire des copépodes	Producteurs primaires (faible), protistes et détritus (fort)	Producteurs primaires (fort), protistes et détritus (modéré)
Contrôle des producteurs primaires par le broutage	Impact faible (1 à 10 % stock)	Impact important (> 100 % de la production primaire)
Contrôle des producteurs primaires par la production régénérée	-	Impact important (> 100 % des besoins de la production primaire)
Contrôle du microzooplancton par prédation du métazooplancton	Potentiellement important	Potentiellement limité

Table 5-1. Principales caractéristiques des deux écosystèmes pélagiques étudiés : le plateau des Kerguelen et la mer Méditerranée.

des conditions moyennes de températures très contrastées. Ainsi des relations encore plus fortes entre « Environnement » et « Zooplancton » ont été mises en évidence avec la même technique d'analyse de données (Coinertie) dans des eaux tropicales avec des $R^2 > 0,9$ (Kâ et al., 2006 ; Etilé et al., 2009).

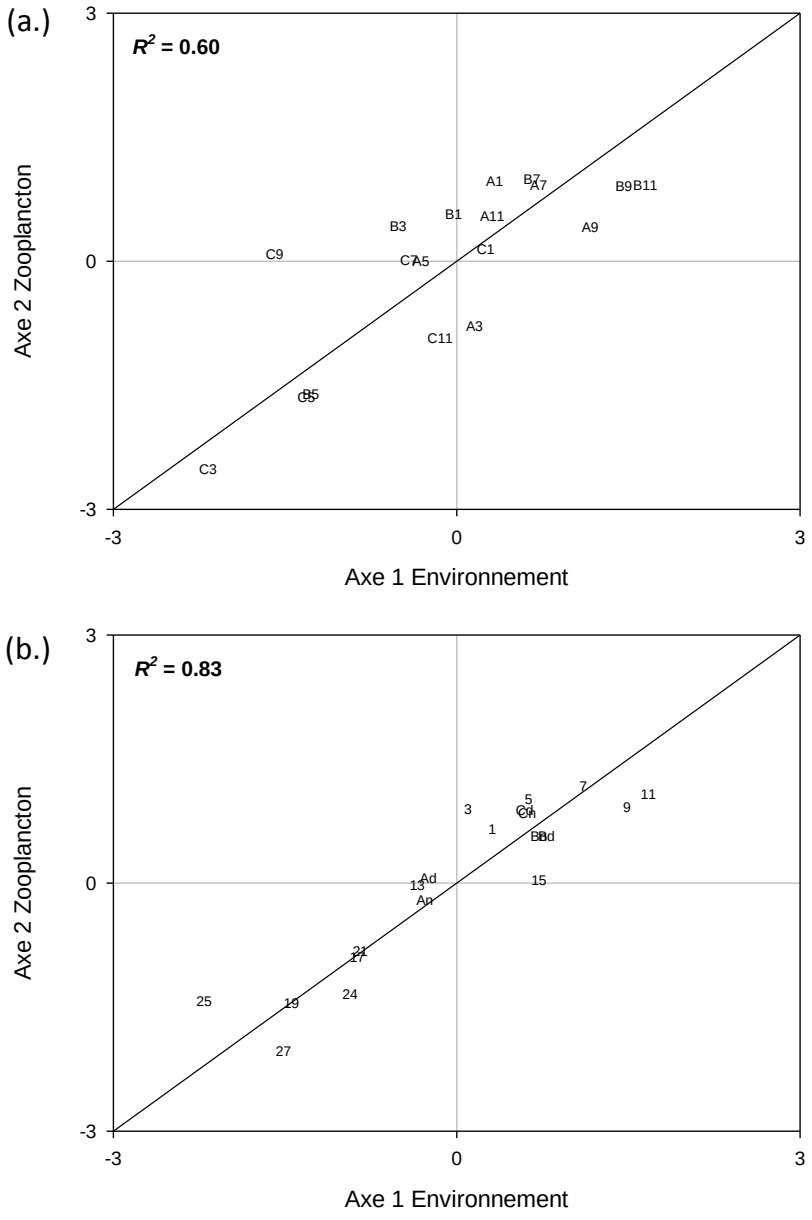

Figure 5-1. Analyse de co-inertie : relation entre les coordonnées normalisées des stations dans le premier axe des deux systèmes (« Environnement » et « Zooplancton ») échantillonnés lors de la campagne KEOPS (a.) et lors de la campagne BOUM (b.). La droite représente l'égalité entre les coordonnées dans les deux systèmes.

Ainsi dans un milieu tempéré-chaud (BOUM) le métabolisme des organismes est plus actif qu'en milieu froid (KEOPS) ce qui implique des temps de réaction plus courts. En Méditerranée, en milieu oligotrophe, la réponse à un stimulus comme l'ajout de phosphore est quasi instantanée et ne met que 3 jours pour se traduire par une augmentation des pontes de copépodes (Pasternak et al., 2005). Au contraire le délai de réponse maximale après un apport en fer dans l'océan Austral est de 29 jours après le stimulus pour *R. gigas* (Jansen et al., 2006). Dans la plupart des expériences d'enrichissement en fer, on n'observe pas de réponse à court terme du mésozooplancton dont la biomasse reste sensiblement constante pendant la période du suivi. Ainsi, la réponse du zooplancton à un stimulus est ainsi d'autant plus rapide que la température du milieu est élevée. Le degré de relation entre les paramètres trophiques et les communautés du zooplancton est donc très dépendant du niveau moyen de température de l'habitat.

5.2 Ecorégionalisation

Nous avons mis en évidence des distributions régionales de l'abondance et de structure des communautés zooplanctoniques fortement liées à la quantité de phytoplancton en Méditerranée. Cependant les structures physiques à méso-échelle (tourbillons anticycloniques, zones frontales) peuvent modifier ce schéma de distribution régionale et ajouter un niveau supplémentaire de variabilité. Ainsi la Méditerranée présente un nombre important de niches écologiques liées à cette variabilité spatiale, favorisant la diversité planctonique. L'hétérogénéité spatiale de la disponibilité nutritive (gradient est-ouest) qui se répercute rapidement sur les échelons trophiques serait à la base de l'hétérogénéité spatiale des communautés zooplanctoniques permettant de définir des écorégions à l'échelle du bassin.

Sur le plateau des Kerguelen, l'abondance et la biomasse du zooplancton sont plus fortes qu'en Méditerranée mais la diversité y est plus faible. Par opposition à la Méditerranée, cette plus faible richesse spécifique peut s'expliquer par un nombre plus réduit de niches écologiques en relation avec l'absence de structure hydrologique à méso-échelle, une faible variabilité spatiale à la fois sur le plateau et entre le plateau et la zone HNLC, et un lien moins fort entre la disponibilité trophique et les communautés de consommateurs.

5.3 Impact du mésozooplancton sur le milieu

En Méditerranée, nous avons mis en évidence un fort impact du métazooplancton sur la production phytoplanctonique, aussi bien en termes de broutage (contrôle « top down ») que de régénération de nutriments par l'excrétion (contrôle « bottom up »). Cependant, la durée de la floraison printanière est limitée par le contrôle « top down » du mésozooplancton mais également par l'épuisement des sels nutritifs. Ainsi, en période estivale, l'excrétion du zooplancton contribue au maintien d'une certaine concentration des producteurs primaires. Ce système planctonique fonctionne donc en équilibre.

A l'opposé, sur le plateau des Kerguelen, le mésozooplancton a un impact négligeable sur le phytoplancton et n'exerce donc pas de contrôle « top down » sur les producteurs primaires. La valeur maximale du broutage des copépodes mesurée en janvier sur KERFIX est de 4.6 % de la production primaire (Razouls et al., 1998). Pour équilibrer ses dépenses, le métazooplancton se nourrit également de protozoaires exerçant ainsi un fort effet « top down » sur le microzooplancton (Atkinson, 1996; Mayzaud et al., 2002b; Razouls et al., 1998 ; Carlotti et al., 2008). Il contribue ainsi, par effet cascade, à diminuer la pression trophique du microzooplancton sur les producteurs primaires. Ce phénomène contribue en partie à expliquer en partie la durée assez longue (> 3 mois) de la floraison phytoplanctonique et notamment de celle des diatomées (Henjes et al., 2007).

5.4 Perspectives

Les grandes campagnes océanographiques multidisciplinaires permettent d'obtenir simultanément de larges jeux de données sur de nombreux compartiments pélagiques et sur les facteurs environnementaux tels que les paramètres physiques et chimiques qui peuvent contrôler la productivité du système. Ce type d'approche a permis, lors de cette thèse, de mettre en évidence certaines différences au niveau de la distribution des communautés planctoniques et des interactions entre les échelons trophiques entre deux milieux océaniques contrastés, bien qu'il s'agisse de biotopes identiques (marins pélagiques) et d'organismes de même groupe taxonomique (métazoaires planctoniques). Il est clair qu'une étude complète de ces paramètres permet à la fois de mettre en évidence les variations spatiales à grande échelle mais également certaines variations à mésoéchelle. Cependant, mon étude a seulement

considéré les relations entre les premiers niveaux trophiques pélagiques. Il faudrait développer des études prenant également en compte les échelons supérieurs de manière à évaluer notamment l'effet « top down » des prédateurs (en particulier des larves et juvéniles) en s'appuyant sur des études intégrées de type « End to End ».

Au cours de cette étude, nous avons étudié l'impact du métazooplancton uniquement sur les organismes autotrophes. Cependant, nous avons mis en évidence sur le plateau des Kerguelen, que bien que la concentration des producteurs primaires soit importante, les copépodes ne se nourrissent que très peu sur cette communauté. De même, en mer Méditerranée, les copépodes de grandes tailles ne peuvent pas subvenir à leurs besoins journaliers en ne broutant seulement que le phytoplancton autotrophe. Cependant ces mesures indirectes de broutage ne sont qu'une estimation puisque certains paramètres peuvent sur ou sous-estimer le calcul du taux de broutage. Par exemple, la dégradation de la chlorophylle *a* dans le tractus digestif des copépodes en pigments non chlorophylliens peut être comprise entre 0 et 95 % bien qu'un grand nombre d'étude estime cette perte entre 10 et 20 % (Båmstedt et al., 1998). De même, les pertes de matière occasionnées par le sloppy feeding peuvent ne pas être négligeables (26 à 35 % de la matière ingérée) (Roy et al., 1989) mais dépendent bien sûr du type de brouteur étudié. Ainsi, nous avons montré que ces copépodes avaient besoin d'un autre type de nourriture tels que les unicellulaires hétérotrophes ou les détritus. Bien que le métazooplancton soit suspecté d'exercer un contrôle direct sur ces communautés (Batten et al., 2001 ; Schnetzer & Caron, 2005 ; Sánchez et al., 2011), très peu d'études sont réalisées sur cette problématique. Il est donc important de réaliser des efforts concernant le comptage des micro-organismes permettant d'étudier et d'identifier l'impact du métazooplancton sur ces communautés.

La compréhension de la structure de l'écosystème pélagique à grandes échelles spatiales et temporelles est le plus souvent réalisée à partir des compilations de données. Celles ci sont issues de différentes campagnes étalées sur plusieurs années, à différentes saisons et dont les stratégies d'échantillonnages sont parfois différentes. Lorsque l'on s'intéresse à l'écosystème pélagique du plateau des Kerguelen et de la zone hauturière proche, on s'aperçoit que le nombre de données sur le métazooplancton reste limité notamment en ce qui concerne les études taxonomiques fines. La campagne BOUM, bien que ponctuelle, a permis de compléter la compilation réalisée par Siokou-Frangou et al. (2011) qui permet une vision synoptique des données sur l'ensemble de la méditerranée.

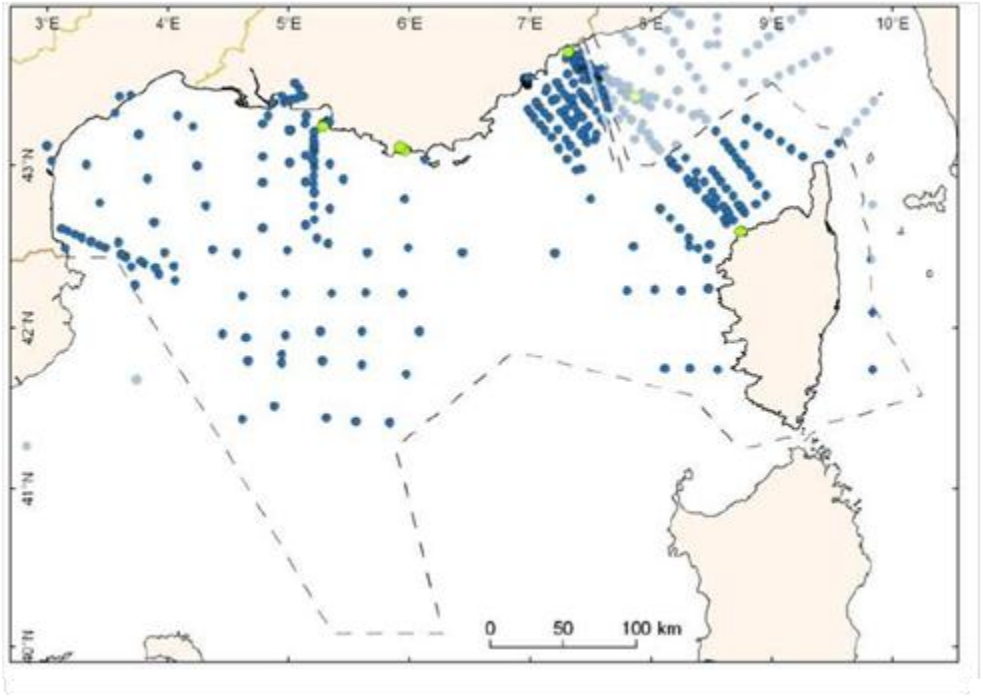

Figure 5-2. Distribution spatiale de l'ensemble des prélèvements du mésozooplancton dans la sous région méditerranée nord-occidentale recensés depuis 1960. (sources des données : CNRS, IFREMER, Universités (Paris 6, Méditerranée, Toulon-var, Liège, Montpellier). (Issue de Sautour et al., 2011).

Un exemple de travail de recensement des données et métadonnées disponibles sur le zooplancton réalisé dans le cadre de la DCSMM (Directive Cadre Stratégique sur le Milieu Marin) en Méditerranée Nord Occidentale est présenté dans la figure 5-2. Une des difficultés majeures est liée à l'homogénéisation de données issues de protocoles différents selon l'objectif scientifique (Fig. 5-3). Une autre difficulté vient de l'hétérogénéité des engins de prélèvements (filet à nappe, filet simple, bouteilles, pompe, CPR) et des mailles (le plus souvent ≥ 200 µm) utilisés pour échantillonner le zooplancton et des capteurs utilisés pour estimer sa distribution *in situ* (LISST, ADCP, OPC laser, PVM). Il est donc nécessaire de développer des protocoles communs (standardisation). Par exemple, au cours de notre étude en Méditerranée nous avons utilisé un filet de 120 µm afin d'obtenir la totalité du spectre de taille du mésozooplancton. En effet les métazoaires < 200 µm présentent une forte abondance. Zervoudaki et al. (2006) montrent qu'une maille de ce type entraîne une sous-estimation de 2 à 20 fois en termes d'abondance par rapport à un filet de 45 µm de vide de maille avec des différences maximales observées pour les stades copépodites d'*Oithona* spp. et d'*Oncaea* spp. qui sont respectivement 51 et 76 fois moins abondants dans les échantillons issus d'un filet de

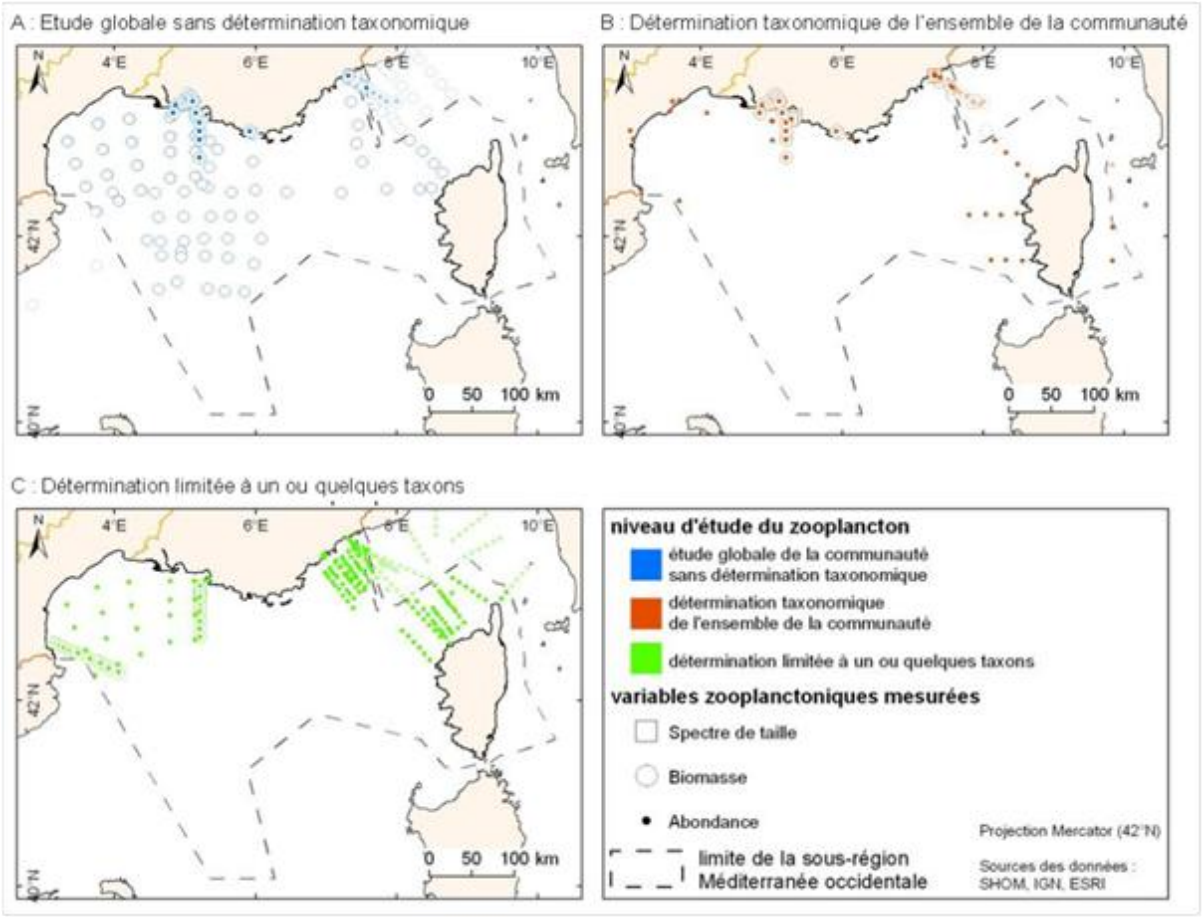

Figure 5-3. Détail du type d'étude réalisée sur le mésozooplancton recensé depuis 1960. (sources des données : CNRS, IFREMER, Universités (Paris 6, Méditerranée, Toulon-var, Liège, Montpellier). (Issue de Sautour et al., 2011).

200 µm. De plus, la contribution de la biomasse des organismes dont la taille est < 1 mm obtenue avec une maille de 45 µm peut être importante puisqu'elle atteint 69 à 77 % de la biomasse totale en mer Egée (Zervoudaki et al., 2007). Ainsi il est maintenant clair de prendre en compte les petites classes de tailles notamment dans les eaux oligotrophes où les copépodes de petites tailles sont abondants (Turner, 2004). Lors de la campagne KEOPS, nous avons utilisé un filet de 330 µm de vide de maille afin de pouvoir échantillonner efficacement les copépodes de grandes tailles (*Rhincalanus gigas*, *Calanus simillimus* et *C.propinquus*) qui sont largement plus abondants qu'en mer Méditerranée. Cependant, il est fort possible que les copépodes de petites tailles, notamment les jeunes stades copépodites ont été sous échantillonnés lors de cette campagne. Ainsi lors de la deuxième campagne KEOPS qui s'est déroulée en septembre-octobre 2011, les organismes ont été prélevés avec un double filet Bongo monté d'un filet de 330 µm et un second de 120 µm de vide de maille. Cependant il serait également intéressant d'effectuer des prélèvements avec des filets de mailles

inférieures car, à ma connaissance, aucune étude du plateau des Kerguelen voir de l'océan Austral, n'a été réalisé avec des filets < 100 µm.

Néanmoins, l'approche par les filets est de plus en plus fréquemment doublée par une approche par des capteurs acoustiques et optiques. Ces instruments non intrusifs permettent l'acquisition de données numériques facilement comparables entre elles. Dans le cas d'échantillons prélevés aux filets, les analyseurs d'images comme l'OPC (Optical Plankton Counter) et le ZooScan, utilisés au cours de cette thèse, permettent d'analyser rapidement l'abondance, la biomasse, la structure en taille et, dans une moindre mesure, la composition en grands taxons des communautés zooplanctoniques (García-Comas et al., 2011; Vandromme et al., 2010). Ces données permettent ainsi de constituer des archives digitales à long terme.

6 REFERENCES BIBLIOGRAPHIQUES

Abou Debs, C., 1984. Carbon and nitrogen budget of the calanoid copepod *Temora stylifera*: effect of concentration and composition of food. Marine Ecology Progress Series 15, 213-223.

Agassiz, A., 1888. Three cruises of the United States coast and Geodetic survey: Stearner Blake in the Gulf of Mexico, in the Carribbean Sea, and along the Atlantic coast of the United States, from 1877 to 1880. Bulletin of the Museum of Comparative Zoology, Harvard University 14, pp 314.

Alcaraz, M., 1985. Vertical distribution of zooplankton biomass during summer stratification in the Western Mediterranean. Proceedings of the 19th European Marine Biology Symposium, Plymouth, Devon, UK, 16–21 September 1984, 135-143.

Alcaraz, M., 1988. Summer zooplancton metabolism and its relation to primary production in the Western Mediterranean. Eds Minas, J. H. and Nival, P., Océanographie pélagique méditerranéenne, Oceanologica Acta SP 9, 185-191.

Alcaraz, M., Saiz, E., Fernandez, J.A., Trepat, I., Figueiras, F., Calbet, A., 1998. Antarctic zooplankton metabolism: carbon requirements and ammonium excretion of salps and crustacean zooplankton in the vicinity of the Bransfield Strait during January 1994. Journal of Marine Systems 17, 347-359.

Alcaraz, M., Saiz, E., Calbet, A., Trepat, I., Broglio, E., 2003. Estimating zooplankton biomass through image analysis. Marine Biology 143, 307-315.

Alcaraz, M., Calbet, A., Estrada, M., Marrasé, C., Saiz, E., Trepat, I., 2007. Physical control of zooplankton communities in the Catalan Sea. Progress in Oceanography 74, 294-312.

Alldredge, A.L., Passow, U., Haddock, S.H.D., 1998. The characteristics and transparent exopolymer particle (TEP) content on marine snow formed from thecate dinoflagellates. Journal of Plankton Research 20, 393-406.

Almeda, R., Augustin, C.B., Alcaraz, M., Calbet, A., Saiz, E., 2010. Feeding rates and gross growth efficiencies of larval developmental stages of *Oithona davisae* (Copepoda, Cyclopoida). Journal of Experimental Marine Biology and Ecology 387, 24-35.

Andersen, V., Sardou, J., Nival, P., 1993. Vertical distributions and migrations of macrozooplankton and micronekton in the Ligurian Sea (NW Mediterranean). Annales de l'Institut océanographique, Paris 69, 129-131.

Andersen, V., François, F., Sardou, J., Picheral, M., Scotto, M., Nival, P., 1998. Vertical distributions of macroplankton and micronekton in the Ligurian and Tyrrhenian Seas (northwestern Mediterranean). Oceanologica Acta 21, 655-676.

Andersen, V., Gubanova, A., Nival, P., Ruellet, T., 2001a. Zooplankton community during the transition from spring bloom to oligotrophy in the open NW Mediterranean and effects of wind events. 2. Vertical distributions and migrations. Journal of Plankton Research 23, 243-261.

Andersen, V., Nival, P., Caparroy, P., Gubanova, A., 2001b. Zooplankton community during the transition from spring bloom to oligotrophy in the open NW Mediterranean and effects of wind events. 1. Abundance and specific composition. Journal of Plankton Research 23, 227-242.

Andersen, V., Devey, C., Gubanova, A., Picheral, M., Melnikov, V., Tsarin, S., Prieur, L., 2004. Vertical distributions of zooplankton across the Almeria-Oran frontal zone (Mediterranean Sea). Journal of Plankton Research 26, 275-293.

Armand, L.A., Cornet-Barthau, V., Mosseri, J., Quéguiner, B., 2008. Late summer diatom biomass and community structure on and around the naturally iron-fertilised Kerguelen Plateau in the Southern Ocean. Deep Sea Research II 55, 653-676.

Ashjian, C.J., Rosenwaks, G.A., Wiebe, P.H., Davis, C.S., Gallager, S.M., Copley, N.J., Lawson, G.L., Alatalo, P., 2004. Distribution of zooplankton on the continental shelf off Marguerite Bay, Antarctic Peninsula, during Austral Fall and Winter, 2001. Deep Sea Research II 51, 2073-2098.

Ashjian, C.J., Davis, C.S., Gallager, S.M., Wiebe, P.H., Lawson, G.L., 2008. Distribution of larval krill and zooplankton in association with hydrography in Marguerite Bay, Antarctic Peninsula, in austral fall and winter 2001 described using the Video Plankton Recorder. Deep Sea Research II 55, 455-471.

Atienza, D., Saiz, E., Skovgaard, A., Trepat, I., Calbet, A., 2008. Life history and population dynamics of the marine cladoceran *Penilia avirostris* (Branchiopoda : Cladocera) in the Catalan Sea (NW Mediterranean). Journal of Plankton Research 30, 345-357.

Atkinson, A., Ward, P., Williams, R., Poulet, S.A., 1992a. Diel vertical migration and feeding of copepods at an oceanic site near South Georgia. Marine Biology 113, 583-593.

Atkinson, A., Ward, P., Williams, R., Poulet, S.A., 1992b. Feeding rates and diel vertical migration of copepods near South Georgia: comparison of shelf and oceanic sites. Marine Biology 114, 49-56.

Atkinson, A., 1994. Diets and feeding selectivity among the epipelagic copepod community near South Georgia in summer. Polar Biology 14, 551-560.

Atkinson, A., 1995. Omnivory and feeding selectivity in five copepod species during spring in the Bellingshausen Sea, Antarctica. ICES Journal of Marine Science 52, 385-396.

Atkinson, A., Shreeve, R.S., 1995. Response of copepod community to a spring bloom in the Bellingshausen Sea. Deep Sea Research I 42, 1291-1311.

Atkinson, A., 1996. Subantarctic copepods in an oceanic, low chlorophyll environment: ciliate predation, food selectivity and impact on prey populations. Marine Ecology Progress Series 130, 85-96.

Atkinson, A., Schnack-Schiel, S.B., Ward, P., Marin, V., 1997. Regional differences in the life cycle of *Calanoides acutus* (Copepoda: Calanoida) within the Atlantic sector of the Southern Ocean. Marine Ecology Progress Series 150, 99-111.

Atkinson, A., 1998. Life cycle strategies of epipelagic copepods in the Southern Ocean. Journal of Marine Systems 15, 289-311.

Atkinson, A., Sinclair, J.D., 2000. Zonal distribution and seasonal vertical migration of copepod assemblages in the Scotia Sea. Polar Biology 23, 46-58.

Atkinson, A., Siegel, V., Pakhomov, E., Rothery, P., 2004. Long-term decline in krill stock and increase in salps within the Southern Ocean. Letters to Nature 432, 101-103.

Azam, F., Fenchel, T., Field, J., Gray, J.S., Meyer-Reil, L.A., Thingstad, F.T., 1983. The ecological role of water-column microbes in the sea. Marine Ecology Progress Series 10, 257-263.

Azzaro, F., Decembrini, F., Raffa, F., Crisafi, E., 2007. Seasonal variability of phytoplankton fluorescence in relation to the Straits of Messina (Sicily) tidal upwelling. Ocean Science 3, 451-460.

Båmstedt, U., Gifford, D.J., Irigoien, X., Atkinson, A., Roman, M., 2000. Feeding. ICES Zooplankton Methodology Manual, Eds. Harris, R., Wiebe, P.H., Lenz, J., Skjoldal, H.R., Huntley, M., Academic, London, 297-399.

Banse, K., 1995. Zooplankton: Pivotal role in the control of ocean production. ICES Journal of Marine Science 52, 265-277.

Barale, V., Jaquet, J.M., Ndiaye, M., 2008. Algal blooming patterns and anomalies in the Mediterranean Sea as derived from the Sea WIFS data set (1998-2003). Remote Sensing of Environment 112, 3300-3313.

Basedow, S., Tande, K.S., 2006. Cannibalism by female *Calanus finmarchicus* on naupliar stages. Marine Ecology Progress Series 327, 247-255.

Batistić, M., Jasprica, N., Carić, M., Lučić, D., 2007. Annual cycle of the gelatinous invertebrate zooplankton of the eastern South Adriatic coast (NE Mediterranean). Journal of Plankton Research 29, 671-686.

Beaulieu, S.E., Mullin, M.M., Tang, V.T., Pyne, S.M., King, A.L., Twining, B.S., 1999. Using an optical plankton counter to determine the size distributions of preserved zooplankton samples. Journal of Plankton Research 21, 1939-1956.

Bergamasco, A., Malanotte-Rizzoli, P., 2010. The circulation of the Mediterranean Sea: a historical review of experimental investigations. Advances in Oceanography and Limnology 1, 11-28.

Berland, B.R., Bonin, D.J., Maestrini, S.Y., 1980. Azote ou phosphore? Considérations sur le "paradoxe nutrionnel" de la mer Méditerranée. Oceanologica Acta 3, 135-142.

Berline, L., Stemmann, L., Vichi, M., Lombard, F., Gorsky, G., 2011. Impact of appendicularians on detritus and export fluxes: a model approach at DyFAMed site. Journal of Plankton Research 33, 855-872.

Béthoux, J.P., 1989. Oxygen consumption, new production, vertical advection and environmental evolution in the Mediterranean Sea. Deep Sea Research 36, 769-781.

Bianchi, C.N., Morri, C., 2000. Marine biodiversity of the Mediterranean Sea: situation, problems and prospects for future research. Marine Pollution Bulletin 40, 367-376.

Bianchi, C.N., 2004. Proposta di suddivisione dei mari italiani in settori biogeografici. Notiziario della Società Italiana di Biologia Marina 46, 57-59.

Bianchi, C.N., 2007. Biodiversity issues for the forthcoming tropical Mediterranean Sea. Hydrobiologia 580, 7-21.

Blain, S., Tréguer, P., Belviso, S., Bucciarelli, E., Denis, M., Desabre, S., Fiala, M., Martin Jézéquel, V., Le Fèvre, J., Mayzaud, P., Marty, J.C., Razouls, S., 2001. A biogeochemical study of the island mass effect in the context of the iron hypothesis: Kerguelen Islands, Southern Ocean. Deep Sea Research I 48, 163-187.

Blain, S., Quéguiner, B., Armand, L., Belviso, S., Bombled, B., Bopp, L., Bowie, A., Brunet, C., Brussaard, C., Carlotti, F., Christaki, U., Corbière, A., Durand, I., Ebersbach, F., Fuda, J.L., Garcia, N., Gerringa, L., Griffiths, B., Guigue, C., Guillerm, C., Jacquet, S., Jeandel, C., Laan, P., Lefèvre, D., Lomonaco, C., Malits, A., Mosseri, J., Obernosterer, I., Park, Y.H., Picheral, M., Pondaven, P., Remeny, T., Sandroni, V., Sarthou, G., Savoye, N., Scouarnec, L., Souhaut, M., Thuiller, D., Timmermans, K., Trull, T., Uitz, J., van-Beek, P., Veldhuis, M., Vincent, D., Viollier, E., Vong, L., Wagener, T., 2007. Impacts of natural iron fertilisation on the Southern Ocean. Nature 446, 1070-1074.

Boyd, P.W., Watson, A.J., Law, C.S., Abraham, E.R., Trull, T., Murdoch, R., Bakker, D.C.E., Bowle, A.R., Buesseler, K.O., Chang, H., Charette, M., Croot, P., Downing, K., Frew, R., Gall, M., Hadfield, M., Hall, J., Harvey, M., Jameson, G., LaRoche, J., Liddlcoat, M., Ling, R., Maldonado, M.T., McKay, R.M., Nodder, S., Pickmere, S., Pridmore, R., Rintoul, S., Safl, K., Sutton, P., Strzepek, R., Tanneberger, K., Turner, S., Walte, A., Zeldis, J., 2000. A mesoscale phytoplankton bloom in the polar Southern Ocean stimulated by iron fertilization. Nature Geoscience 407, 695-702.

Boyd, P.W., Jickells, T., Law, C.S., Blain, S., Boyle, E.A., Buesseler, K.O., Coale, K.H., Cullen, J.J., de Baar, H.J.W., Follows, M., Harvey, M., Lancelot, C., Levasseur, M.,

Owens, N.P.J., Pollard, R., Rivkin, R.B., Sarmiento, J., Schoemann, V., Smetacek, V., Takeda, S., Tsuda, A., Turner, S., Watson, A.J., 2007. Mesoscale Iron Enrichment Experiments 1993–2005: Synthesis and Future Directions. Science 315, 612-617.

Bradford-Grieve, J.M., Boyd, P.W., Chang, F.H., Chiswell, S., Hadfield, M., Hall, J.A., James, M.R., Nodder, S.D., Shushkima, E.A., 1999. Pelagic ecosystem structure and functioning in the Subtropical Front region east of New Zealand in austral winter and spring 1993. Journal of Plankton Research 21, 405-428.

Brugnano, C., Bergamasco, A., Granata, A., Guglielmo, L., Zagami, G., 2010. Spatial distribution and community structure of copepods in a central Mediterranean key region (Egadi Islands-Sicily Channel). Journal of Marine Systems 81, 312-322.

Buat-Ménard, P., Lambert, C.E., 1993. Overview of the *DYFAMED* program. Annales Institut océanographique, Paris 69, 101-105.

Buesseler, K.O., Andrews, J.E., Pike, S.M., Charette, M.A., 2004. The Effects of Iron Fertilization on Carbon Sequestration in the Southern Ocean. Science 304, 414-417.

Calbet, A., Garrido, S., Saiz, E., Alcaraz, M., Duarte, C.M., 2001. Annual zooplankton succession in coastal NW Mediterranean waters: the importance of the smaller size fractions. Journal of Plankton Research 23, 319-331.

Calbet, A., Saiz, E., 2005. The ciliate-copepod link in marine ecosystems. Aquatic Microbiology and Ecology 38, 157-167.

Caparroy, P., Pérez, M.T., Carlotti, F., 1998. Feeding behaviour of *Centropages typicus* in calm and turbulent conditions. Marine Ecology Progress Series 113, 110-115.

Carlotti, F., Thibault-Botha, D., Nowaczyk, A., Lefèvre, D., 2008. Zooplankton community structure, biomass and role in carbon fluxes during the second half of a phytoplankton bloom in the eastern sector of the Kerguelen Shelf (January–February 2005). Deep Sea Research II 55, 720-733.

Carlotti, F., Poggiale, J.C., 2010. Towards methodological approaches to implement the zooplankton component in ‘‘end to end” food-web models. Progress in Oceanography 84, 20-38.

Cataletto, B., Feoli, E., Fonda Umani, S., Cheng-Yong, S., 1995. Eleven years of time-series analysis on the net-zooplankton community in the Gulf of Trieste. ICES Journal of Marine Science 52, 669-678.

Champalbert, G., 1996. Characteristics of zooplankton standing stock and communities in the Western Mediterranean Sea: relations to hydrology. Scientia Marina 60, 97-113.

Chinnery, F.E., Williams, J.A., 2004. The influence of temperature and salinity on *Acartia* (Copepoda: Calanoida) nauplii survival. Marine Biology 145, 733-738.

Christaki, U., Van Wambeke, F., Christou, E.D., Conan, P., Gaudy, R., 1996. Food web structure variability in the surface layer, at a fixed station influenced by the North Western Mediterranean Current. Hydrobiologia 321, 145-153.

Christaki, U., Giannakourou, A., Van Wambeke, F., Grégori, G., 2001. Nannoflagellate predation on auto- and heterotrophic picoplankton in the oligotrophic Mediterranean Sea. Journal of Plankton Research 23, 1297-1310.

Christaki, U., Obernosterer, I., Van Wambeke, F., Veldhuis, M., Garcia, N., Catala, P., 2008. Microbial food web in a naturally iron-fertilized area in the Southern Ocean (Kerguelen Plateau). Deep Sea Research II 55, 706-719.

Christaki, U., Van Wambeke, F., Lefevre, D., Lagaria, A., Prieur, L., Pujo-Pay, M., Grattepanche, J.D., Colombet, J., Psarra, S., Dolan, J.R., Sime-Ngando, T., Conan, P., Weinbauer, M.G., Moutin, T., 2011. Microbial food webs and metabolic state across oligotrophic waters of the Mediterranean Sea during summer. Biogeosciences 8, 1939-1852.

Christou, E.D., Moraitou-Apostolopoulou, M., 1995. Metabolism and feeding of mesozooplankton in the eastern Mediterranean (Hellenic coastal waters). Journal of Plankton Research 126, 39-48.

Christou, E., 1998. Interannual variability of copepods in a Mediterranean coastal area Saronikos Gulf, Aegean Sea. Journal of Marine Systems 15.

Christou, E.D., Stergiou, K.I., 1998. Modelling and forecasting the fortnightly cladoceran abundance in the Saronikos Gulf (Aegean Sea). Journal of Plankton Research 20, 1313-1320.

Clarke, K.R., Warwick, R.M., 1995. Changes in marine communities: an approach to statistical analysis and interpretation, Natural environment research council, Plymouth marine laboratory, pp144.

Coale, K.H., Johnson, K.S., Chavez, F.P., Buesseler, K.O., Barber, R.T., Brzezinski, M.A., Cochlan, W.P., Millero, F.J., Falkowski, P.G., Bauer, J.E., Wanninkhof, R.H., Kudela, R.M., Altabet, M.A., Hales, B.E., Takahashi, T., Landry, M.R., Bidigare, R.R., Wang, X., Chase, Z., Strutton, P.G., Friederich, G.E., Gorbunov, M.Y., Lance, V.P., Hilting, A.K., Hiscock, M.R., Demarest, M., Hiscock, W.T., Sullivan, K.F., Tanner, S.J., Gordon, R.M., Hunter, C.N., Elrod, V.A., Fitzwater, S.E., Jones, J.L., Tozzi, S., Koblizek, M., Roberts, A.E., Herndon, J., Brewster, J., Ladizinsky, N., Smith, G., Cooper, D., Timothy, D., Brown, S.L., Selph, K.E., Sheridan, C.C., Twining, B.S., Johnson, Z.I., 2004. Southern Ocean iron enrichment experiment: carbon cycling in high- and low-Si waters. Science 304, 408-414.

Coll, M., Piroddi, C., Steenbeek, J., Kaschner, K., Ben Rais Lasram, F., 2010. The biodiversity of the Mediterranean Sea: estimates, patterns, and threats. PLoS ONE 5(8): e11842 doi:101371/journalpone0011842.

Collins, M.A., Ross, K.A., Belchier, M., Reid, K., 2007. Distribution and diet of juvenile Patagonian toothfish on the South Georgia and Shag Rocks shelves (Southern Ocean). Marine Biology 152, 135-147.

Conway, H.L., Whitledge, T.E., 1979. Distribution, fluxes and biological utilization of inorganic nitrogen during a spring bloom in the New York Bight. Journal of Marine Research 37, 657-668.

Conway, D.V.P., 1997. Interactions of inorganic nitrogen in the uptake and assimilation by marine phytoplankton. Marine Biology 39, 221-232.

Cornet-Barthau, V., Armand, L., Quéguiner, B., 2007. Biovolume and biomass estimates of key diatoms in the Southern Ocean. Aquatic Microbial Ecology 48, 295-308.

Costa, D.P., Crocker, D.E., 1996. Marine mammals in the Southern Ocean. Antarctic Research Series, Eds. Ross, R.M., Hofmann, E.E., Quetin, L.B., Foundations for Ecological Research West of the Antarctic Peninsula, Washington, DC 70, 287–301.

Crise, A., Allen, J.I., Baretta, J., Crispi, G., Mosetti, R., Solidoro, C., 1999. The Mediterranean pelagic ecosystem response to physical forcing. Progress in Oceanography 44, 219-243.

Crombet, Y., Leblanc, K., Quéguiner, B., Moutin, T., Rimmelin, P., Ras, J., Claustre, H., Leblond, N., 2011. Deep silicon maxima in the stratified oligotrophic Mediterranean Sea. Biogeosciences 8, 459-575.

Cruzado, A., Velasquez, Z.R., 1990. Nutrients and phytoplankton in the Gulf of Lions. Continental Shelf Research 10, 931-942.

Cury, P., Shannon, L., Shin, Y.J., 2001. The functioning of marine ecosystems, Reykjavik Conference on Responsible Fisheries in the Marine Ecosystem, 1-4 October, Reykjavik, Iceland.

D'Ortenzio, F., Ribera d'Alcalà, M., 2009. On the trophic regimes of the Mediterranean Sea: a satellite analysis. Biogeosciences 6, 139-148.

Daly Yahia, N., 1998. Contribution à l'étude du milieu et du zooplancton de la lagune de Bou Grara. Systematique, biomasse et relations trophiques. Diplôme d'Etudes Approfondies. Faculté des Sciences de Tunis, Université de Tunis II. pp215.

Dam, H.G., Peterson, W.T., 1988. The effect of temperature on the gut clearance rate constant of planktonic copepods. Journal of Experimental Marine Biology and Ecology 123, 1-14.

Dauby, P., 1980. Cycle annuel du zooplancton de surface de la baie de Calvi (Corse). Biomasse totale et plancton copépodien. Oceanologica Acta 3, 403-407.

Davoll, P.J., Youngbluth, M.J., 1990. Heterotrophic activity on appendicularian (Tunicata: Appendicularia) houses in mesopelagic regions and their potential contribution to particle flux. Deep Sea Research Part A 37, 285-294.

Deacon, G.E.R., 1982. Physical and biological zonation in the Southern Ocean. Deep Sea Research Part A 29, 1-15.

Defant, A., 1961. Physical Oceanography, Pergamon Press, New York, 1.

Di Capua, I., Mazzocchi, M.G., 2004. Population structure of the copepods *Centropages typicus* and *Temora stylifera* in different environmental conditions. ICES Journal of Marine Science 61, 632-644.

Dolan, J.R., 2005. Marine ecology: Different measures of biodiversity. Nature 433, 27, E9.

Dolan, J.R., Claustre, H., Carlotti, F., Plounevez, S., Moutin, T., 2002. Microzooplankton diversity: relationships of tintinnid ciliates with resources, competitors and predators from the Atlantic Coast of Morocco to the Eastern Mediterranean. Deep Sea Research I 49, 1217-1232.

Dolan, J.R., Rassoulzadegan, F., Caron, D.A., 2005. The first decade of 'Aquatic Microbial Ecology' (1995–2005): evidence for gradualism or punctuated equilibrium? Aquatic Microbial Ecology 39, 3-6.

Dolan, J.R., Vidussi, F., Claustre, H., 1999. Planktonic ciliates in the Mediterranean Sea: longitudinal trends. Deep Sea Research I 46, 2025-2039.

Dolédec, S., Chessel, D., 1994. Co-inertia analysis: an alternative method for studying species-environment relationships. Freshwater Biology 31, 277-294.

Drits, A.V., Pasternak, A.F., Kosobokova, K.N., 1994. Physiological characteristics of the Antarctic copepod *Calanoides acutus* during late summer in the Weddell Sea. Hydrobiologia 292/293, 201-207.

Duhamel, G., Hautecoeur, M., 2009. Biomass, abundance and distribution of fish in the Kerguelen Islands EZ (CCAMLR Statistical Division 58.5.1). CCAMLR Science 16, 1-32.

Durrieu de Madron, X., Guieu, C., Sempéré, R., Conan, P., Cossa, D., D'Ortenzio, F., Estournel, C., Gazeau, F., Rabouille, C., Stemmann, L., Bonnet, S., Diaz, F., Koubbi, P., Radakovitch, O., Babin, M., Baklouti, M., Bancon-Montigny, C., Belviso, S., Bensoussan, N., Bonsang, B., Bouloubassi, I., Brunet, C., Cadiou, J.F., Carlotti, F., Chami, M., Charmasson, S., Charrière, B., Dachs, J., Doxaran, D., Dutay, J.C., Elbaz-Poulichet, F., Eléaume, M., Eyrolles, F., Fernandez, C., Fowler, S., Francour, P., Gaertner, J.C., Galzin, R., Gasparini, S., Ghiglione, J.F., Gonzalez, J.L., Goyet, C., Guidi, L., Guizien, K., Heimbürger, L.E., Jacquet, S.H.M., Jeffrey, W.H., Joux, F., Le Hir, P., Leblanc, K., Lefèvre, D., Lejeusne, C., Lemé, R., Loÿe-Pilot, M.D., Mallet, M., Méjanelle, L., Mélin, F., Mellon, C., Mérigot, B., Merle, P.L., Migon, C., Miller, W.L., Mortier, L., Mostajir, B., Mousseau, L., Moutin, T., Para, J., Pérez, T., Petrenko, A., Poggiale, J.C., Prieur, L., Pujo-Pay, M., Pulido, V., Raimbault, P., Rees, A.P.,

Ridame, C., Rontani, J.F., Ruiz Pino, D., Sicre, M.A., Taillandier, V., Tamburini, C., Tanaka, T., Taupier-Letage, I., Tedetti, M., Testor, P., Thébault, H., Thouvenin, B., Touratier, F., Tronczynski, J., Ulses, C., Van Wambeke, F., Vantrepotte, V., Vaz, S., Verney, R., 2011. Marine ecosystems' responses to climatic and anthropogenic forcings in the Mediterranean. Progress in Oceanography 91, 97-166.

Edvardsen, A., Zhou, M., Tande, K.S., Zhu, Y., 2002. Zooplankton population dynamics: measuring in situ growth and mortality rates using an optical plankton counter. Marine Ecology Progress Series 227, 205-219.

Eisenhauer, L., Carlotti, F., Baklouti, M., Diaz, F., 2009. Zooplankton population model coupled to a biogeochemical model of the North Western Mediterranean Sea ecosystem. Ecological Modelling 220, 2865-2876.

Errhif, A., Razouls, C., Mayzaud, P., 1997. Composition and community structure of pelagic copepods in the Indian sector of the Antarctic Ocean during the end of the austral summer. Polar Biology 17, 418-430.

Estrada, M., Salat, J., 1989. Phytoplankton assemblages of deep and surface water layers in a Mediterranean frontal zone. Scientia Marina 53, 203-214.

Etilé, R.N., Kouassi, A.M., Aka, M.N., Pagano, M., N'douba, V., Kouassi, N.J., 2009. Spatio-temporal variations of the zooplankton abundance and composition in a West African tropical coastal lagoon (Grand-Lahou, Côte d'Ivoire). Hydrobiologia 624, 171-189.

Fernández de Puelles, M.L., Grás, D., Hernandez-León, S., 2003. Annual cycle of zooplankton biomass, abundance and species composition in the neritic area of the Balearic Sea, Western Mediterranean. PSZN Marine Ecology 123, 123-139.

Fernández de Puelles, M.L., Valencia, J., Jansa, J., Morillas, A., 2004. Hydrographical characteristics and zooplankton distribution in the Mallorca channel (Western Mediterranean): spring 2001. ICES Journal of Marine Science 61, 654-666.

Fernández de Puelles, M.L., Alemany, F., Jansá, J., 2007. Zooplankton time-series in the Balearic Sea (Western Mediterranean): Variability during the decade 1994–2003. Progress in Oceanography 74, 329-354.

Fernández de Puelles, M.L., Lopez-Urrutia, A., Morillas, A., Mollinero, J.C., 2009. Seasonal variability of copepod abundance in the Balearic region (Western Mediterranean) as an indicator of basin scale hydrological changes. Hydrobiologia 167, 3-16.

Fonda Umani, S., 1996. Pelagic production and biomass in the Adriatic Sea. Scientia Marina 60 (Sup 2), 65-77.

Fonda Umani, S., Monti, M., Bergamasco, A., Cabrini, M., De Vittor, C., Burba, N., Del Negro, P., 2005. Plankton community structure and dynamics versus physical structure from Terra Nova Bay to Ross Ice Shelf (Antarctica). Journal of Marine Systems 55, 31-46.

Fragopoulu, N., Siokoi-Frangou, I., Christou, E. D., Mazzocchi, M. G., 2001. Patterns of vertical distribution of Pseudocalanidae and Paracalanidae (Copepoda) in pelagic waters (0 to 300 m) of the Eastern Mediterranean Sea. Crustaceana 74, 49-68.

Frangoulis, C., Christou, E.D., Hecq, J.H., 2005. Comparison of Marine Copepod Outfluxes: Nature, Rate, Fate and Role in the Carbon and Nitrogen Cycles. Advances in Marine Biology 47, 253-309.

Fransz, H.G., Gonzales, S.R., 1995. The production of *Oithona similis* (Copepoda: Cyclopoida) in the Southern Ocean. ICES Journal of Marine Science 52, 549-555.

Fransz, H.G., Gonzalez, S.R., 1997. Latitudinal metazoan plankton zones in the Antarctic Circumpolar Current along 61W during austral spring 1992. Deep Sea Research II 44, 395-414.

Fraser, W.R., Trivelpiece, W.Z., 1996. Factors controlling the distribution of seabirds: winter-summer heterogeneity in the distribution of Adélie penguin populations. Eds. Ross, R.M., Hofmann, E.E., Quetin, L.B., Antarctic Research Series, Foundations for Ecological Research West of the Antarctic Peninsula, Washington, DC 70, 257-272.

Froneman, P.W., Ansorge, I.J., Pakhomov, E.A., Lutjeharms, J.R.E., 1999. Plankton community structure in the physical environment surrounding the Prince Edward Islands (Southern Ocean). Polar Biology 22, 145-155.

Furnestin, M.-L., 1968. Le zooplancton de la Méditerranée (Bassin Occidental). Essai de synthèse. ICES Journal of Marine Science 32, 25-69.

Gacic, M., Civitarese, G., Miserocchi, S., Cardin, V., Crise, A., Mauri, E., 2002. The open-ocean convection in the southern Adriatic: A controlling mechanism of the spring phytoplankton bloom. Continental Shelf Research 22, 1897-1908.

Gallienne, C.P., Robins, D.B., 1998. Trans-oceanic characterization of zooplankton community size structure using an optical plankton counter. Fisheries Oceanography 7, 147-158.

Gallienne, C.P., Robins, D.B., 2001. Is *Oithona* the most important copepod in the world's oceans? Journal of Plankton Research 23, 1421-1432.

Gallucci, F., Ólafsson, E., 2007. Cannibalistic behaviour of rock-pool copepods: An experimental approach for space, food and kinship. Journal of Experimental Marine Biology and Ecology 342, 325-331.

García-Comas, C., Stemmann, L., Ibanez, F., Berline, L., Mazzocchi, M.G., Gasparini, S., Picheral, M., Gorsky, G., 2011. Zooplankton long-term changes in the NW Mediterranean Sea: Decadal periodicity forced by winter hydrographic conditions related to large-scale atmospheric changes? Journal of Marine Systems 87, 216-226.

Gaudy, R., 1962. Biologie des copépodes pélagiques du Golfe de Marseille. Recueil des Travaux de la Station Marine d'Endoume Bulletin 27, Fasc. 42, 93-184.

Gaudy, R., 1985. Features and pecularities of zooplankton communities from the western Mediterranean. in Mediterranean Marine Ecosystems, Eds. Moraitou-Apostopoulos, M., Kiortsis, V., Plenum Publishing Corporation, New York, 279-301.

Gaudy, R., Youssara, F., 2003. Variations of zooplankton metabolism and feeding in the frontal area of the Alboran Sea (western Mediterranean) in winter. Oceanologica Acta 26, 179-189.

Gaudy, R., Youssara, F., Diaz, F., Raimbault, P., 2003. Biomass, metabolism and nutrition of zooplankton in the Gulf of Lions (NW Mediterranean). Oceanologica Acta 26, 357-372.

Gentleman, W., Leising, A., Frost, B., Strom, S., Murray, J., 2003. Functional responses for zooplankton feeding on multiple resources: a review of assumptions and biological dynamics. Deep Sea Research II 50.

Gervais, F., Riebesell, U., Gorbunov, M.Y., 2002. Changes in primary productivity and chlorophyll a in response to iron fertilization in the Southern Polar Frontal Zone. Limnology and Oceanography 47, 1324-1335.

Gómez, F., Gorsky, G., Striby, L., Vargas, J.M., Gonzalez, N., Picheral, M., García-Lafuente, J., Varela, M., Goutx, M., 2001. Small-scale temporal variations in biogeochemical features in the Strait of Gibraltar, Mediterranean side—the role of NACW and the interface oscillation. Journal of Marine Systems 30, 207-220.

Gorsky, G., Fisher, N.S., Fowler, S.W., 1984. Biogenic debris from the pelagic tunicate, *Oikopleura dioica*, and its role in the vertical transport of a transuranium element. Estuarine Coastal and Shelf Sciences 18, 13-23.

Gorsky, G., Chrétiennot-Dinet, M.J., Blanchot, J., Palazzoli, I., 1999. Pico- and nanoplankton aggregation by appendicularians: fecal pellet contents of *Megalocercus huxleyi* in the equatorial Pacific. Journal of Geophysical Research 104, 3381-3390.

Gorsky, G., Ohman, M.D., Picheral, M., Gasparini, S., Stemmann, L., Romagnan, J.B., Cawood, A., Pesant, S., Garcia-Comas, C., Prejge, F., 2010. Digital zooplankton image analysis using the ZooScan integrated system. Journal of Plankton Research 32, 285-303.

Grant, S., Ward, P., Murphy, E., Bone, D., Abbott, S., 2000. Field comparison of an LHPR net sampling system and an optical plankton counter (OPC) in the Southern Ocean. Journal of Plankton Research 22, 619-638.

Grosjean, P., Picheral, M., Warembourg, C., Gorsky, G., 2004. Enumeration, measurement, and identification of net zooplankton samples using the ZOOSCAN digital imaging system. ICES Journal of Marine Science 61, 518-525.

Guerzoni, S., Chester, R., Dulac, F., Herut, B., Loÿe-Pilot, M.D., Measures, C., Migon, C., Molinaroli, E., Moulin, C., Rossini, P., Saydam, C., Soudine, A., Ziveri, P., 1999. The role of atmospheric deposition in the biogeochemistry of the Mediterranean Sea. Progress in Oceanography 44, 147-190.

Hafferssas, A., Seridji, R., 2010. Relationships between the hydrodynamics and changes in copepod structure on the Algerian coast. Zoological Studies 49, 353-366.

Hammer, M., Hammer, P., 2000. Behavior of Antarctic krill (*Euphausia superba*): schooling, foraging, and antipredatory behavior. Canadian Journal of Fisheries Aquatic Science 57 (Sup 3), 192-202.

Hargrave, B.T., Geen, G.H., 1968. Phosphorus excretion by zooplankton. Limnology and Oceanography 13, 332-342.

Harrison, W.G., Harris, L.R., Irwin, B.D., 1996. The kinetics of nitrogen utilization in the oceanic mixed layer: Nitrate and ammonium interactions at nanomolar concentrations. Limnology and Oceanography 41, 16-32.

Harvey, H.W., 1955. The chemistry and fertility of sea waters, Univ. Press, Cambridge, pp 224.

Harvey, M.J., Law, C.S., Smith, M.J., Hall, J.A., Abraham, E.R., Stevens, C.L., Hadfield, M.G., Ho, D.T., Ward, B., Archer, S.D., Cainey, J.M., Currie, K.I., Devries, D., Ellwood, M.J., Hill, P., Jones, G.B., Katz, D., Kuparinen, J., Macaskill, B., Main, W., Marriner, A., McGregor, J., McNeil, C., Minnett, P.J., Nodder, S.D., Peloquin, J., Pickmere, S., Pinkerton, M.H., Safi, K.A., Thompson, R., Walkington, M., Wright, S.W., Ziolkowski, L.A., 2011. The SOLAS air–sea gas exchange experiment (SAGE) 2004. Deep Sea Research II 58, 753-763.

Henjes, J., Assmy, P., Klaas, C., Verity, P., Smetacek, V., 2007. Response of microzooplankton (protists and small copepods) to an iron-induced phytoplankton bloom in the Southern Ocean (EisenEx). Deep Sea Research I 54, 363-384.

Henriksen, C.I., Saiz, E., Calbet, A., Hansen, B.W., 2007. Feeding activity and swimming patterns of *Acartia grani* and *Oithona davisae* nauplii in the presence of motile and non-motile prey. Marine Ecology Progress Series 331, 119-129.

Herbland, A., Le Bouteiller, A., P, R., 1985. Size structure of phytoplankton biomass in the equatorial Atlantic Ocean. Deep Sea Research I 32, 819-836.

Herman, A.W., 1983. Vertical distribution patterns of copepods, chlorophyll, and production in northeastern Baffin Bay. Limnology and Oceanography 28, 709-719.

Herman, A.W., 1988. Simultaneous measurement of zooplankton and light attenuance with a new optical plankton counter. Continental Shelf Research 8, 205-221.

Herman, A.W., 1992. Design and calibration of a new optical plankton counter capable of sizing small zooplankton. Deep Sea Research 39, 395-415.
Herman, A.W., Harvey, M., 2006. Application of normalized biomass size spectra to laser optical plankton counter net intercomparisons of zooplankton distributions. Journal of Geophysical Research 111, 1-9.
Hernández-León, S.C., Almedia, C., Portillo Hahnefeld, A., Gómez, M., Montero, I., 2000. Biomass and potential feeding, respiration and growth of zooplankton in the Bransfield Strait (Antarctic Peninsula) during austral summer. Polar Biology 23, 679-690.
Hernández-León, S.C., Montero, I., 2006. Zooplankton biomass estimated from digitalized images in Antarctic waters: A calibration exercise. Journal of Geophysical Research 111, C05S09.
Holm-Hansen, O., Lorenzen, C.J., Holmes, R.W., Strickland, J.D.H., 1965. Fluorometric determination of chlorophyll. Journal du Conseil Permanent International Pour L'Exploration de la Mer 30, 3-15.
Holmes, R.M., Aminot, A., Kérouel, R., Hooker, B.A., Peterson, B.J., 1999. A simple and precise method for measuring ammonium in marine and freshwater ecosystems. Canadian Journal of Fisheries Aquatic Sciences 56, 1801-1808.
Hopcroft, R.R., Clarke, C., Chavez, S.P., 2002. Copepod communities in Monterey Bay during the 1997-1999 El Niño and La Niña. Progress in Oceanography 654, 251-264.
Hopkins, T.L., 1971. Zooplankton standing crop in the Pacific sector of the Antarctic. Eds. Llano, G.W., Wallen, I.E., Biology of the Antarctic Seas, American Geophysical Union, Washington, DC, vol. 17, pp 347–362.
Hopkins, T.L., 1987. Midwater food web in McMurdo Sound, Ross Sea, Antarctica. Marine Biology 96, 96-106.
Hopkins, T.L., Lancraft, T.M., Torres, J., Donnelly, J., 1993. Community structure and trophic ecology of zooplankton in the Scotia Sea marginal ice zone in winter (1988). Deep Sea Research I 40, 81-105.
Hunt, B.P.V., Pakhomov, E.A., 2003. Mesozooplankton interactions with the shelf around the sub-Antarctic Prince Edward Islands archipelago. Journal of Plankton Research 25, 885-904.
Huntley, M., 1981. Nonselective, nonsaturated feeding by three calanid copepod species in the Labrador Sea. Limnology and Oceanography 26, 831-842.
Huntley, M.E., Zhou, M., Nordhausen, W., 1995. Mesoscale distribution of zooplankton in the California Current in late spring, observed by optical plankton counter. Journal of Marine Systems 53, 647-674.
Hygum, B.H., Petersen, J.W., Sondergaard, M., 1997. Dissolved organic carbon released by zooplankton grazing activity—a high-quality substrate pool for bacteria. Journal of Plankton Research 19, 97-111.
Ibanez, F., Bouchez, J., 1987. Anisotropie des populations zooplanctoniques dans la zone frontale de Mer Ligure. Oceanologica Acta 10, 205-216.
Ignatiades, L., 2005. Scaling the trophic status of the Aegean Sea, eastern Mediterranean. Journal of Sea Research 54, 51-57.
Ignatiades, L., Gotsis-Skretas, O., Pagou, K., Krasakopoulou, E., 2009. Diversification of phytoplankton community structure and related parameters along a large-scale longitudinal east–west transect of the Mediterranean Sea. Journal of Plankton Research 31, 411-428.
Ikeda, T., Fay, A.W., 1981. Metabolic activity of zooplankton of the Antarctic Ocean. Australian Journal of Marine and Freshwater Research 32, 921-930.

Ikeda, T., Mitchell, A.W., 1982. Oxygen Uptake, Ammonia Excretion and Phosphate Excretion by Krill and Other Antarctic Zooplankton in Relation to Their Body Size and Chemical Composition. Marine Biology 71, 283-298.

Ikeda, T., 1985. Metabolic rates of epipelagic marine zooplankton as a function of body mass and temperature. Marine Biology 85, 1-11.

Ikeda, T., 1990. Ecological and biological features of a mesopelagic ostracod, *Conchoecia pseudodiscophora*, in the Japan Sea. Marine Biology 107, 453-461.

Ikeda, T., Torres, J.J., Hernández-León, S., Geiger, S.P., 2000. Metabolism. ICES Zooplankton Methodology Manual, Eds. Harris, R., Wiebe, P.H., Lenz, J., Skjoldal, H.R., Huntley, M., Academic, London, 455-532.

Irigoien, X., Huisman, J., Harris, R.P., 2004. Global biodiversity patterns of marine phytoplankton and zooplankton. Nature 429, 863-867.

Isla, J.A., Ceballos, S., Huskin, I., Anadón, R., Alvarez-Marqués, F., 2004. Mesozooplankton distribution, metabolism and grazing in an anticyclonic slope water oceanic eddy (SWODDY) in the Bay of Biscay. Marine Biology 145, 1201-1212.

Jamet, J.L., Bogé, G., Richard, S., Geneys, C., Jamet, D., 2001. The zooplankton community in bays of Toulon area (northwest Mediterranean Sea, France). Hydrobiologia 457, 155-165.

Jansen, S., Klaas, C., Kragefsky, S., von Harbou, L., Bathmann, U., 2006. Reproductive response of the copepod *Rhincalanus gigas* to an iron-induced phytoplankton bloom in the Southern Ocean. Polar Biology 29, 1039-1044.

Jeandel, C., Ruiz-Pino, D., Gjata, E., Poisson, A., Brunet, C., Charriaud, E., Dehairs, F., Delille, D., Fiala, M., Fravalo, C., Miquel, J.C., Park, Y.H., Pondaven, P., Quéguiner, B., Razouls, S., Shauer, B., Tréguer, P., 1998. KERFIX, a time-series station in the Southern Ocean: a presentation. Journal of Marine Systems 17, 555-569.

Johnson, K.M., Sieburth, J.M., Williams, P.J.l., Bändström, L., 1987. Coulometric total carbon dioxide analysis for marine studies: Automation and calibration. Marine Chemistry 21, 117-133.

Kâ, S., Pagano, M., Bâ, N., Bouvy, M., Leboulanger, C., Arfi, R., Thiaw, O.T., Ndour, E.H.M., Corbin, D., Defaye, D., Cuoc, C., Kouassi, E., 2006. Zooplankton Distribution Related to Environmental Factors and Phytoplankton in a Shallow Tropical Lake (Lake Guiers, Senegal, West Africa). International Review of Hydrobiology 91, 389-405.

Karlson, K., Bamstedt, U., 1994. Planktivorous predation on copepods. Evaluation of mandible remains in predator guts as a quantitative estimate of predation. Marine Ecology Progress Series 108, 79-89.

Kattner, G., Graeve, M., Hagen, G., 1994. Ontogenetic and seasonal changes in lipid and fatty acid/alcohol compositions of the dominant Antarctic copepods *Calanus propinquus*, *Calanoides acutus* and *Rhincalanus gigas*. Marine Biology 118, 637-644.

Kattner, G., Hagen, W., 1995. Polar herbivorous copepods – different pathways in lipid biosynthesis. ICES Journal of Marine Science 52, 329-335.

Klein Breteler, W.C.M., Schogt, N., Van der Meer, J., 1994. The duration of copepod life stages estimated from stage-frequency data. Journal of Plankton Research 16, 1039-1057.

Kobari, T., Steinberg, D.K., Ueda, A., Tsuda, A., Silver, M.W., Kitamura, M., 2008. Impacts of ontogenetically migrating copepods on downward carbon flux in the western subarctic Pacific Ocean. Deep Sea Research II 55, 1648-1660.

Kopczynska, E.E., H, W.L., El Sayed, S.Z., 1986. Phytoplankton species composition and abundance in the Indian Sector of the Antarctic Ocean. Polar Biology 6, 161-169.

Koppelmann, R., Weikert, H., 2007. Spatial and temporal distribution patterns of deep-sea mesozooplankton in the eastern Mediterranean – indications of a climatically induced shift? Marine Ecology 28, 259-275.

Koroleff, F., 1969. Direct determination of ammonia in natural waters as indophenol blue. Council for the Exploration of the Sea Commission Meeting C9, 1-6.

Koski, M., Møller, E.E., Maar, M., Visser, A.W., 2007. The fate of discarded appendicularian houses: degradation by the copepod, *Microsetella norvegica*, and other agents. Journal of Plankton Research 29, 641-657.

Koski, M., Jonasdottir, S.H., Bagøien, E., 2011. Biological processes in the North Sea: vertical distribution and reproduction of neritic copepods in relation to environmental factors. Journal of Plankton Research 33, 63-84.

Kouassi, E., Pagano, M., Saint-Jean, L., Sorbe, J.C., 2006. Diel vertical migrations and feeding behavior of the mysid *Rhopalophthalmus africana* (Crustacea: Mysidacea) in a tropical lagoon (Ebrie, Cote d'Ivoire). Estuarine Coastal and Shelf Science 67, 355-368.

Kremer, P., 1977. Respiration and excretion by the ctenophore *Mnemiopsis leidyi*. Marine Biology 44, 43-50.

Krom, M.D., Kress, N., Brenner, S., Gordon, L.I., 1991. Phosphorus limitation of primary productivity in the Eastern Mediterranean Sea. Limnology and Oceanography 36, 424-432.

Krom, M.D., Groom, S., Zohary, T., 2003. The Eastern Mediterranean. Eds.Black, K. D., Shimmield, G. B., The Biogeochemistry of Marine Systems, Blackwell Publishing, Oxford, pp 91-122.

Krom, M.D., Woodward, E.M.S., Herut, B., Kress, N., Carbo, P., Mantoura, R.F.C., Spyres, G., Thingstad, T.F., Wassmann, P., Wexels-Riser, C., Kitidis, V., Law, C.S., Zodiatis, G., 2005. Nutrient cycling in the south east Levantine basin of the eastern Mediterranean: Results from a phosphorus starved system. Deep Sea Research II 52, 2879-2896.

L'Helguen, S., Le Corre, P., Madec, C., Morin, P., 2002. New and regenerated production in the Almeria-Oran front area, eastern Alboran Sea. Deep Sea Research I 49, 83-99.

Labat, J.P., Mayzaud, P., Dallot, S., Errhif, A., Razouls, S., Sabini, S., 2002. Mesoscale distribution of zooplankton in the Sub-Antarctic Frontal system in the Indian part of the Southern Ocean: a comparison between optical plankton counter and net sampling. Deep Sea Research I 49, 735-749.

Lakkis, S., 1990a. Composition, diversity and successions of planktonic copepods in the Lebanese waters (eastern Mediterranean). Oceanologica Acta 13, 489-501.

Lakkis, S., 1990b. Vingt ans d'observations sur le plancton des eaux libanaises:structure et fluctuations interannuelles. Eds. Godeaux, A propos de migrations lessepsiennes, Institut Oceanographique de Monaco, Monaco, pp 51–66.

Latasa, M., Estrada, M., Delgado, M., 1992. Plankton-pigment relationships in the Northwestern Mediterranean during stratification. Marine Ecology Progress Series 88, 61-73.

Le Borgne, R.P., 1986. The release of soluble end products of metabolism. Eds. Corner, S. C., O'Hara, M, The Biological Chemistry of Marine Copepods, Oxford, Clarendon Press, 109-164.

Legendre, L., Rassoulzadegan, F., 1995. Plankton and nutrient dynamics in marine waters. Ophelia 41, 153-172.

Lévy, M., Memery, L., André, J.M., 1998. Simulation of primary production and export fluxes in the Northwestern Mediterranean Sea. Journal of Marine Research 56, 197-238.

Licandro, P., Ibanez, F., 2000. Changes of zooplankton communities in the Gulf of Tigullio (Ligurian Sea, Western Mediterranean) from 1985 to 1995. Influence of hydroclimatic factors. Journal of Plankton Research 22, 2225-2253.

Licandro, P., Icardi, P., 2009. Basin scale distribution of zooplankton in the Ligurian Sea (north-western Mediterranean) in late autumn. Hydrobiologia 617, 17-40.

Lombard, F., Kiørboe, T., 2010. Marine snow originating from appendicularian houses: Age-dependent settling characteristics. Deep Sea Research I 57, 1304-1313.

Longhurst, A.R., Bedo, A.W., Harrison, W.G., Head, E.J.H., Sameoto, D.D., 1990. Vertical flux of respiratory carbon by oceanic diel migrant biota. Deep Sea Research Part A 37, 685-694.

Longhurst, A.R., 1998. Ecological Geography of the Sea, Elsevier Science Publishers, New York, pp 560.

Ludwig, W., Dumont, E., Meybeck, M., Heussner, S., 2009. River discharges of water and nutrients to the Mediterranean and Black Sea: Major drivers for ecosystem changes during past and future decades? Progress in Oceanography 80, 199-217.

Maar, M., Visser, A.W., Nielsen, T.G., Stips, A., Saito, H., 2006. Turbulence and feeding behaviour affect the vertical distributions of *Oithona similis* and *Microsetella norwegica*. Marine Ecology Progress Series 313, 157-172.

Mackas, D., Bohrer, R., 1976. Fluorescence analysis of zooplankton gut contents and an investigation of diel feeding patterns. Journal of Experimental Marine Biology and Ecology 25, 77-85.

Margalef, R., 1985. Western Mediterranean, Key environments. Pergamon Press, Oxford, pp 363.

Marshall, S.M., Orr, A.P., 1958. Some uses of antibiotics in physiological experiments in sea water. Journal of Marine Research 17, 341-346.

Martin, J.H., Gordon, R.M., Fitzwater, S.E., 1990. Iron in Antarctic waters. Nature Geoscience 345, 156-158.

Mauchline, J., 1998. The biology of calanoid copepods. Eds. Blaxter, J.H.S., Southward, A.J., Tyler, P.A., Advances in Marine Biology, Academic Press, London, pp 710.

Mayzaud, P., Conover, R.J., 1988. O:N atomic ratio as a tool to describe zooplankton metabolism. Marine Ecology Progress Series 45, 289-302.

Mayzaud, P., Razouls, S., 1992. Degradation of gut pigment during feeding by a subantarctic copepod: importance of feeding history and digestive acclimation. Limnology and Oceanography 37, 393-404.

Mayzaud, P., Boutoute, M., Gasparini, S., Mousseau, L., Lefevre, D., 2005. Respiration in marine zooplankton—the other side of the coin: CO_2 production. Limnology and Oceanography 50, 291-298.

Mayzaud, P., Razouls, S., Errhif, A., Tirelli, V., Labat, J.P., 2002a. Feeding, respiration and egg production rates of copepods during austral spring in the Indian sector of the Antarctic Ocean: role of the zooplankton community in carbon transformation. Deep Sea Research I 49, 1027-1048.

Mayzaud, P., Tirelli, V., Errhif, A., Labat, J.P., Razouls, S., Perissinotto, R., 2002b. Carbon intake by zooplankton. Importance and role of zooplankton grazing in the Indian sector of the Southern Ocean. Deep Sea Research II 49, 3169-3187.

Mayzaud, P., Lacombre, S., Boutoute, M., 2011. Seasonal and growth stage changes in lipid and fatty acid composition in the multigeneration copepod *Drepanopus pectinatus* from Iles Kerguelen. Antarctic Science 23, 3-17.

Mazzocchi, M.G., Ribera d'Alcalà, M., 1995. Recurrent patterns in zooplankton structure and succession in a variable coastal environment. ICES Journal of Marine Science 52, 679-691.

Mazzocchi, M.G., Christou, E., Fragopoulu, N., Siokou-Frangou, I., 1997. Mesozooplankton distribution from Sicily to Cyprus (Eastern Mediterranean): I. General aspects. Oceanologica Acta 20, 521-535.

Mazzocchi, M.G., Nervegna, D., D'Elia, G., Di Capua, I., Aguzzi, L., Boldrin, A., 2003. Spring mesozooplankton communities in the epipelagic Ionian Sea in relation to the Eastern Mediterranean Transient. Journal of Geophysical Research, 108, 8114, doi:10.1029/2002JC001640.

Mazzocchi, M.G., Christou, E., Di Capua, I., Fernández de Puelles, M.L., Fonda-Umani, S., Molinero, J.C., Nival, P., Siokou-Frangou, I., 2007. Temporal variability of *Centropages typicus* in the Mediterranean Sea over seasonal-to-decadal scales. Progress in Oceanography 72, 214-232.

Mazzocchi, M.G., Licandro, P., Dubroca, L., Di Capua, I., Saggiomo, V., 2011. Zooplankton associations in a Mediterranean long-term time-series. Journal of Plankton Research 33, 1163-1181.

Metz, C., Schnack-Schiel, S.B., 1995. Observations on carnivorous feeding in Antarctic calanoid copepods. Marine Ecology Progress Series 129, 71-75.

Metz, C., 1996. Life strategies of dominant Antarctic Oithonidae (Cyclopoida, Copepoda) and Oncaeidae (Poecilostomatoida, Copepoda) in the Bellingshausen Sea. Berichte zur Polarforschung, Avances in Marine Biology, Alfred Wegener Institut für Polar und Meeresforschung, Bremen, 207,pp 123.

Meybeck, M., Dürr, H., Roussennac, S., Ludwig, W., 2007. Regional seas and their interception of riverine fluxes to oceans. Marine Chemistry 106, 301-325.

Michels, J., Schnack-Schiel, S.B., 2005. Feeding in dominant Antarctic copepods—does the size of the mandibular gnathobases relate to diet? Marine Biology 146, 483-495.

Millot, C., 1999. Circulation in the Western Mediterranean Sea. Journal of Marine Systems 20, 423-442.

Millot, C., Taupier-Letage, I., 2005. Circulation in the Mediterranean Sea. Eds. Saliot, A., The handbook of environmental chemistry, Heidelberg, Springer-Verlag, 5 (K), 29-66.

Minutoli, R., Guglielmo, L., 2009. Zooplankton respiratory Electron Transport System (ETS) activity in the Mediterranean Sea: spatial and diel variability. Marine Ecology Progress Series 381, 199-211.

Molinero, J.C., 2003. Abundance variability of planktonic copepods in the Mediterranean sea. Mechanisms and characteristic scales: the *Centropages typicus* Case Study. Ph.D. Thesis, Paris VI University, Paris, France, pp 200.

Molinero, J.C., Ibanez, F., Nival, P., 2005. North Atlantic climate and northwestern Mediterranean plankton variability. Limnology and Oceanography 50, 1213-1220.

Molinero, J.C., Ibanez, F., Souissi, S., Bosc, E., Nival, P., 2008a. Surface patterns of zooplankton spatial variability detected by high frequency sampling in the NW Mediterranean. Role of density fronts. Journal of Marine Systems 69, 271-282.

Molinero, J.C., Ibanez, F., Souissi, S., Buecher, E., Dallot, S., Nival, P., 2008b. Climate control on the long-term anomalous changes of zooplankton communities in the Northwestern Mediterranean. Global Change Biology 14, 11-26.

Molinero, J.C., Vukanič, V., Lučić, D., Ibanez, F., Nival, P., Licandro, P., Calbet, A., Christou, E., Daly-Yahia, N., Fernández de Puelles, M.L., Mazzocchi, M.G., Siokou-Frangou, I., 2009. Mediterranean marine copepods: basin-scale trends of the calanoid *Centropages typicus*. Hydrobiologia 617, 41-53.

Mongin, M., Molina, E., Trull, T., 2008. Seasonality and scale of the Kerguelen Plateau phytoplankton bloom: a remote sensing and modeling analysis of the influence of natural iron fertilization in the Southern Ocean. Deep Sea Research II 55, 880-892.

Moore, J.K., Abbott, M.R., 2000. Phytoplankton chlorophyll distributions and primary production in the Southern Ocean. Journal of Geophysical Research 105, 28,709-28,722.

Mosseri, J., Quéguiner, B., Armand, L., Cornet-Barthaux, V., 2008. Impact of iron on silicon utilization by diatoms in the Southern Ocean: a case of Si/N cycle decoupling in a naturally iron-enriched area. Deep Sea Research II 55, 801-819.

Mousseau, L., Lefèvre, D., Narcy, F., Nival, P., Andersen, V., 2009. A one-month study of the zooplankton community at a fixed station in the Ligurian Sea: the potential impact of the species composition on the mineralization of organic matter. Biogeosciences Discussions 6, 995-1019.

Moutin, T., Raimbault, P., 2002. Primary production, carbon export and nutrients availability in western and eastern Mediterranean Sea in early summer 1996 (MINOS cruise). Journal of Marine Systems 33-34, 273-288.

Moutin, T., Van Wambeke, F., Prieur, L., soumis. Introduction to Biogeochemistry from the Oligotrophic to the Ultraoligotrophic Mediterranean (BOUM) experiment. Biogeosciences Discuss.

Nakamura, Y., Turner, J.T., 1997. Predation and respiration by the small cyclopoid copepod *Oithona similis*: How important is feeding on ciliates and heterotrophic flagellates? Journal of Plankton Research 19, 1275-1288.

Nicol, S., 2003. Living krill, zooplankton and experimental investigations: a discourse on the role of krill and their experimental study in marine ecology. Marine Freshwater Behavior Physiology 36, 191-205.

Nival, P., Malara, G., Charra, R., Palazzoli, I., Nival, S., 1974. Etude de la respiration et de l'excrétion de quelques copépodes planctonique (Crustacea) dans la zone de remontée d'eau profonde des côtes Marocaines. Journal of Experimental Biology and Ecology 15, 231-260.

Nowacek, D.P., Friedlaender, A.S., Halpin, P.N., Hazen, E.L., Johnston, D.W., Read, A.J., Espinasse, B., Zhou, M., Zhu, Y., 2011. Super-Aggregations of Krill and Humpback Whales in Wilhelmina Bay, Antarctic Peninsula. PLoS ONE 6, e19173.

Nowaczyk, A., Carlotti, F., Thibault-Botha, D., Pagano, M., 2011. Distribution of epipelagic metazooplankton across the Mediterranean Sea during the summer BOUM cruise. Biogeosciences 8, 2159-2177

Obernosterer, I., Christaki, U., Lefevre, D., Catala, P., Van Wambeke, F., Le Baron, P., 2008. Rapid bacterial mineralization of organic carbon produced during a phytoplankton bloom induced by natural iron fertilization in the Southern Ocean. Deep Sea Research II 55, 777-789.

Orsi, A.H., Whitworth Iii, T., Nowlin Jr, W.D., 1995. On the meridional extent and fronts of the Antarctic Circumpolar Current. Deep Sea Research I 42, 641-673.

Paffenhöfer, G.-A., Mazzocchi, M.G., 2003. Vertical distribution of subtropical epiplanktonic copepods. Journal of Plankton Research 25, 1139-1156.

Pagano, M., Gaudy, R., Thibault, D., Lochet, F., 1993. Vertical migrations and feeding rythms of mesozooplanktonic organisms in the Rhône River Plume area (North-west Mediterranean Sea). Estuarine Coastal and Shelf Science 37, 251-269.

Pakhomov, E.A., McQuaid, C.D., 1996. Distribution of surface zooplankton and seabirds across the Southern Ocean. Polar Biology 16, 271-286.

Palomares, M.L.D., Pauly, D., 2011. A brief history of fishing in the Kerguelen Islands. Eds. Harper, S., Zeller, D., Fisheries catch reconstructions: Islands, Part II. Fisheries Centre Research Reports, France, Fisheries Centre, University of British Columbia, 19 (4), 15-20.

Park, Y.H., Gambéroni, L., Charriaud, E., 1991. Frontal structure, transport and variability of the Antarctic Circumpolar Current in the South Indian Ocean sector, 401-801E. Marine Chemistry 35, 45-62.

Park, Y.H., Gambéroni, L., 1997. Cross-frontal exchange of Antarctic Intermediate Water and Antarctic Bottom Water in the Crozet Basin. Deep Sea Research II 44, 963-986.

Park, Y.-H., Roquet, F., Durand, I., Fuda, J.-L., 2008a. Large-scale circulation over and around the Northern Kerguelen Plateau. Deep Sea Research II 55, 566-581.

Park, Y.H., Gasco, N., Duhamel, G., 2008b. Slope currents around the Kerguelen Islands from demersal longline fishing records. Geophysical Research Letters 35, L09604.

Pasternak, A., Schnack-Schiel, S.B., 2001. Feeding patterns of dominant Antarctic copepods: an interplay of diapause, selectivity, and availability of food. Hydrobiologia 453/454, 25-36.

Pasternak, A., Wassmann, P., Wexels Riser, C., 2005. Does mesozooplankton respond to episodic P inputs in the Eastern Mediterranean? Deep Sea Research II 52, 2975-2989.

Pedrotti, M.L., Fenaux, L., 1996. Distribution of echinoderm larval populations in the geostrophic frontal jet of the eastern Alboran Sea. Oceanologica Acta 19, 189-475.

Peralba, A., Mazzocchi, M.G., 2004. Vertical and seasonal distribution of eight *Clausocalanus* species (Copepoda: Calanoida) in oligotrophic waters. ICES Journal of Marine Sciences 61, 645-653.

Pérez, M.T., Dolan, J.R., Fukai, E., 1997. Planktonic oligotrich ciliates in the NW Mediterranean: growth rates and consumption by copepods. Marine Ecology Progress Series 155, 89-101.

Perissinotto, R., 1992. Mesozooplankton size-selectivity and grazing impact on the phytoplankton community of the Prince Edward Archipelago (Southern Ocean). Marine Ecology Progress Series 79, 243-258.

Peters, R.H., 1983. The ecological implications of body size. Cambridge, University Press, pp 329.

Pinardi, N., Masetti, E., 2000. Variability of the large scale general circulation of the Mediterranean Sea from observations and modelling: a review. Palaeogeography, Palaeoclimatology, Palaeoecology 158, 153-173.

Pinca, S., Dallot, S., 1995. Meso- and macrozooplankton composition patterns related to hydrodynamic structures in the Ligurian Sea (Trophos-2 experiment, April-June 1986). Marine Ecology Progress Series 126, 49-65.

Pitta, P., Giannakourou, A., 2000. Planktonic ciliate in the oligotrophic Eastern Mediterranean: vertical, spatial distribution and mixotrophy. Marine Ecology Progress Series 194, 269-282.

Porter, K.G., Feig, Y.S., 1980. The use od DAPI for identifying and counting aquatic microflora. Limnology and Oceanography 25, 943-948.

Postel, L., Fock, H., Hagen, W., 2000. Biomass and abundance. ICES Zooplankton Methodology Manual, Biomass and abundance, Eds. Harris, R., Wiebe, P.H., Lenz, J., Skjoldal, H.R., Huntley, M., Academic, London, 83-192.

Pujo-Pay, M., Conan, P., Oriol, L., Cornet-Barthaux, V., Falco, C., Ghiglione, J.F., Goyet, C., Moutin, T., Prieur, L., 2011. Integrated survey of elemental stoichiometry (C, N, P) from the Western to Eastern Mediterranean Sea. Biogeosciences 8, 883-899.

Putzeys, S., Yebra, L., Almeida, C., Bécognée, P., Hernández-León, S., 2011. Influence of the late winter bloom on migrant zooplankton metabolism and its implications on export fluxes. Journal of Marine Systems 88, 553-562.

Qiu, Z.F., Doglioli, A.M., Hu, Z.Y., Marsaleix, P., Carlotti, F., 2010. The influence of hydrodynamic processes on zooplankton transport and distributions in the North Western Mediterranean: Estimates from a Lagrangian model. Ecological Modelling 221, 2816-2827.

Quéguiner, B., Tréguer, P., Peeken, I., Scharek, R., 1997. Biogeochemical dynamics and the silicon cycle in the Atlantic sector of the Southern Ocean during austral spring 1992. Deep Sea Research II 44, 69-89.

Raimbault, P., Diaz, F., Pouvesle, W., Boudjellal, B., 1999. Simultaneous determination of particulate organic carbon, nitrogen and phosphorus collected on filters, using a semi-automatic wet-oxydation method. Marine Ecology Progress Series 180, 289-295.

Rakusa-Suszcewski, S., McWinnie, M.A., Cahoon, M., 1976. Respiration of the Antarctic copepod, *Rhincalanus gigas*. Limnology and Oceanography 21, 763-765.

Ramfos, A., Isari, S., Somarakis, S., Georgopoulos, D., Koutsikopoulos, C., Fragopoulu, N., 2006. Mesozooplankton community structure in offshore and coastal waters of the Ionian Sea (eastern Mediterranean) during mixed and stratified conditions. Marine Biology 150, 29-44.

Raymont, J.E.G., Krishnaswamy, S., 1968. A method for determining the oxygen uptake and carbon dioxide output in *Neomysis integer*. International Revue der Gesemten Hydrobiologia 53, 563-572.

Razouls, C., 1972. Estimation de la production secondaire (copépodes pélagiques) dans une province néritique méditerranéenne (Golfe de Lion). Thèse de Doctorat d'Etat, Université de Paris VI, Paris, France, pp. 301.

Razouls, C., 1994. Manuel d'identification des principales espèces de copépodes pélagiques Antarctique et sub-Antarctique. Annales Institut Océanographique, Paris 70, 204.

Razouls, C., de Bovée, F., Kouwenberg, J., Desreumaux, N., 2005-2011. Diversity and geographic distribution of marine planktonic copepods. http://copepodes.obs-banyuls.fr/en/.

Razouls, S., Koubbi, P., Mayzaud, P., 1996. Spatio-temporal distribution of mesozooplankton in a sub-Antarctic coastal basin of the Kerguelen Archipelago (southern Indian Ocean). Polar Biology 16, 581-587.

Razouls, S., De Bovée, F., Delille, D., Fiala, M., Mayzaud, P., 1997. Temporal variability of bacteria, phytoplankton and zooplankton assemblages of the sub-Antarctic Morbihan Bay (Kerguelen Archipelago). Eds. Battaglia, B., Valencia, J.V., Antarctic communities: species, structure and survival, Cambridge, Cambridge University Press, 86-92.

Razouls, S., Du Réau, G., Guillot, P., Maison, J., Jeandel, C., 1998. Seasonal abundance of copepod assemblages and grazing pressure in the Kerguelen Island area (Southern Ocean). Journal of Plankton Research 20, 1599-1614.

Razouls, S., Razouls, C., De Bovée, F., 2000. Biodiversity and biogeography of Antarctic copepods. Antarctic Science 12, 343-362.

Redfield, A.C., Ketchum, B.H., Richards, F.A., 1963. The influence of organisms on the composition of seawater. Eds. Hill, M.N., The sea, v. 2. Interscience, 26-77.

Revelante, N., Gilmartin, M., 1992. The lateral advection of particulate organic matter from the PO delta during summer stratification, and its implications for the northern Adriatic. Estuarine Coastal and Shelf Science 35, 191-212.

Reynolds, C.S., 2008. A changing paradigm of pelagic food webs. Hydrobiologia 93, 517-531.

Riandey, V., 2005. Etude de la structure de taille des populations zooplanctoniques dans différents écosystèmes marins. Apports des nouveaux appareils automatisés d'observation. Université de la Méditerranée - Aix Marseille II, Marseille, pp 372.

Riandey, V., Champalbert, G., Carlotti, F., Taupier-Letage, I., Thibault-Botha, D., 2005. Zooplankton distribution related to the hydrodynamic features in the Algerian Basin (western Mediterranean Sea) in summer 1997. Deep Sea Research I 52, 2029-2048.

Ribera d'Alcalà, M., Conversano, F., Corato, F., Licandro, P., Mangoni, O., Marino, D., Mazzocchi, M.G., Modigh, M., Montresor, M., Nardella, M., Saggiomo, V., Sarno, D., Zingone, A., 2004. Seasonal patterns in plankton communities in a pluriannual time series at a coastal Mediterranean site (Gulf of Naples): an attempt to discern recurrences and trends. Scientia Marina 68 (Sup 1), 65-83.

Richardson, A.J., Bakun, A., Hays, G.C., Gibbons, M.J., 2009. The jellyfish joyride: causes, consequences and management responses to a more gelatinous future. Trends in Ecology and Evolution 24, 312-322.

Robinson, A.R., Wayne, G.L., Theocharis, A., Lascaratos, A., 2001. Mediterranean Sea circulation, Ocean Currents. Eds, Indira, Academic Press, 1-19.

Robinson, C., Steinberg, D.K., Anderson, T.R., Arístegui, J., Carlson, C.A., Frost, J.R., Ghiglione, J.F., Hernández-León, S., Jackson, G.A., Koppelmann, R., Quéguiner, B., Ragueneau, O., Rassoulzadegan, F., Robison, B.H., Tamburini, C., Tanaka, T., Wishner, K.F., Zhang, J., 2010. Mesopelagic zone ecology and biogeochemistry - a synthesis. Deep Sea Research II 57, 1504-1508.

Rollwagen Bollens, G.C., Landry, M.R., 2000. Biological response to iron fertilization in the eastern equatorial Pacific (IronEx II). 2. Mesozooplankton abundance, biomass, depth distribution and grazing. Marine Ecology Progress Series 201, 43-56.

Roquet, F., Park, Y.H., Guinet, C., Bailleul, F., Charrassin, J.-B., 2009. Observations of the Fawn Trough Current over the Kerguelen Plateau from instrumented elephant seals. Journal of Marine Systems 78, 377-393.

Rose, M., 1933. Copépodes pélagiques. Faune de France 26, 1-377.

Saba, G.K., Steinberg, D.K., Bronk, D.A., 2011. The relative importance of sloppy feeding, excretion, and fecal pellet leaching in the release of dissolved carbon and nitrogen by *Acartia tonsa* copepods. Journal of Experimental Marine Biology and Ecology 404, 47-56.

Saiz, E., Calbet, A., Irigoien, X., Alcaraz, M., 1999. Copepod egg production in the western Mediterranean: response to food availability in oligotrophic environments. Marine Ecology Progress Series 187, 179-189.

Saiz, E., Calbet, A., Atienza, D., Alcaraz, M., 2007. Feeding and production of zooplankton in the Catalan Sea (NW Mediterranean). Progress in Oceanography 74, 313-328.

Sarthou, G., Vincent, D., Christaki, U., Obernosterer, I., 2008. The fate of biogenic iron during a phytoplankton bloom induced by natural fertilization: impact of copepod grazing. Deep Sea Research II 55, 734-751.

Sautour, B., Raud, T., Brylinski, J.M., Heroin, D., Raybaud, V., Thibault-Botha, D., Stemmann, L., 2011. Contribution à l'Evaluation Initiale, volet « Etat Ecologique »,

Compartiment Zooplancton, Directive Cadre Stratégie pour le Milieu Marin, Sous-Région Marine « Méditerranée Occidentale » (SRM MO), pp 9.

Schlitzer, R., 2002. Carbon export fluxes in the Southern Ocean: results from inverse modelling and comparison with satellite based estimates. Deep Sea Research II 49, 1623–1644.

Schnack-Schiel, S.B., Smetacek, V., Bodungen, B., Stegmann, P., 1985. Utilisation of phytoplankton by copepods in Antarctic water during spring. Eds. Gray, J., Christiansen, M.E., Marine Biology of Polar Region and Effects of Stress on Marine Organisms. Wiley, New York, 65–81.

Schnack-Schiel, S.B., Hagen, W., Mizdalski, E., 1991. Seasonal comparison of *Calanoides acutus* and *Calanus propinquus* (Copepoda: Colanoida) in the southeastern Weddell Sea, Antarctica. Marine Ecology Progress Series 70, 17-27.

Schultes, S., Verity, P.G., Bathmann, U., 2006. Copepod grazing during an iron-induced diatom bloom in the Antarctic Circumpolar Current (EisenEx): I. Feeding patterns and grazing impact on prey populations. Journal of Experimental Marine Biology and Ecology 338, 16-34.

Scotto di Carlo, B., Ianora, A., Fresi, E., Hure, J., 1984. Vertical zonation patterns for Mediterranean copepods from the surface to 3000 m at a fixed station in the Tyrrhenian Sea. Journal of Plankton Research 6, 1031-1056.

Seguin, G., Gaudy, R., Errhif, A., Thibault, D., 1993. Observations on the abundance, taxonomic composition and ecological affinities of pelagic copepods collected from the Almeria-Oran frontal region. Marine Life 3, 19-29.

Semelkina, A.N., 1993. Development of the zooplankton in the Kerguelen Island region in the years 1987–1988. Eds. Duhamel, G., Campagnes SKALP 1987 et 1988 aux îles Kerguelen à bord des navires 'SKIF' et 'KALPER'. Institut Français pour la recherche et la technologie polaires, Rapports des campagnes à la mer 93–01, 90-103.

Shreeve, R.S., Ward, P., 1998. Moulting and growth of the early stages of two species of Antarctic calanoid copepod in relation to differences in food supply. Marine Ecology Progress Series 175, 109-119.

Shreeve, R.S., Ward, P., Whitehouse, M.J., 2002. Copepod growth and development around South Georgia: relationships with temperature, food and krill. Marine Ecology Progress Series 233, 169-183.

Sieburth, J.M., Smetacek, V., Lenz, J., 1978. Pelagic ecosystem structure: Heterotrophic compartments of the plankton and their relationship to plankton size fractions. Limnology and Oceanography 23, 1256-1263.

Siokou-Frangou, I., 1996. Zooplankton annual cycle in a Mediterranean coastal area. Journal of Plankton Research 18, 203-223.

Siokou-Frangou, I., Christou, E.D., Fragopoulu, N., Mazzocchi, M.G., 1997. Mesozooplankton distribution from Sicily to Cyprus (Eastern Mediterranean): II. Copepod assemblages. Oceanologica Acta 20, 537-548.

Siokou-Frangou, I., Bianchi, M., Christaki, U., Christou, E.D., Giannakourou, A., Gotsis, O., Ignatiades, L., Pagou, K., Pitta, P., Psarra, S., Souvermezoglou, E., Van Wambeke, F., Zervakis, V., 2002. Carbon flow in the planktonic food web along a gradient of oligotrophy in the Aegean Sea (Mediterranean Sea). Journal of Marine Systems 33-34, 335-353.

Siokou-Frangou, I., 2004. Epipelagic mesozooplankton and copepod grazing along an east-west transect in the Mediterranean Sea. Rapports de la Commission international pour l'Exploration Scientifique de la Mer Méditerranée 37, 439.

Siokou-Frangou, I., Zervoudaki, S., Christou, E., Zervakis, V., Georgopoulos, D., 2009. Variability of mesozooplankton spatial distribution in the North Aegean Sea, as influenced by the Black Sea waters outflow. Journal of Marine Systems 78, 557-575.

Siokou-Frangou, I., Christaki, U., Mazzocchi, M.G., Montresor, M., Ribera d'Alcala, M., Vaqué, D., Zingone, A., 2010. Plankton in the open Mediterranean Sea: a review. Biogeosciences 7, 1543-1586.

Smith, S.L., 1978. The role of zooplankton in the nitrogen dynamics of a shallow estuary. Estuarine and Coastal Marine Science, 555-565.

Solic, M., Krstulovic, N., Marasovic, I., Baranovic, A., Pucher-Petkovic, T., Vucetic, T., 1997. Analysis of time series of planktonic communities in the Adriatic Sea: Distinguishing between natural and man-induced changes. Oceanologica Acta 20, 131-143.

Sommer, U., Stibor, H., 2002. Copepoda - Cladocera - Tunicata: The role of three major mesozooplankton groups in pelagic food webs. Ecological Research 17, 161-174.

Sommer, U., Stibor, H., Katechakis, A., Sommer, F., Hansen, T., 2002. Pelagic food web configurations at different levels of nutrient richness and their implications for the ratio fish production: primary production. Hydrobiologia 484, 11-20.

Sourisseau, M., 2002. Etude de la structure de taille de la communauté des copépodes par l'analyse de spectres mesurés avec un compteur optique et par la modélisation de la dynamique des populations. Thèse de doctorat, Université de Paris VI.

Sourisseau, M., Carlotti, F., 2006. Spatial distribution of zooplankton size spectra on the French continental shelf of the Bay of Biscay during spring 2000 and 2001. Journal of Geophysical Research 111, C05S09.

Sournia, A., 1973. La production primaire planctonique en Méditeranée: Essai de mise à jour. Bulletin de l'Étude en Commun de la Méditerranée, Vol 5, pp 128.

Spiridonov, V.A., Kosobokova, K.N., 1997. Winter ontogenetic migrations and the onset of gonad development in large dominant calanoid copepods in the Weddell Gyre (Antarctica). Marine Ecology Progress Series 157, 233-246.

Stergiou, K.I., Christou, E.D., Georgopoulos, D., Zenetos, A., Souvermezoglou, C., 1997. The Hellenic Seas: physics, chemistry, biology and fisheries. UCL Press, London 35, 415-538.

Sundquist, E.T., 1993. The global carbon dioxide budget. Science 259, 934-941.

Sutherland, K.R., Madin, L.P., Stocker, R., 2010. Filtration of submicrometer particles by pelagic tunicates. PNAS, 1-6.

Thibault, D., Gaudy, R., Le Fèvre, J., 1994. Zooplankton biomass, feeding and metabolism in a geostrophic frontal area (Almeria-Oran Front, western Mediterranean). Significance to pelagic food webs. Journal of Marine Systems 5, 297-311.

Thingstad, F.T., Rassoulzadegan, F., 1995. Nutrient limitations, microbial food webs, and "biological C-pumps": Suggested interactions in a P-limited Mediterranean. Marine Ecology Progress Series 117, 299-306.

Thingstad, T.F., Krom, M.D., Mantoura, R.F.C., Flaten, G.A.F., Groom, S., Herut, B., Kress, N., Law, C.S., Pasternak, A., Pitta, P., Psarra, S., Rassoulzadegan, F., Tanaka, T., Tselepides, A., Wassmann, P., Woodward, E.M.S., Riser, C., Zodiatis, G., Zohary, T., 2005. Nature of Phosphorus Limitation in the Ultraoligotrophic Eastern Mediterranean. Science 309, 1068-1071.

Thioulouse, J., Chessel, D., Dolédec, S., Olivier, J.M., 1997. ADE-4: a multivariate analysis and graphical dispay software. Statistics and Computing 7, 75-83.

Tirelli, V., Mayzaud, P., 1999. Gut evacuation rates of Antarctic copepods during austral spring. Polar Biology 21, 197-200.

Trégouboff, G., Rose, M., 1957. Manuel de planctonologie méditerranéenne. Centre National de la Recherche Scientifique, 1-587.

Tréguer, P., Le Corre, P., 1975. Manuel d'analyses des sels nutritifs dans l'eau de mer, Laboratoire d'Océanographie Chimique, Université de Bretagne Occidentale, Brest, pp 110.

Tsuda, A., Saito, H., Nishioka, J., Ono, T., 2005. Mesozooplankton responses to iron-fertilization in the western subarctic Pacific (SEEDS2001). Progress in Oceanography 64, 237-251.

Tsuda, A., Saito, H., Nishioka, J., Ono, T., Noiri, Y., Kudo, I., 2006. Mesozooplankton response to iron enrichment during the diatom bloom and bloom decline in SERIES (NE Pacific). Deep Sea Research II 53, 2281-2296.

Tsuda, A., Takeda, S., Saito, H., Nishioka, J., Kudo, I., Nojiri, Y., Suzuki, K., Uematsu, M., Wells, M., Tsumune, D., Yoshimura, T., Aono, T., Aramaki, T., Cochlan, W., Hayakawa, M., Imai, K., Isada, T., Iwamoto, Y., Johnson, W., Kameyama, S., Kato, S., Kiyosawa, H., Kondo, Y., Levasseur, M., Machida, R., Nagao, I., Nakagawa, F., Nakanishi, T., Nakatsuka, S., Narita, A., Noiri, Y., Obata, H., Ogawa, H., Oguma, K., Ono, T., Sakuragi, T., Sasakawa, M., Sato, M., Shimamoto, A., Takata, H., Trick, C., Watanabe, Y., Wong, C., Yoshie, N., 2007. Evidence for the grazing hypothesis: Grazing reduces phytoplankton responses of the HNLC ecosystem to iron enrichment in the western subarctic pacific (SEEDS II). Journal of Oceanography 63, 983-994.

Turley, C., Bianchi, M., Christaki, U., Conan, P., Harris, J.R.W., Psarra, S., Ruddy, G., Stutt, E., Tselepides, A., Van Wambeke, F., 2000. Relationship between primary producers and bacteria in an oligotrophic sea- the Mediterranean and biogeochemical implications. Marine Ecology Progress Series 193, 11-18.

Turner, J.T., 2002. Zooplankton fecal pellets, marine snow and sinking phytoplankton blooms. Aquatic Microbial Ecology 27, 57-102.

Turner, J.T., 2004. The importance of small copepods and their roles in pelagic marine food webs. Zoological Studies 43, 255-266.

Uitz, J., Claustre, H., Garcia, N., Griffiths, B.F., Ras, J., Sandroni, V., 2009. A phytoplankton class-specific primary production model applied to the Kerguelen Islands region (Southern Ocean). Deep Sea Research I 56, 541-560.

Uye, S.-I., 1982. Lenght-weight relationships of important zooplankton from the Inland Sea of Japan. Journal of the Oceanographical Society of Japan 38, 149-158.

Van Beek, P., Bourquin, M., Reyss, J.L., Souhaut, M., Charette, M., Jeandel, C., 2008. Radium isotopes to investigate the water mass pathways on the Kerguelen Plateau (Southern Ocean). Deep Sea Research II 55, 622-637.

Van Wambeke, F., Christaki, U., Giannakourou, A., Moutin, T., Souvemerzoglou, K., 2002. Longitudinal and vertical trends of bacterial limitation by phosphorus and carbon in the Mediterranean sea. Microbial Ecology 43, 119-133.

Van Wambeke, F., Catala, P., Pujo-Pay, M., Lebaron, P., 2011. Vertical and longitudinal gradients in HNA-LNA cell abundances and cytometric characteristics in the Mediterranean Sea. Biogeosciences 8, 1853-1863.

Vanderploeg, H.A., Roman, M.R., 2006. Introduction to special section on analysis of zooplankton distributions using the optical plankton counter. Journal of Geophysical Research 111, C05S09.

Vandromme, P., Stemmann, L., Berline, L., Gasparini, S., Mousseau, L., Prejge, F., Passafuime, O., Guarini, J.M., Gorsky, G., 2010. Zooplankton communities fluctuations from 1995 to 2005 in the Bay of Villefranche-sur-Mer (Northern Ligurian Sea, France). Biogeosciences Discussions 7, 9175-9217.

Vehmaa, A., Kremp, A., Tamminen, T., Hogfors, H., Spilling, K., Engström-Öst, J., 2011. Copepod reproductive success in spring-bloom communities with modified diatom and dinoflagellate dominance. ICES Journal of Marine Science: Journal du Conseil doi:10.1093/icesjms/fsr138.

Verity, P.G., 1985. Ammonia excretion rates of oceanic copepods and implications for estimates of primary production in the Sargasso Sea. Biological Oceanography 3, 249-283.

Vinogradov, M.E., 1962. Feeding of the deep-sea zooplankton. Rapport de Procès Verbal du Conseil Internional de l'Exploration de la Mer 153, 114-120.

Vives, F., 1966. Zooplancton neritico de las aguas de Castellon (Mediterraneo Occidental). Investigacion Pesquera 30, 49-166.

Vukanič, V., 1971. Kopepodi Bokokotorskog Zaliva. Studia Marina 5, 21-60.

Vukanič, V., 1975. Contributions to the study of zooplankton in the coastal waters of the South Adriatic Sea. Ecology 10, 79-106.

Wang, R., Conover, R.J., 1986. Dynamics of gut pigment in the copepod *Temora longicornis* and the determination of *in situ* grazing rates. Limnology and Oceanography 31, 867-877.

Ward, P., Atkinson, A., Murray, A.W.A., Wood, A.G.W., Williams, R., Poulet, S.A., 1995. The summer zooplankton community at South Georgia: biomass, vertical migration and grazing. Polar Biology 15, 195–208.

Ward, P., Shreeve, R.S., 1999. The spring mesozooplankton community at South Georgia: a comparison of shelf and oceanic sites. Polar Biology 22, 289-301.

Webber, M.K., Roff, J.C., 1995. Annual biomass and production of the oceanic copepod community off Discovery Bay, Jamaica. Marine Biology 123.

Weikert, H., Trinkaus, S., 1990. Vertical mesozooplankton abundance and distribution in the deep Eastern Mediterranean Sea SE of Crete. Journal of Plankton Research 12, 601-628.

Wiebe, P.H., Madin, L.P., Haury, L.R., Harbison, G.R., Philbin, L.M., 1979. Diel vertical migration by Salpa aspera and its potential for large-scale particulate organic matter transport to the deep-sea. Marine Biology 53, 249-255.

Woodd-Walker, R.S., Gallienne, C.P., Robins, D.B., 2000. A test for optical plankton counter (OPC) coincidence and a comparison of OPC derived and conventional measures of plankton abundance. Journal of Plankton Research 22, 473-483.

Würtz, M., 2010. Mediterranean pelagic habitat: Oceanographic and biological processes, an ovreview. Gland, Switzerland and Malaga, Spain: IUCN., pp.90.

Yam, E.M., Tang, K.W., 2006. Encounter of the first kind: bacterial colonization of marine snow and implications for DOM dynamics in the oceans. EOS Trans Am Geophys Union 87 suppl.

Yebra, L., Almeida, C., Hernández-León, S., 2005. Vertical distribution of zooplankton and active flux across an anticyclonic eddy in the Canary Island waters. Deep Sea Research I 52, 69-83.

Yentsch, C.S., Menzel, D.W., 1963. A method for the determination of phytoplankton chlorophyll and phaeophytin by fluorescence. Deep Sea Research I 10, 221-231.

Youssara, F., Gaudy, R., 2001. Variations of zooplankton in the frontal area of the Alboran sea (Mediterranean sea) in winter 1997. Oceanologica Acta 24, 361-376.

Yurista, P., Kelly, J.R., Miller, S., 2005. Evaluation of optically acquired zooplankton size-spectrum data as a potential tool for assessment of condition in Great Lakes. Environment management 35, 34-44.

Zeldis, J., 2001. Mesozooplankton community composition, feeding, and export production during SOIREE. Deep Sea Research II 48, 2615-2634.

Zervoudaki, S., Nielsen, T.G., Christou, E., Siokou-Frangou, I., 2006. Zooplankton distribution and diversity in a frontal area of the Aegean Sea. Marine Biology Research 2, 149-168.

Zervoudaki, S., Christou, E.D., Nielsen, T.G., Siokou-Frangou, I., Assimakopoulou, G., Giannakourou, A., Maar, M., Pagou, K., Krasakopoulou, E., Christaki, U., Moraitou-Apostolopoulou, M., 2007. The importance of small-sized copepods in a frontal area of the Aegean Sea. Journal of Plankton Research 29, 317-338.

Zhang, X., Dam, H.G., 1997. Downward export of carbon by diel migrant mesozooplankton in the central equatorial Pacific. Deep Sea Research II 44, 2191-2202.

Zhou, M., Huntley, M.E., 1997. Population dynamics theory of plankton based on biomass spectra. Marine Ecology Progress Series 159, 61-73.

Zhou, M., Tande, K., 2001. Global Ocean Ecosystem Dynamics, Optical Plankton Counter Workshop. GLOBEC Report No. 17, GLOBEC International Project Office, Plymouth, UK, pp. 67.

Zhou, M., Zhu, Y., Peterson, J.O., 2004. *In situ* growth and mortality of mesozooplankton during the austral fall and winter in Marguerite Bay and its vicinity. Deep Sea Research II 51, 2099-2118.

7 ANNEXES

Annexe 7-1. Abondances (ind m^{-3}) mésozooplanctoniques intégrées sur les 200 premiers mètres lors de la campagne KEOPS.

Taxons	Symboles	A1	A3	A5	A7	A9	A11	B1	B3	B5	B7	B9	B11	C1	C3	C5	C7	C9	C11	KERFIX
Copépodes:																				
Calanoides acutus	Cac	0.00	0.00	0.00	0.00	0.00	0.00	0.00	0.00	0.00	0.00	0.00	0.00	0.00	0.00	5.40	0.00	2.08	0.00	0.20
Calanoides acutus C		18.81	32.03	124.99	433.31	1298.27	110.43	9.29	119.32	19.09	293.98	340.06	143.65	45.25	103.49	151.25	34.29	0.00	10.80	13.42
Calanus simillimus /*C. propinquus*	Csi/Cpr	0.00	1.28	20.00	31.51	11.29	0.00	9.29	0.00	28.64	27.56	1.26	0.69	5.14	1.75	5.40	4.29	0.00	0.34	8.88
Calanus simillimus /*C. propinquus* C		244.58	256.23	480.88	551.49	1490.19	55.76	473.84	257.74	553.66	937.06	415.63	215.48	292.05	326.26	934.50	120.01	166.24	43.21	157.92
Candacia cheirura	Cma/Cch	0.00	0.00	0.00	0.00	0.00	0.00	0.00	0.00	0.00	0.00	0.00	0.00	0.00	0.00	5.40	0.54	0.00	0.00	0.00
Candacia maxima	Cma/Cch	0.00	0.00	0.00	0.00	11.29	0.00	0.00	4.77	0.60	0.00	0.00	0.00	0.00	0.00	0.00	0.00	0.00	0.00	0.00
Clausocalanus laticeps	Cla	0.00	0.00	0.00	15.76	79.03	0.00	0.00	0.00	0.00	0.00	0.00	0.00	0.00	0.00	5.40	0.00	2.08	29.71	7.90
Clausocalanus laticeps C		0.00	192.17	179.98	55.15	0.00	7.65	65.04	0.00	486.84	27.56	132.24	16.58	0.00	1.75	0.00	2.09	12.47	13.50	1.58
Clausocalanidae C		301.03	749.47	35.06	204.84	225.79	30.61	901.22	357.97	773.21	358.29	314.87	276.25	563.53	254.35	891.28	81.44	118.44	156.65	26.06
Ctenocalanus vanus		0.00	0.00	0.00	0.00	0.00	0.00	0.00	0.00	0.00	0.00	0.00	0.00	0.00	0.00	0.00	2.14	0.00	0.00	0.00
Drepanopus pectinatus	Dpe	0.00	1.28	0.00	7.88	0.00	0.00	0.00	0.00	0.00	0.00	0.00	0.00	0.00	0.00	0.00	19.29	0.00	0.00	0.00
Drepanopus pectinatus C		206.96	12.81	5.00	126.05	158.05	20.77	232.27	162.28	19.09	156.18	264.49	171.28	28.79	0.00	0.00	0.00	108.05	2.70	0.00
Heterorabdus sp.		0.00	0.00	0.00	0.00	0.00	0.00	0.00	0.00	0.00	0.00	0.00	0.00	0.00	0.00	0.34	0.00	0.00	0.34	0.00
Metridia lucens	Mlu	0.00	6.41	0.00	0.00	0.00	0.00	0.00	0.00	9.55	0.00	0.00	13.81	0.00	0.00	0.00	0.35	0.00	1.35	1.58
Metridia lucens C		235.18	121.71	209.98	55.15	124.18	44.83	55.75	95.46	124.10	73.49	144.84	176.80	4.11	7.02	5.40	10.72	78.96	132.34	13.42
Microcalanus pigmaeus		0.00	0.00	0.00	0.00	0.00	0.00	0.00	0.00	0.00	0.00	0.00	0.00	0.00	1.75	0.00	0.00	0.00	0.00	0.00
Oithona frigida	Ofr	37.63	152.48	10.00	31.51	56.45	5.47	40.82	42.96	35.64	27.56	6.30	0.00	4.11	15.79	0.00	8.57	16.62	32.36	7.50
Oithona similis	Osi	28.22	609.94	64.99	464.83	214.50	0.00	120.10	124.10	1425.51	128.62	62.97	11.05	12.34	21.05	21.61	10.72	54.03	46.23	5.00
Oithona C		1260.55	640.44	259.97	1079.35	1128.93	28.43	2477.72	1217.09	142.55	799.26	566.76	270.73	0.00	12.28	43.21	45.00	147.53	41.60	2.50
Oncaea/Triconia spp.		0.00	0.00	1.20	0.00	11.29	0.00	0.00	0.00	9.55	0.00	0.00	0.00	0.00	7.02	5.40	1.39	4.16	2.03	15.20
Paraeuchaeta spp. C	Par	0.00	1.28	0.00	0.00	5.64	0.00	0.00	0.00	4.18	0.00	6.30	0.00	4.11	0.00	1.01	0.00	0.00	2.36	3.41
Pleuromamma robusta	Pro	0.00	2.56	2.50	0.00	0.00	0.00	0.00	0.00	0.60	0.00	0.00	0.00	0.00	0.00	0.00	0.00	0.52	2.03	0.39
Pleuromamma robusta C		0.00	0.00	0.00	0.00	0.00	0.00	0.00	0.00	0.00	0.00	0.00	0.00	0.00	0.00	0.34	0.00	0.00	0.34	0.00
Rhincalanus gigas	Rgi	18.81	8.97	3.12	0.00	11.29	0.00	9.29	0.00	1.79	18.37	0.00	0.00	3.09	1.75	0.00	0.00	2.08	0.34	0.20
Rhincalanus gigas C		28.22	57.65	69.99	118.18	124.18	75.44	92.91	119.32	85.91	119.43	6.30	27.63	1.03	52.62	70.22	42.86	16.62	27.01	11.05
Nauplii		159.92	179.36	0.00	55.15	11.29	1.09	362.35	19.09	38.18	18.37	0.00	5.53	0.00	0.00	0.00	0.00	4.16	0.34	0.00
Nauplii de *Rhincalanus*		169.33	204.98	0.00	86.66	146.76	25.15	74.33	9.55	171.82	18.37	44.08	49.73	0.00	0.00	16.21	4.29	8.31	1.35	1.58
Exuvies		0.00	0.00	0.00	0.00	0.00	0.00	0.00	0.00	114.55	82.68	100.76	0.00	0.00	47.36	129.64	17.14	0.00	41.86	37.90
Autres taxons:																				
Amphipodes	AM	0.00	0.00	1.25	0.98	2.82	0.00	0.00	0.00	0.60	1.15	0.00	0.00	0.26	0.00	5.40	0.35	0.78	0.34	2.57
Larves d'amphipodes		4.70	0.00	0.00	1.97	4.23	0.00	0.00	0.00	0.00	0.00	0.00	0.00	0.00	0.00	0.00	0.00	0.00	0.00	0.00
Appendiculaires	AP	0.00	44.84	0.00	0.00	0.00	0.00	0.00	0.00	38.18	0.00	0.00	0.00	0.00	0.00	0.00	0.35	0.00	10.80	2.37
Chaetognathes	CH	9.41	25.62	0.00	4.92	0.00	1.64	7.90	4.77	57.27	2.30	12.59	5.53	0.00	8.77	10.80	1.39	0.00	5.40	3.16
Euphausiacés	EU	23.52	96.09	4.37	11.82	36.69	1.64	25.67	20.28	105.00	10.34	5.04	2.76	4.37	7.02	54.02	4.18	5.71	6.75	8.69
Larves d'euphausiacés		4.70	0.00	0.00	6.89	1.41	7.11	11.85	0.00		0.00	1.26	0.69	0.00	0.00	0.00	0.00	0.00	0.00	0.00
Limacina sp.	Lim	470.35	512.46	0.00	15.76	146.76	8.75	464.55	109.78	38.18	64.31	88.16	22.10	2.57	22.80	172.86	20.89	20.78	23.29	26.06
Oeufs poissons		0.00	0.00	0.00	0.00	0.00	0.00	0.00	0.00	0.00	0.00	0.00	0.00	3.34	0.00	0.00	9.75	54.03	0.00	0.00
Ostracodes	OS	0.00	6.41	0.62	0.00	0.00	1.09	0.00	0.00	19.09	0.00	3.15	0.00	0.51	10.52	10.80	0.35	0.00	0.34	2.37
Polychetes	PO	0.00	25.62	0.00	3.94	0.00	0.00	0.00	0.00	38.18	0.00	0.00	0.00	1.54	0.00	0.00	0.00	0.00	0.00	0.00
Larves de polychetes		0.00	0.00	0.00	0.00	0.00	0.00	92.91	38.18	0.00	0.00	0.00	5.53	2.83	0.00	0.00	0.00	6.23	0.34	0.00
Salpes		0.00	0.00	0.00	0.00	0.00	0.00	0.00	0.00	0.00	0.00	0.02	0.00	0.00	0.00	0.00	0.02	0.00	0.00	0.00
Siphonophores	SI	1.00	0.00	0.00	0.00	0.00	0.00	0.00	0.02	0.00	0.00	0.00	0.00	0.00	0.00	0.00	0.02	0.00	0.00	0.00
Spongodiscus sp.	Spo	18.81	19.22	0.00	55.15	67.74	0.00	0.00	38.18	66.82	82.68	44.08	11.05	1.03	0.00	37.81	62.68	91.43	10.80	12.63

Annexe 7-2. Article 1 : *Blastodinium* spp. Infect copepods in the ultra-oligotrophic marine waters of the Mediterranean Sea. C. Alves-de-Souza, C. Cornet, **A. Nowaczyk**, S. Gasparini, A. Skovgaard, L. Guillou. Biogeosciences, 8, 2125-2136, 2011.

Biogeosciences, 8, 2125–2136, 2011
www.biogeosciences.net/8/2125/2011/
doi:10.5194/bg-8-2125-2011

Biogeosciences

Blastodinium spp. infect copepods in the ultra-oligotrophic marine waters of the Mediterranean Sea

C. Alves-de-Souza[1,2,3], **C. Cornet**[1,2,4,5], **A. Nowaczyk**[6], **S. Gasparini**[4,5], **A. Skovgaard**[7], **and L. Guillou**[1,2]

[1]INSU-CNRS, UMR7144, Station Biologique de Roscoff, Place Georges Teissier, 29682 Roscoff, France
[2]Université Pierre et Marie Curie, UMR7144, Station Biologique de Roscoff, Place Georges Teissier, 29682 Roscoff, France
[3]Instituto de Biología Marina, Universidad Austral de Chile, Campus Isla Teja, P.O. Box 567, Valdivia, Chile
[4]Université Pierre et Marie Curie, UMR7093, Laboratoire d'Océanographie de Villefranche, Villefranche-sur-Mer, France
[5]INSU-CNRS, UMR7093, Laboratoire d'Océanographie de Villefranche, Villefranche-sur-Mer, France
[6]INSU-CNRS, UMR6535, Aix-Marseille Université, Laboratoire d'Océanographie Physique et Biogéochimique, Centre d'Océanologie de Marseille, Campus de Luminy, Case 901, 13288 Marseille, France
[7]University of Copenhagen, Department of Veterinary Disease Biology, Laboratory of Aquatic Pathobiology, Stigbøjlen 7, 1870 Frederiksberg C, Denmark

Received: 26 February 2011 – Published in Biogeosciences Discuss.: 11 March 2011
Revised: 25 July 2011 – Accepted: 26 July 2011 – Published: 9 August 2011

Abstract. *Blastodinium* are chloroplast-containing dinoflagellates which infect a wide range of copepods. They develop inside the gut of their host, where they produce successive generations of sporocytes that are eventually expelled through the anus of the copepod. Here, we report on copepod infections in the oligotrophic to ultra-oligotrophic waters of the Mediterranean Sea sampled during the BOUM cruise. Based on a DNA-stain screening of gut contents, 16 % of copepods were possibly infected in samples from the Eastern Mediterranean infected, with up to 51 % of Corycaeidae, 33 % of Calanoida, but less than 2 % of Oithonidae and Oncaeidae. Parasites were classified into distinct morphotypes, with some tentatively assigned to species *B. mangini*, *B. contortum*, and *B.* cf. *spinulosum*. Based upon the SSU rDNA gene sequence analyses of 15 individuals, the genus *Blastodinium* was found to be polyphyletic, containing at least three independent clusters. The first cluster grouped all sequences retrieved from parasites of Corycaeidae and Oncaeidae during this study, and included sequences of *Blastodinium mangini* (the "mangini" cluster). Sequences from cells infecting Calanoida belonged to two different clusters, one including *B. contortum* (the "contortum" cluster), and the other uniting all *B. spinulosum*-like morphotypes (the "spinulosum" cluster). Cluster-specific oligonucleotidic probes were designed and tested by fluorescence in situ hybridization (FISH) in order to assess the distribution of dinospores, the *Blastodinium* dispersal and infecting stage. Probe-positive cells were all small thecate dinoflagellates, with lengths ranging from 7 to 18 µm. Maximal abundances of *Blastodinium* dinospores were detected at the Deep Chlorophyll Maximum (DCM) or slightly below. This was in contrast to distributions of autotrophic pico- and nanoplankton, microplanktonic dinoflagellates, and nauplii which showed maximal concentrations above the DCM. The distinct distribution of dinospores and nauplii argues against infection during the naupliar stage. Dinospores, described as autotrophic in the literature, may escape the severe nutrient limitation of ultra-oligotrophic ecosystems by living inside copepods.

Correspondence to: L. Guillou
(laure.guillou@sb-roscoff.fr)

1 Introduction

Blastodinium species are gut parasites of a wide range of marine copepods. They have the particularity of being apparently autotrophic dinoflagellates, as they have chloroplasts thought to be functional inside the copepod gut in at least 10 of the 13 species formally described to date (Chatton, 1920; Sewell, 1951; Shields, 1994; Skovgaard and Salomonsen, 2009). Infestation is believed to occur during early stages of the copepod life by the ingestion of small (<15 µm) free-living stages called dinospores (Chatton, 1920, p. 121). This supposition is supported by the failure to produce infection

inside parasite-free adults exposed to freshly produced dinospores (Skovgaard, 2005). The parasites grow inside the lumen of the alimentary canal, where they develop a quite complex structure. The primary parasitic cell is the trophocyte, a single cell of considerable size (up to several 100 µm long), which contains two nuclei and absorbs nutrients. In most cases, this cell undergoes rapid sporogenetic cycles that in some species may occur every day (Chatton, 1920, p. 109). Eventually, the trophocyte divides into a secondary trophocyte and a gonocyte, with both cells remaining inside the outer membrane of the original trophocyte. The gonocyte undergoes sporogony by rapid sequential mitotic divisions producing hundreds of sporocytes. Sporulation starts with the rupture of the membrane, and immature spores, with two nuclei, generally exit the host via the anus. After several series of divisions, mature dinospores with a single nucleus acquire flagella and the typical appearance of peridinioid dinoflagellates (Skovgaard et al., 2007). The fate of these spores is still unknown to date, although they are able to quickly encyst after few days of observation in the laboratory (Chatton, 1920) and rapidly declined when incubated in f/2-enriched seawater (Skovgaard, 2005).

Infections by *Blastodinium* spp. are not directly lethal but have negative effects on host fitness. For instance, infected populations are reported to be smaller and potentially sterile, with females having immature gonads and undeveloped genital oviducts and males unable to accomplish their final moulting (Sewel, 1951; Chatton, 1920). However, neutering of infected adult females was not always observed (Ianora et al., 1990). *Blastodinium* reportedly acquires part of its energy from photosynthesis, the rest being ensure by the assimilation of host digestive substances (Pasternak et al., 1984). Thus, the copepod dwarfism and sterility are supposed to be linked to nutritional problems, either provoked by the direct uptake from the parasite or by a reduced capacity to ingest food by the host when *Blastodinium* trophonts occupy most of the digestive tract (Chatton, 1920, p. 221). On the other hand, the copepod host may in turn benefit from exudates release by the microalgae. However, primary production released from *Blastodinium* to the host is thought to be low, accounting for only 1 % of the host food demand (Pasternak et al., 1984). In addition, under starvation conditions, survival time of infested copepods is significantly lower than uninfected copepods indicating a negative effect of infection (Skovgaard, 2005).

The majority of *Blastodinium* species were described by Chatton (1920), mostly from copepods collected in coastal waters of Banyuls-sur-Mer (France, N.W. Mediterranean Sea). Indeed, most observation of *Blastodinium* species are from warm temperate and tropical waters (Chatton, 1920; Coats et al., 2008; Ianora et al., 1987; Pasternak et al., 1984; Sewell, 1951; Skovgaard and Saiz, 2006). Infection prevalences are generally low (1–10 %), although epizootic outbreaks up to 60 % were reported for the North Sea (Vane, 1952). To date, most studies have focussed mainly on the parasitic stage of *Blastodinium* spp., growing and sporulating inside the copepod host. However, knowledge concerning the free-living spores released into the water is fundamental to understanding the dynamics of such parasitic infections. Additionally, because dinospores are supposed to be in majority photosynthetically active, production of this biomass escapes to the natural assumption that growth and size of phytoplankton are mainly controlled by nutrient availability.

The main objectives of the BOUM oceanographic cruise (Biogeochemistry from the Oligotrophic to the Ultra-oligotrophic Mediterranean), were to simultaneously investigate biochemistry and marine food web structures. This manuscript reports copepod infections by *Blastodinium* spp. at the three long-term stations of the cruise. We first characterized individual specimens of *Blastodinium* by morphology and when possible by SSU rDNA gene sequences. These sequences revealed the existence of at least 3 clusters and allowed us to design oligonucleotidic probes specific to the different *Blastodinium* clusters. Using these probes, we quantified the presence of infective unicellular stages, the dinospores, for each cluster, in the water column between 160 m depth and the surface. We compared dinospore distribution to a range of biotic and abiotic parameters measured during the BOUM cruise.

2 Material and methods

2.1 Sampling strategy

The BOUM cruise (Biogeochemistry from the Oligotrophic to the Ultra-oligotrophic Mediterranean sea) took place in the Mediterranean Sea during June–July 2008 and covered a transect from the coastal waters off Marseille (France, West Mediterranean) to the open sea off Israel (East Mediterranean). The three main stations (A, B, and C) located in the Western, Central and Eastern basins, respectively (Fig. 1) were sampled for our study. The stations, while geographically distant, were each inside anticyclonic eddies, characterized by a marked stratification, and very low nutrient levels typical of oligotrophic to ultra-oligotrophic marine waters (Moutin et al., 2010). They were characterized by relatively low concentrations of heterotrophic organisms (bacteria, nanoflagellates, and ciliates) within the microbial food web (Christaki et al., 2011).

Copepods were sampled by a net haul from 200 m depth to surface at stations A, B and C, using a 120 µm mesh Bongo net of 60 cm of diameter aperture. The samples were subsequently concentrated to less than 50 ml by filtration through a 20 µm mesh, rapidly fixed with paraformaldehyde (1 % final concentration) and then stored for one hour at dark and 4 °C. The fixative was removed by filtration using a 20 µm mesh and samples were rinsed twice using Phosphate Buffer Saline (PBS). Samples were then stored into PBS/ethanol 1:1 at −20 °C into 50 ml flasks.

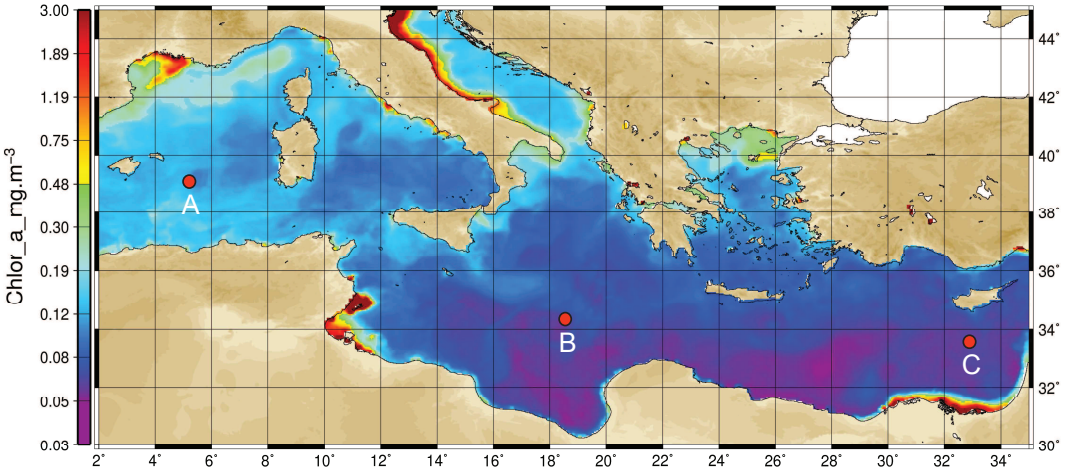

Fig. 1. Location of the stations A, B, and C sampled during the BOUM cruise, superimposed on a SeaWIFS ocean color composite indicating values of total chlorophyll-*a* (15 June–15 July 2008).

Water column samples were taken at 5–6 discrete depths between from 5 to 160 m using 12 l Niskin bottles on a rosette equipped with a conductivity-temperature-depth (CTD) and fluorescence sensors. These water samples were used for the enumeration of *Blastodinium* dinospores by fluorescent in situ hybridization method (FISH). Fifty to 200 ml were fixed with paraformaldehyde (1 % final concentration) and stored for one hour in the dark at 4 °C. Fixed seawater was filtered onto 0.22 µm Anodisc filters (Whatman) with a vacuum pump (∼200 mm Hg). The filters were dehydrated in an ethanol series (50 %, 80 %, 100 %; 3 min each), briefly dried at room temperature, and stored at −80 °C.

2.2 Detection of infections and SSU rDNA gene sequencing

Blastodinium spp. can be easily detected inside the copepod gut in fresh specimens based on the brownish-greenish color and chlorophyll autofluorescence of the photosynthetic parasite (Skovgaard, 2005). However, our fixation protocol uses ethanol to maximise sequencing success and destroys chlorophyll. Consequently, we developed a method based on DNA staining with propidium iodide (PI, 10 µg ml^{-1}) to detect infections. As dinoflagellates have typical, characteristic condensed chromatin at all stages of their life cycle, DNA staining allowed us to easily distinguish *Blastodinium* nuclei from those of the host tissues. This method detected mature and sporulating individuals but was probably less suitable to detect early stages of infections (young trophocytes).

The most abundant copepod taxa were divided into four groups, i.e. Calanoida, Corycaeidae, Oncaeidae and Oithonidae. For each group, copepods were randomly selected and single individuals placed into a 96 well culture plate (Nalgene) containing PBS/ethanol 1:1. After DNA staining, copepods were examined using an inverted microscope equipped with an epifluorescence light source (Olympus, IX71) and a fluorescent filter set for IP (excitation: 536 nm; emission: 617 nm) to determine the presence or absence of *Blastodinium*. In order to evaluate if *Blastodinium* infection affected copepod development, the prosome sizes of infected and uninfected individuals (Corycaeidae only) were compared through Mann-Whitney analyses. This test was used because data were not normally distributed and not homocedastic. From Station C, some of the infected individuals were individually transferred into 0.5 ml tubes and stored in PBS/ethanol 1:1 at −20 °C for further examination. Dissections were done under a steroscope. The very top of the copepod head was finely cut using a scalpel, and *Blastodinium* individuals were extracted from the copepod gut by gently lacerating the gut. When possible, *Blastodinium* were photographed using a standard microscope equipped with a camera (Olympus, BX51). Large sporulating *Blastodinium* generally fragmented during copepod dissection and sporocytes were directly placed into microtubes for subsequent genetic analyses. Parasites were either solitary or gregarious (i.e. more than one individual per copepod). All *Blastodinium* individuals extracted from the same copepod host were pooled inside the same tube. *Blastodinium* individuals were also found outside of their copepod host, probably due to damaging the host through manipulation. These specimens were also placed into 0.5 ml tubes for DNA extraction. Infected copepods were also stained using Gill's Hematoxylin (Polysciences, Inc., Warrington, PA 18976, USA) and then photographed.

DNA was extracted from individual parasites using a modified GITC (Guanidinium isothiocyanate, protocol (Chomczynski and Sacchi, 2006). Individuals were placed in 50 µl of the GITC extraction buffer and crushed using an adjusted micro-pilon (Kimble Chase®). Tubes were incubated at 72 °C for 20 min. Next, one volume of cold isopropanol was

Table 1. List of primers and probes used in this study.

Name	Sequence	Purpose
18S 328F	5′ ACCTGGTTGATCCTGCCAG 3′	Primer for PCR in forward
18S 528F	5′ CCGCGGTAATTCCAGCTC 3′	Primer for PCR in forward and sequencing
18S 63F	5′ ACGCTTGTCTCAAAGATTA 3′	Primer for PCR in forward
18S 329R	5′ GTGAACCTGCRGAAGGATCA 3′	Primer for PCR in reverse
18S 1818R	5′ ACGGAAACCTTGTTACGA 3′	Primer for PCR in reverse
18S 18r71	5′ GCGACGGGCGGTGTGTAC 3′	Primer for PCR in reverse
18S 690R	5′ ATCCAAGAATTTCACCTCTGAC 3′	Primer for sequencing
18S 1055F	5′ GGTGGTGCATGGCCGTTCTT 3′	Primer for sequencing
18S 1055R	5′ ACGGCCATGCACCACCACCCAT 3′	Primer for sequencing
BMANG1	5′ CACTCTCCAAGAAGATGC 3′	Specific probe for *Blastodinium*, clade "mangini"
BCON2	5′ CATACAGTCAAGCACAGC 3′	Specific probe for *Blastodinium*, clade "contortum"
BLA2	5′ TGCGCTAGACGCACAAGG 3′	Specific probe for *Blastodinium*, clade "spinulosum"

added at −20 °C overnight for DNA precipitation. The following day, samples were centrifuged (14 000 rpm, 15 min at 4 °C) and supernatants removed. The DNA pellet was cleaned using 70 % ethanol (100 µl), followed by a last centrifugation (14 000 rpm, 10 min). Supernatant was removed and the DNA pellet was hydrated into 20 µl of sterile distilled water and stored at −20 °C.

DNA extraction products were used for PCR amplification of SSU rDNA (or 18S) gene using different combinations of primers (Table 1). The PCR mix (15 µl final volume) contained 1–6 µl of the DNA extract, 330 µM of each deoxynucleoside triphosphate (dNTP), 2.5 mM of $MgCl_2$, 1.25 U of GoTaq® DNA polymerase (Promega Corporation), 0.17 µM of both primers, 1× of buffer (Promega Corporation). The PCR cycle, run in an automated thermocycler (GeneAmp® PCR System 9700, Applied Biosystem), was programmed to give an initial denaturating step at 95 °C for 5 min, 35 cycles of denaturating at 95 °C for 1 min, annealing at 55 °C for 45 s and extension at 72 °C for 1 min 15 s, and a final extension step at 72 °C for 7 min. PCR products were cloned into a TOPO TA cloning kit (Invitrogen®), following manufacturer's recommendations. Inserts inside white colonies were screened by PCR (same procedure as before). Positive PCR products were purified (ExoSAP-IT® For PCR Product Clean-Up, USB®) and sequenced using the Big Dye Terminator Cycle Sequencing Kit version 3.0 (PE Biosystems®) and an ABI PRISM model 377 (version 3.3) automated sequencer with specific primers. Sequences were edited in the BioEdit 7.0.5.3 program and complete sequences deduced from runs using both external and internal primers (Table 1).

2.3 Phylogeny

Available sequences were aligned using the online version 6 MAFFT, (http://mafft.cbrc.jp/alignment/software/index.html). The best nucleotide substitution model was determined using JModeltest 0.1.1 (Posada, 2008) and a transitional model with six free parameters and unequal base frequencies (TIM2 + G) was selected with the following parameters: Lset base = (0.2622 0.1894 0.2606 0.2878), rmat = (1.4098 3.4396 1.4098 1.0000 8.3362 1.0000), shape = 0.4100. Maximum Likelihood was conducted using PhyML 3.0 (Guindon et al., 2005) and the robustness of inferred topology was supported by bootstrap resampling (100). Bayesian inference was conducted using MrBayes 3.1.2 (Huelsenbeck and Ronquist, 2001) and started with a random tree, run for 2 000 000 generations, sampling the chains every 100th cycle, and burn-in of 5000 generations in order to ensure the use of only stable chains. Data remaining after discarding burn-in samples were used to generate a majority-rule consensus tree where the percentage of samples recovering any particular clade of the consensus tree represented the clade's posterior probability (Huelsenbeck and Ronquist, 2001). The sequences obtained during this study have been deposited in GenBank (JN257667-JN257681).

2.4 Detection of dinospores by FISH

Oligonucleotide probes were designed after visual inspections of the previously described aligned sequences. Beside specificity, main criteria for probe construction were a length of 18 mers and GC content ≥50 %. Probe specificity was tested in silico on a database containing more than 150 000 sequences of SSU rDNA, including 3400 dinoflagellate sequences. Positive controls were obtained using sporulating *Blastodinium* extracted from copepods by disrupting the external cuticle. Dinospores were placed inside PBS:ethanol 50:50 and then filtered throughout a 5 µm polycarbonate filter and dehydrated as previously described.

Oligonucleotide probes were purchased directly labelled with horseradish peroxidase (HRP) in complement to tyramide signal amplification (FISH-TSA). FISH-TSA was

performed separately for each probe. Anodisc filters with samples or positive controls were thawed and cut into pieces (ca. 1/4). For each piece of filter, the face supporting the cells was marked with a pen. Filters were covered with 18 µl of 40 % formamide hybridization buffer (40 % deionized formamide, 0.9 M NaCl, 20 mM Tris-HCl pH 7.5, 0.01 % sodium dodecylsufate (SDS), 10 % Blocking agent (Boehringer Mannheim) and 2 µl of oligonucleotide probe (50 ng µl^{-1} final concentration). Filters were incubated for 3 h at 35 °C for hybridization and subsequently washed twice at 37 °C during 20 min with 3 ml freshly made washing buffer (56 mM NaCl, 5 mM EDTA, 0.01 % SDS, 20 mM Tris-HCl pH 7.5). Filters were then equilibrated in 3 ml TNT buffer (100 mM Tris-HCl pH 7.5, 150 mM NaCl, 0.05 % Tween 20) for 15 min at room temperature in the dark. Each piece of filter was transferred onto a slide for TSA reaction (Kit NEN Life Science Products); 20 µl of freshly made TSA mix (1:1 dextran sulfate and amplification diluent, 1:50 fluorescein tyramide and the mixture of dextran sulfate) were put on the top of each filter piece and slides were incubated for 30 min in the dark. In order to stop the enzymatic reaction and wash the filters, they were transferred in two successive 5 ml 55 °C pre-warmed TNT buffer baths for 20 min each. Filters were then rinsed in water, dried at 55 °C and counterstained with calcofluor (100 ng ml^{-1}) for visualization of dinoflagellate theca. Slides were covered with a cover glass, together with a mix of the antifading reagent Citifluor AF1 and PI for visualization of nucleus (10 µg ml^{-1}), sealed with nail varnish and stored at 4 °C in the dark. All hybridized and stained filters were observed with an Olympus BX-51 epifluorescence microscope (Olympus Optical) equipped with a mercury light source, a 11012v2-Wide Blue filters set (Chroma Technology, VT, USA) and a CCD camera (Spot-RT, Diagnostic Instrument, Sterling Heights, MI, USA). Cells were observed with fluorescence filters sets for calcoluor (excitation: 345 nm; emission: 455 nm), PI (excitation: 536 nm; emission: 617 nm) and fluorescein tyramide (excitation: 495 nm; emission: 520 nm). For each probe, *Blastonidium* dinospores, and small thecate dinoflagelates (STD) were counted on the entire surface representing about 1/4 of the original filter at 40× magnification. After the counting, the pieces of filter were photographed and the precise area was calculated using ImageJ software in order to estimate cell abundances.

2.5 Statistical analysis

The possible relationship between *Blastodinium* dinospore abundances and other abiotic and biotic variables, i.e. nauplii abundances (Nowaczyk et al., 2011), microplanktonic dinoflagellates (Z. Gomez et al., personal communication, 2010), tintinnids (J. Dolan, personal communication, 2010), autotrophic pico- and nanoeukaryotes (C. Courties and L. Bariat, personal communication, 2010), and total eukaryotes (Siano et al., 2011) were examined using Spearman correlation analysis. All the statistical analyses were performed using Statistica 6.0 (StatSoft). Prior to the analyses, all abundance data were log-transformed [ln $(x+1)$].

3 Results

3.1 Copepod infections by *Blastodinium* spp.

At Station C, low infection frequencies (<2 %) were estimated for Oithonidae ($n = 60$) and Oncaeidae ($n = 96$). In contrast, up to 51 % of Corycaeidae ($n = 96$) and 33 % of Calanoida (*Clausocalanus* and *Paracalanus*, $n = 84$) appeared infected based on results of the DNA-stain screening test. These groups represented 86.8 % of the total copepod communities (Nowaczyk et al., 2011). Overall, 16 % of copepods were possibly infected at this station.

Infections of Corycaeidae indicated by the DNA-screening method were further confirmed by dissections in 30 of 35 randomly selected individuals. Among Calanoida, the genus *Clausocalanus* was one of the most abundant groups with at least four species; *C. furcatus*, *C. paululus*, *C. parapergens*, and *C. jobei*. Among them, *C. furcatus* and *C. parapergens* were observed to be infected (list not exhaustive). The Corycaeidae was dominated by a single species, *Farranula rostrata*, although *Corycaeus* sp. and *Onchocorycaeus* sp. were also observed. Males and females of Corycaeidae, distinguishable by the shape of their genital segment, were equally infected. The mean prosome length of females suspected to be infected was 536.1 µm ± 29.5 µm ($n = 33$) compared to 551 ± 61.7 µm ($n = 26$) when uninfected. In males, the mean prosome length of individuals suspected to be infected was 459 µm ± 52.2 µm ($n = 22$) and 517.9 µm ± 47.6 µm ($n = 24$) when uninfected. However, Mann-Whitney analyses indicated that for both sexes the differences between infected and uninfected individuals were not significant ($P = 0.086$). Infections of Corycaeidae were lower at stations A and B, with only 8 and 18 % ($n = 96$) positively screened by the DNA-staining method, respectively (data not available for other groups).

A total of 51 *Blastodinium* individuals were isolated from station C which were either obtained from copepod dissections or found directly in the samples outside their hosts. They differed in location inside the gut of the host as well as their general shape (Fig. 2). *Blastodinium* infecting Corycaeidea were elongated (Fig. 2a) or globular (Fig. 2b and c) and were located anterior-dorsal (Fig. 2b), to dorso-ventral (Fig. 2c). Within Calanoidea, parasites were globular (Fig. 2d), spirally-twisted (Fig. 2e and g), or spindle-shaped (Fig. 2f). When observed inside their host, spirally-twisted individuals were always solitary (see Fig. 2h). Figure 3 represents spindle-shaped *Blastodinium* morphotypes, rounded at the anterior pole and more or less pointed at the posterior pole. Exceptions were individuals that had cylindrical to horizontal extremities on both sides (Fig. 3h and i). In

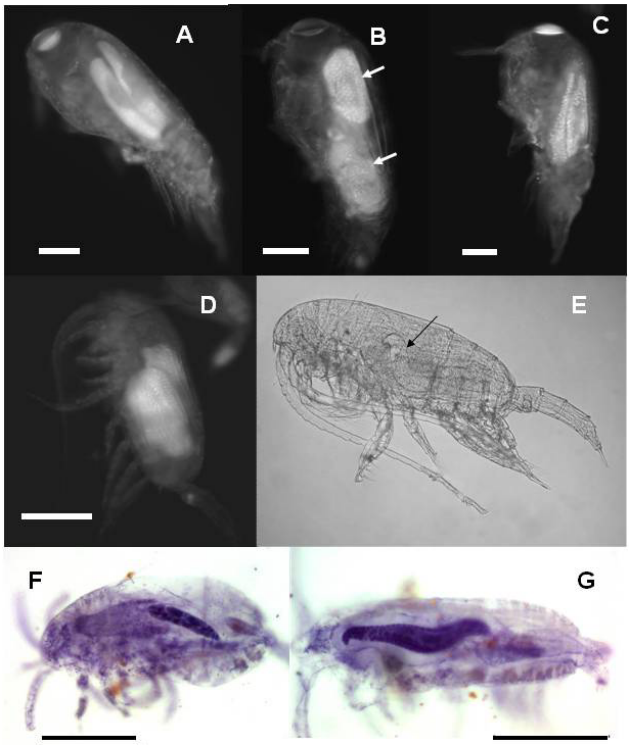

Fig. 2. Observations of *Blastodinium* spp. located inside the gut of their hosts. **(A)** Three individuals of *Blastodinium mangini* infecting *Farranula* cf. *rostrata* (BOUM19). **(B)** At least two individuals (arrows) of an unknown *Blastodinium* with a globular shape infecting *Farranula* cf. *rostrata* (BOUMD9). **(C)** Unknown *Blastodinium* infecting *Farranula* cf. *rostrata* (BOUM18). **(D)** Two individuals of an unknown *Blastodinium* with a globular shape infecting *Clausocalanus furcatus* (BOUM17). **(E)** *Blastodinium contortum* infecting *Clausocalanus furcatus* (BOUMB). **(F)** *Blastodinium* cf. *spinulosum* infecting a probable *Clausocalanus* sp. **(G)** Hypertwisted *Blastodinium contortum* infecting a probable *Haloptilus* sp. Individuals from **(A)** to **(D)** were observed after DNA-staining by Propidium Iodide. Individuals from **(F)** and **(G)** were stained using Gill's Hematoxylin. Scale bars = 100 µm.

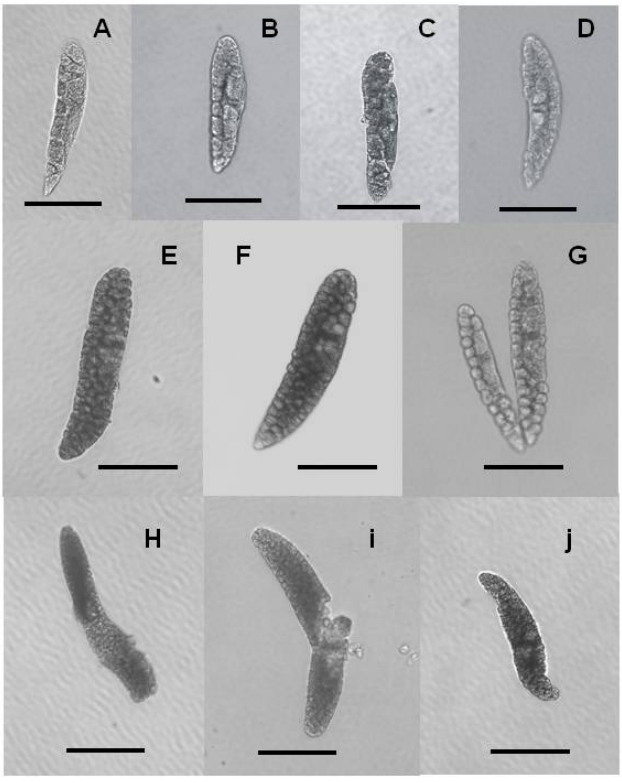

Fig. 3. Different morphotypes of *Blastodinium* spp. with a spindle shape. **(A)**: BOUM5, **(B)**: BOUM27, **(C)**: BOUM21, **(D)**: BOUM29, **(E)**: BOUM3, **(F)**: BOUM35, **(G)**: BOUMPARE4 (see also Fig. S1), **(H)**: BOUM19 (see also Fig. 2), **(I)**: BOUM26, **(J)**: BOUM4. Scale bars = 100 µm.

most cases, a more or less marked straight or concave face (called the ventral side) and a rounded or convex face (the dorsal side) were easily observable (as examples Fig. 3a, b and d). All *Blastodinium* individuals observed were sporulating, and thus were surrounded by one or several layers of sporocytes. In some cases, the trophocyte apical to median was still visible and in direct contact with the external cuticle (Fig. 3a and b for examples), a region that was called the hilum by Chatton (1920, the hile in French). When visible, these trophocytes were dorsal (Fig. 3a, b, c, e and g) except in one individual which showed a ventral trophocyte (Fig. 3d). More or less pronounced twisted morphotypes are showed in the Fig. 4a–c, formed by one and half (Fig. 4b–c) to two (Fig. 4a) turns of a spiral. The trophocyte was more or less central, surrounded by several generations of sporocytes. A presence of the hilum was clearly noticed for Fig. 4b. The largest individual was BOUM7 (470 µm in length, Fig. 4d). This diblastic individual was characterised by the extreme position of its trophocyte that emerged at the anterior pole.

3.2 Phylogeny

A total of 15 *Blastodinium* individuals were successfully amplified by PCR and sequenced. Among them, five were extracted from Corycaeidae, two from Calanoida, one from *Oncaea* sp., and six from individuals found outside their hosts. Four of them (BOUM21, BOUM27, BOUMPARE4, and BOUMF5) could not be amplified using the most external primers (primer 528F was used in forward, Table 1) and consequently these sequences were shorter than others (1157 to 1173 bp) and not included in Fig. 5.

The fifteen sequences belong to the Dinoflagellata. Both Bayesian and Maximum Likelihood (ML) inferences separated *Blastodinium* sequences into three main clusters (Fig. 5). All sequences obtained from Corycaeida and Oncaeidae, grouped into a first cluster well supported by Bayesian posterior probabilities and ML bootstrap values. This cluster also grouped with published sequences of *B.*

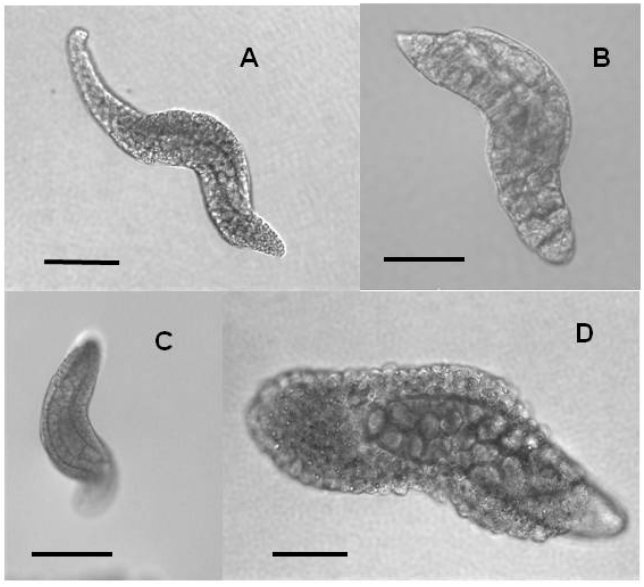

Fig. 4. Different morphotypes of *Blastodinium* spp. showing a more or less pronounced spirally twisted shape. **(A)**: BOUM8, **(B)**: BOUM37, **(C)**: BOUM50, **(D)**: BOUM7. Scale bars = 50 µm.

navicula and of *B. galatheanum* (Skovgaard et al., 2007; Skovgaard and Salomonsen, 2009). Within this group, sequences BOUM4, 19 and 26 had more than 99 % nucleotide sequence identities. All other sequences (BOUME4, BOUMD9, BOUMF5, and BOUMB12) were not particularly affiliated to other sequences within this cluster. A second cluster was formed by all available sequences of *B. spinulosum*, *B. inornatum*, and *B. crassum* from one part, and sequences BOUMPARE4, 3, 21, 27, 29 and 35 in other part. This cluster was only supported by Bayesian posterior probabilities. BOUMPARE4 (not in Fig. 5) was closely related to BOUM35, with a 99.8 % sequence identity. Finally, a last cluster grouped all sequences of *B. contortum* available to date and individual BOUM50 from this work, with high statistical supports. Sequence BOUM7 was completely separated from the rest of *Blastodinium* sequences, and grouped with other dinoflagellate sequences with a long branch.

3.3 Detection of dinospores

A general probe specific for the entire *Blastodinium* genus and targeting all available sequences could not be designed, in agreement with the apparent polyphyletic nature of the genus. Consequently, three different probes were designed for the main clusters described above (probes BMANG1, BLA2, and BCON2, Fig. 5). Probes BMANG1 and BCON2 perfectly matched all known sequences of their groups. Considering only sequences long enough to cover the portion of the probe, 8 out of the 12 sequences belonging to the second cluster perfectly matched the probe BLA2. Indeed, this probe had 1 to 2 mismatches with sequences BOUM3, 21, 27 and the environmental sequence AY664982. However, this probe was the best motif detected for this cluster.

In addition to an intensive in silico screening (see the methods), the specificity of these probes was tested by fluorescent in situ hybridization (FISH) on *Blastodinium* individuals directly extracted from copepods. Based upon previous results, several parasites extracted from Corycaeida were pooled onto the same filter (considered to be the targeted cells for probe BMANG1). *Blastodinium* extracted from Calanoida were separated into two categories, more or less straight individuals in one part (considered as positive cells for BLA2) and more or less spirally twisted in other (considered as positive cells for BCON2). Sporocytes of these parasites were isolated from the external cuticle and prepared for FISH analyses (see material and methods section). The three specific probes were individually tested. Positive signals were only detected between cluster-specific probes and their corresponding *Blastodinium* morphotypes. These three probes were then tested on microphytoplankton collected at stations A, B, and C, containing various species belonging to Dinophysiales, Gonyaulacales, Prorocentrales, and Peridiniales (similar filters as were processed by Siano et al., 2010). No positive signal was detected.

From water column samples, all probe-positive cells were small thecate dinoflagellates (STD) with a single more or less diffuse condensed nucleus, evidenced by the calcofluor and the IP stains (Fig. 5b–d). Most of these cells had a relatively large transversal cingulum. Thecae were relatively thick for cells targeted by probes BCON2 and BMANG1. This was not the case for majority of BLA2-targeted cells, which exhibited thinner thecae (Fig. 5c). The smallest cells were detected using the probe BMANG1 (7–10 µm in length and 5–10 µm in width), whereas larger cells were observed using the probe BCON2 (11–18 µm in length and 9.5–13 µm in width). Beside these general characteristics, a given probe was associated with several distinct morphotypes, especially within the BMANG1 cluster (Fig. 5b).

BLA2 targeted cells were the most abundant, peaking at 2.2 cells ml^{-1} at 100 m depth in station A. BMANG1 probe-positive cells were lower in abundance, with a maximal density of 0.83 cells ml^{-1} observed at station A at 110 m. Finally, maximal abundance of BCON2 targeted cells was observed at station B and for 160 m, with 0.84 cells ml^{-1}. BMANG1 targeted cells were not observed in surface, whereas cells targeted by probes BCON2 and BLA2 were detected at 12.5 m at stations B and C. The sum total of cells targeted by the 3 probes followed the vertical distribution of total STD, which ranged from 3.3 cells ml^{-1} at station C to 7.3 cells ml^{-1} at station B. Maximum densities of STD were detected 10 to 20 m below the deep chlorophyll maximum at stations A and C and at the DCM at station B (Fig. 6). FISH-positive cells represented a substantial proportion of STD communities at their maximal abundances (56 % at station A and 26 % at stations B and C).

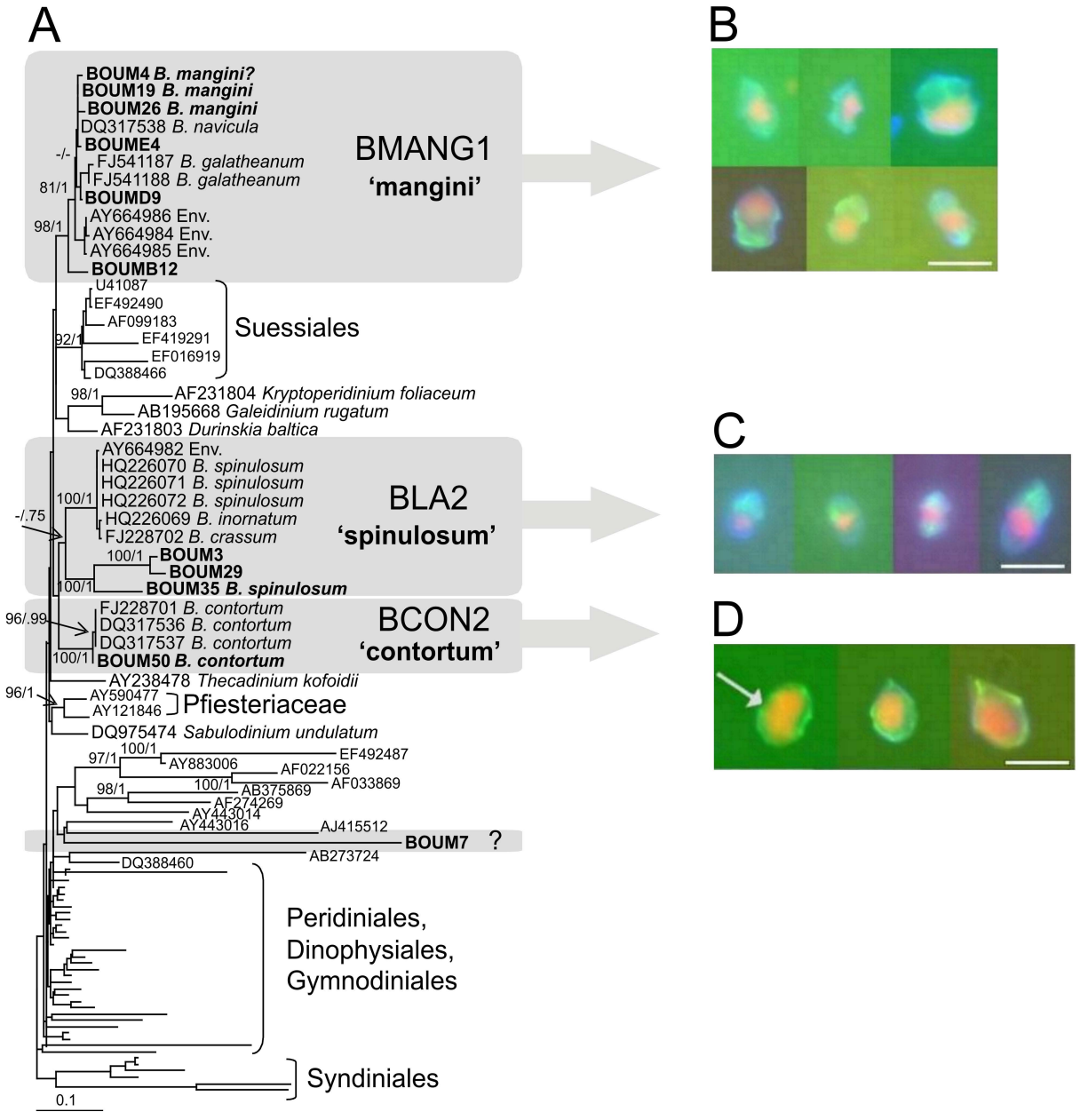

Fig. 5. Phylogeny of *Blastodinium* spp. and detection of dinospores by fluorescent in situ hybridization. **(A)** Maximum likelihood analyses of SSU rDNA gene sequences of *Blastodinium* spp. Sequences obtained in this study are in bold. Complete list of sequences available in Supplement (Table S1). Maximum likelihood bootstrap values (higher than 70 %) and posterior probabilities of Bayesian inferences (higher than 0.7) are reported at the nodes of the principal clusters, respectively. Scale bar corresponds to 0.1 % divergence. **(B)** *Blastodinium* dinospores observed in BOUM samples using the probe BMANG1, specific for the "mangini" cluster. **(C)** *Blastodinium* dinospores observed in BOUM samples using the probe BLA2, specific for the "spinulosum" cluster. **(D)** *Blastodinium* dinospores observed in BOUM samples using the probe BCON2, specific for the "contortum" cluster. Scale bars = 10 µm.

Blastodinium dinospores were negatively correlated with copepod nauplii (−0.54; $P < 0.001$), which were observed mainly above the DCM at station A, B, and C, with similar concentrations during night and day. Similarly, negative correlations were detected between dinospores and other phytoplankton communities mainly occurring above the DCM, such as autotrophic pico- (−0.55) and nanoplankton (−0.58) and total eukaryotes (−0.60; $P < 0.001$). No correlation was detected between *Blastodinium* dinospores, microplanktonic dinoflagellates, and tintinnids.

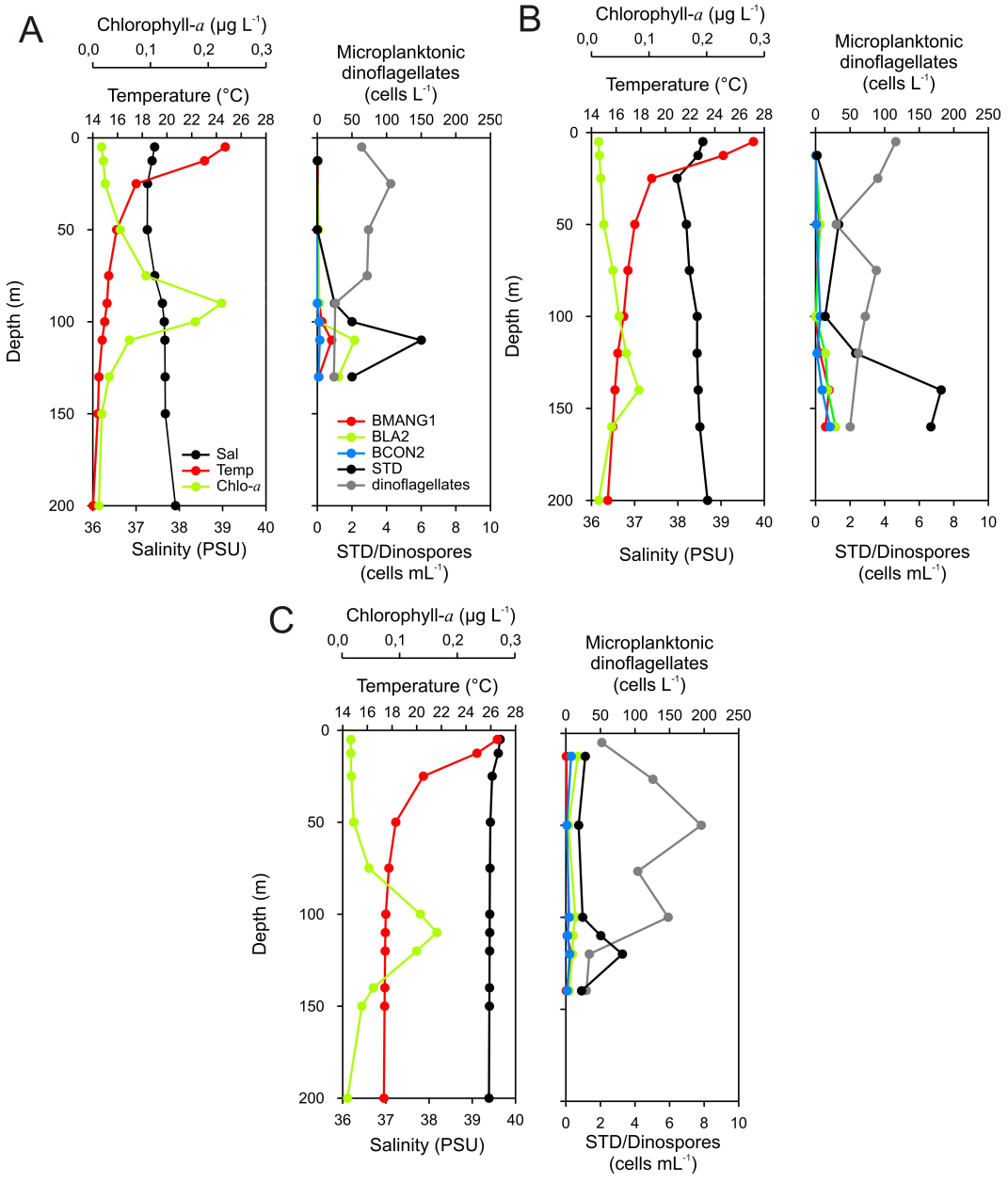

Fig. 6. Vertical distribution of abiotic and biotic parameters at sampling stations A, B, and C. Panels at left: total chlorophyll-*a* ($\mu g\, l^{-1}$), Temperature (°C), and Salinity (PSU). Panels at right: total abundances of microplanktonic dinoflagellates (cells l^{-1}), Small thecate dinoflagellates (STD, cells ml^{-1}), and *Blastodinium* dinospores detected by fluorescent in situ hybridization using corresponding probes (BMANG1, BLA2, and BCON2, cells ml^{-1}).

4 Discussion

4.1 Identification of parasites

Species within the genus *Blastodinium* are distinguished based on the cell shape and size, the location of the trophocyte in sporulating individuals, and the presence or absence of a helicoidal crest of small spinules at the surface of the trophocyte, although this last criterion is often difficult to observe using classical microscopy (Coats et al., 2008; Sewell, 1951). We found that some parasites were characteristic enough to be tentatively assigned to known species. This was the case for individuals BOUM19 and BOUM26, typical of *B. mangini* with a spindle-shape with almost rounding posterior ends, cylindrical to truncate, and lengths ranging from 200 to 350 µm (Chatton, 1920, p. 163). Chatton (1920) described this species as found exclusively in *Farranula rostrata* in Banyuls-sur-Mer (Chatton, 1920, p. 161), as was also the case at Station C. *Blastodinium mangini* is gregarious,

mostly observed in groups of three individuals, as it was also the case for individual BOUM19. In Banyuls-sur-Mer, this species was frequently observed in September–October, infesting up to 10 % of the host populations (Chatton, 1920). A closely related morphotype infecting *Oncaea media* was also described as the variety *B. mangini* var. *oncae* (Chatton, 1920). However, Sewell (1951) remarked that *B. mangini* and *B. mangini* var. *oncae* could not be distinguished based upon morphological criteria. Indeed, Sewell (1951) illustrated a large degree of morphological variability and some of them could be well in the range of the observed globular individuals (Fig. 2b and S1). SSU rDNA failed to properly separate taxa within this cluster, as suggested by the interconnection of other species such as *B. navicula* and *B. galatheanum* in Fig. 5, and more sequences from more variable genetic regions are required to settle this point.

All S-shaped spirally twisted individuals (Fig. 4a to c) were in the range of morphological variation described for *B. contortum*. This identification was also confirmed by the close relationship between sequence BOUM50 and all sequences of *B. contortum* available in the public databases. Indeed, individuals BOUM50 and BOUM37 were typical, solitary inside their host, the cell twisted into a helix in one and a half turns. The sizes were also in the range of this species (150–350 µm for diblastic stages, Chatton, 1920). Individual BOUM8 (Fig. 2g) was closest to the larger morphotype "hypertwisted" (300–400 µm with at least two turns of the helix) described by Chatton. *Paracalanus parvus* is the host type for *B. contortum*. However, this species is known from a wide range of calanoid hosts, including *C. furcatus* and *C. arcuicornis* (Chatton, 1920; Sewell, 1951).

The parasite BOUMPARE4 was also tentatively assigned to *B.* cf. *spinulosum* for several reasons. First, this species is gregarious (11 individuals were retrieved from the same copepod host) and its general shape and size was typical for this species: a spindle shape, two well differentiated poles, with a marked pointed posterior end, and the trophocyte generally submedian and posterior, size of 150–280 µm (Chatton, 1920). *Clausocalanus furcatus*, the most common host for this species, was well represented in BOUM samples. However, the relative distance between all sequences retrieved from the BOUM cruise and sequences of *B. crassum*, *B. inornatum*, and *B. spinulosum* prevented placing this parasite within *B. spinulosum*. Again, more variable regions are required to unveil affiliations within the group.

Other parasites had very unusual features. In particular, individuals BOUM21 and 27 have relatively rounded posterior pole and BOUM29 have a very unusual position for the trophont forming a hilum in ventral position (Fig. 3). BOUM7 is similar in shape and size to *Blastodinium* sp. γ described by Chatton (1920, p. 205). However, because the host was unknown and because of the long branch of this sequence in phylogenetic analyses, identification of this individual was not possible nor its eventual classification inside the *Blastodinium* genus.

Chatton (1920) proposed an arrangement of the *Blastodinium* genus into three main groups established based upon morphological characters. These groups correspond well to the different clusters defined in this study based upon the SSU RDNA gene analyses. Indeed, these clusters have been called "*mangini*", "*contortum*" and "*spinulosum*" in Fig. 5 in homology with Chatton's description. However, the genus *Blastodinium* is confirmed to be polyphyletic based upon the SSU rDNA gene (Skovgaard et al., 2007). More genetic markers (such as LSU rDNA genes (28S) or mitochondrial genes) are required to independently confirm this position.

4.2 Dinospore distributions

Blastodinium dinospores detected by FISH were thecate peridinioid dinoflagellates, in agreement with previous descriptions (Skovgaard et al., 2007; Skovgaard and Salomonsen, 2009). Although the three different probes were associated to relatively resembling individuals (by their mean size for example), several different morphotypes were in fact observed inside each cluster. This is congruent with the huge genetic diversity recorded, leading to the conclusion that each cluster cannot be simply reduced to a single morphotype. Indeed, this work likely underestimates the genetic diversity of *Blastodinium* since several morphotypes (BOUM17 and hyper-twisted *B. contortum*) could not be amplified by PCR, and probe BLA2 did not cover all of the sequences retrieved from this study. Thus, dinospore abundances in this study were likely underestimated. Observations of STD ($<$15 µm) are rare for oligotrophic waters, even in the relatively well-studied Mediterranean Sea (Siokou-Frangou et al., 2010), probably because they are generally grouped with the nanoplanktonic flagellates. We detected maximal abundances of STD below the deep chlorophyll maximum (DCM) at station A and C, an intriguing distribution in contrast with that of larger photosynthetic dinoflagellates which peak in the surface layer. Below the DCM, availability of photosynthetically active radiation is probably a limiting factor. Because chlorophyll was lost during the FISH procedure, we can but speculate on the trophic mode of *Blastodinium* dinospores. Most of *Blastodinium* species described are presumed to be at least partially autotrophic and produced spores that have chloroplasts (Chatton, 1920; Skovgaard et al., 2007). Photosynthetic thecate dinoflagellates resembling *Blastodinium* dinospores were recently reported from a large transect covering the Chile upwelling to the hyper-oligotrophic waters of the South-East Pacific Ocean gyre based upon DAPI counts (Masquelier and Vaulot, 2008).

On the other hand, densities of *Blastodinium* dinospores may simply reflect the vertical distribution of their hosts rather than an ecological preference of the dinospore stage. If this is true, most of *Blastodinium* dinospores were produced at the DCM or just below at the three stations explored. This is in agreement with the maximal copepod abundance, which is generally observed close to the DCM (Herman,

1983; Paffenhöfer and Mazzocchi, 2003; Peralba and Mazzocchi, 2004; Nowaczyk et al., 2011). Considered more in detail, it is known that *Farranula* and *Oncaea*, the two main copepod genera detected in our samples among Cyclopoida, rarely occur in the upper 30 m depth (Siokou-Frangou et al., 1997; Paffenhöfer and Mazzocchi, 2003). This distribution could then explain the absence of BMANG1-targeted cells in surface waters at the three stations. Similarly, *C. paululus*, *C. pergens*, *C. arcuicornis*, *C. parapergens*, and *C. jobei* avoid the surface (upper 25–50 m) when temperatures exceed 20 °C. However, *C. furcatus* is almost exclusively restricted to the upper part of the thermocline during the same period (Paffenhöfer and Mazzocchi, 2003; Peralba and Mazzocchi, 2004). These observations may help explain the presence of *Blastodinium* dinospores in surface waters belonging to the "*contortum*" and "*spinulosum*" clusters, both known to infect *C. furcatus*.

4.3 Ecological relevance in marine oligotrophic waters

Infections on crustaceans by unicellular parasites is well known as a powerful factor controlling host mortality and fecundity in freshwater systems, where prevalences could reach values higher than 80 % in highly productive systems with dense populations of planktonic crustaceans (Green, 1974; Duncan et al., 2006). However, this is not the case for marine pelagic systems where parasite-host interactions are poorly investigated. Based on these antecedents, the prevalences recorded in this study are impressive, especially considering the situation of low biological production and low densities of host populations. Frequencies of infection reported in our study, based on our DNA-stain screening method, are likely over-estimates as only 85 % of probable infections suspicions in Corycaeida at station C were subsequently confirmed by dissections. However, even considering a false-positive error rate of 15 %, the infection rates within Corycaeida and Calanoida groups are among the highest values reported from the literature. However, it should be noted that these frequencies represent grouped infections by very different *Blastodinium* species found coexisting at station C (some inside the same copepod species). This is in agreement with Sewell (1951) who reported the presence of up to 9 different *Blastodinium* species from a single sample collected in the Arabian Sea infecting a wide range of copepods.

Blastodinium occurrences are reported to have a marked seasonality, with highest prevalences observed during warmer period of the year in the Mediterranean Sea (Chatton, 1920; Skovgaard and Saiz, 2006). Concomitantly, Chatton (1920) also reported slower sporulations at low temperature. Thus, the summer conditions during the BOUM cruise were probably likely favourable for *Blastodinium* spp. Such parasitic association may be favoured by the severe depletion of nutrients, generally linked to summer time in more coastal waters. Although more data are required to explore this hypothesis, we can conclude that ultra-oligotrophy of waters is not a limiting factor for these parasites. This was also the case for another parasite, the Amoebophryidae (Syndiniales), which were found infecting several microplanktonic dinoflagellate species at high prevalences at same stations (Siano et al., 2011). The maximal density of Syndiniales dinospores were estimated to be around 50 cells ml^{-1} in oligotrophic waters, 10 times more concentrated than *Blastodinium* dinospores. Converted to biomass, both parasites substantially contribute to the organic carbon, which would be directly consumable by herbivores and/or secondary predators. Indeed, the fate of these free-living parasitic stages is an intriguing question in both cases.

Blastodinium infections are supposed to be initiated during the early stages of copepod development (Chatton, 1920). However, there is a drastic partitioning between nauplii and dinospores (with a significant negative correlation). In other part, nauplii are known to largely consume prey items smaller than the *Blastodinium* dinospores. In contrast, copepodites do feed on prey of dinospore-size, 10–20 µm (Wilson, 1973). Based on these considerations, it appears likely that copepodites are the first stage infected by *Blastodinium* spp.

5 Conclusions

Substantial copepod infections by *Blastodinium* spp. occur in the oligotrophic to ultra-oligotrophic waters of the Mediterranean Sea. *Blastodinium* spp. are polyphyletic and infect a wide range of copepod taxa. The free-living stages (or dinospores) of the parasite *Blastodinium* spp. occur in the water column and can be detected by FISH technique. They formed relatively dense communities located at the DCM or slightly below, a vertical distribution similar to that of their copepod hosts. Interestingly, deep intense blooms of diatoms were also detected during the BOUM transect, especially at station C (Crombet et al., 2011). Such phenomenon may be favoured by hydrophysical meso- and microscale mechanisms. The trophic mode of the dinospores and their ability to persist outside a copepod host at relatively high density are among the many questions which remain concerning these organisms.

Supplementary material related to this article is available online at: http://www.biogeosciences.net/8/2125/2011/ bg-8-2125-2011-supplement.pdf.

Acknowledgements. Authors wish to thank Thierry Moutin, chief of the operation during BOUM cruise and E. M. Bendif for collecting samples on board. We would like to thank F. Gomez for phytoplanktonic counts made on BOUM samples, Claude Courties and Laëtitia Bariat for their analyses of nanoplantkon by flow cytometry, and E. Bigeard for technical help with sequences. We

would like to warmly thank D. Wayne Coats that kindly made micrographs in Fig. 2f–g, Sergey Karpov for its dexterity to extract *Blastodinium* from infected copepods, and John Dolan for data on ciliates and to critically read this manuscript. C. A. S. was financed by a Conicyt doctoral fellowship (Chilean government). This work was financially supported by the French ANR AQUAPARADOX.

Edited by: T. Moutin

References

Chatton, E.: Les péridiniens parasites. Morphologie, reproduction, éthologie, Arch. Zool. Exp. Gen., 59, 1–475, 1920.

Chomczynski, P. and Sacchi, N.: The single-step method of RNA isolation by acid guanidinium thiocyanate-phenol-chloroform extraction: twenty-something years on, Nat. Protoc., 1, 581–585, 2006.

Christaki, U., Van Wambeke, F., Lefevre, D., Lagaria, A., Prieur, L., Pujo-Pay, M., Grattepanche, J.-D., Colombet, J., Psarra, S., Dolan, J. R., Sime-Ngando, T., Conan, P., Weinbauer, M. G., and Moutin, T.: Microbial food webs and metabolic state across oligotrophic waters of the Mediterranean Sea during summer, Biogeosciences, 8, 1839–1852, doi:10.5194/bg-8-1839-2011, 2011.

Coats, D. W., Bachvaroff, T., Handy, S. M., Kim, S., Gárate-Lizárraga, I., and Delwiche, C. F.: Prevalence and phylogeny of parasitic dinoflagellates (genus *Blastodinium*) infecting copepods in the Gulf of California, CICIMAR Oceánides, 23, 67–77, 2008.

Crombet, Y., Leblanc, K., Quéguiner, B., Moutin, T., Rimmelin, P., Ras, J., Claustre, H., Leblond, N., Oriol, L., and Pujo-Pay, M.: Deep silicon maxima in the stratified oligotrophic Mediterranean Sea, Biogeosciences, 8, 459–475, doi:10.5194/bg-8-459-2011, 2011.

Duncan, A. B., Mitchell, S. E., and Little, T. J.: Parasite-mediated selection and the role of sex and diapauses in *Daphnia*, J. Evolution. Biol., 19, 1183–1189, 2006.

Green, J.: Parasites and epibionts of *Cladocera*, Trans. Zool. Soc. Lond., 32, 417–515, 1974.

Guindon, S., Lethiec, F., Duroux, P., and Gascuel, O.: PHYML Online – a web server for fast maximum likelihood-based phylogenetic inference, Nucleic Acids Res., 33, W557–W559, 2005.

Herman, A. W.: Vertical distribution patterns of copepods, chlorophyll, and production in northeastern Baffin Bay, Limnol. Oceanogr., 28, 709–719, 1983.

Huelsenbeck, J. P. and Ronquist, F.: MrBayes: Bayesian inference of phylogenetic trees, Bioinformatics, 17, 754–755, 2001.

Ianora, A., Mazzocchi, M. G., and Scotto di Carlo, B.: Impact of parasitism and intersexuality on Mediterranean populations *Paracalanus parvus* (Copepoda:Calanoida), Dis. Aquat. Organ., 3, 29–36, 1987.

Ianora, A., Scotto di Carlo, B., Mazzocchi, M. G., and Mascellaro, P.: Histomorphological changes in the reproductive condition of parasitized marine planktonic copepods, J. Plankton Res., 12, 249–258, 1990.

Masquelier, S. and Vaulot, D.: Distribution of micro-organisms along a transect in the South-East Pacific Ocean (BIOSOPE cruise) using epifluorescence microscopy, Biogeosciences, 5, 311–321, doi:10.5194/bg-5-311-2008, 2008.

Moutin, T., Van Wambeke, F., and Prieur, L.: Introduction to the Biogeochemistry from the Oligotrophic to the Ultraoligotrophic Mediterranean (BOUM) experiment, Biogeosciences, in preparation, 2010.

Nowaczyk, A., Carlotti, F., Thibault-Botha, D., and Pagano, M.: Metazooplankton diversity, community structure and spatial distribution across the Mediterranean Sea in summer: evidence of ecoregions, Biogeosciences Discuss., 8, 3081–3119, doi:10.5194/bgd-8-3081-2011, 2011.

Paffenhöfer, G.-A. and Mazzocchi, M. G.: Vertical distribution of subtropical epiplanktonic copepods, J. Plankton Res., 25, 1139–1156, 2003.

Pasternak, A. F., Arashkevich, Y. G., and Sorokin, Y. S.: The role of the parasitic algal genus *Blastodinium* in the ecology of planktic copepods, Oceanology, 24, 748–751, 1984.

Peralba, A. and Mazzocchi, M. G.: Vertical and seasonal distribution of eight *Clausocalanus* species (Copepoda: Calanoida) in oligotrophic waters, ICES J. Mar. Sci., 61, 645–653, 2004.

Posada, D.: jModelTest: Phylogenetic model averaging, Mol. Biol. Evol., 25, 1253–1256, 2008.

Sewell, R. B. S.: The epibionts and parasites of the planktonic Copepoda of the Arabian Sea. John Murray expedition 1933–34, Sci. Rep. Br. Mus. Nat. Hist., 9, 255–394, 1951.

Shields, J. D.: The parasitic dinoflagellates of marine crustaceans, Annual Review of Fish Diseases, 4, 241–271, 1994.

Siano, R., Alves-de-Souza, C., Foulon, E., Bendif, El M., Simon, N., Guillou, L., and Not, F.: Distribution and host diversity of Amoebophryidae parasites across oligotrophic waters of the Mediterranean Sea, Biogeosciences, 8, 267–278, doi:10.5194/bg-8-267-2011, 2011.

Siokou-Frangou, I., Christou, E. D., Fragopoulu, N., and Mazzocchi, M. G.: Mesozooplankton distribution from Sicily to Cyprus (Eastern Mediterranean): II. Copepod assemblages, Oceanol. Acta, 20, 537–548, 1997.

Siokou-Frangou, I., Christaki, U., Mazzocchi, M. G., Montresor, M., Ribera d'Alcalá, M., Vaqué, D., and Zingone, A.: Plankton in the open Mediterranean Sea: a review, Biogeosciences, 7, 1543–1586, doi:10.5194/bg-7-1543-2010, 2010.

Skovgaard, A.: Infection with the dinoflagellate parasite *Blastodinium* spp. in two Mediterranean copepods, Aquat. Microb. Ecol., 38, 93–101, 2005.

Skovgaard, A. and Saiz, E.: Seasonal occurrence and role of protistan parasites on coastal marine zooplankton, Mar. Ecol.-Prog. Ser., 327, 37–49, 2006.

Skovgaard, A. and Salomonsen, X. M.: *Blastodinium galatheanum* sp. nov. (Dinophyceae) a parasite of the planktonic copepod *Acartia negligens* (Crustacea, Calanoida) in the central Atlantic Ocean, Eur. J. Phycol., 44, 425–438, 2009.

Skovgaard, A., Massana, R., and Saiz, E.: Parasitic species of the genus *Blastodinium* (Blastodiniphyceae) are peridinioid dinoflagellates, J. Phycol., 43, 553–560, 2007.

Vane, F. R.: The distribution of *Blastodinium hyalinum* in the North Sea, Challenger Soc., 3, 23–24, 1952.

Wilson, D. S.: Food size selection among copepods, Ecology, 54, 909–914, 1973.

Annexe 7-3. Article 2 : The crustacean parasites *Ellobiopsis* Caullery, 1910 and *Thalassomyces* Niezabitowski, 1913 form a monophyletic divergent clade within the Alveolata. Fernando Gómez, Purificatión López-García, **Antoine Nowaczyk**, David Moreira. Systematic Parasitology, 74, 65-74, 2009.

Syst Parasitol (2009) 74:65–74
DOI 10.1007/s11230-009-9199-1

The crustacean parasites *Ellobiopsis* Caullery, 1910 and *Thalassomyces* Niezabitowski, 1913 form a monophyletic divergent clade within the Alveolata

Fernando Gómez · Purificación López-García · Antoine Nowaczyk · David Moreira

Received: 4 February 2009 / Accepted: 19 May 2009

Abstract The Ellobiopsidae are enigmatic parasites of crustaceans that have been grouped together exclusively on the basis of morphological similarities. Ultrastructural studies have revealed their affiliation within the alveolates, which was confirmed by the phylogenetic analysis of the ribosomal RNA gene (SSU rDNA) sequences of two species of *Thalassomyces* Niezabitowski, 1913. However, their precise systematic position within this group remains unresolved, since they could not be definitively allied with any particular alveolate group. To better determine the systematic position of ellobiopsids by molecular phylogeny, we sequenced the SSU rDNA from the type-species of the Ellobiopsidae, *Ellobiopsis chattoni* Caullery, 1910. We found *E. chattoni* infecting various copepod hosts, *Acartia clausi* Giesbrecht, *Centropages typicus* Kröyer and *Clausocalanus* sp., in the Bay of Marseille, NW Mediterranean Sea, which allowed us to study several stages of the parasite development. A single unicellular multinucleate specimen provided two different sequences of the SSU rDNA gene, indicating the existence of polymorphism at this locus within single individuals. *Ellobiopsis* Caullery, 1910 and *Thalassomyces* formed a very divergent and well-supported clade in phylogenetic analyses. This clade appears to be more closely related to the dinoflagellates (including the Syndiniales/Marine Alveolate Group II and the Dinokaryota) and Marine Alveolate Group I than to the other alveolates (Ciliophora, Perkinsozoa and Apicomplexa).

F. Gómez (✉)
Observatoire Océanologique de Banyuls sur Mer, Université Pierre et Marie Curie, CNRS-INSU UMR 7621, Avenue du Fontaulé, BP 44, 66651 Banyuls sur Mer, France
e-mail: fernando.gomez@fitoplancton.com

P. López-García · D. Moreira
Unité d'Ecologie, Systématique et Evolution, CNRS UMR 8079, Université Paris-Sud, Bâtiment 360, 91405 Orsay Cedex, France

A. Nowaczyk
Laboratoire d'Océanographie Physique et de Biogéochimie, CNRS UMR 6535, Aix-Marseille II Université, Station Marine d'Endoume, Rue de la Batterie des Lions, 13007 Marseille, France

Introduction

The ellobiopsids, parasites of crustaceans, are multinucleate protists with a trophomere that possesses an absorbing 'root'. The trophomere root penetrates the host and reproductive structures, the gonomeres, protrude through, or are attached to, the host carapace. They look superficially like fungi, each individual consisting of one or several tubes which are generally transversally septate and ramified. Ellobiopsid parasites consist of five genera grouped on the basis of morphological similarities and distinguished by criteria, including the presence or absence of the attachment organs, the number, size and shape

of trophomeres and gonomeres, the host type, and the position where they settle on the host. Four genera, *Ellobiocystis* Coutière, 1911, *Ellobiopsis* Caullery, 1910, *Parallobiopsis* Collin, 1913 and *Thalassomyces* Niezabitowski, 1913 (syns *Amallocystis* Fage, 1936; *Staphylocystis* Coutière, 1911), are chiefly ectoparasites of pelagic crustaceans, although they also include epibionts (some species of *Ellobiocystis*), whereas the type-species of the monotypic *Rhizellobiopsis* Zachs, 1923 parasitises a benthic polychaetous worm. Currently, the group consists of about 20 species, most of them belonging to *Thalassomyces* (see Shields, 1994).

The first ellobiopsid described, the type-species, *Ellobiopsis chattoni* Caullery, 1910, was an ectoparasite of a calanoid copepod in the NW Mediterranean Sea (Caullery, 1910). *Ellobiopsis* spp. are widespread, infecting several marine and freshwater copepod species; they adversely affect fertility in females (Albaina & Irigoien, 2006) and cause feminisation in males (Théodoridès, 1989; Shields, 1994). This genus consists of three species, *E. chattoni*, *E. elongata* Steuer, 1932 and *E. fagei* Hovasse, 1951, which share a characteristic morphology with a well-defined stalk, a trophomere and one (*E. chattoni*) or two (*E. elongata*) gonomeres. *E. fagei*, with features intermediate between the other two species, has been suggested as being synonymous with *E. chattoni* (see Shields, 1994). The *Ellobiopsis* life-cycle follows several steps. Firstly, a dispersion phase, consisting of spores which settle onto the setae of the new host's appendages, where they metamorphose into trophomeres that extrude a root-like organelle through the copepod's cuticle. When the parasite body reaches a certain size, it becomes transversally septate and forms the gonomere in the distal segment. The distal gonomere becomes granulated and leads progressively to the formation of small groups of pre-spores that fall from the segregating mass. Each bud undergoes a series of divisions to form spores. Although the spores were reported to be flagellate (Shields, 1994), there is no evidence with regard to the number, and type of insertion, of the flagella in *Ellobiopsis* (see Hovasse, 1952).

Ellobiopsis was tentatively placed within the parasitic dinoflagellates (Caullery, 1910; Chatton, 1920; Reichenow, 1930). Hovasse (1926) observed that *Parallobiopsis coutieri* Collin, 1913 produce uniflagellate zoospores, which led him to conclude that ellobiopsid parasites were not dinoflagellates but a separate group in the Flagellata *incertae sedis*. Niezabitowski (1913) described *Thalassomyces* as fungi, and other authors agreed that the whole group was probably fungal (Jepps, 1937; Grassé, 1952; Dick, 2001), but ultrastructural studies have shown that the trophomere is not surrounded by a cell wall, as might be expected for a fungus. In contrast, *Thalassomyces* is bounded by a complex pellicle occasionally interrupted by flask-shaped organelles resembling mucocysts (Galt & Whisler, 1970; Whisler, 1990). Both the pellicle and the zoospore differentiation suggest an affiliation within the alveolates, the entire group being characterised by the presence of membrane-bound flattened vesicles named alveoli (Cavalier-Smith, 1993). Galt & Whisler (1970) placed the ellobiopsid parasites among the dinoflagellates, because the spores of *Thalassomyces marsupii* Kane, 1964 possess one flagellum directed posteriorly and the other circumferentially, which is reminiscent of dinoflagellate flagellar structure. However, the spore of *Thalassomyces* lacks an obvious sulcus and cingulum and also the highly organised interphasic chromosomes of the dinokaryotic dinoflagellates. Schweikert & Elbrächter (2006) observed in *Ellobiopsis* unique ultrastructural features, such as a peculiar organisation of the centrioles that is unknown in other protist groups, so that they discarded any relationship with the dinoflagellates. Cavalier-Smith & Chao (2004) proposed that the infraphylum Ellobiopsa Cavalier-Smith, which, together with the Dinoflagellata Bütschli, comprise the subphylum Dinozoa Cavalier-Smith.

The Alveolata Cavalier-Smith, 1991, one of the major eukaryotic lineages, is composed of three major classes: the Ciliophora Doflein, 1901, the Apicomplexa Levine, 1970 and the Dinoflagellata Bütschli, 1885, and minor groups, such as the Perkinsozoa Norén, Moestrup & Rehnstam-Holm, 1999 (*Perkinsus* Levine, 1978/*Parvilucifera* Norén & Moestrup, 1999), *Colpodella* Cienkowski, 1865 and *Rastrimonas* Brugerolle, 2003, among others (Cavalier-Smith & Chao, 2004). The Apicomplexa and the Perkinsozoa are obligate parasites, while ciliates and dinoflagellates include both parasitic and free-living species. In general, the parasites tend to simplify their morphologies and lose diagnostic morphological characters used for classification. The advent of molecular techniques has provided new tools to clarify the

evolutionary relationships among protist species, including parasites, with the small subunit ribosomal RNA gene (SSU rDNA) as the most popular marker. In the last few years, environmental molecular surveys of SSU rRNA genes has revealed the existence of novel alveolate sequences indicating two large and diverse clades that were initially named Marine Alveolate Groups I and II (MAGI and MAGII, respectively) (López-García et al., 2001; Moreira & López-García, 2002). Subsequently, it has been shown that these groups correspond to parasitic dinoflagellates previously placed within the order Syndiniales Loeblich based on a few morphologically characterised representatives for which SSU rDNA sequences are available (*Amoebophrya* Koeppen, 1894, *Syndinium* Chatton, 1920, *Hematodinium* Chatton & Poisson, 1931, *Duboscquella* Chatton, 1920 and *Ichthyodinium* Hollande & Cachon, 1952) (Skovgaard et al., 2005; Harada et al., 2007; Mori et al., 2007). Silberman et al. (2004) placed *Thalassomyces* within the alveolates using SSU rDNA phylogenetic analysis. However, they concluded that their analyses were unable to resolve whether *Thalassomyces* belonged to a described lineage (e.g. Perkinsozoa or Dinoflagellata) or represented a novel phylum within the alveolates. Moreover, it remains unclear whether the different ellobiopsids form a monophyletic assemblage or not. In order to determine the phylogenetic position of *Ellobiopsis* and to test whether this genus is phylogenetically related to *Thalassomyces*, we amplified, cloned and sequenced the SSU rDNA from the type-species, *E. chattoni*, collected from its type-locality, the NW Mediterranean Sea.

Materials and methods

Sampling and isolation

Infected copepods were collected in the SOMLIT-Marseille station in the Bay of Marseille (43°14′30″N, 05°17′30″E; bottom depth 60 m), using a 200 µm WP2 plankton net mounted with filtering cod ends. Hauls were carried out between 55 m and the surface at 1 m s^{-1}. The host copepods were identified according to Rose (1933). Infected copepods were isolated and placed individually in vials with absolute ethanol. The specimens of *Ellobiopsis* and host were photographed with a digital camera (Nikon Coolpix E995) connected to an inverted microscope (Nikon Eclipse TE200). In order to avoid contamination with copepod DNA, the parasite was separated from the host by cutting off the root or separating the gonomere from the trophont. Then, this was micropipetted individually using a fine capillary into another chamber and washed three times with ethanol. Finally, the specimen was picked up and placed into a 1.5 ml Eppendorf tube filled with absolute ethanol. Samples were kept at laboratory temperature and in darkness until the molecular analysis could be performed.

PCR amplification of small subunit rRNA genes (SSU rDNAs) and sequencing

The ethanol-fixed specimen was centrifuged for 5 minutes at 3,000 rpm. Ethanol was removed by evaporation in a vacuum desiccator and the specimen resuspended directly in 50 µl of Ex TaKaRa (TaKaRa) PCR reaction mix containing 10 pmol of the eukaryotic-specific SSU rDNA primers EK-42F (5′-CTC AARGAYTAAGCCATGCA-3′) and EK-1520R (5′-CYGCAGGTTCACCTAC-3′). PCR reaction conditions were: 2 min denaturation at 94°C; 10 cycles of 'touch-down' PCR (denaturation at 94°C for 15 s; a 30-s annealing step at decreasing temperature from 65 down to 55°C (1°C decrease with each cycle), extension at 72°C for 2 min); 20 additional cycles with 55°C of annealing temperature; and a final elongation step of 7 min at 72°C. A nested PCR reaction was then carried out using 2 µl of the first PCR reaction in a GoTaq (Promega) polymerase reaction mix containing the eukaryotic-specific primers EK-82F (5′-GAAACTGCGAATGGCTC-3′) and EK-1498R (5′-CACCTACGGAAACCTTGTTA-3′) and similar PCR conditions as above except for an increase in the total number of cycles from 30 to 35. The amplified product was subsequently cloned using the Topo TA Cloning system (Invitrogen) following the instructions provided by the manufacturers. Twelve clones were picked and the corresponding insert amplified using vector primers. Amplicons of the expected size were fully sequenced (Cogenics, Meylan, France) with vector primers.

Phylogenetic analyses

Sequences were compared by BLAST (Altschul et al., 1997) to those in the GenBank database. Using the profile alignment option of MUSCLE 3.7 (Edgar, 2004), sequences were aligned to a large multiple sequence alignment containing 1,200 published

alveolate complete or nearly complete SSU rDNA sequences, which included representatives of the major alveolate groups available in public databases. The resulting alignment was manually inspected with the program ED of the MUST package (Philippe, 1993). Ambiguously aligned regions and gaps were excluded from phylogenetic analyses. Preliminary phylogenetic trees with all sequences were constructed using the Neighbor Joining (NJ) method (Saitou & Nei, 1987) implemented in the MUST package (Philippe, 1993). Phylogenetic trees enabled identification of the closest relatives of our sequences, which were selected, together with a sample of other alveolates species and some environmental sequences, to carry out computationally-intensive Maximum Likelihood (ML) and Bayesian Inference (BI) analyses. The extremely divergent *Oxyrrhis marina* Dujardin, 1841 sequence was omitted from phylogenetic analyses in order to avoid long-branch attraction artefacts. A selection of 50 sequences representing different alveolates was thus determined to reconstruct the ML and BI trees. ML analyses were conducted using the program TREEFINDER (Jobb et al., 2004) by applying a GTR + Γ + I model of nucleotide substitution, taking into account a proportion of invariable sites, and a Γ-shaped distribution of substitution rates with four rate categories. BI analyses were carried out using both the program PHYLOBAYES, through the application of a GTR + CAT Bayesian mixture model (Lartillot & Philippe, 2004), and MrBayes v. 3.1.2 (Huelsenbeck & Ronquist, 2001) with the model GTR (Lanave et al., 1984; Rodríguez et al., 1990), with the number of invariable sites being estimated, and a gamma-shaped distribution of variable sites with four rate categories (GTR + Γ + I). Four chains were run up to 1,000,000 generations from a random starting tree well beyond convergence. The first 5,000 trees were discarded as the burn in. Sequences were deposited in GenBank with the following accession numbers: FJ593705-FJ593708.

Results

In late spring of 2008, we observed several copepod species infected with ellobiopsid parasites. Since the phylogenetic position of these parasites remains uncertain, we collected ten individual specimens to carry out molecular phylogenetic studies (see below). In addition, we completed previous observations concerning the life-cycle of these parasites. The copepod assemblage of the Bay of Marseille (NW Mediterranean) was dominated by *Acartia clausi* Giesbrecht, *Centropages typicus* Kröyer and *Pseudocalanus* sp. in the late spring of 2008. Both copepodites and adult stages of the three species appeared infected with specimens of *Ellobiopsis.* On May 29th, *c*.15% of the 200 examined specimens of *A. clausi* appeared infected with this parasite. Parasites were attached to various parts of the host's body, with a higher occurrence on the anterior appendices. Up to five parasites at different developmental stages were found on a single host. This number may be even higher, because younger specimens of *Ellobiopsis* may go unnoticed under optical microscopy due to their small size. The presence of one gonomere suggested that the parasite found in all the infected copepod species corresponded to the type-species, *E. chattoni*.

The *Ellobiopsis* life-cycle

Ellobiopsis chattoni first appeared as a small knob, and then developed into an oval test with a stalk which pierces the host's body (Fig. 1). The shape of the parasite changes throughout its life-cycle. The youngest cells are pyriform, while mature stages may be ellipsoidal or cylindrical (Figs. 2–4). An ellipsoidal or spherical gonomere (sporogenetic stage) is formed from the trophomere by means of a more or less marked constriction at the distal end (Figs. 5–8). In contrast to the live cells, the protoplast of ethanol-fixed specimens shrank and separated from the external membrane. A tube-like structure connected the membrane and protoplast in the distal extreme of the gonomere (Figs. 5–6). This structure seems to be related to the release of the spores. In mature specimens, the gonomere had a knobbly surface with small buds of pre-spores that underwent a series of divisions to give rise to non-flagellate spores (Figs. 9–14). We were unable to determine whether the spores required a post-maturation process to develop the flagella. On a live infected copepod, a specimen of *Ellobiopsis* was observed under the microscope to produce spores after half an hour. Spore formation did not apparently require the differentiation of the gonomere (Figs. 15–17).

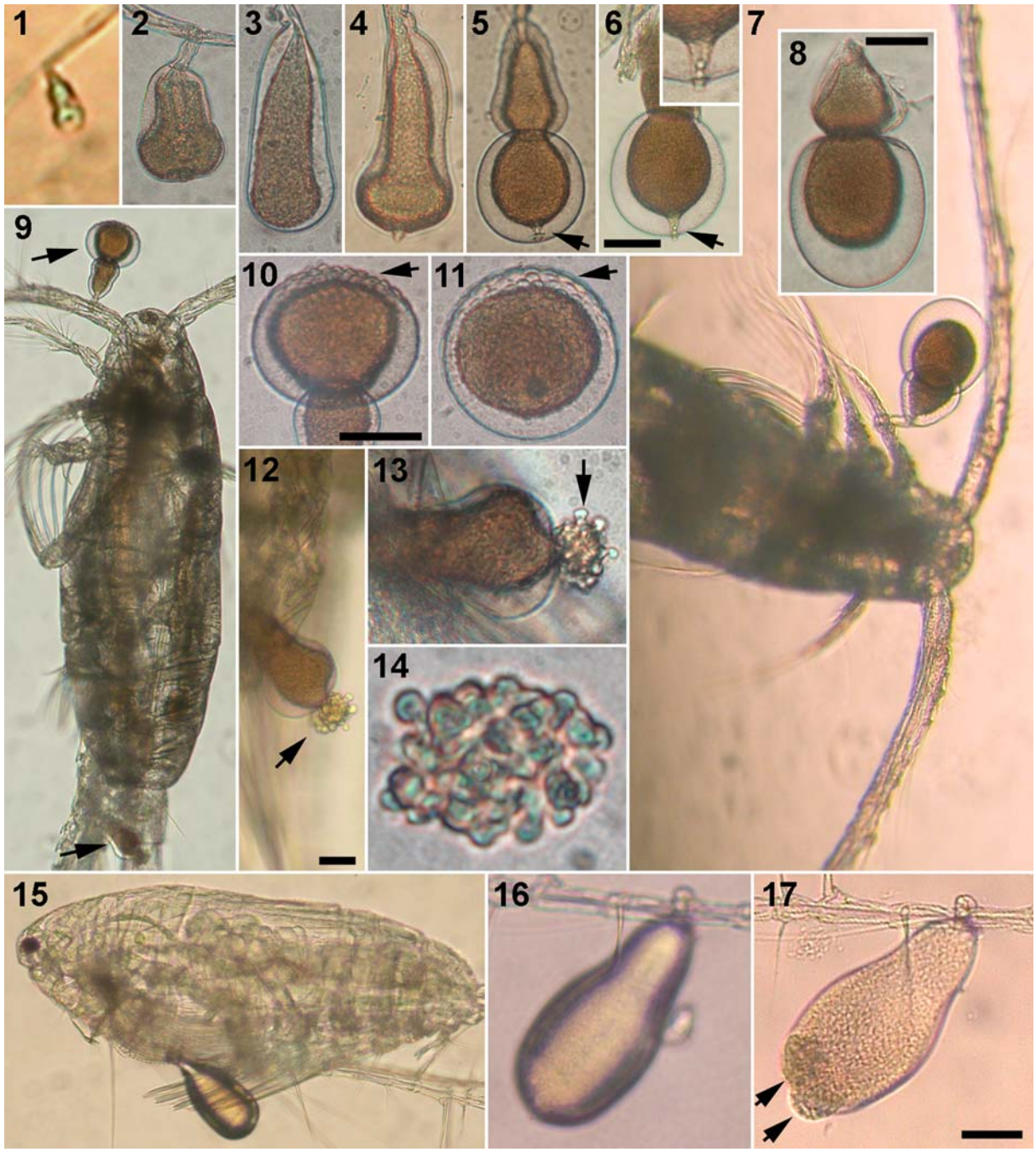

Figs. 1–17 Light micrographs of different life-cycle stages of *Ellobiopsis chattoni* parasitising copepods collected from the Bay of Marseille, NW Mediterranean Sea. 1–6. Different stages of the development; 5–6. the *arrows* indicate a tube-like structure in the distal part of the gonomere. 7–8. Specimen infecting *Acartia clausi* used for single-cell PCR. 9–14. Two parasites at different degrees of maturation in the same host; 10–11. the *arrows* indicate the irregular surface on the distal part of the gonomere; 12–13. the *arrows* indicate the budding of immature spores. 15–17. Live infected copepod; the *arrows* indicate the budding of spores formed after half an hour of observation. 1–14. Ethanol-fixed specimens collected on May 29th, 2008. 15–17. Live specimen collected on June 10th, 2008. *Scale-bar*: 50 μm

Molecular phylogenetic analysis of *Ellobiopsis chattoni*

We attempted to amplify the SSU rRNA gene from the ten *Ellobiopsis* specimens collected. Only four of them yielded DNA fragments of the expected size. Direct sequencing of the amplified products either failed or yielded copepod sequences, except for one partial sequence of poor quality that had *Thalassomyces* as its closest relative (specimen FG144, 87% identity). We then chose one different specimen that had yielded an amplicon of the expected size, FG141, and we cloned the PCR product as a means to discriminate copepod or other potential contaminant amplicons from parasite sequences. The specimen FG141 came from a multinucleate gonomere and a partial trophomere of *E. chattoni* that infected a copepodite stage IV of *Acartia clausi* (Figs. 7–8). We sequenced several clone inserts and consistently obtained two slightly different sequences (Fig. 18). The two SSU rDNA copies differed in 14 substitutions for a length of 1,739 characters. Substitutions occurred all along the sequences in the SSU rDNA variable regions. Since co-infection by two different *Ellobiopsis* species producing a single infecting structure is highly improbable, the presence of two different SSU rDNA sequences suggests the existence of two polymorphic copies of this gene in *Ellobiopsis* cells.

Initial BLAST comparisons showed that, with the exception of the partial environmental sequence MB07.44 (accession EF539153, retrieved from the western Pacific coast, which shared 99% identity with our *Ellobiopsis* sequences, but was not included in our phylogenetic analyses because of its much shorter length), the closest relatives in the database were alveolate sequences that had only low similarity values (<90%). Thus, the second closest relative was *Thalassomyces* sp. JDS-2003 (AY340591) with only 82% identity at the SSU rDNA locus.

We carried out phylogenetic analyses using various reconstruction methods (see Materials and methods). All phylogenetic analyses were congruent in showing that *Ellobiopsis chattoni* formed a monophyletic lineage with *Thalassomyces fagei* Boschma, 1948 and *Thalassomyces* sp. (100% bootstrap support (BS) and posterior probabilities (PP) of 1). The long-branch sequences revealed both ellobiopsid genera as members of the same highly divergent alveolate group.

Fig. 18 Maximum likelihood phylogenetic tree of alveolate SSU rDNA sequences, based on 1,096 aligned positions. Names in *bold* represent the four sequences of different clones from the same isolate of *Ellobiopsis chattoni* obtained in this study. Numbers at the nodes are bootstrap proportions (values <50% are omitted). Nodes supported by posterior probability values >0.90 in Bayesian Inference analyses are indicated by black circles. Several branches leading to fast-evolving species have been shortened to a half or a third (indicated by 1/2 or 1/3). Accession numbers are provided in brackets. The scale-bar represents the number of substitutions for a unit branch length ▶

The inclusion of the ellobiopsids in the SSU rDNA phylogeny of the major alveolate lineages yielded a group that diverged after the Perkinsozoa (with 82% BS and PPs, for the two Bayesian methods used, of 0.94 and 0.86), formed by three clades: the ellobiopsids, the Marine Alveolate Group I and the dinoflagellates (Dinokaryota, Noctilucea and Syndinea). The order of emergence of these three groups remained unresolved. Within the Dinokaryota, the aberrant dinoflagellate *Noctiluca scintillans* (Macartney, 1810) Kofoid, 1920 and the parasite *Haplozoon* Dogiel, 1906 diverged at a basal position, although with very low support (Fig. 18).

Discussion

Systematic position of ellobiopsids within the alveolates

The few available ultrastructural studies showed that the genera *Thalassomyces* and *Parallobiopsis* differed markedly in the complex cytology of the gonomere and number of flagella (Collin, 1913; Hovasse, 1926; Galt & Whisler, 1970; Whisler, 1990). In addition to these morphological differences, differences in the types of hosts parasitised (crustaceans versus polychaete worms) led to the view that ellobiopsids constituted a heterogeneous assemblage of protists with diverse affinities (Boschma, 1949, 1959). In contrast, our results based on SSU rDNA phylogenetic analysis have shown that the most representative taxa, *Ellobiopsis* and *Thalassomyces*, form a monophyletic group. We observed two slightly different SSU rDNA sequences (0.8% divergence) in a single *Ellobiopsis* specimen. The presence of divergent SSU rDNAs in a single species, although not frequent, is not exceptional in eukaryotes (see references in Alverson &

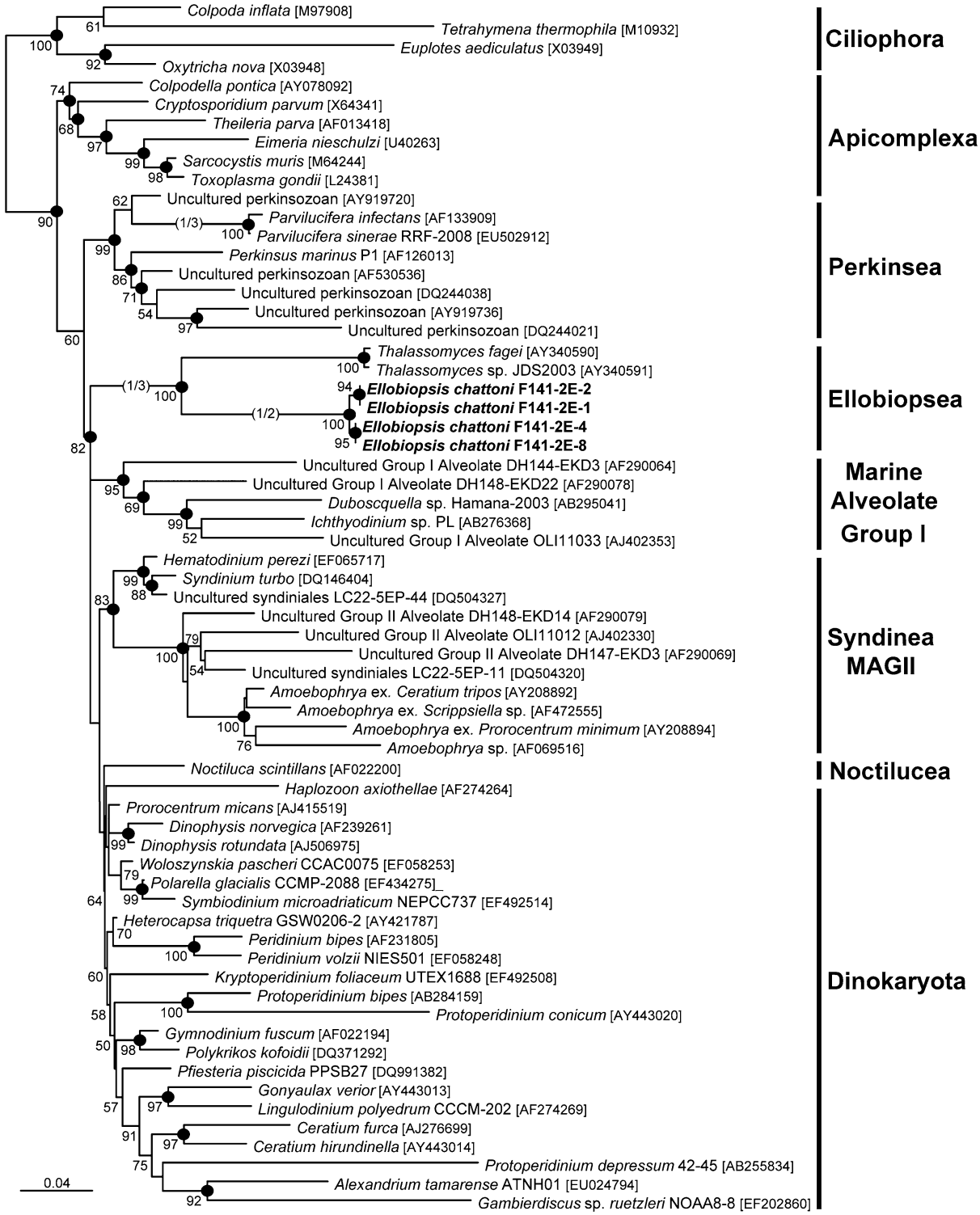
Colpoda inflata [M97908]
Tetrahymena thermophila [M10932]
Euplotes aediculatus [X03949]
Oxytricha nova [X03948]
Ciliophora
Colpodella pontica [AY078092]
Cryptosporidium parvum [X64341]
Theileria parva [AF013418]
Eimeria nieschulzi [U40263]
Sarcocystis muris [M64244]
Toxoplasma gondii [L24381]
Apicomplexa
Uncultured perkinsozoan [AY919720]
Parvilucifera infectans [AF133909]
Parvilucifera sinerae RRF-2008 [EU502912]
Perkinsus marinus P1 [AF126013]
Uncultured perkinsozoan [AF530536]
Uncultured perkinsozoan [DQ244038]
Uncultured perkinsozoan [AY919736]
Uncultured perkinsozoan [DQ244021]
Perkinsea
Thalassomyces fagei [AY340590]
Thalassomyces sp. JDS2003 [AY340591]
Ellobiopsis chattoni F141-2E-2
Ellobiopsis chattoni F141-2E-1
Ellobiopsis chattoni F141-2E-4
Ellobiopsis chattoni F141-2E-8
Ellobiopsea
Uncultured Group I Alveolate DH144-EKD3 [AF290064]
Uncultured Group I Alveolate DH148-EKD22 [AF290078]
Duboscquella sp. Hamana-2003 [AB295041]
Ichthyodinium sp. PL [AB276368]
Uncultured Group I Alveolate OLI11033 [AJ402353]
Marine Alveolate Group I
Hematodinium perezi [EF065717]
Syndinium turbo [DQ146404]
Uncultured syndiniales LC22-5EP-44 [DQ504327]
Uncultured Group II Alveolate DH148-EKD14 [AF290079]
Uncultured Group II Alveolate OLI11012 [AJ402330]
Uncultured Group II Alveolate DH147-EKD3 [AF290069]
Uncultured syndiniales LC22-5EP-11 [DQ504320]
Amoebophrya ex. Ceratium tripos [AY208892]
Amoebophrya ex. Scrippsiella sp. [AF472555]
Amoebophrya ex. Prorocentrum minimum [AY208894]
Amoebophrya sp. [AF069516]
Syndinea MAGII
Noctiluca scintillans [AF022200]
Haplozoon axiothellae [AF274264]
Noctilucea
Prorocentrum micans [AJ415519]
Dinophysis norvegica [AF239261]
Dinophysis rotundata [AJ506975]
Woloszynskia pascheri CCAC0075 [EF058253]
Polarella glacialis CCMP-2088 [EF434275]_
Symbiodinium microadriaticum NEPCC737 [EF492514]
Heterocapsa triquetra GSW0206-2 [AY421787]
Peridinium bipes [AF231805]
Peridinium volzii NIES501 [EF058248]
Kryptoperidinium foliaceum UTEX1688 [EF492508]
Protoperidinium bipes [AB284159]
Protoperidinium conicum [AY443020]
Gymnodinium fuscum [AF022194]
Polykrikos kofoidii [DQ371292]
Pfiesteria piscicida PPSB27 [DQ991382]
Gonyaulax verior [AY443013]
Lingulodinium polyedrum CCCM-202 [AF274269]
Ceratium furca [AJ276699]
Ceratium hirundinella [AY443014]
Protoperidinium depressum 42-45 [AB255834]
Alexandrium tamarense ATNH01 [EU024794]
Gambierdiscus sp. ruetzleri NOAA8-8 [EF202860]
Dinokaryota
0.04

Kolnick, 2005). For example, among the alveolates, multiple polymorphic sequences have been reported from clonal cultures of perkinsid parasites (Burreson et al., 2005). They were interpreted as the result of a relatively recent hybridisation of two different species. Similarly, species of *Protoperidinium* Bergh, 1881, the most speciose dinoflagellate genus, have shown a relatively high intra-individual variability in the SSU and LSU rDNAs (Yamaguchi et al., 2006; Gribble & Anderson, 2007). The intragenomic sequence variation in *E. chattoni* should be taken into account, especially to avoid an overestimation of species diversity, in future environmental sequencing studies.

Although the monophyly of the genera *Ellobiopsis* and *Thalassomyces* was firmly demonstrated by our SSU rDNA phylogenetic analysis, the branching position of the ellobiopsids within the alveolates was much less certain. The ellobiopsids have unique ultrastructural peculiarities, such as the nuclear dimorphism and centriolar complexes (Galt & Whisler, 1970; Whisler, 1990; Schweikert & Elbrächter, 2006). Cavalier-Smith & Chao (2004) justified the ellobiopsids as sisters of dinoflagellates because they share centrioles associated with cytoplasmic channels through the nucleus and both the posterior flagellum and circumferential transverse flagellum. However, other typical dinoflagellate features, such as the dinokaryon characterised by condensed chromosomes in interphase, the two grooves (cingulum, sulcus) and the transverse ribbon-like flagellum (with mastigonemes and paraxial rod), are lacking in ellobiopsids (Galt & Whisler, 1970; Whisler, 1990; Schweikert & Elbrächter, 2006). The only described species of the Marine Alveolate Group I belong to *Duboscquella* and *Ichthyodinium*, endoparasites of tintinnid ciliates and fish eggs, respectively (Harada et al., 2007; Mori et al., 2007). They have biflagellate spores with a sulcus and cingulum that are reminiscent of the dinoflagellates (Chatton, 1952; Cachon & Cachon, 1987). However, if we restrict the dinoflagellates based on the occurrence of a dinokaryon, we must exclude *Duboscquella* and *Ichthyodinium* from them because there is no evidence of condensed interphase chromosomes in any stage of their life-cycle (Harada et al., 2007). The level of organisation of the chromosomes is also variable among the Syndinea, and the dinokaryon is missing in vegetative cells of *Noctiluca scintillans* (see Fukuda & Endoh, 2008). This character is also uneven in perkinsid parasites. For example, *Parvilucifera prorocentri* Leander & Hoppenrath, 2008 has been described with condensed chromosomes, whereas they have not been reported in *P. infectans* Norén & Moestrup, 1999 (Norén et al., 1999; Leander & Hoppenrath, 2008). Therefore, the lack of condensed chromosomes in the highly aberrant ellobiopsids is probably a poor ultrastructural criterion for discarding the possible phylogenetic relationship with the dinoflagellates that appears to be supported by the SSU rDNA phylogeny.

Another of the apparent anomalies of the ellobiopsid parasites is the number of flagella. The spores of *Thalassomyces* are unequivocally biflagellate, whereas they are apparently uniflagellate or non-flagellate in *Parallobiopsis* and *Ellobiopsis*, respectively (Collin, 1913; Hovasse, 1926, 1952; Galt & Whisler, 1970; Whisler, 1990). However, we might expect the occurrence of biflagellate spores in all the ellobiopsids, taking into account that this is a common feature in all known relatives (Apicomplexa, Perkinsozoa, Syndinea, *Colpodella*, Dinokaryota and *Duboscquella*). Whereas, a second flagellum might have been unnoticed in the earlier and only study of *Parallobiopsis*, the production of biflagellate spores after a post-maturation process needs to be demonstrated in *Ellobiopsis*. In this study, we observed from a live *Ellobiopsis* specimen that spore formation did not apparently require the differentiation of the gonomere (Figs. 15–17). This phenomenon may be interpreted as a fast response of the parasite to the forthcoming death of the host and subsequently its own death. The mechanism of dispersion and motility of the spores remains unknown.

Ecological aspects

Copepods are the most abundant metazoans in the oceans (Mauchline, 1998) and *Ellobiopsis chattoni* has been reported infecting at least 25 copepod species and even crab larvae (Shields, 1994). Environmental sequencing surveys have revealed that the spores of parasitic alveolates, such as the Syndinea, are widely distributed throughout the oceans (Moreira & López-García, 2002; Guillou et al., 2008). In contrast, only one ellobiopsid environmental sequence is found in the GenBank database (accession EF539153). This might be explained either by the potential inefficiency of eukaryote-specific primers to amplify the highly divergent ellobiopsid sequences or, perhaps, by the

fact that the infective spores of the ellobiopsids are not abundant in the oceans or have short-lived stages.

All described Syndinea obligatorily kill their hosts and produce infective spores in massive numbers. In contrast, *Ellobiopsis* keeps the host alive for a long time, although it reduces its fecundity, presumably by decreasing the host reserves available for reproduction (Shields, 1994). In this study, we observed that specimens of *Ellobiopsis* rapidly form spores as a response to the host's death. It might be possible that they also have the capacity to induce the fast formation and release of spores under favourable conditions, such as high host population densities. This would limit the distribution of ellobiopsid spores to very discrete periods and locations, explaining the almost complete absence of ellobiopsid sequences in environmental surveys.

In our study, the three dominant copepod species from a single zooplankton sample were infected with specimens of *Ellobiopsis*. We assumed that a single *Ellobiopsis* species is responsible for the infection of multiple host species, although it has been reported that different copepod species appear to have different susceptibilities to the ellobiopsid infection. For example, in the North Atlantic, *Calanus helgolandicus* Claus is commonly infected by *E. chattoni*, whereas the co-occurring species, *C. carinatus* Kröyer, appears to be unaffected (Albaina & Irigoien, 2006). Several parasitic alveolates with a broad host range are well known. This is the case for the perkinsid *Parvilucifera infectans*, capable of infecting several species of dinoflagellates (Norén et al., 1999), whereas the congeneric *P. prorocentri* is only known to infect a single dinoflagellate species (Leander & Hoppenrath, 2008). A syndinian that parasitises dinoflagellates of the genus *Amoebophrya* has strains that show a high degree of host-specificity, whereas others have a relatively broad host range (Kim et al., 2008). Experimental infection studies will help elucidating whether a single strain of *Ellobiopsis* is able to infect different copepod species. In addition, further molecular and ultrastructural studies, including the survey of different seasons, hosts and geographical locations, will address the question of whether *E. chattoni* constitutes an independent species or a species complex with independent species in each host.

Acknowledgements This is a contribution to the project DIVERPLAN-MED supported by a post-doctoral grant to F.G. of the Ministerio Español de Educación y Ciencia No. 2007-0213. P.L.G. and D.M. acknowledge financial support from the French CNRS and the ANR Biodiversity project 'Aquaparadox'. This is a part of SOMLIT (Service d'Observation en Milieu LITtoral) national grid.

References

Albaina, A., & Irigoien, X. (2006). Fecundity limitation of *Calanus helgolandicus*, by the parasite *Ellobiopsis* sp. *Journal of Plankton Research, 28*, 413–418.

Altschul, S. F., Madden, T. L., Schaffer, A. A., Zhang, J., Zhang, Z., et al. (1997). Gapped BLAST and PSI-BLAST: A new generation of protein database search programs. *Nucleic Acids Research, 25*, 3389–3402.

Alverson, A. J., & Kolnick, L. (2005). Intragenomic nucleotide polymorphism among small subunit (18S) rDNA paralogs in the diatom genus *Skeletonema* (Bacillariophyta). *Journal of Phycology, 41*, 1248–1257.

Boschma, H. (1949). Ellobiopsidae. *Discovery Report, 25*, 281–314.

Boschma, H. (1959). Ellobiopsidae from the tropical West Africa. *Atlantide Report, 5*, 145–175.

Burreson, E. M., Dungan, C. F., & Reece, K. S. (2005). Molecular, morphological, and experimental evidence support the synonymy of *Perkinsus chesapeaki* and *Perkinsus andrewsi*. *Journal of Eukaryotic Microbiology, 52*, 258–270.

Cachon, J., & Cachon, M. (1987). Parasitic dinoflagellates. In F. J. R. Taylor (Ed.), *The biology of dinoflagellates* (pp. 571–610). Oxford: Blackwell.

Caullery, M. (1910). *Ellobiopsis chattoni*, n. g., n. sp., parasite de *Calanus helgolandicus* Claus, appartenant probablement aux Péridiniens. *Bulletin Scientifique de la France et la Belgique, 44*, 201–214.

Cavalier-Smith, T. (1993). Kingdom Protozoa and its 18 phyla. *Microbiological Reviews, 57*, 953–994.

Cavalier-Smith, T., & Chao, E. E. (2004). Protalveolae phylogeny and systematics and the origins of Sporozoa and dinoflagellates (phylum Myzozoa nom nov.). *European Journal of Protistology, 40*, 185–212.

Chatton, E. (1920). Les Péridiniens parasites. Morphologie, reproduction, éthologie. *Archives de Zoologie Experimentale et Générale, 59*, 1–475.

Chatton, E. (1952). Classe des Dinoflagellés ou Péridiniens. In P. Grassé (Ed.), *Traité de Zoologie* (Vol. 1, pp. 1309–1406). Paris: Masson et Cie.

Collin, B. (1913). Sur un Ellobiopside nouveau parasite des Nebalies (*Parallobiopsis coutieri* n. g., n. sp.). *Comptes Rendus de l'Academie des Sciences, 156*, 1332–1333.

Dick, M. W. (2001). *Straminipilous fungi: Systematics of the peronosporomycetes, including accounts of the marine straminipilous protists, the plasmodiophorids, and similar organisms*. Dordrecht: Kluwer, 654 pp.

Edgar, R. C. (2004). MUSCLE: Multiple sequence alignment with high accuracy and high throughput. *Nucleic Acids Research, 32*, 1792–1797.

Fukuda, Y., & Endoh, H. (2008). Phylogenetic analyses of the dinoflagellate *Noctiluca scintillans* based on β-tubulin and

Hsp90 genes. *European Journal of Protistology, 44*, 27–33.

Galt, J. H., & Whisler, H. C. (1970). Differentiation of flagellate spores in *Thalassomyces* Ellobiopsid parasite of marine Crustacea. *Archiv für Mikrobiologie, 71*, 295–303.

Grassé, P. P. (1952). Les Ellobiopsidae. In P. Grassé (Ed.), *Traité de Zoologie* (Vol. 1, pp. 1023–1030). Paris: Masson et Cie.

Gribble, K. E., & Anderson, D. M. (2007). High intraindividual, intraspecific, and interspecific variability in large-subunit ribosomal DNA in the heterotrophic dinoflagellates *Protoperidinium*, *Diplopsalis*, and *Preperidinium* (Dinophyceae). *Phycologia, 46*, 315–324.

Guillou, L., Viprey, M., Chambouvet, A., Welsh, R. M., Kirkham, A. R., Massana, R., et al. (2008). Widespread occurrence and genetic diversity of marine parasitoids belonging to Syndiniales (Alveolata). *Environmental Microbiology, 10*, 3349–3365.

Harada, A., Ohtsuka, S., & Horiguchi, T. (2007). Species of the parasitic genus *Duboscquella* are members of the enigmatic marine alveolate Group I. *Protist, 158*, 337–347.

Hovasse, R. (1926). "Parallobiopsis coutieri" Collin. Morphologie, cytologie, évolution, affinités des Ellobiopsidés. *Bulletin Scientifique de la France et la Belgique, 60*, 409–446.

Hovasse, R. (1952). *Ellobiopsis fagei* Hovasse, Ellobiopsidé parasite, en Méditerranée, de *Clausocalanus arcuicornis* Dana. *Bulletin de l'Institut Océanographique, Monaco, 1016*, 1–12.

Huelsenbeck, J. P., & Ronquist, F. (2001). MrBayes: Bayesian inference of phylogenetic trees. *Bioinformatics, 17*, 754–755.

Jepps, M. W. (1937). On the protozoan parasites of *Calanus finmarchicus* in the Cycle Sea area. *Quarterly Journal of Microscopical Science, 79*, 589–658.

Jobb, G., von Haeseler, A., & Strimmer, K. (2004). TREEFINDER: A powerful graphical analysis environment for molecular phylogenetics. *BMC Evolutionary Biology, 4*, 18.

Kim, S., Park, M. G., Kim, K. Y., Kim, C. H., Yih, W., Park, J. S., et al. (2008). Genetic diversity of parasitic dinoflagellates in the genus *Amoebophrya* and its relationship to parasite biology and biogeography. *Journal of Eukaryotic Microbiology, 55*, 1–8.

Lanave, C., Preparata, G., Saccone, C., & Serio, G. (1984). A new method for calculating evolutionary substitution rates. *Journal of Molecular Evolution, 20*, 86–93.

Lartillot, N., & Philippe, H. (2004). A Bayesian mixture model for across-site heterogeneities in the amino-acid replacement process. *Molecular Biology and Evolution, 21*, 1095–1109.

Leander, B. S., & Hoppenrath, M. (2008). Ultrastructure of a novel tube-forming, intracellular parasite of dinoflagellates: *Parvilucifera prorocentri* sp. nov. (Alveolata, Myzozoa). *European Journal of Protistology, 44*, 55–70.

López-García, P., Rodríguez-Valera, F., Pedrós-Alió, C., & Moreira, D. (2001). Unexpected diversity of small eukaryotes in deep-sea Antarctic plankton. *Nature, 409*, 603–607.

Mauchline, J. (1998). The biology of calanoid copepods. *Advances in Marine Biology, 33*, 1–710.

Moreira, D., & López-García, P. (2002). The molecular ecology of microbial eukaryotes unveils a hidden world. *Trends in Microbiology, 10*, 31–38.

Mori, K., Yamamoto, K., Teruya, K., Shiozawa, S., Yoseda, K., Sugaya, T., et al. (2007). Endoparasitic dinoflagellate of the genus *Ichthyodinium* infecting fertilized eggs and hatched larvae observed in the seed production of leopard coral grouper *Plectropomus leopardus*. *Fish Pathology, 42*, 49–57.

Niezabitowski, E. L. (1913). Die pfianzlichen Parasiten der Tiefsee-Decapoden-Gattung *Pasiphaea*. *Kosmos, 38*, 1563–1572.

Norén, F., Moestrup, O., & Rehnstam-Holm, A.-S. (1999). *Parvilucifera infectans* Norén *et* Moestrup sp. nov. (Perkinsozoa phylum nov.): A parasitic flagellate capable of killing toxic microalgae. *European Journal of Protistology, 35*, 233–254.

Philippe, H. (1993). MUST, a computer package of management utilities for sequences and trees. *Nucleic Acids Research, 21*, 5264–5272.

Reichenow, E. (1930). Parasitische Peridinea (einschließlich Ellobiopsidae). *Die Tierwelt der Nord- und Ostsee, 19*(2.d3), 85–100.

Rodríguez, F., Oliver, J. L., Marín, A., & Medina, J. R. (1990). The general stochastic model of nucleotide substitution. *Journal of Theoretical Biology, 142*, 485–501.

Rose, M. (1933). Copépodes pélagiques. *Faune France, 26*, 1–374.

Saitou, N., & Nei, M. (1987). The neighbor-joining method: A new method for reconstructing phylogenetic trees. *Molecular Biology and Evolution, 4*, 406–425.

Schweikert, M., & Elbrächter, M. (2006). First ultrastructural investigations on *Ellobiopsis* spec. (incertae sedis) a parasite of copepods. *Endocytobiosis Cell Research, 17*, 73.

Shields, J. D. (1994). The parasitic dinoflagellates of marine crustaceans. *Annual Review of Fish Diseases, 4*, 241–271.

Silberman, J. D., Collins, A. G., Gershwin, L. A., Johnson, P. J., & Roger, A. J. (2004). Ellobiopsids of the genus *Thalassomyces* are alveolates. *Journal of Eukaryotic Microbiology, 52*, 246–252.

Skovgaard, A., Massana, R., Balague, V., & Saiz, E. (2005). Phylogenetic position of the copepod-infesting parasite *Syndinium turbo* (Dinoflagellata, Syndinea). *Protist, 156*, 413–423.

Théodoridès, J. (1989). Parasitology of marine zooplankton. *Advances in Marine Biology, 25*, 117–177.

Whisler, H. C. (1990). Incertae Sedis Ellobiopsida. In L. Margulis, J. O. Corliss, M. Melkonian, & D. J. Chapman (Eds.), *Handbook of Protoctista* (pp. 715–719). Boston: Jones & Bartlett.

Yamaguchi, A., Kawamura, H., & Horiguchi, T. (2006). A further phylogenetic study of the heterotrophic dinoflagellate genus, *Protoperidinium* (Dinophyceae) based on small and large subunit ribosomal RNA gene sequences. *Phycological Research, 54*, 317–329.

Résumé
Le mésozooplancton de la couche épipélagique (0-200 m) a été étudié dans deux écosystèmes contrastés ; le premier se situe au niveau de la partie sud du plateau des Kerguelen et d'une partie de la zone HNLC (High Nutrient Low Chlorophyll) de l'océan Austral, à la fin de floraison estivale entretenue par des apports naturels en fer (KEOPS : janvier-février 2005). La deuxième étude s'est intéressée à l'ensemble de la Méditerranée, le long d'une radiale de 3 000 km caractérisée par un degré d'oligotrophie croissant d'Ouest en Est (BOUM juin-juillet 2008). La communauté mésozooplanctonique a été caractérisée à la fois par la description des stocks (abondance et biomasse) et de sa structure (composition taxonomique et spectre de taille). La distribution spatiale à l'échelle régionale a été étudiée et mise en relation avec différents paramètres environnementaux et trophiques. L'impact de la communauté sur les producteurs primaires a été également estimé à partir de l'analyse de différents processus physiologiques (ingestion, respiration et excrétion). La communauté mésozooplanctonique australe était caractérisée par de fortes abondance et biomasse sur le plateau des Kerguelen et plus faible en zone HNLC. Elle était composée essentiellement de stades copépodites avec une présence importante de mues et des taux élevés de respiration indiquant une croissance active. Cependant l'impact du broutage sur la production primaire était faible ce qui suggère l'utilisation d'autres ressources alimentaires tel que le microzooplancton. En Méditerranée, l'abondance zooplanctonique présentait un gradient croissant est-ouest auquel s'ajoutait un gradient nord-sud décroissant dans le bassin occidental. Cette distribution était fortement liée à la quantité de chlorophylle *a*. Le broutage du mésozooplancton sur les producteurs primaires était important. Les flux de matière liés à l'activité métabolique supportaient plus de 100 % des besoins de la production primaire en carbone, azote et phosphore. L'étude des relations entre la diversité spécifique et les variables environnementales (physique, chimique et biologique) a révélé une forte régionalisation en Méditerranée alors que sur le plateau des Kerguelen ces relations sont faibles.

Abstract
Mesozooplankton from the epipelagic layer (0-200 m) was studied in two contrasted ecosystems: the first one is located in the Austral Ocean, around the Southern part of the Kerguelen shelf and over the HNLC (High Nutrient Low Chlorophyll) area, at the end of summer bloom period supported by natural iron enrichment (KEOPS, January-February 2005). The second study focused on the whole Mediterranean Sea, along a 3 000 km transect characterized by an oligotrophy gradient decrease from West to East (BOUM, June-July 2008) with low phosphorus concentration. Mesozooplanktonic community was characterized by both its stock composition (abundance and biomass) and its structure (taxonomic composition and size spectrum). Spatial distribution at the regional scale was studied and linked to different environmental and trophic parameters. The community impact on primary production was also estimated from different physiological process analyses (ingestion, respiration and excretion). Mesozooplanktonic community showed higher abundance and biomass over the Kerguelen shelf than in HNLC area. The community was essentially composed by copepodite stages, large quantity of exuviae and high respiration rates suggesting active growth. However, phytoplankton based ingestion rates were low implying the use of other food source such as microzooplankton. In the Mediterranean, abundance showed an increasing westward gradient with a southward decreasing gradient in the Occidental Basin. This distribution was strongly linked to the chlorophyll concentration. Mesozooplankton grazing on primary producers was important. Biogeochemical flux associated with the metabolic activities supported in excess of 100 % of the primary production needs in term of carbon, nitrogen and phosphorus. Relationships between the specific diversity and the environmental variables (physical, chemical and biological) showed a high regionalization in the Mediterranean Sea whereas in the Kerguelen shelf these relations are weak.